

Skeletal muscle in cancer:
Exploration of the local immune environment and its association to muscle mass in cancer

by
Ana Teresa Anoveros Barrera

A thesis submitted in partial fulfillment of the requirements for the degree of
Doctor of Philosophy
in
Nutrition and Metabolism

Department of Agricultural, Food and Nutritional Science
University of Alberta

©Ana Teresa Anoveros Barrera, 2020

Abstract

Low muscle mass and muscle wasting are concerning issues as they are associated with poor outcomes and reduced survival in the oncological setting. Inflammation is a recognized contributor to disease-associated muscle loss; however, the biological characteristics of muscle tissue exhibiting aberrant muscle features such as low muscle mass or muscle wasting are not known in the cancer setting. . Immune cells are participants of the cycle of inflammation which have been associated with low muscle mass in a variety of cancer populations; however, there is limited knowledge on the immune environment of skeletal muscle during cancer. Lymphocyte and neutrophil tissue migration is suspected as relevant event occurring in the host as part of the response to cancer and it has been linked to cancer-induced tissue wasting. In the present study, we explored clinical and animal models to expand the knowledge on the involvement of immune cells within skeletal muscle in association with muscle mass during cancer.

In a clinical model, we investigated the relationships between immune cells from the innate and adaptive response and muscle mass of a cancer population ($n = 30$, 91% gastrointestinal malignancies and 67%). Muscle fiber CSA was positively correlated ($r = > 0.45$; $p = < 0.05$) with total number of T cells, CD4, and CD8 T cells and CD11b+ granulocytes/phagocytes. Consistently, patients with a higher number of CD8 T cells had larger muscle fiber CSA and higher skeletal muscle index. Further exploration on gene-array data generated in a second identical patient cohort revealed inverse associations between CD8 T cell-related genes with key genes involved in muscle catabolic pathways: (Caspase 8), autophagy (Beclin 1), catabolic signaling (ACVR2B and ACVR1B receptors) and ubiquitin proteasome (FBXO32, FOXO4, MUL1 and TRIM63) ($r = \geq 0.5$; $p = < 0.0001$).

In a preclinical cancer model, we explored the effect of cancer and chemotherapy treatment in lymphocyte and neutrophil migration into skeletal muscle. A global gene expression dataset was generated from skeletal muscle of a wild colorectal tumor-bearing rat model developed to study the effect of chemotherapy exposure (irinotecan/5-Fluorouracil) and which is known to exhibit mild muscle atrophy. Differential expression of genes encoding toll-like receptors (TLR5 and CD14), chemokines (CXCL14, CX3CL1 and CXCR4) and cellular adhesion molecules (SELE, ITGAD and ITGB2A) revealed the involvement of immune cell migration in muscle as part of the response to tumor burden, while chemotherapy exposure promoted the differential expression on additional genes encoding TLR-adaptor MAL/TIRAP and TLR-associated enzyme IRAK4, as well as chemokine ligand CCL6. Gene exploration with Ingenuity Pathway Analysis® resulted in the identification of three genes (ITGAD, ITGB2, CD6) encoding surface molecules exclusively expressed in lymphocytes and/or myeloid cells, providing initial evidence of their presence within skeletal muscle in tumor-bearing rodents, as well as chemotherapy exposed rodents.

In conclusion, findings from clinical and preclinical models suggest an involvement of immune cells from innate and adaptive immune response with muscle mass in cancer. Lymphocyte and phagocyte tissue migration, which has been linked to muscle loss, is a relevant event occurring in muscle in response to cancer. In addition, exposure to chemotherapy influences the local immune environment of muscle and promotes upregulation of genes involved in immune cell migration; however, more studies are needed to understand its effect to repeated exposures. Further exploration is required to understand the dynamics of immune cells and skeletal muscle, and their implications in muscle mass in cancer. Overall the present work is an important contribution to the fields of skeletal muscle abnormalities in cancer, cancer cachexia and muscle disease.

Preface

This doctoral thesis is an original work of Ana Anoveros Barrera. Human studies presented in Chapter 3 and 4 was approved by the Health Research Ethics Board of Alberta-Cancer Committee, and performed under the auspices of Protocol ETH-21709: *The Molecular Profile of Cancer Cachexia*. Animal work presented in Chapter 5 was approved by the University of Alberta Institutional Animal Care Committee and conducted under the Protocol AC12200: “*Nutritional modulation of antineoplastic therapy*” in accordance with the Guidelines of the Canadian Council on Animal Care. Present work was funded by Canadian Institutes of Health Research.

Chapter 3 has an equal contribution from Ana Anoveros and Amritpal S. Bhullar. This chapter has been published as Ana Anoveros-Barrera, Amritpal S. Bhullar, Cynthia Stretch, Nina Esfandiari, Abha R. Dunichand-Hoedl, Karen J. B. Martins, David Bigam, Rachel G. Khadaroo, Todd McMullen, Oliver F. Bathe, Sambasivarao Damaraju, Richard J Skipworth, Charles T. Putman, Vickie E. Baracos and Vera C. Mazurak. “Clinical and biological characterization of skeletal muscle tissue biopsies of surgical cancer patients”. *Journal of Cachexia Sarcopenia and Muscle*. 2019. jcsm.12466. Conceptualization, design, analysis, writing, and interpretation: Ana Anoveros and Amritpal S. Bhullar. Gene array data analysis and interpretation: Cynthia Stretch. Data collection and analysis: Nina Esfanidari. CT image analysis and experimental optimization: Abha R. Duhichand-Hoedl. Experimental optimization and image analysis: Karen J.B. Martins. Patient recruitment, biopsy and clinical data collection: David Bigam, Todd McMullen, Rachel G. Khadaroo and Oliver F. Bathe. Data interpretation and manuscript editing: Sambasivarao Damaraju, Richard J Skipworth and Charles T. Putman. Conceptualization, design, analysis, interpretation, and editing: Vera C. Mazurak and Vickie E. Baracos.

Chapter 4 has been published as Anoveros-Barrera A, Bhullar AS, Stretch C, Dunichand-Hoedl AR, Martins KJB, Rieger A, Bigam D, McMullen T, Bathe OF, Putman CT, Field CJ, Baracos VE, Mazurak VC. “Immunohistochemical phenotyping of T cells, granulocytes, and phagocytes in the muscle of cancer patients: association with radiologically defined muscle mass and gene expression”. *Skeletal Muscle*. 2019. 14;9(1):24. Conceptualization, design, analysis, writing, and interpretation: Ana Anoveros. Conceptualization, design, experimental optimization and tissue processing: Amritpal S. Bhullar. Gene array data analysis, interpretation, and creation of

correlation matrix figures: Cynthia Stretch. CT image analysis and experimental optimization: Abha R. Duhichand-Hoedl. Experimental optimization and immunohistochemistry image analysis: Karen JB Martins. Flow cytometry experimental design and data analysis: Aja Rieger. Patient recruitment, biopsy and clinical data collection: David Bigam, Todd McMullen, Oliver F. Bathe. Interpretation and editing: Charles T. Putman. Experimental design, data interpretation and manuscript development: Catherine J. Field. Conceptualization, design, analysis, interpretation, and editing: Vera C. Mazurak and Vickie E. Baracos.

Chapter 5 was done in collaboration of Dr. Vera Mazurak and Dr.Sambasivarao Damaraju Laboratories. It was written in a manuscript format, part of this chapter will be prepared for publication. Ana Anoveros contributed with conceptualization, data analysis, interpretation and manuscript writing. Bhumi Batt contributed with the performing and interpretation of transcriptomic and functional annotations, and methodology writing. Gauhar Ali contributed with conceptualization and data analysis. Alaa Almasud contributed to animal characteristics analysis. Alaa Almasud, Kait St. Pierre and Abha R Dunichand-Hoedl contributed with rodent experiments, animal care and sample collection. Catherine J. Field and Vickie Baracos contributed with conceptualization and manuscript editing. Vera C. Mazurak and Sambasivarao Damaraju contributed with conceptualization, global gene database generation, analysis methodology and interpretation, and manuscript editing.

Dedication

To

My parents, Julio Añoveros and Ana Teresa Barrera

This project and degree would have not be possible without you. Thank you for all the effort and love to provide me with the best tools to start and complete the present and other life challenges. You are my greatest inspiration and I love you immensely.

Ing. Javier Torres

My love and best friend, you have been an amazing partner in this crazy dance that we call life. I love you and thank you for your encouragement to explore the world and pursue the present doctoral degree. Your support, guidance and love have been invaluable elements during this whole process.

My brother, Julio Añoveros

Thank you for your support, for listening and giving words of encouragement in difficult times. Thank you for being the best big brother any one can ask, for your support and love. You are amazing, I love you so much.

Victoria Torres

The lady that came to turn my world 360°, you brought a new light and purpose into our lives. I am grateful for your life and love. Thank you to you and the Buttons for your patience and support in the past year. Managing motherhood and a PhD program has been an extreme experience, but I would not change any part of this process in the way it came to be.

Mafer Maxil Salchita

Thank you for being such an important part of the conception and completion of this journey. Thank you for your love, friendship, support, for listening and for believing in me for the past 30 years.

Irina Vázquez and Roxy Malagón

Thank you for your unconditional support and love. It has meant a lot to share one more life adventure with mis queridas amigas del jardín de la tercera edad.

ACKNOWLEDGMENTS

I would like to thank the Consejo Nacional de Ciencia y Tecnología (CONACyT) from the government of Mexico for providing the financial support for this degree. Thank you for giving me the opportunity and honour to represent Mexico abroad. I am confident that my training and everything obtained from this degree will have a positive impact in many ways in Mexico and all over the world.

Dr. Vera Mazurak you are one of my greatest mentors in life and grad school. I am truly grateful for the opportunity to be part of your team and to contribute to the knowledge of the world in the area of Cancer, Muscle wasting and Nutrition. You have been an inspiration to me, to pursue my dreams, motherhood, to be confident of myself, skills, knowledge, and most important to learn that compassion and positive feedback are the best tools to nourish the essence of a person and lead them to their success. Since day one of my degree, I felt your commitment and unconditional support, and as proof I am taking a PhD when I thought I was coming for Master degree. Thank you.

Dr. Vickie Baracos (Momma Vickie), thank you for all the love, support and brain exercise. You are truly the Stephen Hawkins of Cancer Cachexia, and I feel extremely lucky to be one of your science children. Thank you for taking the time to explain many concepts that once were extremely hard to connect, if something I have learned from you is that “there is always a way and there is always an answer for every question”. Thank you for sharing with me your passion for science, your love for horses, and the importance of collaborating and believing in the potential of others. Thank you for believing in me and for your support in many ways so I could accomplish this goal.

Dr. Catherine Field, it has been an honour to be your mentee in the PhD program and the Nutrition field. Thank you for sharing your passion, love and enthusiasm for Nutrition with me which was something I was in very much need of. I am extremely grateful for having your guidance and encouragement to develop my leadership, project management, networking, and public speaking skills. Thank you so much for all the support and love during this program, and for believing in me.

Dr. Sambasivarao Damaraju, with deep appreciation I share with you that the last part of this thesis was quite a challenge. Achieving that objective was possible thanks to your extensive contribution and constant support, thank you very much for everything. Dr. Charles Putman (Ted), thank you for your contribution for many parts of this work, you always gave me encouragement and kindness when I was in much need of them, you are an amazing person... thank you. Thank you to Dr. Jerome Frenette and Dr. Richard Uwiera for serving as external examiners of this final exam. Thank you to Dr. Rene Jacobs for being the chair of the exam, and for his contribution of many memories during the last five years at the 4th floor.

Dr. David Bigam, our famous oncology surgeon and father of the biopsies, thank you for your great passion and commitment to this project and research. I am very grateful for having you on our side, for your support and kindness. Also, an immense thank you to all the patients in our cohorts for your contribution to the knowledge on muscle abnormalities during cancer, without your enthusiasm and trust this research would not be here.

Amritpal Bhullar and Abha R. Dunichand-Hoedl, you have been critical people in the achievement of this degree. I will be forever thankful for your encouragement, support, love, kindness and friendship. Thank you giving me perspective in the moments were my mind was cloudy and the tea times. Jacqueline Krysa and Yumna Zia, thank you for your friendship, support, for the memories and all the art that we did together and the one that you made for me. You are amazing. Thank you to the amazing friends from the Mazurak/Baracos lab: Alaa, Maryam, Sara, Luana, Caitlyn, Magaly, Bhumi, Lisa, Gauhar, Asifa, Cynthia, Lorena, Dalton, Nathalja, Kevin, summer students, visitors and many more. Thank you to my friends from other labs, for your support and friendship: Paoli, Blanca, Paulina A, Jessy, Paulina B, Marjorie, Jingjie, Sue, Marnie, Kelly-Ann, Rabban and many more amazing people.

Javier Torres, thank you for all the effort and emotional support during these five years and specially the last year (sorry if I wasn't very nice some days). I am extremely grateful for your love and to share this achievement with you. Also, thank you to my family and friends from Mexico for their support and encouragement. Special thanks my mom, Miss Ana Barrera, for taking time off to take care of Victoria so I could finish writing the papers and the present thesis.

Table of contents

Chapter 1: Literature review

1.1 Relevance of skeletal muscle mass in the clinical and cancer setting	1
1.2 Radiological assessment of muscle in cancer patients.....	2
1.2.1 Advantages and limitations of CT as a body composition assessment tool.....	3
1.2.2 Identification of low muscle mass individuals with muscle CT-derived assessment in cancer	4
1.3 Muscle biopsies as an emerging tool to understand low muscle mass and muscle wasting in cancer	5
1.4 Inflammation as a contributor to muscle loss in cancer.....	5
1.4.2 Potential mechanisms and involvement of immune cells in cancer-associated muscle loss	9
1.4.3 Immune cell accumulation into skeletal muscle during cancer: migratory signals and its relation to cancer-associated muscle wasting.....	11
1.4.4 Chemotherapy as an additional source of inflammation impacting muscle mass.....	14
1.5 Summary.....	15

Chapter 2: Research plan

2.1 Rationale	25
2.2 Research objectives and hypotheses	26

Chapter3: Clinical and biological characterization of skeletal muscle tissue biopsies of surgical cancer patients

3.1 Introduction.....	28
3.2 Materials and methods	29
3.2.1 Literature review.....	29
3.2.2 Rectus abdominis biological characterization	30
3.3 Results.....	33
3.3.1 Literature review	33
3.3.2 Rectus abdominis biological characterization.....	35
3.4 Discussion.....	37

Chapter 4: Immunohistochemical phenotyping of T cells, granulocytes and phagocytes in muscle of cancer patients: association with radiologically-defined muscle mass and gene expression

4.1 Introduction.....	63
4.2 Methods.....	64
4.2.1 Study population	64
4.2.2 Radiological assessment of muscle mass by CT scan.....	64
4.2.3 Muscle biopsies	65
4.2.4 Immunohistochemistry	65
4.2.5 Confocal microscopy and histological analysis	66

4.2.6 Gene expression: Microarray analysis	67
4.2.7 Statistical analysis	67
4.3 Results.....	68
4.4 Discussion.....	71

Chapter 5: Immune cell migratory signaling in skeletal muscle in response to a tumor and irinotecan/5-fluorouracil chemotherapy in a ward colorectal cancer rodent model

5.1 Introduction.....	83
5.2 Methods.....	84
5.2.1 Animal model	84
5.2.2 Experimental design	84
5.2.3 Tumor volume and tumor-free body weight.....	85
5.2.4 Diet and food intake	85
5.2.5 Muscle mass: total weight and muscle fiber Cross Sectional Area (CSA)	85
5.2.6 Statistical considerations for animal and tumor characteristics.....	86
5.2.7 Total RNA extraction	86
5.2.8 RNA-sequencing, differential expression analysis and statistical considerations for genomics.....	86
5.2.9 Global gene expression profiling: Candidate gene search and Ingenuity Pathway Analysis® (IPA)	87
5.3 Results.....	88
5.3.1 Changes in food intake, body weight and tumor volume during cancer trajectory.....	88
5.3.2 Moderate muscle atrophy is present in tumor-bearing and chemotherapy exposed rodents	88
5.3.3 Candidate search of immune cell migration genes in muscle of tumor-bearing rodents versus healthy	88
5.3.4 Candidate search of immune cell migration genes in muscle of tumor-bearing exposed to chemotherapy	89
5.3.5 Ingenuity Pathway Analysis® (IPA) biological functions to identify genes associated with the presence of lymphocytes and neutrophils in muscle of tumor-bearing and chemotherapy exposed rodents.....	89
5.4 Discussion.....	90

Chapter 6: Final discussion

6.1 General summary and review of objectives and hypotheses	108
6.2 Considerations for future studies	111
6.3 Conclusion	115

Bibliography	116
---------------------------	------------

Appendix content

Appendix A (Chapter 3): Antibody information used for immunofluorescence experiments: muscle fiber types, laminin/dystrophin and nuclear stain.....	171
Appendix B (Chapter 3): Complete extraction table of the reviewed articles in relevance of muscle biopsy collection in cancer patients.....	172
Appendix C (Chapter 3): Skeletal muscle gene expression for genes associated with cancer cachexia in cancer patients.....	192
Appendix D (Chapter 4): Primary antibody panel for immunohistochemistry	196
Appendix E (Chapter 4): Secondary antibody panel for immunohistochemistry with corresponding primary antibodies.....	197
Appendix F (Chapter 4): Immune cell characterization by immunofluorescence	198
Appendix G (Chapter 4): Immunostaining of serial cross-sections of muscle tissue	199
Appendix H (Chapter 4): Flow cytometry analysis for CD3+ and CD11b+ cells.....	200
Appendix I (Chapter 4): Patient characteristics, secondary cohort with microarray analysis in rectus abdominis muscle	201
Appendix J (Chapter 4): Negative univariate associations ($r \leq -0.50$) between T cell related genes and genes involved in muscle catabolic pathways of rectus abdominis muscle of male cohort (n=69)	202
Appendix K (Chapter 4): Negative univariate associations between T cell related genes and genes involved in muscle catabolic pathways of rectus abdominis muscle of secondary female cohort (n=64)	205
Appendix L (Chapter 4): Gene arrays from rectus abdominis muscle from secondary female cohort (n=64)	207
Appendix M (Chapter 5): Candidate molecules for elaboration of candidate gene list.....	208
Appendix N (Chapter 5): Overlapping of differentially expressed genes between (A) tumor-bearing versus healthy rodents, (B) tumor-bearing chemotherapy exposed versus non-exposed rodents, and (C) tumor-bearing chemotherapy exposed versus healthy rodents.	215
Appendix O (Chapter 6): Granulocytes located in blood vessel and infiltrated in muscle tissue	216

List of Tables

Table 1.1 Published studies with large cancer patient cohorts reporting SMI values

Table 1.2 Studies investigating blood immune cells in relation to low muscle mass or muscle loss

Table 1.3 Molecules involved in cell adhesion during immune cell migration

Table 3.1 Original articles reporting muscle biopsy collection in patients with cancer: assessment of bias and study quality, population characteristics weight loss or cancer cachexia classification criteria.

Table 3.2 Biopsy collection and handling procedures across the studies

Table 3.3 Patient characteristics

Table 3.4 Most common medications prescribed and potential effects on skeletal muscle

Table 3.5 Computed tomography defined muscle composition at L3 for rectus abdominis and total skeletal muscle in cancer patients, stratified by sex and age decade

Table 3.6 Rectus abdominis myosin heavy chain content and mean muscle fiber area of cancer patients

Table 3.7 Skeletal muscle gene expression for genes associated with cancer cachexia in cancer patients

Table 3.8 Summary of recommendations for muscle biopsy processing and population characterization

Table 4.1 Patient characteristics

Table 4.2 Immunohistochemical identification and quantification of immune cells in muscle

Table 4.3 Correlation between number of immune cells and muscle mass variables, all patients (n=30)

Table 4.4 Comparison of characteristics of cancer patients with low muscle mass and normal muscle mass

Table 4.5 Human studies reporting number of CD3+ (T cells) and CD11b+ (Granulocytes/Phagocytes) in muscle

Table 5.1 Composition of rodent diet

Table 5.2 Candidate gene list: genes encoding molecules with a role in immune cell migration

Table. 5.3 Candidate gene search: Differentially expressed genes identified in rodent muscle involved in immune cell migration

Table. 5.4 Tumor-bearing *versus* healthy rats - IPA® biological function analysis for identification of lymphocyte and neutrophil-related genes

Table. 5.5 Tumor-bearing chemotherapy-exposed *versus* non-exposed rats- IPA® biological function analysis for identification of lymphocyte and neutrophil-related genes

Table. 5.6 Tumor-bearing versus healthy rats– Lymphocyte and neutrophil-related differentially expressed genes in rodent muscle identified by IPA® biological function analysis

Table. 5.7 Tumor-bearing chemotherapy-exposed *versus* non-exposed rats – Lymphocyte and neutrophil-related differentially expressed genes in rodent muscle identified by IPA® biological function analysis

Table 5.8 Genes encoding cell surface molecules with relevance to lymphocyte and myeloid cell function identified by IPA *biological functions*

List of Figures

Figure 1.1 Radiological CT-derived body composition assessment at lumbar 3 (L3) vertebrae

Figure 1.2 Contribution of immune cells in cancer-associated muscle wasting

Fig.3.1 Flow chart of search. PRISMA diagram for the identification, screening, eligibility and inclusion of papers (January 1st 1990 – August 16th 2018) from SCOPUS. All articles included investigated cancer, skeletal muscle and muscle biopsies. Excluded records: review articles and ongoing clinical trials

Fig.3.2 SMI distribution for male and female in the present study in comparison to a larger cancer cohort from same region and similar clinical characteristics

Figure 4.1 SMI z-score distribution of cancer patients in the study

Fig. 4.2 Immunohistochemistry of T cells and granulocytes/ phagocytes

Fig. 4.3 Distribution of immune cells within muscle tissue

Fig.4.4 Correlation matrix of T cells genes and muscle catabolic pathway genes

Fig. 4.5 Presence of immune cells in skeletal muscle tissue during cancer and potential role of CD8 T cells in muscle mass preservation

Figure 5.1 Experimental study design

Figure 5.2 Muscle fiber cross sectional area (CSA) of gastrocnemius muscle in various treatment groups (n=4 per group)

Fig.5.3 Tumor-bearing *versus* healthy (reference) - Flow chart of IPA®

Fig. 5.4 Tumor-bearing chemotherapy exposed *versus* non-exposed - Flow chart of IPA®

Figure 5.5 Hypothetical overview of molecules encoded by differentially expressed genes identified using candidate gene search and IPA®

List of symbols and abbreviations

5-FU	5-fluorouracil
β	Beta
C	Celsius
cm	Centimeters
CNS	Central nervous system
CSA	Cross sectional area
CT	Computed tomography
CTP-11	Camptothecin-11 or irinotecan
DEGs	Differentially expressed genes
g	Grams
HU	Hounsfield Units
IFN	Interferon
IL	Interleukin
IPA	Ingenuity ®Pathway Analysis`
L3	Lumbar 3
LMR	Lymphocyte monocyte ratio
m	Meters
MCP-1	Monocyte chemoattractant protein 1
mg	Milligram
MHC	Major histocompatibility complex
MHC	Major histocompatibility complex
MRI	Magnetic resonance image
MyCH	Myosin heavy chain
NF κ B	Nuclear factor kappa B
ng	Nanogram
NGS	Next Generation Sequencing

NLR	Neutrophil Lymphocyte ratio
SD	Standard Deviation
SE	Standard Error
SE	Standard error
SMI	Skeletal muscle index
TGF	Transforming growth factor
TLR	Toll-like receptor
TNF	Tumor necrosis factor
TRIF	TIR-domain-containing adaptor inducing interferon-
μm^2	Micrometer squared

Chapter 1: Literature review

1.1 Relevance of skeletal muscle mass in the clinical and cancer setting

Skeletal muscle is a dynamic tissue involved in body mobility, strength and nutrient/energy metabolism comprising 50 to 75% of body protein stores (Frontera & Ochala, 2015). Muscle mass is regulated by a balance between catabolic and anabolic signals contributing to protein turnover. Genetics, aging, sex, diet, physical activity, chronic disease and medications are factors that impact muscle mass (Arden & Spector, 1997; Burd et al., 2010; Leenders et al., 2013; Malin & Kashyap, 2014; McGlory, et.al., 2019; C. H. Murphy et al., 2018; Nilwik et al., 2013). The importance of muscle mass for human health has been reevaluated in the past decades by the emerging use of body composition techniques such as computed tomography (Fukushima, et.al., 2018; Fukushima, et.al., 2015; Lieffers, et.al., 2012; Martin et al., 2013; Prado et al., 2008a; Voron et al., 2015). Low muscle mass has been associated with reduced quality of life, morbidity and increase costs of hospital care in aging and diverse clinical populations (Beaudart et al., 2015; Gani et al., 2016; Giglio et al., 2018; Kawamura et al., 2018; Mayr et al., 2018; Mori et al., 2019; O'Brien et al., 2018; Otten et al., 2019; Pourhassan, et.al. 2018; Silva de Paula, et.al, 2018; Yadav et al., 2015; Y. Zhang et al., 2019). The cost of patients with low muscle mass is nearly as twice as individuals with normal muscle mass due to post-operative complications and longer hospital stays (Gani et al., 2016; Huang et al., 2017). Low muscle quantity, quality and strength, in addition to a reduced physical performance is termed sarcopenia (Cruz-Jentoft et al., 2019). However, criteria for sarcopenia varies among clinical populations in oncological research, patients with sarcopenia are identified by the sole presence of low muscle mass (Rier, et.al., 2016; Shachar, et.a. 2016). For cancer cachexia, a multifactorial syndrome that involves muscle wasting (with or without loss of adipose tissue), the diagnostic criterion is weight loss >5% in the last 6 months or weight loss of >2% in individuals with body mass index below 20 kg/m² or weight loss of >2% in individuals with sarcopenia (Fearon et al., 2011). Sarcopenia is one-time point measurement, as muscle loss is a dynamic process.

In the cancer population, sarcopenia is a concerning issue as prevalence has been reported up to 69 to 89% (Rier et al., 2016; Shachar et al., 2016). Low muscle mass is an a one-time point assessment that predicts reduced survival, increased post-operative complications, and treatment toxicity during cancer trajectory (Barret et al., 2014; Fukushima et al., 2018, 2015; Kazemi-

Bajestani, Mazurak, & Baracos, 2016; Lieffers et al., 2012; Martin et al., 2013; Mayr et al., 2018; Otten et al., 2019; Prado et al., 2008a; Silva de Paula et al., 2018; Voron et al., 2015). Post-operative complications are related to the surgical procedure (e.g. wound infection, bleeding, anastomotic leakage) or general medical complications (e.g. nosocomial infections, pulmonary embolism, cardiac complications, hepatic dysfunction) (Huang et al., 2017; Lieffers et al., 2012). Importantly, cancer patients appear to have accelerated muscle loss and higher degree of chemotherapy toxicity when sarcopenia is present (Kazemi-Bajestani et al., 2016; R. A. Murphy, Mourtzakis, et.al, 2010). Cancer-associated muscle loss is associated to increased mortality during cancer (Fogelman et al., 2014). The degree of muscle loss that cancer patients experience can be from 2 to 25% within a period of 2 to 9 month (Roeland et al., 2017).

1.2 Radiological assessment of muscle in cancer patients

In cancer research, computed tomography (CT), performed as the clinical standard of care, has emerged as an opportunistic tool for body composition assessment (Mourtzakis et al., 2008). Extensive validation and extreme precision (error values of ~1.4%) have made CT imaging the gold standard technique for body composition assessment in the cancer population (Lieffers et al., 2012; Martin et al., 2013; Mitsiopoulos et al., 1998; Mourtzakis et al., 2008; Carla MM M Prado et al., 2008b; Xiao et al., 2018). CT is an X-ray-based medical device used to create high resolution two and three dimensional images of body structures using computer image reconstruction (Hounsfield, 1973; Ter-Pogossian, 1977). Skeletal muscle, adipose tissue and other body tissues are distinguished by differences in radiodensity, also known as attenuation coefficient, which reflect the ability of radiation to pass through a tissue (Ter-Pogossian, 1977). CT radiodensity is usually reported using Hounsfield Units scale (HU)(Aubrey et al., 2014), a linear transformation of the attenuation coefficient where the radiodensity of distilled water is defined as zero and the radiodensity of air as -1000 HU (Ter-Pogossian, 1977). Pre-defined HU ranges are used in the literature to radiologically define subcutaneous adipose tissue (-190 to -30 HU), visceral adipose tissue (-190 to -50 HU), intermuscular adipose tissue (-190 to -30 HU), and skeletal muscle (-29 to +150 HU) (Fig. 1.1) (Miller et al., 1998; Mourtzakis et al., 2008; Shen et al., 2004; Yoshizumi et al., 1999). Quantification of the anatomical regions from CT images consists of a map of pixels, corresponding to a HU value and the total volume represented by the sum of all pixels (Carla M. Prado & Heymsfield, 2014). Finally, CT assessment enables quantification, which reflects

tissue volume, described as cross-sectional area (CSA, cm²) and mean radiodensity (HU), also known as mean attenuation value.

The use of CT for body composition, specifically for skeletal muscle, was initially validated in limbs from cadavers demonstrating that tissue volume and CT estimated values were strongly related ($r=0.99$, SE of estimate=3.8 cm² $p<0.001$) (Mitsiopoulos et al., 1998). Later, the search to find a landmark that represents whole body values for muscle mass in men and women resulted in the analysis of single abdominal cross-sectional images above and below the lumbar 4 to 5 region where lumbar 3 (L3) had the strongest correlation to whole body muscle volume ($r=0.924$, $p<0.001$) (Shen et al., 2004). The anatomical region at L3 level includes several muscle groups: psoas, erector spinae, quadratus lumborum, transversus abdominis, external and internal oblique muscles of the abdomen, and rectus abdominis muscle. In addition, prediction equation to estimate whole body muscle mass (or volume) from lumbar CSA values were developed by Shen et al. (Shen et al., 2004). Currently, CT is extensively used around the world for the assessment of muscle mass in different clinical populations as cancer, liver disease and healthy kidney donor candidates (Derstine et al., 2018; Ebadi et al., 2018; Johns et al., 2017; Martin et al., 2018; Van Der Werf et al., 2018; Xiao et al., 2018). Increased attention on CT-derived muscle assessment led to the identification of two abnormal muscle phenotypes: low muscle mass and low muscle radiodensity. Low muscle mass is defined with skeletal muscle index (SMI) a measure for relative muscularity calculated from muscle CSA divided by height squared (cm²/m²) (Baumgartner et al., 1998). While low muscle radiodensity (mean muscle HU) is associated with pathological fat accumulation within muscle (Goodpaster et al., 2000). These two muscle abnormalities are considered to be separate but often as coexisting biological processes which was recently revealed by research evaluating gene expression in muscle biopsies of pancreatic cancer patients (Stretch et al., 2018).

1.2.1 Advantages and limitations of CT as a body composition assessment tool

CT is distinguished from other imaging body composition technologies (e.g. Dual Energy X-ray absorptiometry) for clearly differentiating between tissue compartments (i.e. organs, bone, adipose tissue and muscle) (Fig. 1.1), which is an advantage when assessing patients where alterations in hydration status are present (Mourtzakis et al., 2008). CT is highly reproducible with a low coefficient of variation between and within observers (Mitsiopoulos et al., 1998; Carla M. M.

Prado & Heymsfield, 2014). Trained personal and software licensing are required for the use of this technique. CT technology is limited to the clinical setting, as it is exclusively used for diagnostic and follow-up purposes due to elevated cost and high radiation doses. Patients with extremely large body structures (BMI >40 kg/m²) that are not able to fit in the scan field of view are excluded from this medical procedure (Carla Prado & Heymsfield, 2014).

1.2.2 Identification of low muscle mass individuals with muscle CT-derived assessment in cancer

In cancer research, individuals with low muscle mass have been identified using distinct criteria. Rier et al. reviewed these criteria in a variety of cancer populations (Rier et al., 2016). Most studies categorized their patients under the criteria for *sarcopenia*, which involves SMI-derived cut-offs obtained from survival analyses based on cancer cohorts. These cut-offs were defined from the study cohort or selected from already published data. Fewer studies arbitrarily defined low muscle mass based on individuals at the low end of the SMI distribution of the study cohort, bearing in mind that these patients are at most risk of poor outcomes (Rier et al., 2016). For each of these methods, there is potential risk for sampling bias. For instance, when SMI cut-off values are selected from published literature, especially from cancer populations that differ from the study cohort, patient can be miscategorised into sarcopenic or non-sarcopenic groups. Also, for studies focusing on arbitrary cut-offs at the lower end of the SMI distribution, patients might not represent an appropriate sample of individuals with and without sarcopenia. Importantly, statistical analysis for data normality indicate that SMI is normally distributed, which provides insight on the possibility of finding a point of reference for researchers to compare their populations to larger patient cohorts. SMI z-score calculations to evaluate the number of standard deviations from the mean in relation to a population of reference provides a more global perspective of the study population. Importantly, in recent years, SMI values (mean \pm standard deviation) of large cohorts (>1150 patients) of oncological and surgical cancer populations have been published (Table 1.1) (Johns et al., 2017; Martin et al., 2013; Martin, Gioulbasanis, Senesse, & Baracos, 2019; Martin et al., 2018; Xiao et al., 2018). Optimistically, as more research is developed using CT for body composition assessment, emerging and aggregated data for SMI distributions in relation to specific cancer types and geographical regions will be available.

1.3 Muscle biopsies as an emerging tool to understand low muscle mass and muscle wasting in cancer

In oncological research, collection of surgical and needle muscle biopsies from consenting cancer patients is emerging. Exploration of biological and morphological characteristics of muscle tissue is an essential tool to better understand the impact of cancer on muscle and define molecular mechanisms underlying muscle abnormalities and muscle wasting. For example, higher proteolytic activity is suggested in cancer patients, elevated mRNA expression of ubiquitin has been observed in muscle biopsies when compared to individuals without cancer (Williams, Sun, Fischer, & Hasselgren, 1999). A comparison within cancer patients found a smaller muscle fiber diameter (<25%) and reduced mean protein content in patients with low muscle mass experiencing >2% weight loss when compared to non-losing or normal muscle patients (Johns et al., 2014). More recently, muscle biopsy collection is combined with techniques such as Next Generation Sequencing (NGS), a high-end transcriptomics technology (Alekseyev et al., 2018). NGS has enabled extensive exploration of genes potentially involved in cancer cachexia (Fearon et al., 2011; Narasimhan et al., 2017). A critical evaluation of past and current work in this area is needed as relevant sources of variations such as patient selection, classification, and clinical characterization, as well as biopsy collection/manipulation practices, pose limitations in the result interpretation, reliability and comparability.

1.4 Inflammation as a contributor to muscle loss in cancer

Inflammation is a complex process involving a series of physiological and molecular responses with the aim to restore body homeostasis (Medzhitov, 2008). In the presence of cancer, inflammation is persistent (Baracos, Martin, Korc, Guttridge, & Fearon, 2018; Grivennikov, Greten, & Karin, 2010), and recognized as a contributor to cancer-associated muscle wasting (Baracos et al., 2018; Fearon et al., 2011). Cancer-induced inflammation implicates the activation and circulation of immune cells from innate and adaptive immune response. Alterations in circulating immune cell counts occur at diverse time points of disease trajectory (Cespedes Feliciano et al., 2017; Malietzis, Currie, et al., 2016). Importantly, blood immune cell counts are used as biomarkers of systemic inflammation to predict patient outcomes; and more recently, evidence suggests that circulating immune cells are associated to muscle mass in patients with a variety of cancer types (Table 1.2) (Dolan, et.al, 2017; Malietzis et al., 2014). Several types of

immune cells have been investigated in relation with low muscle mass and muscle wasting in cancer patients. For instance, white blood cells (WBC) also referred as leukocytes, have shown a positive association with skeletal muscle index (SMI) in colon cancer patients (W. Z. He et al., 2018). Studies comparing patients with sarcopenia with non-sarcopenic patients have reported conflicting results. For instance, higher values of WBC were reported in the sarcopenia group for head and neck, esophagogastric and non-small cell lung cancer (Black et al., 2017; Cho et al., 2018; Tsukioka et al., 2018); while, no differences have been observed in cancers of gastrointestinal, urothelial and other lung cohorts (Fukushima et al., 2015; Kim et al., 2016a; Lin et al., 2018; Richards et al., 2012; Rollins et al., 2016). Interpretation of the results can be limited by the ability of WBC counts to distinguish immune cell subsets, as they are comprised of all immune cell types.

Literature reporting associations between immune cells and muscle mass was investigated in table 1.2. Lymphocytes account for 25 to 33% of WBC, it includes natural killers, T cells and B cells (George-Gay & Parker, 2003). Elevated counts are associated with favorable clinical prognosis in patients undergoing cancer treatment (Oh et al., 2018). Correlations between lymphocyte counts and SMI, suggest that cancer patients with higher lymphocyte counts have higher SMI (W. Z. He et al., 2018; Kim et al., 2016b; Zheng et al., 2018). For gastric cancer patients with sarcopenia, lymphocyte counts were 20% lower than those without sarcopenia (Peng et al., 2015; Y. Wang et al., 2017); while for endometrial and gastrointestinal cancer cohorts no differences were observed between sarcopenic and non-sarcopenic patients (Black et al., 2017; Kuroki et al., 2015). Subtypes of lymphocytes were investigated in relation to lean muscle mass index, a measurement of muscularity obtained by dual-energy X-ray absorptiometry, in a pilot study of patients with gastrointestinal and lung malignancies (Narsale et al., 2019). Negative correlations observed between lean muscle mass index and CD4 T cells, as well as with inflammatory CD8 T cells (Narsale et al., 2019), suggest a more complex involvement of lymphocyte subtypes that could help to explain an overall positive or absent relationship between lymphocyte counts and muscle mass. For neutrophils, granulocytes/phagocytes that account for 50 to 70% of peripheral WBC (George-Gay & Parker, 2003), a higher neutrophil count has been reported in patients with lower muscle mass in head and neck, gastrointestinal and colon cancer cohorts (Black et al., 2017; Cho et al., 2018). In contrast, no differences were observed in neutrophil counts in patients with low muscle mass in non-metastatic colon cancer, stomach and small cell lung cancer (W. Z. He et al.,

2018; Kim et al., 2016a; Lin et al., 2018). Monocytes account for 3 to 7% of blood WBC (George-Gay & Parker, 2003), and are precursors for macrophages and dendritic cells which are phagocytes with antigen presentation functions. Positive correlations between monocyte counts and SMI have been reported in colon cancer patients (W. Z. He et al., 2018). In addition, exploration of proportions of dendritic cell phenotypes, monocyte-derived but also bone marrow-derived, resulted in positive correlations between mature dendritic cells (CD40+) and SMI values in non-metastatic colorectal cancer patients (Malietzis, Lee, et al., 2016). No relationships were reported for other dendritic phenotypes related to maturity (CD86), migration (CCR7) and cell signaling (CD36) in relation to SMI (Malietzis, Lee, et al., 2016).

Proportions between immune cell types, such as neutrophil lymphocyte ratio (NLR) is a recognized biomarker of systemic inflammation. NLR is used as a predictor of poor clinical outcomes and survival in cancer patients (Dolan et al., 2017; Gonda et al., 2017; Paramanathan, Saxena, & Morris, 2014; Sato et al., 2017). An elevated NLR, neutrophil predominance over lymphocytes, has been observed in patients with sarcopenia in cohorts of lung, upper and lower gastrointestinal cancers (Caan et al., 2017; Cho et al., 2018; Kim et al., 2016b; Lin et al., 2018; Malietzis, Currie, et al., 2016; Malietzis, Johns, et al., 2016; Tsukioka et al., 2018); also, a high NLR (≈ 3) has resulted a predictor of low muscle mass and muscle loss in patients with gastrointestinal malignancies (Basile et al., 2019; Lin et al., 2018; Malietzis, Currie, et al., 2016). Elevated pre-diagnostic NLR values have been related to a higher risk of experiencing low muscle mass in non-metastatic colorectal cancer patients (Cespedes Feliciano et al., 2017; Xiao et al., 2019); multivariate analyses reported consistent results across cancer stage, age and sex (Cespedes Feliciano et al., 2017). Also, positive correlations have been reported between NLR and SMI values in lung cancer patients (Kim et al., 2016b). For pancreatic patients undergoing first line of chemotherapy, higher variations of NLR at baseline and 3 months after treatment were present in patients experiencing $\geq 10\%$ of muscle loss (Basile et al., 2019). A study that evaluated patients with cancer cachexia reported high NLR values between pre-cachectic and non-cachectic cases (Penafuerte et al., 2016). A handful of studies reported no statistical differences in NLR when comparing patients with and without sarcopenia in cohorts of gastrointestinal, urinary and respiratory malignancies (Dolan et al., 2018; Go et al., 2016; Hirasawa et al., 2016; Richards et al., 2012; Rollins et al., 2016; B. H.L. Tan et al., 2015). McSorley *et al.* evaluated NLR based on two sarcopenia definitions (Prado *et al.* and Martin *et al.*) (Martin et al., 2013; Carla MM M Prado

et al., 2008b) in colorectal patients, reporting contradicting results and very weak associations (McSorley, Black, Horgan, & McMillan, 2018).

Lymphocyte monocyte ratio (LMR) is also used as a biomarker of inflammation in cancer, and it has been less studied in relation to muscle mass in comparison to NLR. Having a high LMR reflects predominance of circulating lymphocytes over monocytes; it is associated to better clinical outcomes and increased survival in the cancer population (Gu et al., 2016). Colorectal cancer patients with a high LMR have shown a reduced risk of experiencing low muscle mass (Cespedes Feliciano et al., 2017). However, when evaluating muscle loss in relation to LMR, no associations were observed in a pancreatic cancer cohort receiving chemotherapy (Basile et al., 2019).

Collectively, the present clinical evidence suggests an involvement of peripheral immune cells with muscle mass in cancer patients. Immune cell types and proportions within them, might play specific roles in the preservation or loss of muscle mass in cancer. Evidence on peripheral immune cells suggests that elevated lymphocyte counts and proportions over monocytes might play a role in muscle mass preservation; whereas elevated neutrophil counts and proportions over lymphocytes might promote low muscle mass and muscle wasting during cancer. Nevertheless, current research has limitations in the exploration of the relationships between circulating immune cells and muscle mass. For instance, the criteria or thresholds selected to define sarcopenia or low muscle mass, and high immune cell counts, NLR and LMR ratios could influence the current findings and limits the comparability between studies. Most studies in the present literature review had a consistent body composition assessment technique (Table 1.2), however, comparability of results is challenging for those studies using DXA (Narsale et al., 2019) or CT with a different HU scale or body landmarks that have not been validated for muscle mass assessment (Go et al., 2016). Sex and age are factors that influence muscle mass and immune response (Klein & Flanagan, 2016; Martin et al., 2014; Nilwik et al., 2013), and interpretation of the results in studies with cohorts that include patients with all age groups to studies with mainly elderly individuals (>65 years old) may limit generalizability of findings. A multivariate analysis that accounted for age and sex reported that older age, female gender, in addition to high preoperative NLR and low physical status are predictors of low muscle mass over time in individuals with colorectal cancer (Malietzis, Currie, et al., 2016). In relation to sex, Lin *et al.* observed no differences between men and women in a cohort of stomach cancer patients with age range of 53 to 73 years old (Lin et al.,

2018). Cancer type and stage could limit the comparability of the present studies. Several cohorts included a variety of cancer types, for a study comparing WBC, lymphocyte and neutrophil counts between esophagogastric and colorectal cancer patients showed no relationships to the cancer type (Black et al., 2017). Feliciano *et al.* reported high NLR was related to a higher risk of sarcopenia with no evidence of interaction for cancer stage, age and sex in a colorectal cancer cohort; in addition, those patients with high NLR and sarcopenia were at greater risk of death (Cespedes Feliciano et al., 2017). However, the importance of cancer stage remains unclear as mixed stages are typically included in the studies.

1.4.2 Potential mechanisms and involvement of immune cells in cancer-associated muscle loss

Immune cells have the potential to promote muscle wasting through several mechanisms; nevertheless, their direct role in skeletal muscle is less known. Research in cancer evaluating immune cell accumulation in the central nervous system (CNS), as well as pro-inflammatory mediators as promoters of inflammation and tissue wasting, provides insightful information of the potential role of immune cells in cancer-associated muscle wasting (Fig.1.2). In the CNS, neutrophils and pro-inflammatory cytokine IL-1 β have detrimental effects on food intake impacting energy expenditure and promoting mobilization of protein stores. Accumulation of neutrophils into the brain modulates hypothalamic neuronal signaling pathway playing a role in the development of anorexia as seen in rodents implanted with pancreatic ductal adenocarcinoma (Burfeind et al., 2019a). Anorectic effects are also reported in relation to IL-1 β and its receptor on the hypothalamus of tumor-bearing rodents (Laviano et al., 2000; Turrin et al., 2004). As a result of reduced food intake body protein stores decrease and energy balance is affected. Energy balance is also altered by the increment in resting energy expenditure promoted by inflammatory cytokines such as leukemia inhibitor factor (LIF) (Purcell, Elliott, Baracos, Chu, & Prado, 2016). In animal cancer models, LIF is suggested to be mainly secreted by tumor cells (Kandarian et al., 2018) but production by T cells and monocytes has been reported *in vitro* and *in vivo* in CNS-related inflammatory diseases (Vanderlocht, Hellings, et al., 2006; Vanderlocht, Hendriks, Venken, Stinissen, & Hellings, 2006). LIF induces anorexia by activation of pro-opioid melanocortin neurons in the hypothalamus (Grossberg et al., 2010), and has additional effects in energy balance involving suppression of serum leptin, a hormone involved in food intake, adiposity and as a negative regulator of energy expenditure (Beretta, Dube, Kalra, & Kalra, 2002; Friedman &

Halaas, 1998). Mice with experimental deletion of LIF implanted with C26 tumor cells are protected against muscle loss, and exhibit reduced secretion of IL-6, TNF-alpha and IL1-beta (Kandarian et al., 2018).

Pro-inflammatory mediators evoke activation of protein degradation pathways, and inhibit anabolic activity to promote loss of myofiber proteins leading to an overall reduction of muscle mass over time (Argilés, Busquets, Stemmler, & López-Soriano, 2014; Baracos et al., 2018; Costelli et al., 2002). For instance, IL-1 β activates the hypothalamic–pituitary–adrenal axis inducing upregulation of pro-catabolic genes, such as MAFBX, MURF1 (TRIM63) and FOXO1 (Braun et al., 2011); a similar effect is reported with hypothalamic accumulation of neutrophils in a pancreatic cancer rodent model (Burfeind et al., 2019a). TNF-alpha, IL-6 and IFN-gamma are involved in the activation of NF κ B pathway (Brasier, 2010; Langstein et al., 1991; Ma et al., 2017; Malinin, et al., 1997; Nishikai-Yan Shen et al., 2017; Schütze, et al., 1995; Zhou, et al. 2006), promoting expression of transcription factors from the *forkhead* (FOXO) family which leads to upregulation of ubiquitin proteasome proteins Murf1 and Atrogin 1 (Fbxo32) (Argilés et al., 2014; Baracos et al., 2018). TNF-alpha and IL-6 also activate P38/MAPK which results in increased activity of caspases (Fernando, et al. 2002; Supinski, et al., 2010), a pathway involved in cellular apoptosis (Jameel et al., 2009; Juo et al., 1997; Kralova, et al., 2008). Treatment with anti-TNF-alpha and anti-IL-6, in an experimental model of cachexia, resulted in muscle mass preservation by attenuating the activation of ubiquitin-proteasome and calcium-dependent protease proteolytic pathways (Costelli et al., 2002). In addition, TNF-alpha and IL-6 disrupt anabolic hormone activity (i.e. Insulin and Insulin-growth factor) promoting suppression of RAC serine/threonine-protein kinase (AKT) pathway suppressing protein synthesis and facilitating protein catabolism (Fernández-Celemín, Pasko, Blomart, & Thissen, 2002; Martín, Gómez-SanMiguel, Priego, & López-Calderón, 2018; Plomgaard et al., 2005; Sandri et al., 2004; White et al., 2013). TGF-beta and Activin A, members of the TGF-beta superfamily, are involved in activation of proteolysis and inhibition of protein synthesis (Argilés et al., 2014; Baracos et al., 2018). TGF-beta and Activin A are produced in the presence of malignancy (Jung, et al. 2017; Loomans & Andl, 2014; Yang, et al., 2010), and secreted by a variety of immune cells (Lacy, 2015; Ogawa, et al., 2006; Robson et al., 2008).

Immune cell accumulation in relation to cancer-associated muscle wasting has not been characterized in skeletal muscle of humans or animals with cancer; however, preclinical models suggests a direct involvement of immune cells with skeletal muscle in response to cancer. Presence of neutrophils, macrophages and T cells have been described in muscle of C26 tumor-bearing mice experiencing muscle wasting (Berardi et al., 2008). Relevance of immune cell migration as an event occurring in relation to tumor burden and potential mechanism of cancer-associated muscle loss is supported by rodent models with a variety of tumors. For instance, rodents with experimental deletion of molecules involved in the immune cell migration process, such as toll-like receptors (TLR) and chemokine receptors, have muscle mass preservation (Burfeind et al., 2018, 2019b; Calore et al., 2018a; Cannon et al., 2007; Ruud et al., 2013; G. Zhang et al., 2017). TLRs stimulation activates skeletal muscle proteolytic pathways including apoptosis and ubiquitin-proteasome (Calore et al., 2018b; G. Zhang et al., 2017); however, phagocyte accumulation in brain and adipose tissue has been also associated to tissue wasting (Calore et al., 2018b; G. Zhang et al., 2017). For instance, adipose tissue atrophy was mitigated by reduction of macrophage migration in a TLR4 knockout mice implanted with Lewis lung carcinoma (Henriques et al., 2018). In a CCR2 knockout model, hypothalamic accumulation of neutrophils was reduced with a concurrent attenuated expression of catabolic genes in muscle of mice with pancreatic cancer (Burfeind et al., 2019a).

1.4.3 Immune cell accumulation into skeletal muscle during cancer: migratory signals and its relation to cancer-associated muscle wasting

Immune cell infiltration and accumulation within muscle is part of the inflammatory process in injury and several inflammatory diseases such as muscular dystrophy, polymyositis and dermatomyositis (Loell & Lundberg, 2011; Madaro & Bouché, 2014; Porter et al., 2003); under normal conditions, immune cells are scarcely present in muscle (Beaton, Allan, Tarnopolsky, Tiidus, & Phillips, 2002; C Malm et al., 2000; Christer Malm et al., 2004; Mikkelsen et al., 2009; Paulsen et al., 2013; Tidball, 2017). Following injury, immune cell migration is required to promote tissue repair and restore homeostasis (Madaro & Bouché, 2014; Tidball, 2017). Within muscle, macrophages with an inflammatory phenotype (M1) and neutrophils remove debris and phagocytose necrotic cells (Arnold et al., 2007); while T cells are mobilized by chemokines and antigen presentation by dendritic cells (Liao et al., 2012; C. Zhang et al., 2018). CD8 T cells promote macrophage recruitment, and CD4 T cells induce macrophage polarization into an anti-

inflammatory phenotype (M2) (Burzyn et al., 2013; Deng, Wehling-Henricks, Villalta, Wang, & Tidball, 2012; Liao et al., 2012; Panduro, Benoist, & Mathis, 2018; C. Zhang et al., 2018; J. Zhang et al., 2014). Cross-talk between immune cells and muscle is essential for muscle homeostasis (Costamagna, Costelli, Sampaolesi, & Penna, 2015; Tidball, 2017). Imbalance between lymphocytes and myeloid cells (phagocytes and granulocytes) or absent or persistent recruitment under acute or chronic inflammatory conditions results in aberrant repair and tissue damage with potential loss of muscle mass (Butterfield, et.al., 2006; Castiglioni et al., 2015; Dumont, Bouchard, & Frenette, 2008; Reinhard Hohlfeld & Engel, 1991; Kohno et al., 2011; Loell et al., 2011; Loell & Lundberg, 2011; Rigamonti et al., 2013; Suzuki et al., 2005; J. Zhang et al., 2014). Phagocytes and T cells have been identified in muscle of rodents implanted with the C26 colorectal cancer (Berardi et al., 2008) which further supports the idea of a widespread involvement of immune cells during cancer and a relevant role as contributors of cancer-muscle wasting.

The factors that trigger immune cell mobilization into skeletal muscle in relation to cancer are not completely understood. However, tumor-related proteins and inflammatory mediators are capable of inducing immune cell migration in muscle. Potential mechanisms involve TLR stimulation, chemokine signaling and antigen presentation. TLRs are distributed among a variety of cells including immune cells and muscle. TLRs are located within the cell membrane (TLR1, TLR2, TLR4, TLR5, TLR6 and TLR10) and on cytoplasmic endosomes (TLR3, TLR7, TLR8 and TLR9). TLRs signaling is mediated by recognition of microbial components or molecules released during cell damage (Kawasaki & Kawai, 2014; Lavine & Sierra, 2017; Marino, Scuderi, Provenzano, & Bartoccioni, 2010; G. Zhang et al., 2017). Tumors are known to release membranous particles called exosomes and micro-vesicles acting as a vehicle to carry molecules (cellular cargo) to distant sites and trigger inflammation and promote tumorigenesis (Hernandez, Huebener, & Schwabe, 2016). Such tumor-derived micro-vesicles containing tumor-related microRNA can stimulate endogenous TLRs in muscle (Calore et al., 2018a; W. A. He et al., 2014). MicroRNA activation of TLR7/8 and TLR9 signaling cascade induces cell apoptosis as observed *in vivo* and *in vitro* in muscle exploration of rodents inoculated with Lewis lung carcinoma (Calore et al., 2018a; W. A. He et al., 2014), a well established cancer cachexia model. Immune cell-mediated TLR detection of danger-associated molecules coming from cancer-induced apoptotic muscle cells is thought to promote monocyte and neutrophil migration into muscle (Pillon & Krook, 2017; J. Wang, 2018; Wynn & Vannella, 2016). Also, activation of the TLR-signaling cascade promotes

chemokine synthesis via NFκB pathway (Boyd et al., 2006; Hindi & Kumar, 2016; Sachdev, et al., 2014).

Chemokine-receptors present on immune cell membranes enable cell attraction signals from chemokines to guide them from the periphery into the tissues (Raman & Sobolik-Delmaire, 2011). Chemokine CCL2 (MCP-1), a potent neutrophil/macrophage chemoattractant, is reported to be elevated in plasma of treatment-naïve pancreatic cancer patients experiencing cancer cachexia (Talbert et al., 2018). In addition, elevated circulatory CCL2 levels have been associated with the development of cancer-induced muscle wasting in C26 tumor-bearing rodents (Lerner et al., 2016). Tumor-bearing rodents with experimental deletion of CCL2 receptor (CCR2) resulted in a reduced hypothalamic migration of neutrophils which lead to attenuated muscle proteolysis (Burfeind et al., 2018, 2019b). In muscle, temporary upregulation of chemokine genes CCL2 is observed in acute inflammation models (Pourteymour et al., 2017); while chronic over-expression of CCL2 is reported in muscular dystrophy and inflammatory myopathies, linked to chronic phagocyte recruitment and sustained inflammation (De Bleecker, De Paepe, Vanwalleghem, & Schröder, 2002; Figarella-branger, Civatte, Bartoli, & Ois Pellissier, 2003; Porter et al., 2003). TLRs stimulation and chemokine secretion are direct facilitators of the immune cell migration process. TLR2 and TLR5, as well as chemokines CCL19, CCL21 and CXCL12 induce the expression of beta-2 integrins on immune cells (Chung et al., 2014; Constantin et al., 2000; Fagerholm, Guenther, et al., 2019; Kuwano, et al., 2010; Yago, et al., 2018). Interactions of immune cell-related integrins with epithelial-derived adhesion molecules, such as P and E selectins, are fundamental for facilitating the extravasation of immune cells through the endothelium (Table 1.3) (Fagerholm et al., 2019; Kuwano et al., 2010; Lozano, Kahl, Wong, Stephenson, & Zamboni, 1999; Vestweber, 2015; Yago et al., 2010, 2018). For instance, upregulation of P-selectin gene (SELEP) has been reported in rodents with tumor-induced muscle wasting (Benjamin H.L. Tan et al., 2012).

In injury models, T cell mobilization into muscle is mediated by chemoattraction (CCL3, CCL4 and CCL5) and protein/antigen presentation from monocyte-derived dendritic cells (Liao et al., 2012; C. Zhang et al., 2018). Cancer-related muscle breakdown might provide a source of peptide gathering for antigen presenting cells. Secretion of muscle-related proteins, such as myosin species, is observed in urine of gastro-oesophageal cancer patients with cancer cachexia (Stephens

et al., 2010). T cell interaction with other cells (immune and non-immune) is facilitated by antigen presentation via major histocompatibility complex (MHC) class I and II, molecule complexes expressed in all nucleated cells and critical for cell-mediated immune responses (M. J. Grusby et al., 1994; M. Grusby, Johnson, Papaioannou, & Glimcher, 1991; Yamazaki et al., 1988). Upregulated expression of MHC class I and II in relation to T cell accumulation is reported in undamaged muscle fibers of patients with inflammatory muscle disease (Nalini, Narayanappa, & Nagappa, 2013). Importantly, cytotoxic activity of CD4 and CD8 T cells can compromise integrity of muscle cells as observed in experiments using T cells isolated from muscle or blood of patients with chronic inflammatory myopathy *ex vivo* (Reinhard Hohlfeld & Engel, 1991; Pandya et al., 2016). IFN-gamma can promote tissue expression of both MHC class I and II (Butticè, Miller, Wang, & Smith, 2006; Hsiao et al., 2008). In malignancy, IFN-gamma released by the tumor-environment could potentially induce immune cell-mediated interactions with muscle via MHC class I and II. Increased expression of MHC class I and expression of MHC class II have been reported in human myoblasts treated with IFN-gamma (R Hohlfeld & Engel, 1990). Collectively, preclinical models support immune cell migration as an event occurring in muscle during cancer with a relevant role in cancer-induced muscle loss.

1.4.4 Chemotherapy as an additional source of inflammation impacting muscle mass

Chemotherapy is a collective term wherein administration of various drugs/agents singly, or in combinations, treatment regimens, and use as an adjunct therapy following surgery or radiotherapy. It is a recognized inducer of muscle loss associated with reduced survival in patient with cancer (Barreto, et al., 2016; Barreto, et al., 2016; Blauwhoff-Buskermolen et al., 2016; Daly et al., 2018; Damrauer et al., 2018b; Järvinen, et.al., 2018; Kiss, et.al., 2018; Mayanagi et al., 2017; Pin, et.al. 2019). Chemotherapy is an additional source of inflammation which further modifies host immunity by diverse mechanisms. For instance, doxorubicin, 5-fluorouracil (5-FU), cisplatin, and paclitaxel, agents used as a first line of treatment for a variety of cancer types, promote synthesis of pro-inflammatory cytokines (TNF alpha, IL-1, IL-6, and IL-8) via NFκB pathway (Damrauer et al., 2018a; Vyas, Laput, & Vyas, 2014). Irinotecan (CPT-11), an agent used to treat gastrointestinal cancer, has intestinal toxic effects leading to bacterial translocation and stimulation of the innate immune response (Nakao et al., 2012; Wardill et al., 2016). Increased accumulation of neutrophils and T cells has been observed in rats experiencing intestinal mucositis after irinotecan exposure (Fernandes et al., 2018). In bone marrow, myelosuppression is a common

hematological toxic effect of chemotherapeutic agents reflected on peripheral leukopenia and neutropenia (Gao et al., 2019; Kamimura, et al., 2016; Newman et al., 2016; Weycker et al., 2016; Zalberg, et al., 1998). Low white blood cell counts have been reported in 70% of patients exposed to adjuvant chemotherapy for rectal cancer (Newman et al., 2016). Also, alterations in the proportion of immune cell populations with a reduction in lymphocytes and increase in neutrophil and monocytes have been reported in a ward colorectal tumor rodent model exposed to a two week regimen of irinotecan/5-FU (Hongyu Xue et al., 2009). Chemotherapy invoked immune responses from tissues/organs shows inter-individual variations. A reduced and enhanced immune responses were observed in splenocytes and mesenteric lymph node cells, respectively, in tumor-bearing rodents exposed to irinotecan (H Xue, et. al., 2009). Skeletal muscle, as a site directly involved in pharmacokinetics, is susceptible to a direct damage upon chemotherapy exposure (Schiessel & Baracos, 2018). Activation of NF κ B pathway in muscle was reported upon exposure to chemotherapy (Damrauer et al., 2018a; Schiessel & Baracos, 2018); nevertheless, the implications of chemotherapy in relation to the immune cell mediated response of muscle are less known.

1.5 Summary

In the oncological setting, low muscle mass and muscle wasting are concerning issues as they have been associated with poor clinical prognosis. Inflammation is a recognized contributor to cancer-associated muscle loss. Importantly, immune cells are relevant players of inflammation, and relationships between them and muscle mass have been observed in the cancer population. Preclinical cancer models exploring phagocyte accumulation in the central nervous system and adipose tissue, as well as critical molecules involved in immune cell migration, suggest that immune cell accumulation into muscle tissue is a relevant event occurring during cancer. In addition, resident immune cells within muscle might contribute to cancer-associated muscle wasting. Potential mechanisms involve activities of neutrophils on the central nervous system inducing anorexia and muscle proteolysis, secretion of pro-inflammatory cytokines activating proteolytic pathways and inhibiting anabolic routes. There are suspected triggers that promote immune cell migration into muscle during cancer, potentially activation of TLRs, chemokine secretion, and muscle-related antigen presentation. Persistent migration of phagocytes, granulocytes and lymphocytes is suspected to support chronic inflammation with potential impact in muscle mass. During cancer, patients are commonly exposed to chemotherapy as part of anti-

neoplastic treatment. Chemotherapy as an additional source of inflammation induce perturbations in host immunity with can further alter the involvement of immune cells within muscle.

Author	Sample size (n)	Males (%)	Age mean±SD	Cancer type	Cancer stage (%)	Region	CT Muscle assessment (Landmark and HU)	SMI (cm²/m²) mean±SD	Muscle radiodensity (HU) mean±SD
Martin 2013	1473	56	M:64.7±11.2 F:64.8±11.5	Colorectal, Pancreas, Esophageal, Stomach, other GI and respiratory tract	I - 4.7 II -15.9 III- 27.8 IV- 51.6	Canada	L3 -29 to +150	M: 51.5±9 F:41.3±7	M: 35.5±8.6 F:34.5±10.2
Johns 2017	1276	61	65±13	Esophageal, gastric and pancreatic, lung and other GI	I - 6 II - 9 III- 52 IV -33	Canada, UK, Norway, Switzerland and Greece	L3 -29 to +150	M: 49±9 F:41±7	NR
Martin 2018	2100	61	66.6±11.9	Colorectal, (Colon n=1279 and Rectum n=821)	I - 18 II -34 III- 42 IV -5	Canada and UK	L3 -29 to +150	M:50.0±9 F:39.7±7	M: 32.9±9.4 F:30.8±9.6
Xiao 2018	3051	50	63.2±11.2	Colorectal, (Colon n= 2194 and Rectum n=857)	I - 29.8 II - 31.7 III- 38.5	California, USA	L3 -29 to +150	M:54.1±9.3 F:43.0±7.4	M: 40.4±9.6 F:37.2±10.0
Xiao 2019	3262	50	62.6 ± 11.4	Colorectal, (Colon n=2,315 and Rectum n=947)	I - 30 II - 32.5 III- 36.8	California, USA	L3 -29 to +150	M:54.2±9.2 F:43.1±7.5	M: 40.6±9.6 F:37.5±10.0
Martin 2019	1157	64	63.6±11.4	Head & Neck n=234, lower GI n=475, upper GI n=171, respiratory tract n=295 [only patients with BMI ≥25 kg/m ² - overweight (65.7%) and obese]	I and II -17 III -22 IV -61	Canada	L3 -29 to +150	All patients M: 54.2±8.5 F:43.7±7.8 Overweight M:52.3±7.2 F:41.5 ± 6.6 Obese M:58.5 ± 9.5 F:46.9 ± 8.3	All patients M: 33.5±8.2 F:29.2±9.4 Overweight M:34.1±8.0 F:30.5±9.6 Obese M:32.1±8.8 F:26.9±8.8

SD; Standard deviation, CT: Computed tomography, L3: Lumbar 3, HU: Hounsfield Units, SMI: Skeletal Muscle Index. M: Male, F: Females, NR: Not reported. Other GI: digestive and accessory organs.

Table. 1.2 Studies investigating blood immune cells in relation to low muscle mass or muscle loss								
Author (year)	Study type	Cancer type and Stage	N (% of Men)	Age (years, mean±SD)	Muscle mass assessment / criteria	Low muscle mass prevalence (% of patients)	Blood Immune cells	Results [Statistical analysis]
Basile (2019)	Longitudinal, retrospective	Pancreas IV	94 (55%)	<70, n=45 and >70, n=49 ^e	CT L3, -29 to +150 HU Prado 2008, early loss: decrease of SMI >10% (after 3 months)	73%	NLR	NLR predictor for early loss of muscle mass, less than 10% or higher equal to 10% (1.31 OR, 95% CI 1.06-1.61, p=0.010). [Logistic regression]
							LMR	No associations observed with muscle loss [Logistic regression]
Rollins (2016)	Longitudinal, retrospective	Pancreatic ^a Locally advanced and metastatic	228 (54%)	Palliative chemo: 64.8 ± 8.7 / Non-chemo: 72.9 ± 11.1	CT L3, -29 to +150 HU Martin 2013	60.5%	NLR	No differences between sarcopenic and non sarcopenic [Student T-test]
							WBC: <8.5, 8.5-11 and >11 (x10 ⁹ /L)	No differences between sarcopenic and non sarcopenic [Student T-test]
He (2018)	Longitudinal, retrospective	Colon I to III	561 (61%)	59 (19-87) ^d	CT L3, -29 to +150 HU Low and high SMI groups based on median SMI values for men and women	49.9%	WBC	Positive correlation of SMI with WBC (r=0.135, p=0.001). [Pearson's correlation]
							Neutrophil counts	Positive correlation of the SMI with neutrophil (r= 0.097, p=0.022). [Pearson's correlation]
							Lymphocyte counts	Positive correlation of SMI with lymphocytes (r=0.142, p=0.001). [Pearson's correlation]
							Monocyte counts	Negative correlation of SMI with monocyte counts (r=-0.126 p=0.003). [Pearson's correlation]
Richards (2012)	Cross-sectional	Colorectal I to III	174 (55%)	<64 -n=51, 65-74 - n=63 and >75- n=35 ^e	CT L3, -29 to +150 HU Low tertile	M: 34% F:34%	NLR: <5 and >5	No differences of NLR (p=0.85) between SMI tertiles (low/med/high). [Chi-square]
							WBC count: <8.5, 8.5-11 and >11 (x10 ⁹ /L)	No relationship between SMI and WBC (p=0.51) [Chi-square]
Malietzis (Annals of Surg) (2016)	Cross-sectional	Colorectal I to IV	763 (60%)	<65, n=276, 65-74, n=265 and >75, n=222 ^e	CT L3, -29 to +150 HU Martin 2013	65%	NLR >3 and <3	Patients with NLR >3 had low SMI than those with NLR<3 (p=0.016) . [Fisher exact test]. High NLR predictor of low SMI [odds ratio (OR) = 1.78 (95% confidence interval [CI]: 1.29-2.45), P < 0.001]. Univariate analysis - high NLR: predictor of low SMI. A higher proportion of patients with myopenia (60%) had high NLR >3, compared to non-myopenic (43.1%). [Multivariate regression: age, ASA, UICC stage, albumin, NLR, and tumor site]

Malietzis (Tumor Biol) (2016)	Cross-sectional	Colorectal I to III	21 (62%)	70± 9.2	CT L3, -29 to +150 HU N/A	N/A	Monocyte-derived dendritic cell CD11c+, bone marrow-derived dendritic cell CD11c- / Additional markers: CD40, CD80, CD83, CD86, CCR7 and CD36	Monocyte-derived and bone-derived dendritic cells (CD40+) positively correlated with SMI (r = 0.45, p=0.04). No correlations with dendritic cells expressing CCR7, CD83 or CD36. [Pearson's correlation]
Malietzis (Annals Sur Oncol) (2016)	Longitudinal, prospective	Colorectal I to IV	856 (56%)	<65,n=45.4 , ≥65,n=54.6 ^e	CT L3, -29 to +150 HU 25th percentile	N/R	high NLR: >3	Patients with high NLR preoperatively had significantly lower SMI median values compared with patients with low NLR (p<0.001). [Mann Whitney U] Elevated preoperative NLR >3, had a significant effect on the LSMI trajectory over time. [Multilevel mixed-effect linear regression model]
Feliciano EMC (2017)	Longitudinal , retrospective	Colorectal I to III	2470 (51%)	63±12	CT L3, -29 to +150 HU Feliciano 2017	46%	NLR <3, 3 to <5 and >5 (Evaluated 24 before diagnosis)	Prediagnostic high NLR associated to risk for sarcopenia in a dose-response manner (Independently of race/ethnicity, cancer site, age, stage and BMI). High NLR increased the risk for sarcopenia, this was consistent across stage, age and sex (no evidence of interactions). [Logistic regression]
							LMR <2, 2- <3, 3-<4 and ≥4	High LMR- protective of sarcopenia in a dose dependent manner. [Logistic regression]
Caan (2017)	Longitudinal, retrospective	Colorectal I to III	3262 (50%)	62.6±11.4	CT L3, -29 to +150 HU Optimal stratification and lowest tertile	All: 42%, M: 45% F:39.5%	NLR ≤5 or ≥5	A higher proportion of sarcopenic patients (33.6%) had high NLR, compared to patients without sarcopenia (24%).
McSorley (2018)	Cross-sectional	Colorectal I to III	322 (54%)	<65,n=106, 65-74, n=127 and >74,n= 89 ^e	CT L3, -29 to +150 HU Prado 2007 or Martin 2013	Prado 2007: 49% Martin 2013: 47%	NLR	Correlations between NLR and patients with sarcopenia with Prado et al. (r=0.13, p=not reported) and Martin et al. (r=-0.011, p=not reported) criteria. [Spearman's correlation]
Xiao (2019)	Longitudinal , retrospective	Colorectal I to III	3262 (51%)	62.6 ± 11.4	CT L3,-29 to +150 Optimal stratification	42.4%	NLR <3, 3-5, ≥5	In a dose-respone manner, high NLR associated to risk for sarcopenia. NLR 3-5 (OR=1.48 (1.15, 1.92 – 95%CI) and NLR >5 (OR=2.07 (1.57, 2.74 – 95%CI)). [Univariate analysis / Multivariate: age at diagnosis (either categoric or continuous), sex, race/ethnicity, cancer stage, cancer site, prediagnostic weight change history, Charlson Comorbidity Score, smoking history, alcohol use, neutrophil lymphocyte ratio, albumin, and TAT tertiles at diagnosis]
Doland (2019)	Longitudinal, prospective	Colorectal TNM 0 t 3	650 (55%)	<65,n=234, 65-74, n=251 and >74, n=165 ^e	CT L3,-29 to +150 Martin 2013	All: 43.5%, M:45% Fs:55%	NLR ≤3 and >3	No relationship in NLR >3 in patients with low SMI (47.3%) or in high SMI (40%) [Chi square]
Black (2017)	Longitudinal, retrospective	Esophago-gastric and colorectal I to III	447 (57%)	<64, n=133, 65-74, n=148	CT L3, -29 to +150 HU Martin 2013	Esophagogastic: 21%	Neutrophil count <7.5 or >7.5 x10 ⁹ /L	Esopho-gastric patients and colorectal: High neutrophil counts (>7.5 x 10 ⁹ L) associated to sarcopenia versus to non sarcopenic patients (p<0.03) [Chi square]

				and >75, n=166 ^c		Colorectal: 24%	Lymphocyte counts <1 or >1 x10 ⁹ /L	No differences between sarcopenic and non sarcopenic. [Chi square]
							WBC: <8.5, 8.5-11 and >11 (x10 ⁹ /L)	Esopho-gastric patients: Higher WBC (8 to 11, >11 x 10 ⁹ L) associated to sarcopenic patients versus non sarcopenic (p=0.01). Colorectal patients: No differences in the WBC between sarcopenic and non sarcopenic. [Chi square]
Tan (2015)	Cross-sectional *	Esophago-gastric I to III	89 (75.3%)	65.8 ± 8.1	CT L3, -29 to +150 HU Low tertile	49%	NLR (as a continuous variable), assessed previous to chemotherapy exposure	No differences in NLR values between sarcopenic (2.69 ± 1.23) and non sarcopenic (2.68±2.33) patients. [Student T-test]
Lin (2018)	Cross-sectional	Stomach T stage:1 to 4	670 (75%)	65 years (58–73) ^d	CT L3, -29 to +150 HU Zhuang 2016	15.5%	NLR	High NLR with sarcopenia versus non-sarcopenic, median 3.86 and 2.5, respectively (p<0.001). High NLR >2.67 associated to higher prevalence of patients with sarcopenia (p<0.001) [Mann-Whitney U test, multivariate regression with 14 variables]
							Neutrophil counts	No differences between sarcopenic and non-sarcopenic [Mann-Whitney U test]
							Lymphocyte	Low lymphocytes in sarcopenic versus non sarcopenic, median 1.35 and 1.70, respectively (P<0.001) [Mann-Whitney U test]
							WBC	No differences between sarcopenic and non-sarcopenic [Mann-Whitney U test]
Zheng (2018)	Longitudinal, prospective	Stomach I to III	532 (75.8%)	61.1 ± 11.5	CT L3, -29 to +150 HU Optimal stratification	All: 17.1%, M:12.4% F:32%	Lymphocyte count (mm ³)	Low lymphocytes in patients with low SMI versus high SMI (p<0.001). Positive correlations between SMI and lymphocyte counts (r=0.272, p=N/R). [Student T-test and Spearman's correlation]
Narsale (2019)	Cross-sectional	GI ^b , nasopharyngeal and Respiratory (NSCLC) II to IV	n=11 (100%)	59.3±10	DXA N/A	N/A	CD4+ and CD8+ T cells (naïve, memory and regulatory)	CD4+ T regulatory cells correlated to LMI (r=-0.6, p=0.04). CD8+ T cells (expressing IL2+) negatively correlated to LMI (r=-0.83, p=0.02). No relationships of CD8+ T cells (naive and memory) with LMI. [Spearman's correlation]
Penafuerte (2016)	Cross-sectional	Head and neck, breast, upper GI, colorectal hepatobiliary, pancreas, lung, and prostate III to IV	122 (61.5%)	63.8 ± 12.7	CT L3, -29 to +150 HU Negative SMI z-scores from Fearon 2011	Sarcopenia: 65.6% Cachexia: 50.8% precachexia: 28.7% no-cachexia:20.5%	NLR	High NLR in cachectic ^c versus non-cachectic patients, 5.2 and 2.9, respectively (p=0.02). No differences were found between pre-cachectic ^c and cachectic or non-cachectic. [Student T-test]
							Neutrophils	Neutrophils negatively correlated with SMI z-score (r=-0.244, p=0.014). High neutrophils in cachectic versus non-cachectic 5.7X10 ⁹ L and 3.8X10 ⁹ L, respectively (p=0.007). No differences were found between pre-cachectic and cachectic or non-cachectic [Spearman's correlation and Student T-test]
Cho (2018)	Longitudinal, retrospective	Head and neck III to IV	221 (81.4%)	59 (18-94) ^d	CT L3, -29 to +150 HU <49 cm ² /m ² for men <31 cm ² /m ² for women	48%	NLR	Higher NLR values in patients with sarcopenia versus without sarcopenia, mean 3.5 and 2.8, respectively (p=0.053) [Mann-Whitney-U-test]

							Neutrophil count	Higher neutrophil counts in patients with sarcopenia versus to non-sarcopenic, mean 5.3 x10 ⁹ L and 4.6 x10 ⁹ L, respectively (p=0.023) [Mann-Whitney-U-test]
							WBC	Higher WBCs in patients with sarcopenia versus with those non-sarcopenic, mean 7.9 x10 ⁹ L and 7.1x10 ⁹ , respectively (p=0.023) [Mann-Whitney-U-test]
Hirasawa (2016)	Longitudinal, retrospective	Bladder cancer I to IV	136 (82.4%)	Sarcopenic: 71.6 ± 1 Non-Sarcopenic: 65.8 ± 1.2	CT L3, -29 to +150 HU Martin 2013	40%	NLR	At baseline, no differences between the patients with sarcopenia and non-sarcopenia. [Student T-test]
Kuroki (2014)	Cross-sectional *	Endometrial I to IV	122 (0%)	65.9 ± 10.4	CT L3, -29 to +150 HU Low tertile	50%	Lymphocyte count <1.5 and ≥1.5	No differences in lymphocyte count ≥1.5 same for sarcopenic and non-sarcopenic patients (p=0.83). [Fisher's exact test]
Fukushima (2015)	Longitudinal, retrospective *	Urothelial carcinoma Advanced, metastatic	88 (68%)	68 (39–91) ^d	L3, -29 to +150 HU Martin 2013	All:60%, Males:30% Females:71%	WBC	No differences between sarcopenic and non-sarcopenic [Wilcoxon rank sum test]
Kim EY (2016)	Cross-sectional	Respiratory (SCLC) Limited and extensive disease	186 (84%)	68.6 ± 9.4	CT L3, -29 to +150 HU Fearon 2011	69%	NLR	High NLR in sarcopenic versus non-sarcopenic patients, median 3 and 2.5, respectively (p=0.011). Association between L3 SMI and NLR (r=-0.145, p=0.048). [Mann-Whitney U test and Partial correlation analysis]
							Neutrophils	No differences or associations Mann-Whitney U test and Partial correlation analysis]
							Lymphocytes (x10 ⁹ /L)	Low lymphocytes in sarcopenic versus non-sarcopenic patients, median 1.69 and 2, respectively (p=0.002). Association between L3 SMI and lymphocyte counts (r=0.151, p=0.039) [Mann-Whitney U test and Partial correlation analysis]
							WBC	No differences or associations [Mann-Whitney U test and Partial correlation analysis]
Go (2015)	Cross-sectional	Respiratory (SCLC) Limited and extensive disease	117 (100%)	<65, n=45 and >65, n=72 ^e	CT T4 (pectoralis muscle), -29 to +100 HU Low tertile	25%	NLR <4 and ≥4	No differences between sarcopenic and non sarcopenic [Chi-square/Fisher's exact test]
Tsukioka T (2018)	Longitudinal, prospective	Respiratory (NSCLC) IIIA	69 (68%)	65.9 ± 9.8	CT L3, -29 to +150 HU Prado 2007	Alle:30.4%, Males:40.4% , Females:9%	NLR	Higher values of NLR in patients with sarcopenia compared to non-sarcopenic (p=0.013). [Mann-Whitney-U-test]
							Leucocyte count (μL)	Higher values of leukocytes in patients with sarcopenia compared to non-sarcopenic (p=0.05) [Mann-Whitney-U-test / Values reported as bloxplot]

*Inflammation was not investigated as main objective

^a Pancreatic: ductal adenocarcinoma and distal cholangiocarcinoma

^b Gastrointestinal (GI): esophageal, gastric, pancreas, small bowel, colorectal

^c Number of participants

^d Median (minimum – maximum)

^e Cachexia (58% of patients), criteria: >5% weight (past 6 months), or ongoing weight loss of >2% with a body mass index (BMI) <20 Kg/m², and/or sarcopenia // Precachexia (28.7%), criteria: no cachexia, C-reactive protein >5mg/L

N/R: Not reported, N/A: Not applicable. SCLC: small cell lung cancer. NSCL: Non-small cell lung cancer. CT: Computed tomography. L3: Lumbar 3. HU: Hounsfield Units. SMI: Skeletal muscle index (cm²/m²), LMI: lean mass index (kg/m²). M:Males. F:Females. NLR: Neutrophil lymphocyte ratio. LMR: Lymphocyte monocyte ratio.

Low muscle mass (sarcopenia) criteria by author:

1. Fearon et al. 2011: <55 cm²/m² in men and <39 cm²/m² in women.

2. Feliciano et al. 2017: SMI - 52 cm²/m² and <38 cm²/m² for normal or overweight men and women, respectively, and <54 cm²/m² and <47 cm²/m² for obese men and women, respectively.

3. Martin et al. 2013: BMI <25 kg/m², SMI of <43 cm²/m² for men and <41 for women. BMI >25 kg/m², SMI of <53 cm²/m² for men and <41 cm²/m² for women.

4. Prado et al. 2007: SMI for male patients of <52.4 cm²/m² and <38.5 cm²/m² for female patients.

5. Prado et al. 2008: SMI < 53 cm²/m² for men with body mass index (BMI) > 25, SMI < 43 cm²/m² for men with BMI < 25, SMI < 41 cm²/m² for women.

6. Zhuang et al. 2016: L3 SMI ≤40.8 cm²/m² for men and 34.9 cm²/m² for women.

Table 1.3 Molecules involved in cell adhesion during immune cell migration	
Endothelial cell	Immune cells
Selectin: P-selectin and E-selectin	Selectin: L-selectin and PSGL-1
Intracellular adhesion molecules: ICAM1, ICAM2 and VCAM1	Integrin: LFA-1 [subunit alpha-L (CD11a)/beta-2 (CD18)] Mac-1 [subunit alpha-M (CD11b)/ beta-2 (CD18)] CD11c/CD18 (subunit alpha-X/beta-2) VLA-4 [subunit alpha-4 (CD49d)/ beta-1 (CD29)]
	Others adhesion molecules: CD44

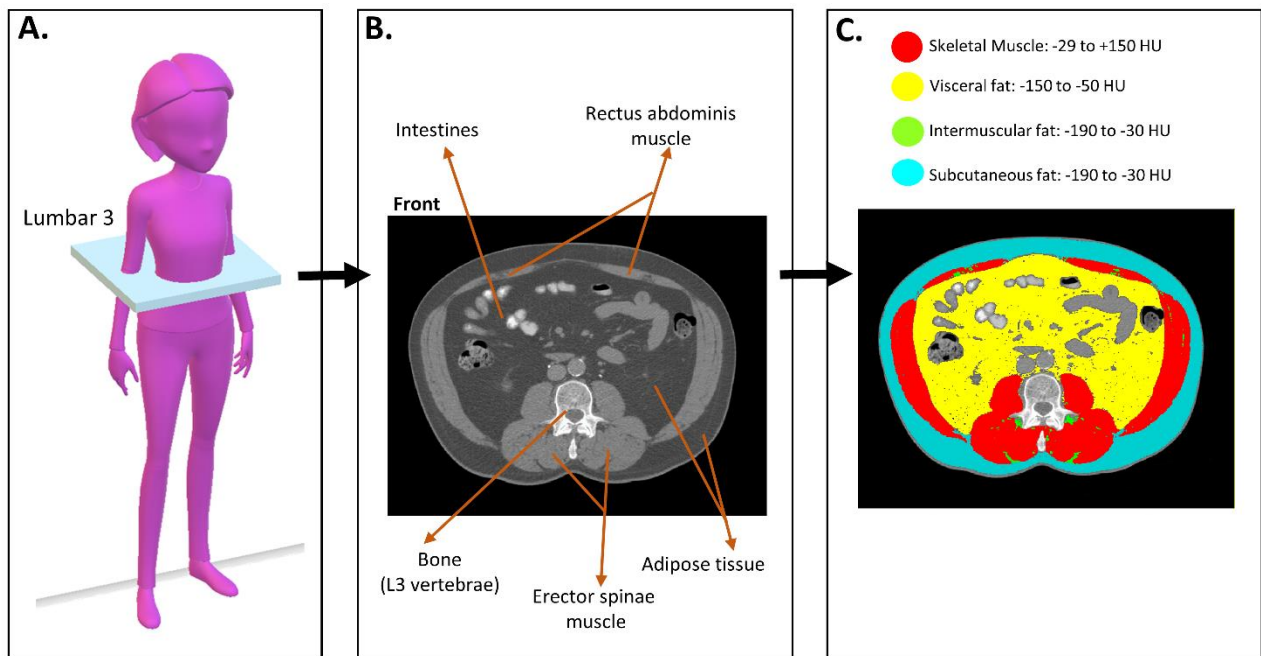


Figure 1.1 Radiological CT-derived body composition assessment at lumbar 3 (L3) vertebrae. A. CT image is obtained at the transverse plane at L3 level (blue squared area). B. Computer image reconstruction enables for visualization of tissues and organs distinguished by their differences in radiodensity as represented in the linear gray scale. C. Image analyzed for body composition using software imaging SliceOmatic®, skeletal muscle (in red) has higher density than adipose tissue (yellow, green and turquoise). Body compartments are identified according to the Hounsfield Unit scale (HU). Quantification of the anatomical regions from CT images consists of a map of pixels, corresponding to a HU value and the total volume represented by the sum of all pixels.

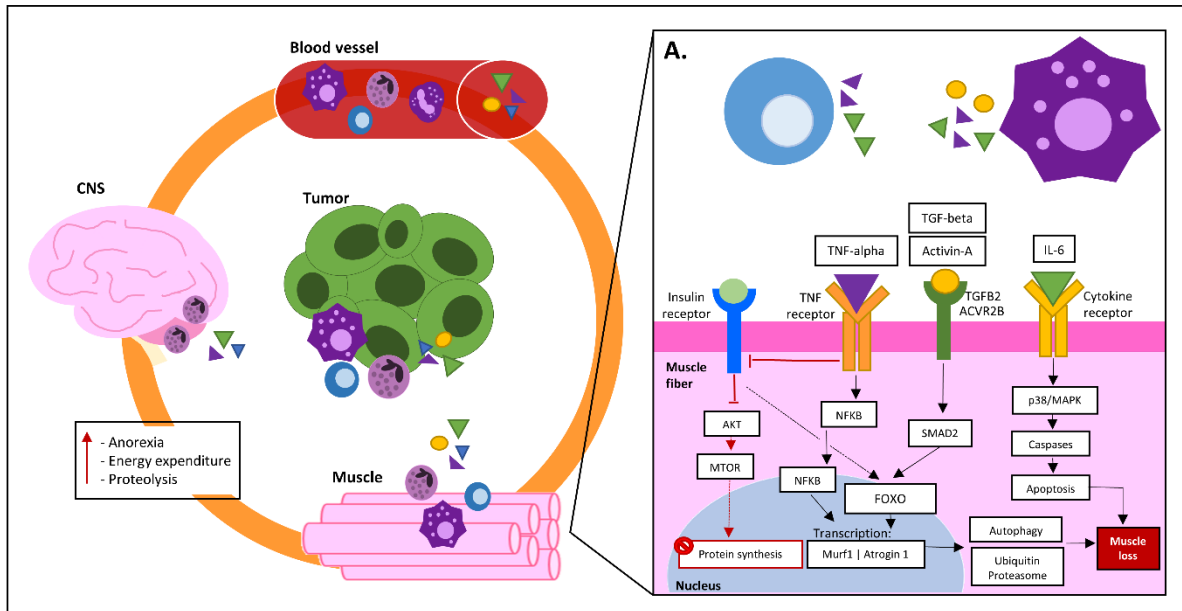


Figure 1.2 Contribution of immune cells to cancer-associated muscle wasting

During cancer, immune cells are mobilized to different tissues. In the CNS, neutrophils and IL-1beta promote anorexia and increased energy expenditure, a reduced food intake leads to protein mobilization in muscle. Hypothalamic infiltration of neutrophils promotes induction of muscle degradation pathways. Pro-inflammatory mediators secreted by infiltrated immune cells, in addition to tumor micro-environment, contribute to the activation of catabolic routes in muscle. Signaling of TNF-alpha receptor interferes with insulin receptor signaling blocking the AKT/MTOR pathway and leading to reduced protein synthesis, and promoting the activity of transcription factors from FOXO family. Activation of NFKB and FOXO promote the transcription of pro-catabolic genes which activate autophagy and ubiquitin proteasome. TGF-beta family promotes the activity of FOXO family via SMAD2. Signaling of the IL-6 receptors promotes caspase activity, leading to muscle cell apoptosis. Collectively and independently these pathways lead to loss of muscle mass.

[Lymphocytes represented by blue circles. Monocytes/Phagocytes represented by dark purple figures. Granulocytes represented by light purple circle. Pro-inflammatory cytokines represented by yellow circle and triangles]

Chapter 2: Research plan

2.1 Rationale

In the oncological setting, low muscle mass and muscle wasting are concerning issues as they are associated with poor outcomes and reduced survival (Kazemi-Bajestani et al., 2016; J R Lieffers et al., 2012; Jessica R Lieffers et al., 2009; Martin et al., 2013; Prado et al., 2008a). Computed tomography (CT) is an opportunistic tool used for body composition assessment with extreme precision that has been extensively validated in cancer patients (J R Lieffers et al., 2012; Martin et al., 2013; Mitsiopoulos et al., 1998; Mourtzakis et al., 2008; Prado et al., 2008b; Xiao et al., 2018). CT has enabled the identification of individuals with low muscle mass or cancer-associated muscle loss. In addition, intraoperative collection of muscle biopsies is emerging in cancer research as a tool to explore and understand biological characteristics in humans with low muscle mass and muscle wasting. Biopsy collection of *rectus abdominis*, a poorly characterized muscle group that is accessible during abdominal surgical procedures, is emerging in cancer research. Therefore, a biological characterization of *rectus abdominis* muscle is essential to evaluate potential sources of variation contributing to result interpretation, as well as reference ranges, to provide context and guidance for current and future research.

Immune cells are essential participants of the inflammatory response (Grivennikov et al., 2010; Madaro et al., 2014; Tidball, 2017). During cancer, activation and mobilization of immune cells is promoted by the tumour micro-environment (Baracos et al., 2018; Grivennikov et al., 2010; Madaro et al., 2014; Odobasic et al., 2016). Importantly, inflammation is recognized as a noted contributor to disease-associated muscle loss (Baracos et al., 2018; Fearon et al., 2011). Current evidence evaluating circulating immune cells as markers of systemic inflammation in cancer patients, has reported an association between the number of circulating granulocytes/phagocytes and lymphocytes with low muscle mass and muscle wasting during the cancer trajectory (Basile et al., 2019; Black et al., 2017; He et al., 2018; Kim et al., 2016; Lin et al., 2018; Oh et al., 2018).

Immune cell migration into muscle is suspected to be a relevant event occurring in the host as a response to cancer and its treatments. Chemotherapy, as an additional source of inflammation, induces perturbations in host immunity, and has direct detrimental effects on muscle tissue that promote muscle loss (Barreto et al., 2017; Daly et al., 2018; Jung et al., 2015; Rollins et al., 2016; Schiessel et al., 2018; Sjøblom et al., 2015; Xue et al., 2009). Few studies have investigated the

presence of immune cells in muscle of humans and in preclinical models with cancer (Berardi et al., 2008; Zampieri et al., 2009), and a link between immune cell migration and muscle loss during cancer has been suggested by the exploration of cancer-associated tissue wasting in experimental models of cancer (Burfeind et al., 2018, 2019a; Calore et al., 2018; Cannon et al., 2007; Henriques et al., 2018; Ruud et al., 2013; Zhang, Liu, Ding, Miao, et al., 2017). Our knowledge of immune cell migratory events occurring in muscle during malignancy and chemotherapy is limited; therefore, a characterization and quantification of immune cell populations within muscle is the first step to further investigate their relationship with low muscle mass and possible immune mechanisms of cancer-associated muscle wasting.

2.2 Research objectives and hypotheses

2.2.1 Clinical and biological characterization of skeletal muscle biopsies of surgical cancer patients (Chapter 3)

Objective

To provide a characterization of *rectus abdominis* muscle biopsies obtained from a well-powered sample size (n=190) to evaluate sources of variations such as risk of sampling bias and sexual dimorphisms. Evaluation of *rectus abdominis* muscle for features of interest will be placed within context of what is known based on a state-of-the-science review of the literature that has muscle biopsy material from cancer patients.

2.2.2 Immunohistochemical phenotyping of T cells and phagocytes in muscle of cancer patients: association with radiologically-defined muscle mass and gene expression (Chapter 4)

Hypothesis

It is hypothesized that cancer patients with lower muscle mass have more granulocytes/ phagocytes (CD11b, CD15 and CD14) and T cells (CD3, CD4 and CD8) within their muscle tissue.

Objective

To investigate the relationship between immune cells from the innate (granulocytes/ phagocytes: CD11b, CD15 and CD14) and adaptive (T cells: CD3, CD4 and CD8) immune response with muscle mass measures in cancer patients.

2.2.3 Immune cell migratory signaling in skeletal muscle in response to a tumor and irinotecan/5-fluorouracil chemotherapy in a ward colorectal cancer rodent model (Chapter 5)

Hypothesis

It is hypothesized that immune cell migration is an event occurring in skeletal muscle in response to the presence of a tumor that is further altered by chemotherapy exposure, revealed by gene transcriptional events generated from rat muscle under conditions of healthy, tumor-bearing (ward colorectal) and tumor-bearing irinotecan/5-fluorouracil exposure.

Objective 1

To investigate if genes transcribing molecules involved in immune cell migration activation, signaling and extravasation, such as Toll-like receptors, chemokines and cell adhesion molecules, are differentially expressed in tumor-bearing rats when compared to healthy rodents.

Objective 2

To investigate if previously investigated genes (objective 1), transcribing Toll-like receptors, chemokines and cell adhesion molecules, are furthered altered by chemotherapy exposure in tumor-bearing rats.

Secondary hypothesis

It is hypothesized that there are differentially expressed genes that encode molecules exclusively or highly expressed in lymphocytes and neutrophils that suggest their presence within muscle in response to tumor burden and following chemotherapy exposure.

Secondary objective

To evaluate global gene expression profiles using *Ingenuity Pathway Analysis*® (IPA) for evidence of differentially expressed genes related to the presence of neutrophils and lymphocytes under conditions of (a) tumor-bearing *versus* non-tumor bearing, and (b) in tumor-bearing with and without chemotherapy exposure.

Chapter 3: Clinical and biological characterization of skeletal muscle tissue biopsies of surgical cancer patients

3.1 Introduction

Several radiologically-defined features of skeletal muscle have been associated with clinical outcomes in patients with cancer. Reduced muscle mass (i.e. sarcopenia), loss of muscle mass over time and reduced muscle radiodensity, are related to mortality, shorter progression – free survival, chemotherapy toxicity and complications of cancer surgery (Kazemi-Bajestani et al., 2016; Lieffers et al., 2012; Martin et al., 2013; Vinet et al., 2011). In light of the associations between muscle and outcomes, researchers are increasingly investigating the pathophysiology of muscle abnormalities (Miyamoto et al., 2016; Mueller et al., 2016; Stretch et al., 2018) and attempting to relate the findings to the much broader base of knowledge that exists from research in animal models. Muscle may be obtained from cancer patients by percutaneous biopsy as well as intraoperatively during cancer surgery. Clinical data aligned with the biopsy provides a comprehensive approach to understand cancer cachexia from the vantage point of muscle wasting. Evaluation of human muscle contributes significantly to the understanding of molecular mechanisms in a variety of primary pathologies of skeletal muscle (Joyce et al., 2012; Lacomis, 2004).

Biopsy and tissue manipulation techniques can induce changes in the muscle that alter enzyme activity, metabolite concentrations and protein metabolism (Chatterjee, 2014; Hers et al., 1966; Varadhan et al., 2018). Also, patient characteristics such as age, sex, cancer type, comorbidities, medications (including chemotherapy) taken at the time of biopsy collection are known factors that influence muscle metabolism (Batchelor et al., 1997; Edwards et al., 1975; Jackson et al., 2014; Salvatore et al., 2014; Stephens et al., 2012). These methodological issues pose limitations in the reliability, interpretation and comparability of the findings on muscle biopsies in patients with cancer. Therefore our first aim was to conduct a state-of-the-science review of the literature on muscle biopsy in cancer patients. This type of review retains many features of a systematic review except that studies are not excluded on the basis of a quality assessment, and thus presents a broader search of the literature. An associated aim was to provide recommendations of components to consider when evaluating and reporting results of muscle biopsies from cancer patients.

The second aim of this study was to evaluate sources of variation in the muscle biopsy material to better understand the risk of sampling bias, to determine variance and effect size to enable sample size calculations, and to determine the possible consequences of sexual dimorphism and age as confounders using a relatively well-powered sample (n=190). Our research group has experience in the radiological characterization of muscle (Martin et al., 2013; Mourtzakis et al., 2008; Xiao et al., 2018) and skeletal muscle morphology, cell biology and biochemistry (Johns et al., 2017; Narasimhan et al., 2017, 2018; Stretch et al., 2018). Our collaborative effort with hepatopancreatobiliary cancer surgeons has enabled muscle biobanking and exploration of muscle biology within large populations. We have published studies on muscle expression of mRNA, microRNA, and alternative splice variants (Narasimhan et al., 2017, 2018; Stretch et al., 2013), alongside specific and precise measures of muscle mass, radiodensity and muscle loss.

3.2 Materials and methods

3.2.1 Literature review

A state-of-the-science review (Grant et al., 2009) is a broad search of the literature that includes all studies in a particular area. Our review protocol follows the Preferred Reporting Items for Systematic Reviews and Meta-Analyses (PRISMA) (Liberati et al., 2009) guidelines to reduce bias (Fig. 3.1). Articles indexed in SCOPUS from January 1, 1900 to August 16, 2018 were queried to capture reports on skeletal muscle biopsies from cancer patients. Search terms included adult humans, malignant disease [(cancer) OR (neoplasm) OR (carcinoma) OR (tumor) OR (malignant) OR (metastasis)], skeletal muscle [(skeletal muscle) OR (muscle mass) OR (lean body mass) OR (rectus abdominis) OR (cachexia) OR terms for other specific muscle] and biopsy. Review articles and studies on experimental models, laboratory animals, non-cancer populations or those not employing muscle biopsies were excluded. Bibliographies of identified articles were hand searched to find additional relevant publications. There were no exclusion criteria regarding number of patients and type of study (retrospective, prospective or cross-sectional). Data were extracted from the result sections, tables and figures of each article. As we did not aggregate the data, no additional data was contributed from the investigators.

Two reviewers independently assessed each of the included studies, disagreements were resolved by consensus. A score for study quality was given using assessment tools provided by the National Heart, Lung and Blood Institute (NIH -U.S. Department of Health & Human Services) for cross-sectional, cohort, case-control, randomized control trials and before-after studies. The

Newcastle-Ottawa scale modified for cross-sectional studies (Modesti et al., 2016) was used to give a bias score based on the a) representativeness, b) size and c) non-respondent report.

3.2.2 Rectus abdominis biological characterization

3.2.2.1 Subjects and acquisition of muscle samples

The study was approved by the Health Research Ethics Board of Alberta-Cancer. Patients undergoing elective abdominal surgery were consecutively approached to participate in tumor and tissue banking at a hepatopancreatobiliary surgical service in Alberta, Canada. Three percent of approached patients declined participation. Patients provided written informed consent for muscle biopsy and tissue banking. Release of n=190 samples from the bank for analysis, as well as patient information (demographic, clinical and operative data) from medical records, was performed under the auspices of Protocol ETH-21709: *The Molecular Profile of Cancer Cachexia*. Patients consent freely to muscle biopsy from the site of incision at the time of surgery, as this entails little if any incremental discomfort or risk, as the surgery is inherently invasive. All patients were either diagnosed as having cancer or were suspected of having cancer due to their symptoms and radiological assessments such as CT imaging.

The study cohort and conditions for acquisition of muscle samples have been described previously (Stretch et al., 2013). Briefly, *rectus abdominis* (0.5 – 3 g) samples were collected during open abdominal surgery scheduled as part of their clinical care. Upper abdominal transverse incision was performed, muscle biopsy was obtained at opening by sharp dissection, without the use of electrocautery.

3.2.2.2 Computed tomography image analysis

Digital axial CT scans performed pre-operatively and used to plan surgery were used to quantify skeletal muscle cross-sectional area (CSA, cm²) as in our prior work (Mourtzakis et al., 2008; Prado et al., 2008). Measures with CT have excellent precision (precision error values of ~1.5%) (Mitsiopoulos et al., 1998). Briefly, images at the 3rd lumbar vertebra (L3) were analyzed for total L3-CSA within a specified Hounsfield Unit (HU) range (-29 to +150) using Slice-O-Matic software (v.4.3, Tomovision, Magog, Canada). Muscle area was normalized for stature and reported as skeletal muscle index (SMI, cm²/m²). Mean radiodensity (HU) was also reported. Adipose tissue CSA at L3 was calculated in a HU range of -150 to -50 and -190 to -30, for visceral and subcutaneous adipose tissue, respectively (Mitsiopoulos et al., 1998). The distribution of SMI of the patients providing biopsy for this study were compared to a previously

described large cohort of oncology patients (n=1,473) to confirm that the population sampled is representative of muscle mass distribution and mean values for our population (Fig. 3.2). Sarcopenia was classified according to previously reported (Caan et al., 2017; Xiao et al., 2018) sex- and body mass index (BMI)- specific criteria: for BMI <30 kg/m² - SMI <52.3 cm²/m² for men and <38.6 cm²/ m² for women, and BMI ≥30 kg/ m²- SMI <54.3 cm²/m² for men and <46.6 cm²/m² for women.

Processing of Muscle Biopsy

From each biopsy, several analysis were performed, each with specific preparation procedures. In the operating room, visible adipose and connective tissue was removed from the biopsy and it was cut into two pieces; one piece to be used for analysis of gene expression, and myosin heavy chain by electrophoresis was immediately frozen in liquid nitrogen in the operating room prior to being transported to the lab for storage in liquid nitrogen until analysis. The other piece of the biopsy to be used for microscopy was transported on ice to the laboratory within 20 to 30 minutes. For morphological preservation, isopentane (2-Methylbutane, C₅H₁₂) was cooled at -160 °C in liquid nitrogen for 20 minutes or until the appearance of a thick frozen layer at the bottom of the container. A piece of muscle was oriented for transverse section and delicately placed on aluminum foil. Tissue was submerged in isopentane for 20 seconds, aluminum foil was turned upside down to allow full exposure of the muscle section. After submersion, tissue was wrapped and left in liquid nitrogen for 5 minutes. Information about surgery date, time, and sample reception was documented.

3.2.2.3 Immunofluorescence: Fiber types, laminin/dystrophin and nuclear stain

Muscle serial sections (10µm) were cryosectioned (cryostat Leica model CM300) transversely at -22°C and stored at -80°C until staining. Myosin Heavy Chain (MyHC) I, IID and IIA were determined as previously described (Gallo et al., 2006). Primary and secondary antibodies are described in Appendix A. After the secondary antibody application, a nuclear stain (4',6-diamidino-2-phenylindole, DAPI) was added for 2 minutes and washed. Slides (Apex™ superior adhesive slides, Leica biosystems) were mounted, covered and let dry for twelve hours. Images for tissue sections were acquired using a 20X/0.85 oil lens with a spinning disk confocal microscope (Quorum Wave FX Spinning Disc Confocal System – Quorum technologies). Individual Z-stacked images were assembled to create a composite image of a whole tissue cross-section. Tissue images were capture and analyzed with Volocity 6.3 software [PerkinElmer,

Waltham, MA, USA]. A software script was established to identify muscle fibres types (I, I/IIA, IIA, IIA/D and D) using intensity of the MyHC stains and quantified automatically by the software. Mean muscle fiber area (μm^2) was calculated by the detection of membrane (laminin/dystrophin antibody) fluorescence of muscle fibers in a cross-section. Percentage of fibers with centralized nuclei was manually assessed by selecting muscle fibers with mispositioned nuclei (clearly separated from sarcolemma, equidistant or not) in a tissue cross-section.

3.2.2.4 *Electrophoretic Analysis of Myosin heavy chain (MyHC) Isoform Content*

Semi-quantitative MyHC isoform analyses were completed on frozen rectus abdominis using Western blotting as previously described (Gallo et al., 2006; Martins et al., 2012; Putman et al., 2007). All three of the adult MyHC isoforms (I, IIA and IID) were clearly visible on all gels and reliably quantified in at least triplicate by integrated densitometry (Syngene ChemiGenius, GeneTools, Syngene).

3.2.2.5 *Triglyceride (TG) content analysis*

A piece of biopsy [50 mg] was ground using a frozen pestle and mortar without letting the tissue thaw. Ground tissue was homogenized in a 1.6 ml calcium chloride [CaCl_2 ; 0.025%] solution with glass beads [0.5 mm diameter; FastPrep [®]-24, MP Biomedicals, Santa Ana, CA, USA] in 20 sec intervals for 1 min. Samples were placed on ice for 15 sec between each homogenization interval. A modified Folch method was used to extract lipids using chloroform/methanol (2:1, vol/vol) as previously described (Murphy et al., 2010; Pratt et al., 2001). The TG fraction was isolated on G-plates and the TG band was identified and scraped. An internal standard C15:0 [10.2 mg/100 ml hexane] was added, followed by saponification and methylation. Samples were analyzed using gas liquid chromatography (flame-ionisation detector) on a Varian 3900 [Varian Instruments, Georgetown, ON, Canada]. Quantity of fatty acids within the TG fraction was calculated by comparison with the known concentration of the internal standard and sum of all fatty acids was reported as total TG.

3.2.2.6 *Gene expression: Microarray*

Microarray was conducted as previously described (Stretch et al., 2013). The data have been deposited in the U.S. National Center for Biotechnology Information (NCBI) Gene Expression Omnibus25 and are accessible through GEO series accession number GSE41726.

3.2.2.7 Statistical analysis

Statistical analyses were conducted in IBM® SPSS ® software, version 24. A test for normal distribution was applied to the continuous variables. Descriptive statistics were reported as mean \pm standard deviation. Comparisons between groups were conducted using independent t-test or Mann-Whitney U according to the variable normal distribution and chi-square test for categorical variables. Statistical significance was considered at p values less than 0.05 (two-sided).

3.3 Results

3.3.1 Literature review

A total of 59 articles reporting analysis of skeletal muscle in cancer populations were reviewed. The Preferred Reporting Items for Systematic Reviews and Meta-Analyses (PRISMA) (Liberati et al., 2009) flow diagram of our search strategy is shown in Fig. 3.1.

Study Quality and Design

Table 3.1 includes all of the extracted data as well as scores for sampling bias (Newcastle-Ottawa scale) and study quality assessments (NIH). In general the study quality rated as low for the majority of studies (Table 3.1). Applying the Newcastle-Ottawa criteria for sampling bias revealed the majority of studies had a high risk of sampling bias with 58% of studies lacking representativeness, 96% lacking sample size justification and no study mentioned non-respondent rate (% of population approached who declined participation). Muscles biopsied were rectus abdominis (n=40), quadriceps (n=20), tibialis anterior (n=1), gastrocnemius (n=1), pectoralis major (n=1), sternocleidomastoid (n=1), serratus anterior (n=1), diaphragm (n=1) and latissimus dorsi (n=1), and in seven studies more than one muscle was collected. Four studies reported evaluation of rectus abdominis from cancer patients and quadriceps for non-cancer controls, and four studies reported biopsied muscle from 2 or 3 different muscles.

Gastrointestinal cancers were the most common diagnoses; 31/59 studies included patients of exclusively one cancer type: colorectal, pancreatic, gastric, breast or prostate. Inclusion of patients with two or more cancer types was reported in 27/59 studies. Cancer stage or presence of metastasis was described in 39/59 studies. Combined data from two or more cancer stages was reported in 38/59 studies.

The majority of studies were cross-sectional (Appendix B). For investigation of patients with cancer cachexia, weight loss was considered as the main reference for classification. In 36

studies weight loss was graded with varying cut points (e.g. 5%, 10% or 15%). Time frame of weight loss was not specified in 16 of these studies (Table 3.1). Percentage weight loss ranged from 5 to 22% in weight-losing groups (Appendix B). Measures of body composition were included in 25 studies, however these measures were used to assess muscle mass or rate of muscle wasting over time in only 7 studies (Appendix B).

Total sample size in each study was generally limited (mean, $n=26$; median $n=18$; range 1 – 134). Seventy-six percent of studies included $n \leq 30$ cancer patients; 48/59 studies included a non-cancer control group, sample size ranging from $n=3$ to 41. Fifty-two studies included men and women, 5 studies only men, 1 study only women and 2 studies did not specify the sex of their patients. For those studies including both sexes, 50 had an imbalance between treatment groups in the % of male and female patients, and only 3 studies matched the number of male and female participants. When reporting the results, almost all of the studies (98%) presented aggregate data from men and women.

When a non-cancer control group was employed in the study, the majority of studies included control groups that went under surgical procedures (i.e. Cholelithiasis and cholecystitis, ovarian cyst, inguinal hernia, laparocoele, abdominal aorta aneurysm, hemangioma of liver, gallstones, chronic pancreatitis), or healthy volunteers (Appendix B). No study defined the criteria used to select healthy volunteers. Table 3.1 highlights the features of the cancer groups compared to control groups. More than 54% of the studies included cancer patients with an average age of ≥ 65 years, and for studies involving non-cancer patients as controls, 26% included patients with an average age of ≥ 65 years.

Most (33/59) reports failed to mention comorbidities as a component of their exclusion criteria or patient's demographics. Commonly excluded diagnoses were: diabetes, chronic obstructive pulmonary disease (COPD), liver failure, renal failure, chronic hepatitis, autoimmune diseases and inflammatory bowel disease. Use of medications (e.g. corticosteroids, anabolic/catabolic agents and/or beta blockers) was described in 17 studies as clinical characteristics or exclusion criteria. Prior exposure to antineoplastic drugs was reported in 14/59 studies. Inclusion of patients naïve to chemotherapy or radiotherapy was stated in 6/59 studies, two studies acknowledged the inclusion of some patients with one or fewer cycles of chemotherapy that concluded 4 weeks previous to biopsy collection.

Technical Considerations

Biobanking protocol and tissue manipulation

Abdominal and thoracic muscle biopsies were collected during a surgical procedure in 43 studies, with collection at the start of surgery being explicitly stated in 31 studies (Table 2). Presence or absence of tissue cauterization was specified in 29/43 studies. Percutaneous procedure (needle biopsy) was the main method for collection of muscles of the lower limb (n=19 studies), open muscle biopsy technique was reported in 1 study and in 1 study the collection method was unspecified. For both surgical and percutaneous biopsies, removal of blood traces and/or fat/fibrotic tissue after collection was mentioned in 7/59 studies (Table 3.2).

Information provided on biopsy manipulation was limited and mainly focused on freezing and storage procedures. In 43/59 studies, immediate freezing in liquid nitrogen was reported. In only one study was it explicitly stated that freezing was done in the operating room versus a laboratory facility. The most common temperatures for sample storage were between -70 and -80°C; storage details were not mentioned in 11/59 studies. Details on time between biopsy and transportation to laboratory facilities and waiting periods were not reported in any study.

3.3.2 Rectus abdominis biological characterization

Study population

Demographics and clinical data from 190 patients are provided in Table 3.1. Nearly all patients (97%) who were approached consented to intraoperative biopsy, as this entails little, if any, incremental discomfort as the surgery is inherently invasive. Therefore there was no selection bias inherent in the cohort. Typical of hepato-pancreatic-biliary case load, 88% of cancers were gastrointestinal, with the largest proportions being colorectal and pancreatic cancer. Surgical procedures included, hepatectomy, liver metastasectomy, pancreatectomy, Whipple procedure, bile duct resection, cholecystectomy, colectomy, and gastrectomy. Metastasis was present in 50% of the patients. Most of the patients were naive to chemotherapeutic agents, 23% had exposure to chemotherapy within 2 to 4 weeks prior to the surgical procedure. The majority of patients were classified as overweight. Diabetes type II and hypertension were the most common comorbidities. Most commonly used medications reported among the population were analgesics, anti-inflammatory, statins, glucose-lowering drugs, anti-hypertensives, anti-reflux and thyroid hormone replacement (Table 3.4).

CT image analysis

Muscle L3-CSA, SMI and muscle radiodensity of rectus abdominis and total muscle are shown in Table 3.5. Sarcopenia was present in 56% of the patients, 60% (n=97) of males and 49% (n=42) of females. Weight history was available for 45 patients. Fifty six percent of patients experienced weight loss ($11\pm 12\%$ in 5 ± 12 months), and 60% of weight losing patients were sarcopenic. Out of 44% (n=20) weight stable patients, 70% were sarcopenic.

Sex differences

In light of the fact that most of the papers in the literature review included samples of mixed sex of varying proportions, we examined all of the biopsy features for sex differences. Sexual dimorphism was prominent in **L3-CSA** total lumbar muscle and RA, muscle radiodensity of RA and total muscle (Table 3.5), mean fibre cross-sectional area (Table 3.6), and in expression of genes associated with muscle growth, apoptosis and inflammation (Table 3.7). Proportions of fiber types using both quantification methods, MyHC isoforms and individual fiber types, were not different between male and female patients (Table 3.6).

For centralized nuclei assessment the mean % of fibers with centralized nuclei was $12\pm 9\%$ (4 to 36%) and $10\pm 8\%$ (3 to 27%) in males and females, respectively. No differences were found between men and women ($p=0.39$) with a combined mean value of $11\pm 8\%$.

Rectus abdominis: proportion of fiber types and muscle fiber area

Electrophoretic Analysis of Myosin heavy chain (MyHC) Isoforms confirmed MyHC I and MyCH IIA to be present at similar proportions, while MyHC IID was less abundant (Table 3.6A). MyHC type IIA was the most abundant isotype, followed by MyHC type I and IID (Table 3.6B). In addition, 15.5% of the fibers were identified as hybrids, which is the sum of MyHC type I/IIA and IIA/D. For individual fiber types, type I fibers comprised the greatest proportion (46.4%) followed by fiber type IIA (36.1%) and hybrid type IIA/D (15%). Presence of fiber type IID, as well as hybrid type I/IIA, was minimal (1.8 and 0.7%). Mean muscle fiber area (μm^2) was calculated by the detection of membrane (laminin/dystrophin antibody) fluorescence on 1069 ± 771 muscle fibers per biopsy (Table 3.6C). Mean muscle fiber area was determined in total and per fiber type, which includes collective results of MyHC isoforms and individual fiber types (Table 3.6C). Mean fiber area of MyHC type I was smaller than MyHC type IIA and IID. For individual fiber types, type I and type I/IIA were smaller compared to type IIA, IIA/D and IID. Type IID had the largest mean fiber area compared to the other individual fiber types.

Age effects

Comparison of older (74±4 years, n=13) and younger (50±6 years, n=13) males revealed no differences between groups with respect to mean muscle fiber area (total, individual fiber types or MyHC isoforms), % of individual fiber types or % of MyHC isoforms. Age effect was evaluated in males (n=26) by comparing mean values of a younger group versus an older group. No significant differences were found in relation to % of MyHC isoform content.

Skeletal muscle gene expression for genes associated with cancer cachexia

Differences in genes encoding proteins commonly explored in cancer-muscle wasting are summarized in table 3.7 (Appendix C). Atrophy, autophagy, apoptosis, muscle growth, and inflammation genes were selected based on reviewed literature on muscle atrophy in cancer [(M Bossola et al., 2001; Maurizio Bossola et al., 2003; Higuchi et al., 2000; JAGOE et al., 2002; Johns et al., 2017; Khal et al., 2005; Noguchi et al., 1998; Stephens et al., 2010; A. Williams et al., 1999)]. Sexual dimorphism exists in pathways related to skeletal muscle anabolism and catabolism illustrating the need for caution when generalizing results from only one sex or discussing results from a mixed group of cancer patients.

3.4 Discussion

There is a perceived need to understand the human biology of cancer-associated muscle atrophy and to frame it in the context of our larger understanding of experimental findings (Argilés et al., 2014; Baracos et al., 2018; Egerman et al., 2014; Johns et al., 2017; Mueller et al., 2016). The emergent literature on human muscle biopsies has been generated with that intent, but has a number of substantial limitations within the study design as well as procedures for collection and preparation of the biopsy material. At the same time there is substantial opportunity for collaboration between cancer surgeons and researchers to obtain intraoperative biopsies with a high rate of patient consent and the additional capability to describe the muscles of these patients with precise radiological metrics. Agreement to a set of standardized procedures and reporting, will enhance the consistency, reliability and comparability of future research in this area. Evaluation of human rectus abdominis muscle presents the expected variation in several measures that may be of interest for emerging studies in this area.

Study Quality and Design

The quality of the studies reporting on biopsy material to characterize varying features of muscle biology was uniformly low. Quality assessment tools revealed several inconsistencies in sample selection strategies, study design, data collection and analysis in the existing literature. Bias assessment of sample selection exposed a clear absence of sample representativeness in 59% of studies and lack of sample size justification in 96% of studies. In 75% of the studies reviewed, samples from a relatively small number of participants ($n \leq 30$) were evaluated without accounting for age or sex variation.

The majority of published studies use weight loss (versus weight stability) to define cachexia. This approach is limited by not accounting for the characteristics of muscle (muscle mass or change in muscle over time), which are the clinically relevant features related to cancer outcomes. Indeed weight stable patients may well be losing muscle over time (Roeland et al., 2017) and they can also be profoundly sarcopenic (Martin et al., 2013; Prado et al., 2008). Weight loss was the most commonly used criteria for cancer cachexia assessment, however, application of this measure alone poses major concerns in misclassification and unintended exclusion of cachectic patients. Many studies were published prior to the widespread use of CT images to quantify muscle, as well as prior to the publication of the international cachexia consensus, which defines muscle mass as a diagnostic criterion for cachexia (Acharyya et al., 2005; Agustsson et al., 2011; Banduseela et al., 2007; M Bossola et al., 2001; Maurizio Bossola et al., 2006, 2003; Busquets et al., 2007; Eley et al., 2008; Higuchi et al., 2000; JAGOE et al., 2002; Khal et al., 2005; Lundholm et al., 1976; Noguchi et al., 1998; Rhoads et al., 2010; Schmitt et al., 2007; Shaw et al., 1991; I. J. Smith et al., 2011; Stephens et al., 2010; Weber et al., 2007, 2009; A. Williams et al., 1999; S. Zampieri, Doria, et al., 2010; S. Zampieri, Valente, et al., 2010; Sandra Zampieri et al., 2009; Zeiderman et al., 1991). The premise of using weight loss when muscle is being evaluated is erroneous. Muscle wasting can be experienced by patients with less than 5% weight loss (Roeland et al., 2017). Also, the arbitrary selection of weight loss percentage and timeframe in different studies complicates the comparison of results between studies. In the cohort of patients we evaluated, 70% of weight stable patients and 60% of weight-losing patients were sarcopenic. Therefore, assessment of muscle mass is essential, this can be easily achieved through the secondary analysis of CT images used to plan the surgery (Caan et al., 2017; Mourtzakis et al., 2008; Xiao et al., 2018).

Some authors reported mortality-defined cutpoints to define sarcopenia according to age and sex of a reference population (Martin et al., 2015; Prado et al., 2008) and these have been secondarily used by other authors (Rier et al., 2016). Caution should be used in applying these cutpoints to define sarcopenia in patients undergoing muscle biopsy, these may not necessarily reflect the population from which biopsies are evaluated (Rier et al., 2016). Here we suggest to use CT to quantify muscle features for the overall population from which the biopsy sampling is done. In this way, patients providing biopsy for our study are clearly representative of the entire L3 SMI distribution of our regional population (Alberta, Canada) (Fig. 3.2). This representation eliminates the possibility of sampling bias. It also allows each patients' skeletal muscle index to be ranked within the population distribution overall as well as compared to values available for healthy young individuals (Derstine et al., 2018).

Age and sex differences exist at the level of muscle function, biochemistry/metabolism and mass (Esfandiari et al., 2014; Jackson et al., 2014; Stephens et al., 2012). The majority of studies reported combined data from both sexes without acknowledging sexual dimorphisms. Age was generally not accounted for. In the first forty years of life, muscle mass is relatively stable in both men and women; then it begins to decline, however, the rate of loss is slower in women than in men (G. I. Smith et al., 2016). In our sample, differences between men and women were observed for muscle fiber area, SMI and muscle radiodensity. Sexual dimorphism in gene expression was not limited to a particular pathway or function but was identified in growth (AKT1, FOXO1, MSTN, PAX7, TGF α 1), apoptosis (CASP9) and inflammation (TNF, STAT3). In relation to the age effect, we did not find any significant differences in mean muscle fiber area and proportion of fiber types when comparing young versus old male cancer patients; this could be potentially explained by the narrow age range in our study. Differences between young (18 to 48 years) and older (66 to 99 years) participants (Marzani et al., 2005) has been reported for fiber type distribution in rectus abdominis and vastus lateralis. Therefore, age differences and sexual dimorphism must be acknowledged when comparing, reporting and interpreting muscle characteristics.

Here we present many characteristics of human rectus abdominis muscle. We obtained a detailed analysis of its radiological features, for the first time. Our analysis of fibre type is multidimensional and confirms the mixed fibre distribution of the rectus abdominis. A prior study in cancer patients with upper gastrointestinal malignancies, reported mean values of 48% and 55%

for MyHC type I and IIa , respectively (Johns et al., 2014) . Muscle gene expression and triglyceride content levels as presented here are new information about rectus abdominis. Future work on rectus abdominis can be usefully planned, using this base of information. The majority of evidence to date (Table 3.1) on muscle from cancer patients is coming from rectus abdominis. Due to the unique characteristics of each muscle type, we suggest that future researchers identify candidate muscles for intensive research using the principle that the muscle(s) most often transected in cancer surgeries would be the greatest resource. This can be decided in function of the common surgical approaches. Thus over time a large base of evidence may be obtained from *latissimus dorsi*, *serratus anterior* or intercostal muscle (for example) from thoracic cancer surgeries.

A key component of case-control studies is to provide details of the control group relative to the research question. However, this is rarely done in the literature that we reviewed (Narasimhan et al., 2017, 2018). Detailed clinical characterization of non-cancer controls is usually missing, and assumption of a healthier status of the control group when compared to cancer patients is common. In many cases the comparator group is a non-cancer surgical patient population, however, there is no documentation provided around diagnosis or medications. Presumably healthy volunteers could have underlying co-morbid conditions or be taking medications that impact skeletal muscle. Comorbidities and use of medications were not generally mentioned either for patients undergoing non-cancer surgery or “healthy” volunteers recruited outside the clinical setting. Approximately 60% of people diagnosed with malignancy are 65 years and older (Edwards et al., 1975). Prevalence of comorbidity in cancer population range from 30-50% depending on type of cancer (Xiao et al., 2018) and a patient with history of cancer has on average three comorbidities (Garman et al., 2003; Seo et al., 2004). Diabetes and hypertension were the most common conditions in our patient population but cardiovascular disorders and mental health problems are also prevalent in the cancer population (Edwards et al., 1975; Xiao et al., 2018). These chronic conditions and medications taken to control them can independently affect muscle physiology (Bouchi et al., 2017; D’Souza et al., 2013; Henriksen et al., 2017; Langen et al., 2013; Larsen et al., 2016; Leenders et al., 2013; Marquis et al., 2002; Salvatore et al., 2014; Vuong et al., 2010; Wang et al., 2016; Wüst et al., 2007) (Table 3.4). COX inhibitors, statins, biguanides, proton pump inhibitors and thyroid hormones were the most common medications prescribed in our patient population apart from those prescribed during

cancer treatment. These classes of drugs have known effects on muscle protein synthesis (Burd et al., 2010; Standley et al., 2013; T. A. Trappe et al., 2002; Todd A Trappe et al., 2013) and catabolism (Bodine et al., 2015; Mammucari et al., 2007; Sandri et al., 2004; Stitt et al., 2004), atrophy pathways (Cetrone et al., 2014), insulin sensitivity (Malin et al., 2014) and mitochondria function (Wessels et al., 2014). Therefore, it is important that for both the cancer group and “control” groups have a detailed medical history that captures diagnosis of other conditions and medications. In addition to drugs prescribed for management of comorbid conditions, antineoplastic treatment previous to tissue biopsy is also a relevant event that may impact interpretation of results as the long lasting effects in the muscle are unknown (Schiessel et al., 2018).

Technical considerations

We suggest recommendations for minimum procedures to follow in biobanking practices, tissue manipulation and patient characterization to enhance the consistency, reliability and comparability of future research (Table 3.8). Acknowledgement of differences between muscle groups is essential when comparing and interpreting results. RA is commonly collected in patients with gastrointestinal disease due to its practicality in relation to the surgical incision while maintaining patient burden to the essential minimum. Its broad extension in the abdominal area enables for collection of muscle tissue from a variety of locations (Pedersen et al., 2014); however, no one has demonstrated how homogeneous the RA is in relation to the biopsy site. On the other hand, quadriceps or tibialis anterior are collected in healthy volunteers serving as controls as there is no justification for surgical intervention. Importantly, physiological variations between muscle groups exist (Johnson et al., 1973; Miller et al., 1993), which strongly suggest that studies collecting different muscles must avoid comparing or combining data of more than one muscle.

Most researchers did not report on surgical procedures and muscle biopsy collection, transport and processing of the samples, each of which can impact on the morphological and molecular profile of the biopsy (Chatterjee, 2014; Srinivasan et al., 2002; Truong et al., 2017). Collecting abdominal muscle biopsies at the start of the surgical procedure and avoidance of electrocautery, is strongly recommended to reduce variations associated with the surgical trauma, variable duration of surgery and intra-operative effect of anesthetics (Chatterjee, 2014; Essen et al., 1992; Lattermann et al., 2002; Luo et al., 1998; Ruel et al., 2003; Varadhan et al., 2018). Skeletal muscle collected at the start and end of a surgery expresses differences in genes associated

with inflammation, growth differentiation and transcription factors (Ruel et al., 2003). For percutaneous biopsies, the Bergstrom protocol is a well-developed method with several adjustments to improve the quality of the muscle biopsies (Shanely et al., 2014; Tarnopolsky et al., 2011). Procedures followed after biopsy collection must also be detailed as sample preservation and storage impacts on muscle integrity and potentially interpretation of the results. Lastly, the numbers of medical conditions and drugs taken by patients in this sample are important and all of these and their different combinations may have an impact on specific aspects of muscle biology. As much as possible, we recommend to annotate the presence of comorbidities and medications in patients consenting to biopsy.

Overall, the literature review reveals a high risk of sampling bias, poorly characterised patient populations. These features make reliable comparison between studies and aggregation of data challenging. Muscle biopsy preparation and biobanking practices are also variable between studies. Data from an unbiased sample of 190 patients presents a variety of measures of interest on rectus abdominis to provide a point of reference for researchers exploring biological characteristics of this muscle. Continued collaboration between researchers and cancer surgeons would enable a more complete understanding of mechanisms of cancer-associated muscle atrophy.

Table 3.1 Original articles reporting muscle biopsy collection in patients with cancer: assessment of bias and study quality, population characteristics weight loss or cancer cachexia classification criteria.

Author	Bias †	Quality ††	Muscle	Cancer site	Cancer Stage	Cancer population		Control group		Patient weight loss or cachexia criteria
						n (% male)	Age (years) mean ± SD	n (%male)	Age (years) mean ± SD	
Acharyya 2005	1/3	3/12	RA	Gastric	NR	27(NR)	NR	14(NR)	NR	N/A
Agustsson 2011	1/3	3/12	RA	Pancreas Other GI	NR	Pancreas 13 (30) Other GI 8 (37)	Pancreas: 70 ± 2 Other: 68 ± 3	Benign: 8 (37) Pancreatiti s : 8 (63)	Benign: 53 ± 4 Pancreatit is 52 ± 3	NR
Aversa 2016	1/3	6/12	RA	Colorectal Pancreas Gastric	1-4	All: 29 (59) WS = 14 WL =15	68 ± 10.7	11 (63)	63 ± 13.2	5% WL (6 months)
Bonetto 2013	1/3	3/12	RA	Gastric	1-4	16(NR)	64 ± 11	6 (NR)	62 ± 17.4	>5% WL
Bossola 2006	1/3	5/12	RA	Gastric	1-4	16 (50)	60.8 ± 11.2	5 (60)	65.6 ± 7.5	WL Mild: 0–5%. WL Moderate: 6–10%. WL Severe: >10%
Bossola 2001	1/3	4/12	RA	Gastric	NR	20 (55)	61 ± 79.6	10 (60)	62 ± 45.8	WL Mild: 0–5%. Moderate 6–10%. Severe: >10%
Bossola 2003	1/3	5/12	RA	Gastric	NR	23 (61)	59.5 ± 16.1	14 (64)	61.2 ± 12.3	>10% WL
Busquets 2007	0/3	3/12	RA	Esophagea l Gastric Pancreas	1-4	16(NR)	66 ± 10	11 (NR)	66 ± 10.2	>5% WL (1 month)
DeJong 2005	0/3	4/12	RA	Pancreas	1-4	16 (63)	66 ± 8	11 (81)	67 ± 13.2	N/A

D'Orlando 2014	1/3	6/12	RA	Gastric	1-4	38 (66)	68.1 ± 11.6	12 (58)	64.2 ± 11.6	>5% WL (6 months)
Eley 2008	1/3	3/12	RA	Esophagea l Gastric	1-4	15 (87)	66 (49 – 83) *	9 (10)	56 (41 – 86) *	N
Johns 2017	2/3	9/12	RA	Esophagea l Gastric Lung and Other	1-4	134 (51)	65 ± 13	N/A	N/A	WL >5% >10% >15% and SMI with any degree of WL (>2%)
Johns 2014	0/3	5/12	RA	Upper GI Pancreas	NR	41 (73)	65 ± 12.8	N/A	N/A	>5% WL (6 months) and low muscularity with 2% WL
Khal 2005	0/3	1/12	RA	Pancreas Colorectal	NR	All: 18 (67) WS = 5 (60) WL = 13 (69)	WS:79.8 ± 2.2 WL:70.6 ± 8.2	10 (80)	69.6 ± 7.3	WL Moderate: 1- 11%. WL Severe: >11%
Lundholm 1976	1/3	3/12	RA	Esophagea l Gastric Pancreas Colorectal Kidney and others	NR	43 (44)	♂:62 ± 13.1 ♀: 63 ± 9.7	55 (51)	56 ± 14.8	N/A
Marzetti 2017	1/3	5/12	RA	Gastric	1-4	All: 18 (94) WS = 9 (100) WL =9 (89)	WS:70.6 ± 8.63 WL:66.8 ± 12.5	9 (88)	57.4 ± 15.9	>5% WL (6 months)
Narasimhan 2017	2/3	8/12	RA	Pancreas Colorectal	1-4	22 (41)	64.9 ± 10	20 (45)	63.6 ± 7.9	>5% WL (6 months) or BMI of <20 with WL >2% and sarcopenia

Narasimhan 2018	1/3	5/12	RA	Pancreas Colorectal	1-4	All: 40 (43) WS =19 (47) WL = 21 (40)	WS:64 ± 8 WL: 66 ± 11	N/A	N/A	WL >5% >10% >15% and sarcopenic (SMI) with any degree of WL (>2%)
Noguchi 1998	0/3	3/12	RA	Esophagea l Gastric Colorectal	1-4	10 (90)	56 (50 to 63)*	N/A	N/A	N/A
Pessina 2010	1/3	6/12	RA	Gastric	1-3	30 (57)	63.8 ± 2.8	8 (62)	64.2 ± 2.6	N/A
Prokopchuk 2016	0/3	4/12	RA	Pancreas	1-4	All: 25 (32) NC=13 (38) CC=12 (25)	NC:67 (36- 87) CC:70 (52-83)*	Benign=15 (80) Pancreatitis= 9 (45)	Benign: 67 (32- 73) Pancreatitis: 49.5 (40- 75)*	>10% WL (6 months)
Ramage 2018	1/3	3/12	RA	Esophagea l Gastric Pancreas	1-4	32 (81)	64.5 (43-83)	N/A	N/A	>5% WL of pre- illness
Rhoads 2009	1/3	6/12	RA	Gastric	1-4	All: 14 (57) WS = 6 (66) WL = 8 (50)	64.2 ± 3.8	10 (60)	63.9 ± 2.8	NR
Schmitt 2007	0/3	2/12	RA	Pancreas	2, 4	All: 16 (63) NC= 8 (37) CC = 8 (88)	NC: 62 ± 8.5 CC:53 ± 11.3	N/A	N/A	>10% WL (6 months)
Skorokhod 2012	0/3	1/12	RA	Pancreas	2-4	All: 23 (61) WS = 13 (69) WL = 10 (50)	WS: 66 (51- 69) WL: 65 (57- 74)	N/A	N/A	>10% WL of pre- illness
Smith 2010	0/3	4/12	RA	Gastric	1-4	15 (67)	66 ± 11.6	15 (80)	57 ± 19.3	>5% WL

Stephens 2011	0/3	2/12	RA	Esophagea l Gastric Pancreas Rectal	2-4	19 (58)	67 ± 10	6 (33)	53 ± 8	>10% WL (6 months)
Stephens 2015	0/3	3/12	RA	Esophagea l Gastric Pancreas and other	1-4	All: 92 (72) NC = 41 (82) CC = 51(63)	All: 65 ± 10 NC:68 ± 9 CC:63 ± 9	15 (53)	56 ± 17	>5% WL
Stretch 2013	0/3	4/12	RA	Liver Bile duct GI tract Pancreas and other	NR	134 (51)	♂:59 ± 13 ♀:63 ± 13	N/A	N/A	N/A
Sun 2012	0/3	5/12	RA	Gastric	1-4	102 (71)	62.13 ± 6.54	29 (72)	61.8 ± 6.4	>10% WL
Taskin 2014	0/3	1/12	RA	Colorectal Pancreas Gastric and other	NR	All: 14 (50) NC= 8 (37) CC = 6 (66)	NC: 68 ± 5 CC: 70 ± 15	5 (40)	77 ± 5	>10% WL (6 months) weight stable <5%
Williams 1999	0/3	2/12	RA	Colorectal	NR	6 (66)	67 (53-76) *	6 (83)	54(22-92) *	N/A
Zeiderman 1991	0/3	5/12	RA	Esophagea l Gastric Colorectal Pancreas	NR	30 (70)	Hospital diet: 67 ± 9.5 3 days intervention: 72 ± 3.2 7 days intervention: 67 ± 6.3	N/A	N/A	> 5 kg WL (3 months)
Zampieri 2010	0/3	3/12	RA, QF	Colorectal	NR	14 (36)	65.1 ± 10.3	Myopathy: 13 (38) Healthy: = 19(NR)	Myopath y: 64.3 ± 6.3 Healthy: 30.1 ± 13.3	N/A

Zampieri 2009	0/3	1/12	RA, QF	Colorectal	2-3	10 (30)	65.1 ± 10.3	10(NR)	22.7 ± 2.6	N/A
Zampieri 2010	1/3	3/12	RA, QF	Colorectal	2-3	11 (36)	65.1 ± 10.3	7 (0)	44.5 ± 18.3	N/A
Aversa 2012	1/3	3/12	RA, SA	NSCLC Gastric	1-4	39 (74)	Lung: 66 ± 9 Gastric :65 ± 10	10 (50)	Abdominal: 63 ± 10 Thoracic :65 ± 12	NR
MacDonald 2015	0/3	2/12	RA, QF	Esophagea l Gastric	1-4	All: 14 (57) WS = 6 (66) WL = 8 (50)	WS: 62.5 (57.0- 70.3)** WL: 63.4 (61.5-66.3)**	7 (42)	52.1 (51.5- 53.1)**	>5% WL
Shaw 1991	0/3	6/14	RA, SCM	Colorectal Pancreas Head & neck thyroid and other	NR	All: 43 (42) WS = 25 (48) WL = 18 (66)	WS:61 ± 20 WL: 64 ± 12.7	18 (33)	57 ± 16.9	>15% WL of pre- illness
Stephens 2010	1/3	3/12	RA, VL, DIAPH	Esophagea l Gastric Pancreas	NR	18 (66) WL	67 ± 8.4	3 (66)	45 ± 3.4	>5% WL
Brzeszczyns ka 2016	0/3	2/12	QF	Esophagea l Gastric Pancreas	2-3	All: 28 (75) NC = 18 (72) CC = 10 (80)	NC: 67 ± 10.5 CC: 65 ± 8.1	Middle age 20 (60) Elderly: 21 (52)	Middle- age: 61 ± 7 Elderly: 79 ± 3.6	>5% WL of pre- illness
Ebhardt 2017	0/3	1/12	QF	Esophagea l Gastric Pancreas	NR	All: 19 (79) NC = 14 (85) CC = 5 (60)	Non- CC: 66.3 ± 10.2 CC:64 ± 4.1	Non- sarcopenic 10 (60) Sarcopenic 8 (50)	Non- sarcopeni c:	>5% WL of pre- illness

									77.4 ± 2.3 Sarcopenia: 80.3 ± 3.9	
Gallagher 2012	1/3	7/14	QF	Esophageal 1 Gastric Pancreas	1-3	12 (83)	65	6 (66)	58	NR
Christensen 2016	N/A	13/14	VL	Testicular germ cell	NR	8 (100)	33.4 ± 7.5	Control =9 (100) Ref=13 (100)	Control: 37.8 ± 7.6 Reference group:32. 1 ± 6.3	N/A
Christensen 2014	N/A	13/14	VL	Testicular germ cell	NR	15 (100)	Intervention: 34.4 ± 7.6 Control: 35.8 ± 8.9	19 (100)	31.5 ± 6.0	N/A
Lamboley 2017	1/3	3/12	VL	Prostate	2	8 (100)	68 ± 5.6	14 (100)	71 ± 3.7	N/A
Nilsen 2016	N/A	9/14	VL	Prostate	NR	12 (100)	67 ± 7	11 (100)	64 ± 6	N/A
Op den Kamp 2015	0/3	6/12	VL	NSCLC	3-4	All: 26 (65) Pre-CC = 10 (80) CC= 16 (56)	Pre-CC: 62.4 ± 10.4 CC: 59.8 ± 8.2	22 (59)	61.4 ± 7.0	>5% WL (6 months)
Op den Kamp 2012	0/3	3/12	VL	NSCLC	1-3	16 (93)	65.9 ± 7.5	10 (70)	63.7 ± 5.6	10% WL (6 months)
Op den Kamp 2013	0/3	5/12	VL	NSCLC	3-4	All: 26 (65) Pre-CC = 10 (80) CC= 16 (56)	Pre-CC: 62.4 ± 10.4 CC:59.8 ± 8.2	22 (59)	61.4 ± 7.02	5% WL (6 months) 2% WL with BMI <20 or sarcopenia

Phillips 2013	0/3	4/14	VL	Colorectal	Early	8 (50)	62.5 ± 23.4	8 (50)	70.7 ± 4.5	N/A
Puig- Vilanova 2014	1/3	3/12	VL	Lung	1-4	10 (100)	65 ± 9	Healthy = 10 (100) COPD = 16 (100)	65 ± 11 64 ± 9	Fat Free Mass Index: <18.5kg/m ²
Weber 2007	0/3	3/12	VL	Gastric Pancreas Leukemia	NR	17 (53)	52.5 ± 6.5	27 (52)	57.9 ± 12.4	>10% WL (6 months)
Weber 2009	0/3	2/12	VL	GI tract (not defined)	NR	19 (52)	58 ± 9	19 (53)	56 ± 7	>10% WL (6 months)
Williams 2012	0/3	5/12	VL	Colorectal	Early	13 (46)	66 ± 10.8	8 (50)	71 ± 5.6	N/A
Banduseela 2007	N/A	N/A	TA	NSCLC	NR	1 (100)	63	6 (50)	Healthy: 49±7 Myopath y: 60±18	NR
Higuchi 2000	N/A	N/A	Gastroc	Gastric	NR	1 (100)	54	N/A	N/A	N/A
Jagoe 2002	0/3	1/12	LD	Lung	3-4	36 (75)	64.1 ± 9	10 (40)	51.3 ± 15.1	Any % WL (6 months)
Bohlen 2018	0/3	4/12	PM	Breast	1-4	14 (0)	56.5 ± 17.2	6 (0)	44.2 ± 7.4	N/A

Values reported as mean \pm standard deviation (SD) unless indicated Otherwise *median (range) and ** median (interquartile range). † Modified Newcastle-Ottawa Scale † † Quality Assessment score-high score means high quality. NIH-NHLBI: National Heart Lung and Blood Institute; RA: Rectus Abdominis; TA: Tibialis anterior; QF: Quadriceps Femoris; VA: Vastus Lateralis; PM: Pectoralis Major; SA: Serratus Anterior; LD: Latissimus Dorsi; Gastroc: Gastrocnemius; SCM: Sternocleidomastoid; DIAPH: Diaphragm; GI: Gastrointestinal; NSCLC: Non-small cell Lung carcinoma; N/A: Not applicable; NR: Not reported. WS: Weight stable WL: Weight loss. NC: non-cachexia .BMI: Body Mass Index. SMI: Skeletal Muscle Index.

Table 3.2 Biopsy collection and handling procedures across the studies				
Author	Biopsy collection (collected in start or end of surgery)	Cauterized	Blood traces, fat or connective tissue removed	Sample handling and storage conditions
Acharyya 2005	NR	NR	NR	NR
Agustsson 2011	Initial phase of surgery	NR	NR	Incubated in vitro
Aversa 2016	Initial phase of surgery	No	NR	Immediately frozen, stored at -80°C
Aversa 2012	Initial phase of surgery	No	NR	Immediately frozen, stored at -70°C
Banduseela 2007	Percutaneous biopsy (local anaesthesia)	N/A	Yes (fat, connective tissue)	Immediately frozen, stored at -80°C
Bohlen 2018	NR	N/A	NR	Stored in RNA stabilization solution at -4°C overnight and then stored at -80°C
Bonetto 2013	Initial phase of surgery	No	NR	Immediately frozen, stored at -80°C
Bossola 2006	Initial phase of surgery	No	NR	Immediately frozen, stored at -70°C
Bossola 2001	Initial phase of surgery	No	NR	Immediately frozen, stored at -70°C
Bossola 2003	Initial phase of surgery	No	NR	Immediately frozen, stored at -70°C
Brzeczynska 2016	Initial phase of surgery	No	Yes (blood)	Immediately frozen, stored at -80°C
Busquets 2007	Initial phase of surgery	No	NR	Immediately frozen, stored at -80°C
Christensen 2016	Percutaneous biopsy (local anaesthesia)	N/A	NR	Immediately frozen, stored at -80°C
Christensen 2014	Percutaneous biopsy (local anaesthesia)	N/A	NR	Immediately frozen, stored at -80°C
DeJong 2005	Initial phase of surgery	No	NR	Immediately frozen, stored at -70°C
D'Orlando 2014	Initial phase of surgery	No	NR	Immediately frozen, stored at -80°C
Ebhardt 2017	Percutaneous biopsy (local anaesthesia)	N/A	Yes (blood)	Immediately frozen, stored at -80°C
Eley 2008	Initial phase of surgery	No	NR	Immediately frozen, stored at -70°C
Gallagher 2012	Percutaneous biopsy (local anaesthesia)	N/A	Yes (blood)	Immediately frozen, stored at -80°C
Higuchi 2000	NR	N/A	NR	NR
Jagoe 2002	Initial phase of surgery	No	NR	Immediately frozen, stored at -80°C
Johns 2017	Initial phase of surgery	No	NR	Immediately frozen, stored in liquid nitrogen
Johns 2014	Initial phase of surgery	NR	Yes (blood)	Immediately frozen, stored at -80°C
Khal 2005	NR	No	NR	Immediately frozen, stored at -70°C
Lamboley 2017	Percutaneous biopsy (local anaesthesia)	N/A	Yes (blood)	Immediately and stored in liquid nitrogen

Lundholm 1976	Initial phase of surgery	NR	NR	Muscle fibre isolation on fresh tissue
MacDonald 2015	Initial phase of surgery and Percutaneous biopsy (local anaesthesia)	NR	NR	Immediately frozen in liquid nitrogen, storage temperature NR
Marzetti 2017	Initial phase of surgery	No	NR	Immediately frozen, stored at -80°C
Narasimhan 2017	Initial phase of surgery	No	NR	Immediately frozen, stored at -80°C
Narasimhan 2018	Initial phase of surgery	No	NR	Immediately frozen, stored at -80°C
Nilsen 2016	Percutaneous biopsy (local anaesthesia)	N/A	Yes (fat)	Frozen by immersion in isopentane, stored at -80°C
Noguchi 1998	Initial phase of surgery	NR	NR	Immediately frozen in situ, stored at -70°C
Op den Kamp 2015	Percutaneous biopsy (local anaesthesia)	N/A	NR	Immediately frozen, stored at -70°C
Op den Kamp 2012	Percutaneous biopsy (local anaesthesia)	N/A	NR	Immediately frozen, stored at -80°C
Op den Kamp 2013	Percutaneous biopsy (local anaesthesia)	N/A	NR	Frozen by immersion in isopentane, stored in -80°C
Pessina 2010	Initial phase of surgery	No	NR	Immediately frozen, stored at -70°C
Phillips 2013	Percutaneous biopsy (local anaesthesia)	N/A	NR	Immunoblotting in fresh tissue
Prokopchuk 2016	NR	NR	NR	Immediately frozen and stored at -80°C
Puig-Vilanova 2014	Open muscle biopsy technique	N/A	NR	NR
Ramage 2018	NR	NR	NR	Immediately frozen, stored at -80°C
Rhoads 2009	Initial phase of surgery	No	NR	Immediately frozen, stored at -70°C
Schmitt 2007	NR	NR	NR	Immediately frozen in liquid nitrogen, storage temperature NR
Shaw 1991	NR	NR	NR	Snap-frozen in liquid nitrogen, thawed after 48 hrs
Skorokhod 2012	Initial phase of surgery	NR	NR	Immediately frozen in liquid nitrogen, storage temperature NR
Smith 2011	Initial phase of surgery	No	NR	Immediately frozen and stored at -80°C
Stephens 2011	Initial phase of surgery	NR	NR	Fixation for microscopy
Stephens 2010	Rectus abdominis – NR Quadriciceps - Percutaneous biopsy (local anaesthesia)	NR	NR	Immediately frozen
Stephens 2015	Initial phase of surgery	NR	Yes (blood)	Immediately frozen, stored at -80°C
Stretch 2013	Initial phase of surgery	No	NR	Immediately frozen and stored in liquid nitrogen.
Sun 2012	Initial phase of surgery	NR	NR	Immediately frozen and stored at -80°C
Taskin 2014	NR	NR	NR	Transferred to lab on ice cold buffer, stored at -20°C

Weber 2007	Percutaneous biopsy (local anaesthesia)	N/A	NR	Immediately frozen, stored at -80°C
Weber 2009	Percutaneous biopsy (local anaesthesia)	N/A	NR	Immediately frozen, stored at -70°C
Williams 2012	Percutaneous biopsy (local anaesthesia)	N/A	NR	NR
Williams 1999	Initial phase of surgery	No	NR	Immediately frozen, stored at -70°C
Zampieri 2010	Rectus abdominis – NR Quadriceps - Percutaneous biopsy (local anaesthesia)	NR	NR	Immediately frozen and stored in liquid nitrogen.
Zampieri 2009	Rectus abdominis – NR Quadriceps - Percutaneous biopsy (local anaesthesia)	NR	NR	Immediately frozen and stored in liquid nitrogen.
Zampieri 2010	Rectus abdominis - NR Quadriceps - Percutaneous biopsy (local anaesthesia)	NR	NR	Immediately frozen and stored in liquid nitrogen.
Zeiderman 1991	Initial phase of surgery	NR	NR	Incubation
NR: NR; N/A: Not applicable				

Table 3.3 Patient characteristics			
	Male (n=122)	Female (n=68)	P values
Age, mean years ± SD (Min-Max)	61 ± 12 (19-87)	65 ± 12 (21-87)	0.049
Tumour type, % (n):			0.006
Colorectal	45 (55)	26 (18)	
Pancreas	23 (28)	31 (21)	
Other gastro-intestinal	25 (31)	22 (15)	
Other ^b	6 (8)	20 (14)	
Presence of metastasis, % (n)	56 (68)	40 (27)	0.03
Chemotherapy exposure within 4 weeks prior to muscle biopsy, % (n):	23 (28)	22 (15)	0.9
Patients with weight lost, % (n)	56 (14) ^c	55 (11) ^d	0.9
Sarcopenia, % (n)	60 (61) ^e	50 (23) ^f	0.2
BMI (kg/m²), mean ± SD	27 ± 5	28 ± 7	0.7
BMI classification, % (n):			0.1
Underweight	1 (1)	1 (1)	
Normal	26 (32)	26 (18)	
Overweight	39 (48)	28 (19)	
Obesity I	17 (21)	6 (4)	
Obesity II	5 (6)	10 (7)	
Obesity III	2 (2)	4 (3)	
Missing BMI	10 (12)	24 (16)	
Comorbidities, % (n):			
Diabetes type II	12 (15)	18 (12)	0.3
Hypertension	24 (29)	29 (20)	0.4
Cardiovascular disease	15 (18)	7 (5)	0.1
Dyslipidemia	7 (9)	7 (5)	0.9
History of smoking habit, % (n)	28 (34)	24 (16)	0.3
Computed tomography, body composition analysis, mean ± SD:			
Subcutaneous adipose tissue (cm ²)	166.4±91.5 ^g	251.1±134.4 ^h	<0.001
Visceral adipose tissue (cm ²)	174.8±105.1 ^g	111.9±65.7 ^h	<0.001
Muscle biopsy triglyceride content (µg/mg), mean ± SD:	13.2±14.8 ⁱ	29.5±21.7 ^j	<0.001
^a Other gastro-intestinal: Stomach, small intestine, liver, intrahepatic bile duct, gallbladder, biliary tract and appendix. ^b Other: adrenal gland, skin, kidney, mesothelium, lymphoma, melanoma, chronic lymphocytic leukemia, prostate, ovary, uterus, head and neck. BMI: Body mass index Patients with weight loss information: ^c n=25 / ^d n=20 Patients with sarcopenia information: ^e n=102 / ^f n=46 CT Adipose tissue information: ^g n=98 / ^h n=44 Patients with muscle biopsy triglyceride content: ⁱ n=69 / ^j n=19 Differences between males and females were analyzed by independent t-test (continuous variables) and chi-square test (categorical variables).			

Table 3.4 Most common medications prescribed and potential effects on skeletal muscle				
Class of drug	% (n)	Common use	Possible implications to skeletal muscle	
Cyclooxygenase inhibitors	Aspirin, Acetaminophen	15 (29)	Pain, fever, inflammation, prevention of cardiovascular disease	Influence muscle prostaglandin synthesis, muscle protein metabolism, and cellular processes regulating muscle protein synthesis. (Burd et al., 2010; Liu et al., 2016; Standley et al., 2013; Todd A Trappe et al., 2013)
HMG-CoA reductase inhibitors	Rosuvastatin, Simvastatin, Atorvastatin	13 (24)	lipid-lowering	Association with myalgia and related symptoms. Associated to mitochondrial oxidative stress (Bouitbir et al., 2016; Diaz et al., 2015)
Biguanide	Metformin	8 (16)	Type 2 diabetes, suppressor of hepatic gluconeogenesis	Mitochondrial dysfunction in skeletal muscle. Sensitizes muscle to insulin; increases glucose disposal in skeletal muscle (Bouitbir et al., 2016; Diaz et al., 2015)
Proton pump inhibitors	Omeprazole, Pantoprazole	8 (16)	Gastroesophageal reflux, erosive esophagitis	Concomitant administration with atorvastatin and dexamethasone is associated to increase risk of myopathy (Bouitbir et al., 2016; Diaz et al., 2015)
Hormones	Levothyroxine	7 (13)	Thyroid hormone (T4) deficiency	Influences myogenesis, associated with sarcopenia and myopathy (Bouitbir et al., 2016; Diaz et al., 2015)
Angiotensin converting enzyme inhibitor	Ramipril	7 (13)	Hypertension, congestive heart failure	Associated with larger muscle cross sectional area and muscle remodeling, associated with cancer cachexia (Bouitbir et al., 2016; Diaz et al., 2015)
Thiazide diuretic	Hydrochlorothiazide	6 (12)	Hypertension, diuretic by reducing sodium reabsorption	None reported or reviewed
Calcium channel blockers	Amlodipine	5 (9)	Hypertension, calcium channel blocker	None reported and reviewed (Bouitbir et al., 2016; Diaz et al., 2015)
Opioid	Oxycodone	3 (5)	Pain	Hypogonadism and testosterone depletion in men. (Bouitbir et al., 2016; Diaz et al., 2015)
Alpha-adrenergic blocker	Tamsulosin	3 (5)	Muscle relaxer of prostate and bladder	None reported or reviewed
Xanthine oxidase inhibitor	Allopurinol	3 (5)	Gout prevention, decrease blood uric acid levels	Prevents skeletal muscle atrophy (Bouitbir et al., 2016; Diaz et al., 2015)
Anticoagulant	Warfarin	3 (5)	Anticoagulant	None reported or reviewed

Percentage of patients prescribed this medication out of a total of 190 patients who had a medical history available with information provided on current medication use.

Table 3.5 Computed tomography defined muscle composition at L3 for rectus abdominis and total skeletal muscle in cancer patients, stratified by sex and age decade

Sex	Age stratum		Rectus Abdominis	Total Lumbar Muscle	Lumbar skeletal muscle index	Rectus Abdominis	Total Lumbar Muscle
		N	L3-CSA (cm ²)		cm ² /m ²	Radiodensity (Hounsfield Units)	
Male	<50	17	15.9 ± 3.8 (9.8-23.4)	188.7 ± 29.1 (123.6-238.2)	58.2 ± 8.9 (42.8-73.3)	36.2 ± 12.3 (7.6-54.8)	39.6 ± 10.5 (15.4-55.3)
	50-60	34	13.6 ± 3.9 (6.6-24.5)	156.2 ± 27.5 (107.2-228.9)	50.6 ± 8.2 (37.1-66.5)	30.9 ± 12.2 (4.4-50.0)	36.5 ± 8.9 (13.8-50.5)
	60-70	23	13.3 ± 3.3 (5.7-19.4)	158.4 ± 20.7 (109.0-192.5)	50.8 ± 6.6 (36.4-60.8)	28.0 ± 12.3 (-10.8-44.3)	33.8 ± 10.1 (7.1-54.4)
	70-80	23	11.5 ± 2.6 (6.0-17.6)	141.4 ± 23.0 (94.6-187.2)	46.6 ± 6.0 (35.6-59.1)	20.0 ± 11.3 (-2.0-44.6)	28.9 ± 7.7 (10.0-42.6)
	>80	4	9.8 ± 4.2 (6.2-15.2)	139.0 ± 16.4 (122.8-160.9)	46.1 ± 7.1 (40.1-56.3)	21.5 ± 8.3 (12.3-30.4)	27.5 ± 3.0 (24.8-31.5)
Female	<50	3	9.3 ± 3.2 (5.9-12.2)	114.9 ± 14.8 (97.8-124.4)	43.8 ± 1.6 (42.9-45.7)	32.0 ± 5.7 (26.6-38.0)	45.1 ± 5.3 (40.5-50.9)
	50-60	11	7.0 ± 2.4 (3.8-10.9)	101.5 ± 16.8 (67.5-125.4)	38.3 ± 6.8 (23.9-46.4)	22.7 ± 13 (4.2-41.1)	35.4 ± 7.6 (20.9-46.1)
	60-70	15	8.7 ± 3.7 (2.8-16.9)	102 ± 16.6 (66.2-122.7)	39.2 ± 7.0 (27.7-52.8)	19.1 ± 10.3 (2.5-39.1)	29.0 ± 7.1 (18.2-39.6)
	70-80	16	6.7 ± 2.3 (1.4-10.9)	101.0 ± 13.8 (79.0-127.3)	40.5 ± 4.8 (33.8-49.7)	13.1 ± 10.0 (-7.7-30.9)	28.9 ± 7.0 (15.0-38.9)
	>80	3	7.7 ± 3.1 (4.2-10.0)	92.8 ± 14.8 (77.9-107.5)	41.1 ± 8.1 (32.9-49.1)	12.2 ± 19.8 (-10.1-27.6)	22.9 ± 4.1 (18.2-25.3)
Total male		101	13.6 ± 3.8 (5.7-24.5)	158.2 ± 29 (94.6-238.2)	50.8 ± 8.3 (35.6-73.3)	28.2 ± 12.9 (-10.8-54.8)	34.3 ± 9.7 (7.1-55.3)
Total female		48	7.6 ± 2.9 (1.4-16.9)	101.7 ± 15.4 (66.2-127.3)	39.8 ± 6 (23.9-52.8)	18.2 ± 12 (-10.1-41.1)	31 ± 8.3 (15-50.9)

Values reported in mean ± SD (range). L3, 3rd Lumbar vertebra. CSA, Cross-sectional area.

Table 3.6 Rectus abdominis myosin heavy chain content and mean muscle fiber area of cancer patients				
	All	Male	Female	P value
A. MyHC content by electrophoresis^a (% ± SD N= 40 M / n=8 F)				
MyHC I (%)	39.3 ± 11.1	39.1 ± 10.3	40.6 ± 15.6	0.73
MyHC IIA (%)	38.4 ± 11.1	37.5 ± 10.0	42.6 ± 15.7	0.24
MyHC IID (%)	22.3 ± 8.9	23.4 ± 8.6	16.8 ± 9.1	0.06
B. MyHC content by immunohistochemistry^a (% ± SD N= 20 M / n=10 F)				
MyHC isoforms (%):				
MyHC type I	47.1 ± 13.0	47.0 ± 12.6	47.3 ± 14.6	0.91
MyHC type IIA	51.8 ± 13.4	52.4 ± 12.6	50.5 ± 15.6	0.53
MyHC type IID	16.7 ± 14.3	19.2 ± 13.7	11.8 ± 15.1	0.19
All Hybrids ^b	15.5 ± 13.5	18.5 ± 13.5	9.6 ± 12.2	0.08
Individual fiber types (%):				
Fiber type I	46.4 ± 12.9	48.9 ± 9.4	46.2 ± 14.2	0.32
Fiber type I/IIA	0.7 ± 1.0	0.6 ± 0.9	1.2 ± 1.6	0.15
Fiber type IIA	36.1 ± 9.5	35.7 ± 9.4	40.7 ± 9.6	0.71
Fiber type IIA/D	15.0 ± 13.7	13.1 ± 12.4	8.5 ± 12.9	0.39
Fiber type IID	1.8 ± 4.6	1.7 ± 3.7	3.4 ± 7.3	0.32
C. Mean muscle fiber area (μm²) (% ± SD N= 20 M / n=10 F)				
All Fibers	3236 ± 1390	3784 ± 1285	2139 ± 854	<0.05
MyHC isoforms (μm²):				
MyHC type I	2323 ± 944	2591 ± 970	1786 ± 635	<0.05
MyHC type IIA	4009 ± 1937	4848 ± 1725	2331 ± 1054	<0.05
MyHC type IID	4026 ± 2060	4722 ± 1895	2461 ± 1546	<0.05
Individual fiber types (μm²):				
Fiber type I	2325 ± 941	2591 ± 970	1795 ± 633	<0.05
Fiber type I/IIA	2253 ± 1209	2726.6 ± 1181	1306 ± 528	<0.05
Fiber type IIA	3940 ± 1970	4760 ± 1820	2299 ± 1012	<0.05
Fiber type IIA/D	4012 ± 2055	4833.5 ± 1841	2266 ± 1268	<0.05
Fiber type IID	5243 ± 2407	5323 ± 2553	4729 ± 1524	0.75
MyHC: Myosin heavy chain				
^a There were no differences in age, BMI, metastasis, chemotherapy exposure, comorbidities nor smoking history between men and women				
^b All hybrids refer to fibers of mixed myosin heavy chain isoforms MyHC type I/IIA and MyHC type I				

Table 3.7 Skeletal muscle gene expression for genes associated with cachexia in cancer patients^a						
Biological function	Gene symbol	Gene name	Agilent transcript ID [Refseq RNA ID]	Female (n=64)	Male (n=69)	p-value
Atrophy	FOXO1	Forkhead Box O1	A_24_P22079	1.53 ± 1.04	1.11 ± 0.68	0.005
Autophagy	BECN1	Beclin 1	A_23_P433071 [NM_003766]	0.91 ± 0.27	1.03 ± 0.3	0.05
			A_23_P89410 [NM_003766]	1.00 ± 0.27	1.11 ± 0.33	0.05
	CTSL2	Cathepsin L2	A_23_P146456 [NM_001333]	1.31 ± 0.57	0.99 ± 0.44	<0.0001
Apoptosis	CASP8	Caspase 8	A_23_P209389 [NM_033355]	0.97 ± 0.32	1.09 ± 0.38	0.08
	CASP9	Caspase 9	A_23_P97309 [NM_001229]	0.95 ± 0.19	1.06 ± 0.25	0.008
A_24_P111342 [NM_001229]			0.97 ± 0.22	1.08 ± 0.31	0.03	
Muscle growth	AKT1	V-Akt Murine Thymoma Viral Oncogene Homolog 1	A_23_P2960 [NM_005163]	1.23 ± 0.52	1.04 ± 0.35	0.03
	DMD	Dystrophin	A_24_P342388 [NM_004019]	1.34 ± 0.67	0.94 ± 0.29	<0.0001
			A_24_P185854 [NM_004010]	1.11 ± 0.27	0.94 ± 0.23	<0.0001
			A_24_P34186 [NM_004010]	1.19 ± 0.55	0.97 ± 0.39	0.01
			A_32_P199796 [NM_004023]	1.27 ± 0.66	0.98 ± 0.42	0.005
	MSTN	Myostatin	A_23_P165727 [NM_005259]	1.71 ± 2.43	2.74 ± 3.74	0.02
	PAX7	Paired Box 7	A_23_P126225 [NM_013945]	0.99 ± 0.49	1.08 ± 0.39	0.05
			A_23_P500985 [NM_013945]	0.96 ± 0.45	1.03 ± 0.33	0.09
	PPARGC1A	Peroxisome Proliferator-Activated Receptor Gamma, Coactivator 1 Alpha	A_24_P303052 [NM_013261]	1.22 ± 0.77	1.00 ± 0.51	0.07
	SMAD3	SMAD Family Member 3	A_23_P48936 [NM_005902]	1.14 ± 0.42	1.00 ± 0.28	0.07
TGFB1	Transforming Growth Factor, Beta 1	A_24_P79054 [NM_000660]	1.42 ± 1.47	1.06 ± 0.54	0.01	
Inflammation	JAK1	Janus Kinase 1	A_24_P410678 [NM_002227]	0.92 ± 0.37	1.15 ± 0.43	0.001
	JAK2	Janus Kinase 2	A_23_P123608 [NM_004972]	1.21 ± 0.48	1.06 ± 0.45	0.03
	JAK3	Janus Kinase 3	A_23_P329112 [NM_000215]	1.03 ± 0.46	1.19 ± 0.57	0.09

	STAT3	Signal Transducer And Activator Of Transcription 3	A_23_P107206[NM_213662]	1.21 ± 1.02	0.53 ± 0.35	0.02
	STAT5A	Signal Transducer And Activator Of Transcription 5A	A_23_P207367 [NM_003152]	1.12 ± 1.01	0.32 ± 0.34	0.03
			A_24_P173088 [NM_003152]	1.19 ± 1.00	0.47 ± 0.45	0.005
	TNF	Tumor Necrosis Factor	A_24_P50759 [NM_000594]	0.99 ± 0.35	1.15 ± 0.44	0.03

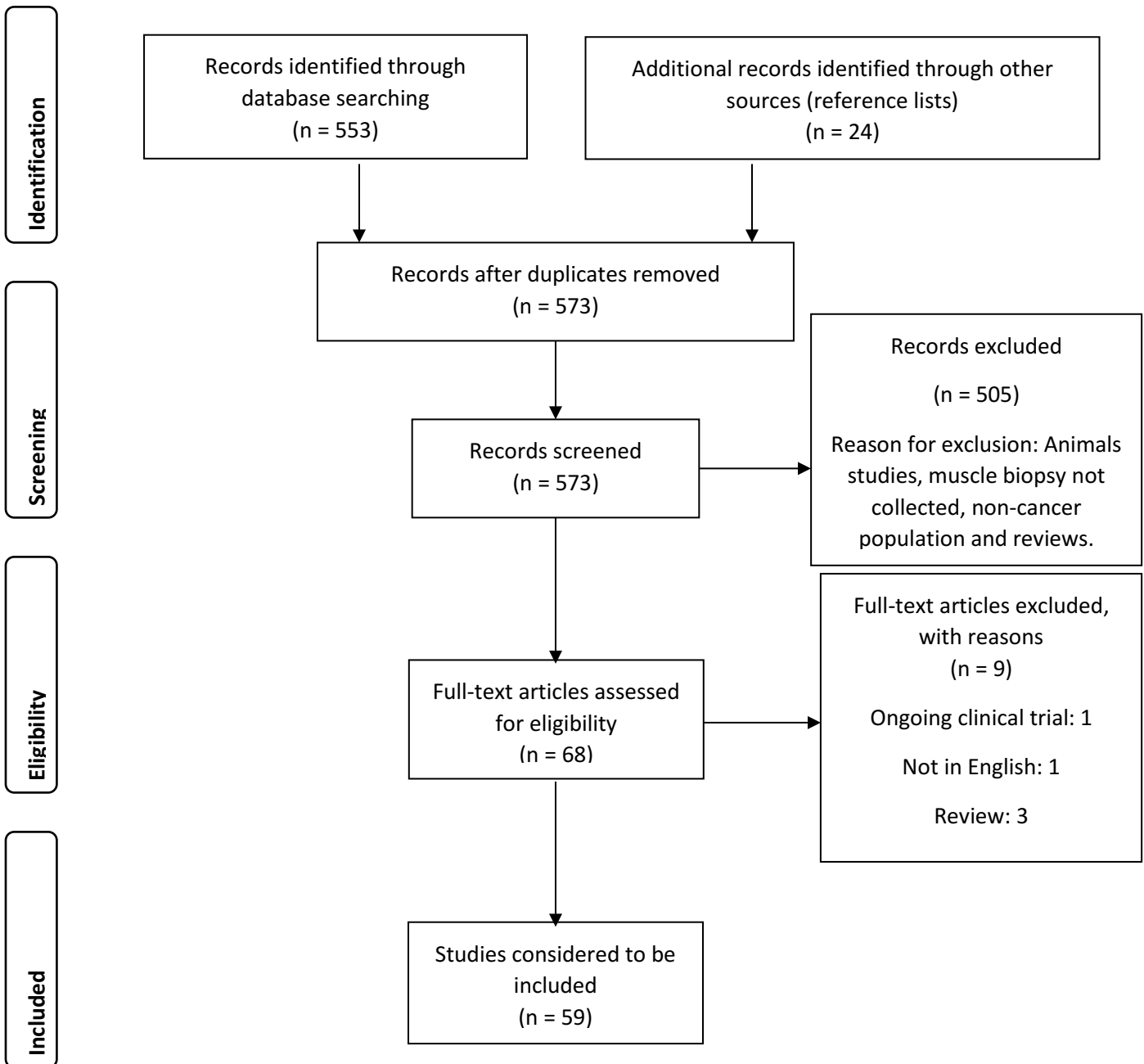
Values (unitless) reported as mean ± standard deviation

^a Cancer type (p=0.003) and metastasis presence (p=0.002) were different between men and women. There were no differences in age, BMI, chemotherapy exposure, comorbidities nor smoking history between men and women.

Table 3.8 Summary of recommendations for muscle biopsy processing and population characterization

- A) Biobanking protocols and tissue manipulation:
- For intraoperative muscle biopsies, collect at the start of the surgical procedure and avoid cauterization.
 - Avoid or report the use of foreign substances (e.g. use of saline-moistened gauzes)
 - Report waiting periods between surgical/needle removal, transportation to other facilities and freezing; include the use or not of crushed ice during the waiting process.
 - Report any removal of blood traces or unrelated tissue from the muscle biopsy.
 - If muscle is “immediately frozen” clarify the location, time and other relevant details (e.g. RNA stabilizer solution) of this action after the surgical removal.
 - Sample storage recommended $\leq -70^{\circ}\text{C}$; however, the temperature selection will depend on the molecules of interest and/or experimental techniques.
- B) Cancer population characterization.
- Clearly state the patient selection method and possible limitations.
 - Report information on metastatic status or tumour classification.
 - Report comorbidities and medications.
 - Report past or current exposure of antineoplastic treatments.
- C) Inclusion of control groups
- Provide a clear characterization of the control group.
 - Report comorbidities and medications.
 - Match age and sex with study population. Provide justification for case-matching criteria
 - Collect same muscle in control and study populations.
- D) Classification and results
- Avoid mixing the results of two or more muscle groups or comparing one muscle group with a different muscle group (e.g. rectus abdominis versus quadriceps).
 - Acknowledge sexual dimorphism in skeletal muscle by reporting results based in male and females, include mean and standard deviation.
 - Classification of cancer cachexia should include both, body composition analysis (muscle mass values) and weight loss

Fig.3.1 Flow chart of search. PRISMA diagram for the identification, screening, eligibility and inclusion of papers (January 1st 1990 – August 16th 2018) from SCOPUS. All articles included investigated cancer, skeletal muscle and muscle biopsies. Excluded records: review articles and ongoing clinical trials



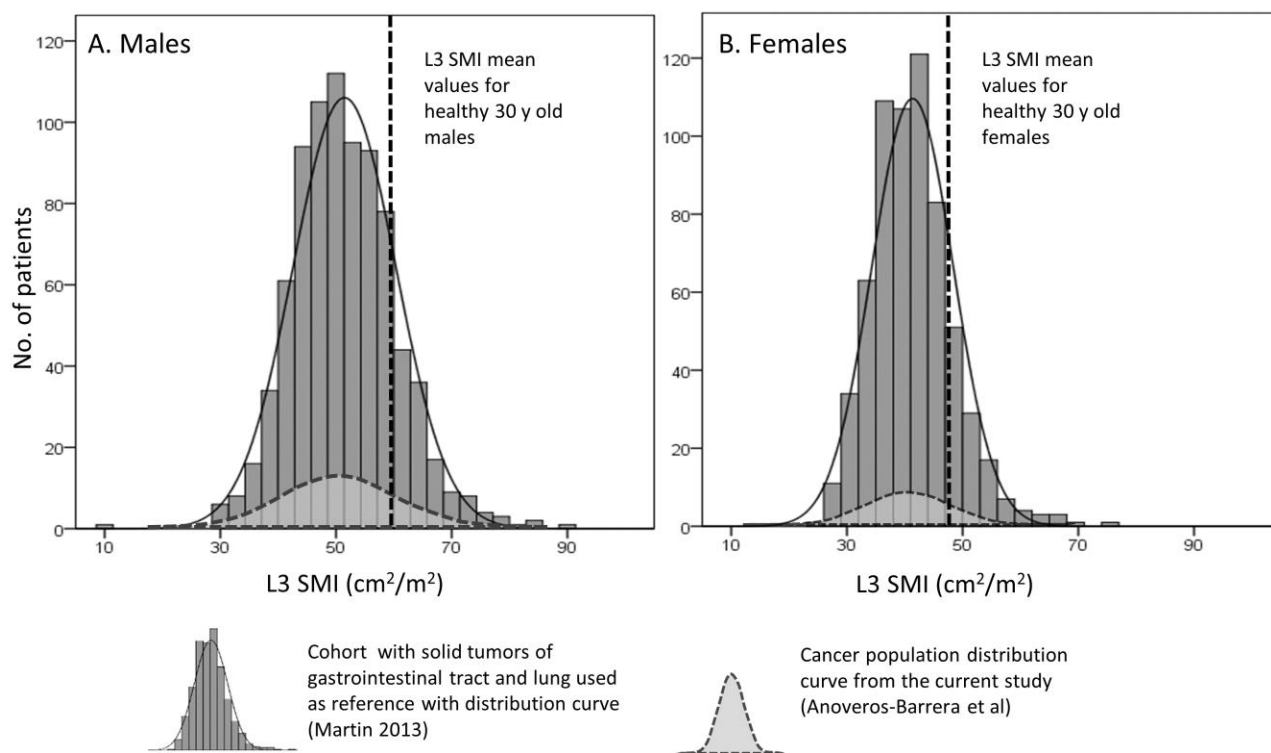


Fig.3.2 SMI distribution for male and female in the present study in comparison to a larger cancer cohort from same region and similar clinical characteristics

Figure represents overlap of L3 SMI distributions for male (A) and female (B) patients of current cancer population (small, light gray distribution) and a cancer cohort with solid tumors of gastrointestinal tract and lung (big, dark gray distribution) (Martin et al. 2013 and Kazemi-Bajestani et al. 2015). A. L3 SMI mean \pm standard deviation values are $50.8 \pm 8.3 \text{ cm}^2/\text{m}^2$ and $51.5 \pm 8.9 \text{ cm}^2/\text{m}^2$ for the current population and Martin et al. gastrointestinal and lung cancer cohort, respectively. B. L3 SMI mean values are $39.8 \pm 6 \text{ cm}^2/\text{m}^2$ and $41.3 \pm 7 \text{ cm}^2/\text{m}^2$ for the current population and Martin et al. gastrointestinal and lung cancer cohort, respectively. L3 SMI mean values for healthy 30 y old kidney donor candidates (dotted line) are placed at 60.9 and $47.7 \text{ cm}^2/\text{m}^2$ for males and females, respectively (Derstine et al.2018).

Chapter 4: Immunohistochemical phenotyping of T cells, granulocytes and phagocytes in muscle of cancer patients: association with radiologically-defined muscle mass and gene expression

4.1 Introduction

Systemic inflammation is a recognized contributor to muscle wasting in cancer. Pro-inflammatory mediators secreted by the tumor microenvironment and host responsive tissues (i.e. adipose tissue) can activate circulating and tissue-resident immune cells (Baracos et al., 2018). In skeletal muscle tissue, interactions between muscle and immune cells can confer an inflammatory environment promoting muscle loss through various mechanisms. For instance, pro-inflammatory cytokines such as tumor necrosis factor (TNF) alpha and interleukin (IL)-6, secreted by innate (e.g. phagocytes and granulocytes) and adaptive (e.g. T cells) immune cells, can stimulate muscle catabolism by activating nuclear factor kappa B (NFκB) (Baracos et al., 2018; Egerman et al., 2014). Studies in experimental models report that these inflammatory cytokines can also inhibit anabolic hormones resulting in the impairment of protein synthesis (De Alvaro et al., 2004). Integrity of muscle fibers can be compromised by the direct cytotoxic effect of T cells, as observed in muscle inflammatory diseases (e.g. polymyositis and dermatomyositis) in humans (Hohlfeld et al., 1991; Pandya, Venalis, et al., 2016).

Immune cell presence has been identified using CD45, a general leukocyte marker, in muscle of patients with early stage colorectal cancer (Zampieri et al., 2010); however, further characterization and quantification has never been performed in the cancer population. Innate immune cells profiled as neutrophils and macrophages with single immune markers such as CD11b or CD15 or CD14 have been identified in muscle tissue of populations with myopathy (polymyositis and dermatomyositis), obesity and exercise-induced stress (Bruun et al., 2006; Englund et al., 2002; C Malm et al., 2000; Christer Malm et al., 2004). Presence of T cells within muscle tissue is commonly explored using CD3 with or without CD4 or CD8 in patients with myopathy and healthy adults undergoing eccentric exercise (Dorph et al., 2006; Englund et al., 2002; C Malm et al., 2000; Christer Malm et al., 2004; Pandya, Loell, et al., 2016).

Exploration of the skeletal muscle immune environment is emerging in human muscle biopsies, which will enable a better understanding of the immune components that contribute to cancer-associated muscle wasting. Also, secondary analysis of oncologic images has enabled the precise characterization of muscle mass distribution in the cancer populations from which these biopsies are derived (Anoveros-Barrera et al., 2019). Comparison of cancer patients with and without

muscle wasting is providing new mechanistic insights into muscle loss in the cancer population (Narasimhan et al., 2017, 2018).

Therefore, in this study we aimed to investigate the skeletal muscle immune-environment by exploring the presence of different immune cell populations and their relationship to muscle mass in cancer patients undergoing abdominal surgery. It was hypothesized that cancer patients with lower muscle mass have more phagocytes/granulocytes (CD11b, CD15 and CD14) and T cells (CD3, CD4 and CD8) within their muscle tissue.

4.2 Methods

4.2.1 Study population

Thirty cancer patients undergoing elective abdominal surgery for purposes of cancer diagnosis, primary treatment or liver metastasis removal were consecutively approached to participate. Previous history of muscle inflammatory disease (i.e. polymyositis, dermatomyositis, and inclusion body myositis) was considered as exclusion criteria. Subject demographics and clinical information were extracted from clinical charts. The majority of patients included in the study were naïve to chemotherapy and radiotherapy (n=23). Three patients had chemotherapy 9 months prior to the biopsy. Three patients had chemotherapy one month prior to the biopsy. One patient received chemotherapy and radiotherapy 4 months prior to the biopsy.

Written consent for participation in the present study was obtained from all patients previous to intraoperative collection of muscle biopsy. This study was approved by the Health Research Ethics Board of Alberta-Cancer Committee, all patients provided informed consent previous to the surgery. Procedures were performed from July 2015 to July 2017 at the University of Alberta Hospital, Edmonton, Canada under the protocol ETH-21709: *The Molecular Profile of Cancer Cachexia*.

4.2.2 Radiological assessment of muscle mass by CT scan

Pre-operative CT scans performed as the standard of care in the cancer were used to quantify skeletal muscle L3-CSA (Mourtzakis et al., 2008; C. M. M. Prado et al., 2008). Briefly, CT images collected at the 3rd lumbar vertebrae (L3) were analyzed with Slice-O-Matic® V4.3 (Tomovision, Montreal, QB, Canada), L3 muscle CSA was identified at a range of -29 to +150 Hounsfield Units (HU). Skeletal muscle index (SMI) was obtained by adjusting muscle CSA for height

(cm²/m²). These pre-operative CT images document the inclusion of male and female patients representing the entire SMI distribution of the population being sampled (n=1473) from our regional cancer center in Alberta, Canada (Fig.4.1) (Martin et al., 2013). SMI z-scores for each subject were calculated based on sex and decade of age using mean values and standard deviation of the population cohort (Kazemi-Bajestani et al., 2016). Further group comparison (low and normal muscle mass) was done based in SMI mean \pm standard deviation of 30 year old healthy individuals (Derstine et al., 2018).

4.2.3 Muscle biopsies

Rectus abdominis (\approx 1 g) was collected at the initial stage of the surgical procedure. Upper abdominal transverse incision was performed, muscle was collected by sharp dissection without the use of electrocautery and biopsies were placed on ice within 10 minutes. On average, a period of 30 minutes occurred between biopsy removal and arrival in the laboratory. Visually evident adipose and connective tissue was removed from the muscle specimen. For morphological assessment, tissue was frozen in cooled isopentane and stored at -80°C. Sample processing time after the arrival of the specimen to the laboratory was within 1.5 hours; procedures were performed under sterile conditions and tissue was kept on ice.

4.2.4 Immunohistochemistry

Immunofluorescence was performed in transverse serial sections of 10 μ m thickness cut with cryostat Leica model CM300 at -22°C. Experiments were done using three serial sections, two slides for immune cell identification [antibody combination: 1) CD3, CD4 and nuclear stain and 2) CD11b, CD14, CD15 and nuclear stain] and one slide for muscle fiber area assessment [antibody combination: 3) Laminin/dystrophin]. Tissue slides (ApexTM superior adhesive slides, Leica Biosystems) were fixed in acetone at -20°C, washed several times in phosphate buffered saline (PBS) and incubated with blocking solution (PBS-Tween 20, 10% normal goat serum and 1% bovine serum albumin) for one hour. Sections were washed in PBS prior to incubation with primary antibodies (Appendix D) at 4°C overnight. Tissue was washed one time in PBS-Tween 20 and six times in PBS before application of secondary antibodies. Secondary antibodies (Appendix E) used with CD3, CD11b and Laminin/Dystrophin was Alexa Fluor® 647 of goat anti-rabbit IgG, with CD4 and CD14 was Alexa Fluor® 568 of goat anti-mouse IgG1 and with CD15 was Alexa Fluor® 488 of goat anti-mouse IgM. After two hours of secondary incubation at

room temperature, sections were washed six times in PBS. Nuclear stain, 4',6-diamidino-2-phenylindole (DAPI), was added for two minutes. Slides were mounted in ProLong® Diamond Antifade medium, covered with 1.5 thick coverslips and let to dry flat for twelve hours.

4.2.5 Confocal microscopy and histological analysis

Muscle sections were visualized with a spinning disk confocal microscope (Quorum Wave FX Spinning Disc Confocal System – Quorum technologies). Z-stacked images taken across a tissue section using the 20X/0.85 oil lens were assembled together and plane-merged to create a composite image to enable the visualization of a whole and clear tissue cross-section. Volocity 6.3 software [PerkinElmer, Waltham, MA, USA] was used to capture, merge and analyze all images.

Immune cell quantification

Immune cells located in the endomysium were quantified. Assessments were performed on a total area of $2.0 \pm 0.7 \text{ mm}^2$ which included information of 398 ± 97 muscle fibers. Manual immune cell quantification was performed using Volocity® software, results were reported as number of cells per 100 fibers. Values were also presented as number of cells per mm^2 for comparison with other study populations reported in the literature. CD3+CD4- cells were defined as CD8 T cells. Areas excluded for immune cell quantification were: large blood vessels and detectable capillaries, nerves, fibrotic tissue and folded areas. Immune cell populations were identified based on the co-expression of cell surface markers, immune cells were quantified only if they had a nucleus surrounded by fluorescent antibody on the surface (Appendix F). Endomysial areas and muscle fibers were located by increasing the brightness of the image as muscle tissue autofluorescence easily allowed the identification of muscle structures. In addition, muscle fibers and endomysium location was corroborated using serial sections of laminin-dystrophin stain (Appendix G).

Muscle fiber CSA analysis

Image assessment of muscle fiber CSA was done using in Volocity® software. First, muscle fiber CSA (μm^2) was obtained from the detection of membrane fluorescence of single muscle fibers. Second, a mean muscle fiber CSA value was calculated from the area assessment of all muscle fibers per cross-section.

Immune cell isolation and flow cytometry analysis

Mononuclear cells were isolated from rectus abdominis muscle in a subset of n=17 (males=12/females=5) patients using similar procedures to those previously described (Mckay et al., 2010). Briefly, 150 mg of muscle was digested in an enzymatic solution (DMEM with collagenase 1%, dispase II and CaCl₂) at 37°C (5% CO₂). After washing, sample was filtered through a mesh. The pellet was resuspended in PBS with 4% FBS, and cells counted using trypan blue. Volume equivalent to one million mononuclear cells was used. Conjugated antibodies (CD3-BV421 and CD11b-PE-Cy7; BD Biosciences) for cell surface antigens were mixed in aliquot cocktails and added into the respective tubes, including fluorescence minus one controls (FMOs). Samples were incubated at 4°C in the dark for 40 minutes. After incubation, cells were washed twice and fixed with 100µL of 1% paraformaldehyde. Tubes were refrigerated for twelve hours until flow cytometry acquisition was performed with a BD Fortessa X-20 analyzer and BD FACS Diva™ software [BD Biosciences]. Finally, flow cytometry analyses were done using FlowJo© software [FlowJo, LLC] (Appendix H)

4.2.6 Gene expression: Microarray analysis

Microarray analysis was conducted in rectus abdominis muscle from a cohort of patients (n=69 males / n=64 females) previously described (Stretch et al., 2013). Briefly, total RNA was isolated, purified, quantified and subjected to linear amplification and Cy3 labeling and Hybridization to Agilent Whole Human Genome Arrays using Agilent kits (One Color Low RNA Input Linear Amplification Kit Plus, One Color RNA Spike-In Kit and Gene Expression Hybridization Kit) according to the manufacturer's protocols. The arrays were scanned using an Agilent Scanner, the data was extracted and quality was evaluated using Feature Extraction Software 10.5.1 (Agilent). The data were normalized using GeneSpring GX 11.5.1 (Agilent). The data used in this publication have been deposited in the U.S. National Center for Biotechnology Information (NCBI) Gene Expression Omnibus25 and are accessible through GEO series accession number GSE41726.

4.2.7 Statistical analysis

All analyses were conducted in IBM® SPSS® Statistics software, version 24. A test for normal distribution was applied to the continuous variables, immune cells were not normally distributed. To assess associations between immune cells and muscle mass values, Spearman's coefficient was selected. Comparisons between sexes or groups were conducted using Mann-Whitney U (non-

categorical variable) and chi-square or Fisher exact test (categorical variables) where appropriated. Statistical significance was considered at p values less than 0.05.

Gene correlation analyses

Pearson correlation analysis was done in R version 3.4.2 (2017-09-28) using the Hmisc (version 4.1-1) and corrplot (version 0.84) packages. Correlation analysis between CD8A and all other genes in the microarray was used to identify significantly correlated genes. The correlation p-values were adjusted for multiple comparisons using the Benjamini-Hochberg procedure. Correlations were considered significant if they had a false discovery rate (FDR) of <0.05. Of those genes significantly correlated with CD8A, genes associated with CD8 T cell function and muscle catabolism were identified based on a review of the current literature and submitted to further analysis. Correlations between all gene-gene combinations were conducted to examine the relationship between CD8 T cell genes and catabolic genes.

4.3 Results

Patient characteristics are presented in Table 4.1 Mean age was 64 ± 11 years, there were no age differences between men and women. Most patients had gastrointestinal malignancies (91%), with colorectal and pancreatic cancer being common among males and females. Advance stage (IV) was present in 60% of men and 80% of women.

Innate and adaptive immune cells are present in the muscle of cancer patients

T cells, CD3-CD4⁺ and granulocytes/phagocytes were identified in the muscle tissue of patients diagnosed with cancer (Table 4.2 and Fig. 4.2). Immune cells were consistently found in the periphery of the muscle fibers, in the area known as endomysium (Fig. 4.2). In general, distribution of immune cells occurred along the tissue with clear separation between cells (Fig. 4.3). T cells accounted for 67% of immune cells identified within the muscle tissue (Table 4.2). CD8 T cells (CD3⁺CD4⁻) were twice as abundant as CD4 T cells (CD3⁺CD4⁺). A population of CD3-CD4⁺ cells was identified, and represented 14% of the immune cells. CD11b⁺ cells comprised 20% of the immune cells identified, two subtypes of CD11b⁺ cells were identified. CD11b⁺CD14⁺CD15⁺ cells were present at 1.6 fold higher than CD11b⁺CD14⁻CD15⁻ cells. Immune cells with single antigens CD14 or CD15 (without CD11b⁺) were not present. Males had

more CD4 T cells than females (Table 4.2). No other differences between men and women were observed.

Flow cytometry analysis enabled confirmation of the immune populations explored in the immunohistochemistry assays. Immune cells comprised a very small percentage of isolated mononuclear cells. CD3⁺ cells comprised of 1.8±1% (mean ± standard deviation) and CD11b⁺ of 1.6±1.3% (mean ± standard deviation). No statistical differences were found between males and females for CD3 (p=0.2) or CD11b cells (p=0.9). No further analyses were pursued given the low numbers of CD3⁺ and CD11b⁺ cells obtained from muscle tissue.

T cells (CD3⁺), CD3-CD4⁺ cells and granulocytes/phagocytes (CD11b⁺) cells are positively correlated with muscle mass

Muscle mass was evaluated by histological and radiological assessments (Table 4.1). Muscle mass measurements are reported as: muscle fiber CSA, L3-CSA, SMI and SMI z-scores. Correlations between immune cells and muscle mass variables are reported in Table 4.3 Muscle fiber CSA was positively correlated with total CD3⁺, CD4 (CD3+CD4⁺) and CD8 (CD3+CD4⁻) T cells, CD3-CD4⁺ cells and granulocytes/phagocytes subtype 1 (CD11b+CD14+CD15⁺). SMI and SMI z-score, were positively correlated with total CD3⁺ T cells and CD8 T cells.

In women, significant correlations between muscle fiber CSA, CD3⁺ T cells (r=0.8, p=0.006) and CD8 (CD3+CD4⁻) T cells (r=0.9, p=0.001) were observed. In men, muscle fiber CSA was positively correlated with total number of CD11b⁺ cells (r=0.5, p=0.01), CD11b+CD14+CD15⁺ (r=0.6, p=0.007), total CD3⁺ T cells (r=0.5, p=0.01) and CD8 (CD3+CD4⁻) T cells (r=0.6, p=0.01). In addition, CD3⁺ T cells were correlated with SMI (r=0.6, p=0.006) and SMI z-scores (r=0.6, p=0.004); CD8 (CD3+CD4⁻) T cells to SMI (r=0.5, p=0.004) and SMI z-scores (r=0.6, p=0.005) in men.

Comparison of patient characteristics based on normal and low muscle mass

Cancer patients participating in the present study represent the entire SMI distribution reported in a population from the same region with solid gastrointestinal and respiratory tumours (Fig.1). A subset of patients (37%) was identified as having SMI values within what is reported for normal muscle mass in 30 year old individuals (Table 4.4) (Derstine et al., 2018). Further comparison of

patient characteristics between normal and low muscle mass revealed no differences in age and number of men between groups. The prevalence of patients with stage IV and chemotherapy was higher in the low muscle mass group. Patients with the highest proportions of CD8 T cells (≥ 9 cells per 100 fibers) were present in the muscle mass group considered as normal level (Table 4.4 and Fig 4.1).

Gene analysis: CD8 T cells negatively associated with catabolic pathways in muscle

Microarray analyses were performed in rectus abdominis muscle of a second cohort with similar clinical characteristics to our main cohort (Appendix I) (Stretch et al., 2013). Forty-six genes were selected for this analysis representing T cells and CD8 T cell function (Crespo et al., 2013; Kaech et al., 2002; Lyons et al., 2017; Mueller et al., 2013; Stoeckle et al., 2009; Weng et al., 2012), as well as muscle catabolic pathways (Appendix J and K) (Argilés et al., 2014; Baracos et al., 2018; Barreto et al., 2017; Belizário et al., 2001; Cottle et al., 2009; Egerman et al., 2014; Fan et al., 2017; Johns et al., 2017; Marchildon et al., 2016; Milan et al., 2015; Sánchez-Espiridión et al., 2012; Silva et al., 2015). The gene correlation matrix is presented in Fig.4.4 for men (Appendix L). CD8 T cell associated genes and muscle catabolic genes were inversely correlated in both men and women, however more consistent and stronger correlation coefficients were observed in men in comparison to women, as we had seen for the immune cell counts and measures of muscle mass. In men, T cell function and CD8 T cell specific genes were negatively correlated with ubiquitin proteasome genes (FOXO4, STUB1, UBE2R2 and USP2) and autophagy/apoptosis genes (BECN1). Genes from the ubiquitin proteasome (TRIM63, MUL1, FBXO32, UBB, UBC, USP4, UBE2B, UBE2L3, UBA52, and DNAJC11), catabolic signaling (ACVR2B and ACVR1B), apoptosis (SIVA1) and autophagy (ATG13) pathways were negatively correlated with T cell function genes. Apoptotic gene CASP8 was negatively correlated with CD8 T cell specific gene GZMA.

Further gene exploration on the correlation of CD8A gene with regulatory cytokine IL-10 and pro-inflammatory cytokine IL-6 was done. A significant positive correlation was found between CD8A and IL-10 receptor subunit α ($r=0.6$, $p<0.001$), and no significant correlations were observed for IL-10 ($r=0.2$, $p=0.2$), IL-6 ($r=0.2$, $p=0.19$) or IL-6 receptor ($r=-0.2$, $p=0.07$).

4.4 Discussion

This is the first study to investigate the local immune-environment of skeletal muscle by identifying immune cell populations in muscle and their relationship to muscle mass in cancer patients. T cells, CD3-CD4⁺ cells and granulocytes/phagocytes were identified. Assessment of the relationship between immune cell numbers and muscle mass, revealed a greater number of T cells (CD3⁺), granulocyte/phagocytes (CD11b⁺CD14⁺CD15⁺) and CD3-CD4⁺ cells in patients with larger muscle fiber size. In particular, CD3⁺CD4⁻ cells, profiled as CD8 T cells by exclusion, were positively correlated with both histological and radiological indices of muscle mass. In support of this finding, CD8 (CD3⁺CD4⁻) T cell associated genes were negatively correlated with genes involved in muscle catabolic pathways.

In cancer preclinical models, mobilization of immune cells participating in innate and adaptive responses has been observed in several tissues and organs (i.e. blood, brain, liver, adipose tissue) (Burfeind et al., 2019). It is suggested that immune mediators originating in the tumor micro-environment could influence the rearrangement of the immune-environment of skeletal muscle influencing muscle mass (Fig.4.5) (Burfeind et al., 2018; Cannon et al., 2007; Madaro et al., 2014; Tidball, 2017; Zhang et al., 2017). In humans, linear relationships between blood immune cell counts, used as markers for systemic inflammation, and radiological assessments of muscle mass have been reported (Feng et al., 2018; Go et al., 2016; He et al., 2018; Kim et al., 2016; Lin et al., 2018; Malietzis, Johns, et al., 2016; Malietzis, Lee, et al., 2016). Similar to our CD3⁺ T cell findings, peripheral lymphocyte counts, which include T cells and other adaptive responders, have been positively associated with higher SMI in gastrointestinal and lung cancers (Baumann, 2010; Feng et al., 2018; He et al., 2018; Kim et al., 2016; Lin et al., 2018; Zheng et al., 2018). Elevated levels of circulating granulocytes, in particular neutrophils, are consistently reported in cancer patients with low muscle mass (Black et al., 2017; Cho et al., 2018; McSorley et al., 2018; Penafuerte et al., 2016), which is contrary our results from CD11b⁺ phagocyte/granulocyte cells. Importantly, this finding could be explained by the relationship between granulocytes and T cells, where cancer patients with low circulatory neutrophil lymphocyte ratios (NLR) seem to have higher SMI compared to those with elevated NLR. For more individual markers, dendritic cells (phagocytes), which can be identified as CD11b⁺ cells (Merad et al., 2013), have been found to be elevated in the blood of patients with high SMI (Malietzis, Lee, et al., 2016). CD3-CD4⁺ cells, which were positively correlated with muscle fiber CSA, might belong to a subtype of T cells with

a low expression of surface CD3, or even, CD4⁺ antigen presenting cells (Bekiaris et al., 2013; Esashi et al., 2004; Merad et al., 2013; Ravoet et al., 2009). Collectively, this evidence suggests that immune cells influence muscle mass during cancer.

Consistent associations of CD8 T cells (CD3⁺CD4⁻) with histological and radiological indices of muscle mass, revealed that low numbers of CD8 T cells are present in patients with low muscle mass. The associations observed here do not imply causal mechanisms; however, one could speculate on the possibility that CD8 T cells could influence muscle mass. Further exploration on the CD8A gene, suggested an inverse association of CD8 T cells with apoptosis (Caspase 8), autophagy (Beclin 1), catabolic signaling (ACVR2B and ACVR1B receptors) and ubiquitin proteasome (FBXO32, FOXO4, MUL1 and TRIM63), pathways which collectively would result in improvement or maintenance of muscle mass (Fig. 4.5) (Baracos et al., 2018; Egerman et al., 2014; Wing, 2016). In accordance with our findings, downregulation of the CD8A T cell gene is observed in blood of patients experiencing loss of muscle mass, when compared to non-losing patients (Penafuerte et al., 2016). A pilot study, evaluating several circulating CD8 T cells subsets (naïve and memory / pro-inflammatory and anti-inflammatory) in a population with mainly gastrointestinal malignancies, provided a more complex perspective in the relationships between CD8 T cells subsets and lean mass, where pro-inflammatory CD8 T cells (expressing IL-2) were negatively associated with lean mass while other phenotypes were not associated (Narsale et al., 2019).

Cross-talk between muscle and immune cells is essential to restore homeostasis and promote muscle tissue repair after a catabolic event (Tidball, 2017). For instance, positive correlation of CD8A gene with IL-10 receptor, suggests an involvement of CD8 T cells (Endharti et al., 2005; Liu et al., 2015) and other anti-inflammatory immune cells (M2 macrophages) (Deng et al., 2012; Dennis et al., 2013) in the IL-10 pathway of skeletal muscle which involves a reduction in the expression of pro-inflammatory mediators (IL-6, IL-1 α IL- β TNF- α and IFN- γ) leading to the support of anabolic hormones activity and regulation of myogenesis (Dagdeviren et al., 2016; Deng et al., 2012; Trendelenburg et al., 2012).

Comparison of our quantifications and observations suggest that muscle immune-environment from cancer patients might differ from both healthy and inflammatory muscle disease (Table 4.5). We did not observe characteristics of inflammatory myopathy such as immune cell clusters,

muscle fiber infiltration and perifascicular atrophy (Dalakas, 2015). Cautious comparisons with immune cell quantifications done in other muscle groups, inform that higher and variable numbers of T cells are present in patients with muscle inflammatory disease when compared to the present cancer population (Dorph et al., 2006; Englund et al., 2002; Pandya, Loell, et al., 2016). In addition, T cells and granulocyte/phagocytes (CD11b+) in muscle are scarce in healthy individuals in comparison to people with cancer or inflammatory myopathy (Dorph et al., 2006; Englund et al., 2002).

The main scientific approach of this study was based on inter-individual variations of across the range of muscle mass in cancer patients. We biopsied a representative sample of patients (Fig. 4.1) across the entire SMI distribution reported for patients with cancers in our geographical region and our study did not have sampling bias issues (Anoveros-Barrera et al., 2019). In this distribution some patients have muscle mass comparable to the normal range expected for healthy 30 year old individuals (Derstine et al., 2018), and others have significant muscle depletion (Fig.4.1 and Table 4.4). We acknowledge the limitations of our current cohort, where is not completely clear how the effect of advanced cancer stage or chemotherapy exposure are accounted for. It is recognized that advanced cancer is associated with intense catabolism which influences muscle mass and immune cells (Lieffers et al., 2009; Lissoni et al., n.d.; Shibata et al., 1998); however, patients with advanced cancer, which were located among the whole SMI distribution in our study, can experience periods of muscle mass maintenance during their disease trajectory (C. M. Prado et al., 2013). Patients exposed to chemotherapy prior to biopsy were observed along most of the SMI distribution, with the exception of the high end of the distribution. Chemotherapeutic agents promote cytotoxicity and metabolic alterations (Cooper et al., 2015; Crouch et al., 2017; Schiessel et al., 2018); however, long term effects of on muscle immune-environment have not been extensively explored.

Whether muscles of cancer patients are different from those of healthy controls is a legitimate question; however, the feasibility of obtaining rectus abdominis from appropriately matched healthy controls is questionable. This would be limited to healthy persons having elective abdominal surgery, and CT imaging for quantification of muscle mass (a relatively infrequent event). The control population would also need to be proven free of any acute or chronic conditions associated with muscle wasting. As a consequence, a very small number of studies

include healthy controls (Anoveros-Barrera et al., 2019). Our study confirms the presence of immune cells within the muscle of cancer patients; further exploration of immune cell phenotypes (i.e. more detailed analysis of maturation and activation) and immune mediators (e.g. cytokines) is necessary to better understand the local immune cell environment in relation to the muscle mass in cancer. Evaluation of changes of immune cells, muscle mass and disease progression over time will expand on the findings of the current research which is limited by its cross-sectional design.

This is the first study to investigate the local immune-environment of skeletal muscle by identifying immune cell populations in muscle and their relationship to muscle mass in cancer patients. The skeletal muscle immune-environment of patients with cancer is comprised of different immune cells from the adaptive and innate immune response. Muscle tissue immune-environment in cancer patients might differ from healthy conditions and muscle inflammatory disease. Correlations of T cells, granulocyte/phagocytes and CD3-CD4+ cells with histological and radiological muscle mass measurements suggest a relationship between immune cells and muscle mass status. Gene correlation analysis suggests an inverse relationship of CD8 T cells with diverse components of muscle catabolic pathways which might have an impact in muscle mass preservation during cancer. These results will serve to better understand the role of the local immune-environment of skeletal muscle and its implications to muscle mass in cancer.

Table 4.1 Patient characteristics				
	All (n=30)	Males (n=20)	Females (n=10)	P
Age, mean years ± SD (Min-Max)	64±11 (38-81)	63±13 (38-81)	67±7 (52-77)	0.71
Tumor type, % (n):				0.68
Colorectal	37 (11)	35 (7)	40 (4)	
Pancreas	30 (9)	25 (5)	40 (4)	
Liver	10 (3)	10 (2)	10 (1)	
Bile duct	7 (2)	10 (2)	0 (0)	
Gallbladder	7 (2)	5 (1)	10 (1)	
Others†	9 (3)	15 (3)	0 (0)	
Tumor stage, % (n):				0.22
I	3.3 (1)	5 (1)	0 (0)	
II	3.3 (1)	5 (1)	0 (0)	
III	13 (4)	10 (2)	20 (2)	
IV	67 (20)	60 (12)	80 (8)	
N/A	13.3 (4)	20 (4)	0 (0)	
BMI (kg/m²), mean ± SD	27±7	27±6	26±9	0.68
BMI classification, % (n):				0.24
Underweight	10 (3)	10 (2)	10 (1)	
Normal	47 (14)	40 (8)	60 (6)	
Overweight	23 (7)	30 (6)	10 (1)	
Obesity I	7 (2)	5 (1)	10 (1)	
Obesity II	10 (3)	15 (3)	0 (0)	
Obesity III	3 (1)	0 (0)	10 (1)	
Comorbidities, % (n):				
Diabetes type II	30 (9)	20 (4)	50 (5)	0.96
Hypertension	50 (15)	50 (5)	50 (5)	1.00
CVD	23 (7)	25 (5)	20 (2)	0.76
Dyslipidemia	23 (7)	25 (5)	20 (2)	0.76
Computed tomography body composition analysis, mean ± SD:				
L3 Muscle CSA (cm ²)	132.1±33.9	146.8±29.5	102.6±20.3	<0.01*
SMI (cm ² /m ²)	45.8±9.2	49±8.5	40.5±8.4	0.39
SMI z-score (SD)	-0.2±1.1	-0.3±1.1	-0.1±1.2	0.59
L3 Muscle radiodensity (HU)	30.8±9.5	31.4±10.5	30.4±7.6	0.72
L3 VAT CSA (cm ²)	172.3±91.9	188±97.2	150.6±79.7	0.29
L3 SAT CSA (cm ²)	192.8±115.2	165.2±110.7	247.5±102.2	0.015*
L3 TAT CSA (cm ²)	377.1±172.3	365.2±173	409.5±168.9	0.45
Muscle histological characteristics:				
Muscle fiber CSA (μm²), mean ± SD	3154±1408	3707±1329	2047±788	<0.01*

† Others: melanoma, chronic lymphocytic leukemia and lymphoma. N/A: No applicable BMI, Body Mass Index; CVD, Cardiovascular disease; L3, Lumbar 3; CSA, Cross sectional area; HU, Hounsfield Unit; VAT, Visceral adipose tissue; SAT, Subcutaneous adipose tissue; TAT, Total adipose tissue; SMI, Skeletal muscle index; SD, Standard deviation.
* Difference between males and females (p=<0.05).

		All (n=30)	Males (n=20)	Females (n=10)	
Immune cell identified	Antibodies	No. of cells per 100 fibers			p value
Granulocytes/phagocytes:	CD11b+	1.6 (0-8)	1.6 (0-6)	1.6 (1-8)	0.98
a. Granulocytes/phagocytes subtype 1	CD11b+CD14+CD15+	1.0 (0-5)	1.3 (0-4)	0.5 (0-5)	0.32
b. Granulocytes/phagocytes subtype 2	CD11b+CD14-CD15-	0.5 (0-3)	0.0 (0-2)	1.1 (0-3)	0.14
T cells:	CD3+	6.5 (1-24)	8.3 (1-24)	5.5 (1-12)	0.07
a. CD4 T cells	CD3+CD4+	2.3 (0-15)	2.7 (0-15)	1.7 (0-6)	0.05*
b. CD8 T cells	CD3+CD4-	4.1 (1-18)	5.6 (1-18)	4 (1-10)	0.21
CD3-CD4+ cells	CD3-CD4+	0.6 (0-12)	2.0 (0-6)	0.7 (0-12)	0.71

Values reported as median (range). P values from Mann-Whitney U test. * Difference between males and females (p<0.05)

		Total T cells	CD4 T cells	CD8 T cells	CD3- CD4+ cells	Total granulocytes/ phagocytes	Granulocytes/ phagocytes subtype 1	Granulocytes/ phagocytes subtype 2
Muscle fiber CSA	r	0.63	0.41	0.63	0.45	0.29	0.46	-0.05
	p	0.0002	0.026	0.0002	0.012	0.126	0.011	0.784
SMI	r	0.49	0.28	0.44	0.2	-0.003	0.14	-0.16
	p	0.006	0.136	0.014	0.59	0.986	0.44	0.395
SMI z-scores	r	0.44	0.12	0.49	0.24	-0.04	0.05	-0.12
	p	0.016	0.517	0.005	0.186	0.823	0.782	0.527

r= Spearman's coefficient of correlation. p = <0.05: statistical significance. CSA: Cross-sectional area. SMI: Skeletal Muscle Index.

	Normal muscle mass	Low muscle mass	P value
Total sample size, n	11	19	
Males, % (n)	55 (6)	74 (14)	0.25
Age, mean years ± SD	63.5±13	64.3±10.4	0.89
SMI (cm²/m²), mean± SD:			
Males	59±4.9	44.6±5.4	<0.01
Females	47.2±4.0	33.8±5.7	<0.01
Patients with stage IV, % (n)	55 (6)	74 (14)	0.25
Patients exposed to chemotherapy, % (n)	0 (0)	37 (7)	0.025
Patients with ≥9 CD8 T cells per 100 fibers, % (n)	45 (5)	11 (2)	0.043

Normal muscle mass: patients with SMI (cm²/m²) within the mean±standard deviation (SD) of 30 year old healthy individuals (Males: 60.9±7.8 cm²/m² // Females: 47.5±6.6 cm²/m²) as reported by Derstine et. al. (Derstine et al., 2018) Differences between groups were analyzed by Mann-Whitney U test (non-categorical variables) and Fisher Exact test (categorical variables) where appropriate. Statistical significance p <0.05

Study	Subjects	Age (years)	Sample size	Muscle group	Number of CD3+/mm ²	Number of CD11b+ /mm ²
Anoveros-Barrera et al. (Current study)	Cancer population, men and women	64 (38-81)	n=30	Rectus abdominis	12.3 (1.6 - 33.3)	3 (0-13)
Pandya et al. 2016	Myopathy, men and women	64 (43-74)	n=16	VA and TA	13.5 (0.5 - 963)	N/A
Dorph et al. 2006	Myopathy, men and women	58 (38-76)	n=11	VA and TA	Symptomatic muscles: 58.1 (0.5 – 159.8) Asymptomatic muscles: 55.9 (1.1 – 126.8)	N/A
	Healthy volunteers, men and women	51 (47-56)	n=6	VL and TA	1.8 (0.4 – 5.0)	
Englund et al. 2002	Myopathy, men and women.	46 (26-64)	n=11	VL	3 (0-7)	1 (0-10)
	Healthy volunteers, men and women	27 (22-46)	n=7	VL	1 (0-2)	0 (0-1)

Values reported as median (Minimum – Maximum). Myopathy: Polymyositis and Dermatomyositis. VL= Vastus lateralis. TA= Tibialis Anterior. N/A=Not assessed.

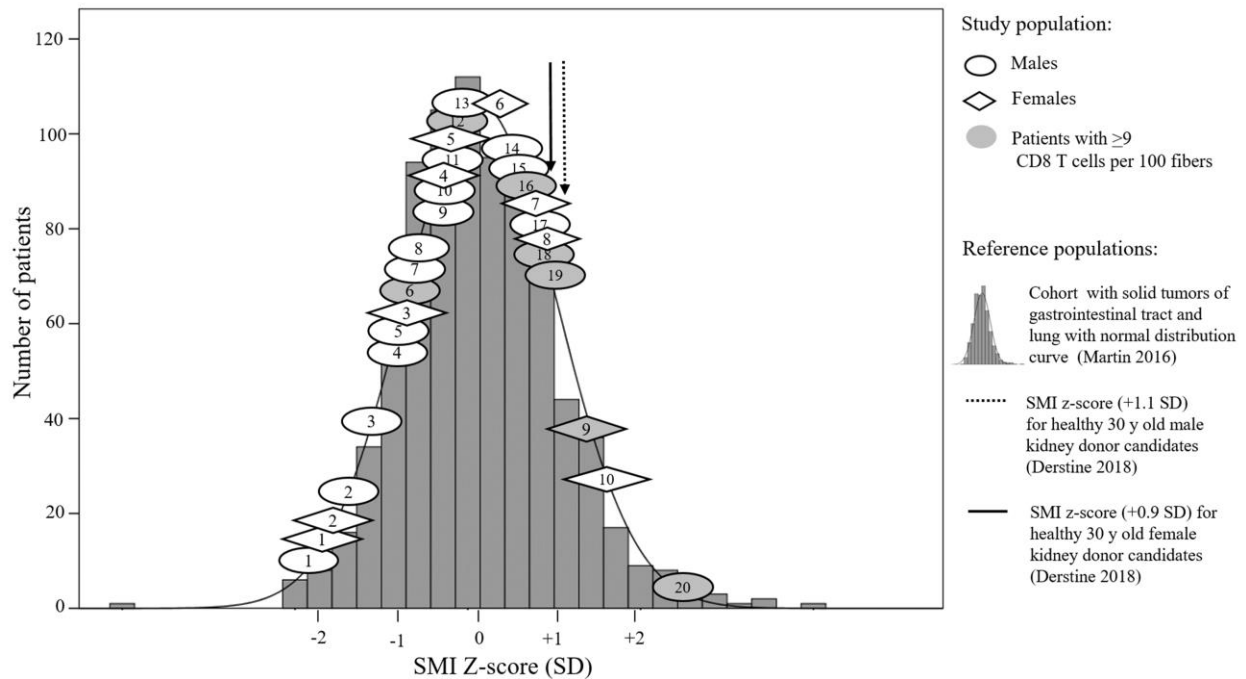


Figure 4.1 SMI z-score distribution of cancer patients in the study

SMI z-scores (SD, standard deviation) for male (n=20, circles) and female (n=10, diamonds) patients of the current study in relation to the SMI z-score distribution (dark gray histogram) from a cancer cohort with gastrointestinal tract and lung solid tumors (n=1473, 58% males) from the same regional cancer centre¹³. SMI z-scores were calculated based in sex and age¹⁵. Circle and diamonds in light gray are patients with highest values of CD8 T cells per 100 fibers. Vertical arrows representing SMI z-scores (SD) for healthy 30 year old kidney donor candidates were placed to highlight cancer patient with SMI z-score values that are similar to the healthy population⁶¹. **Notes:** Only one SMI distribution is shown indistinctively of sex, as male (n=828) and female (n=645) SMI distribution shapes were the same in the Martin et al. cohort¹³. SMI z-scores for healthy kidney donor candidates were calculated by subtracting Martin et al. oncological cohort mean SMI values (males: 51.5 cm²/m² / females: 41.3 cm²/m²) from Derstine et al. healthy 30 year old mean SMI values (males: 60.9 cm²/m² / females: 47.5 cm²/m²) and divided by the SD of Martin et al. oncological cohort (males: ± 8.9 / females: ± 7).

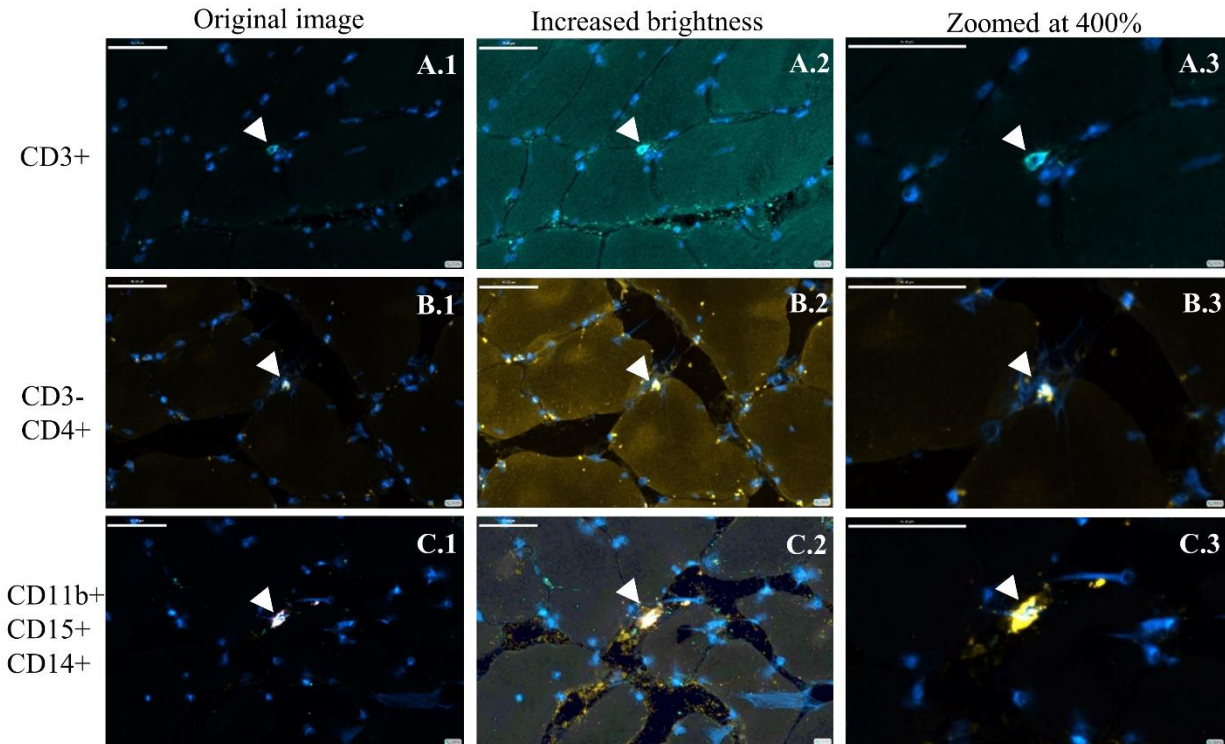


Fig. 4.2 Immunohistochemistry of T cells and phagocyte/granulocytes

Immunostaining of CD3+ (A), CD3-CD4+ (B), and CD11b+CD14+CD15+ (C) cells pointed by the white arrows in muscle tissue of cancer patients. Stained nuclei in blue. A.1, B.1 and C.1 original images with no brightness manipulation. As for images A.2, B.2 and C.2 brightness was increased to visually appreciate the location of the immune cells on the periphery of muscle fibers. A.3, B.3 and C.3 were zoomed to a 400% from the original image. Scale bar 45 μ m.

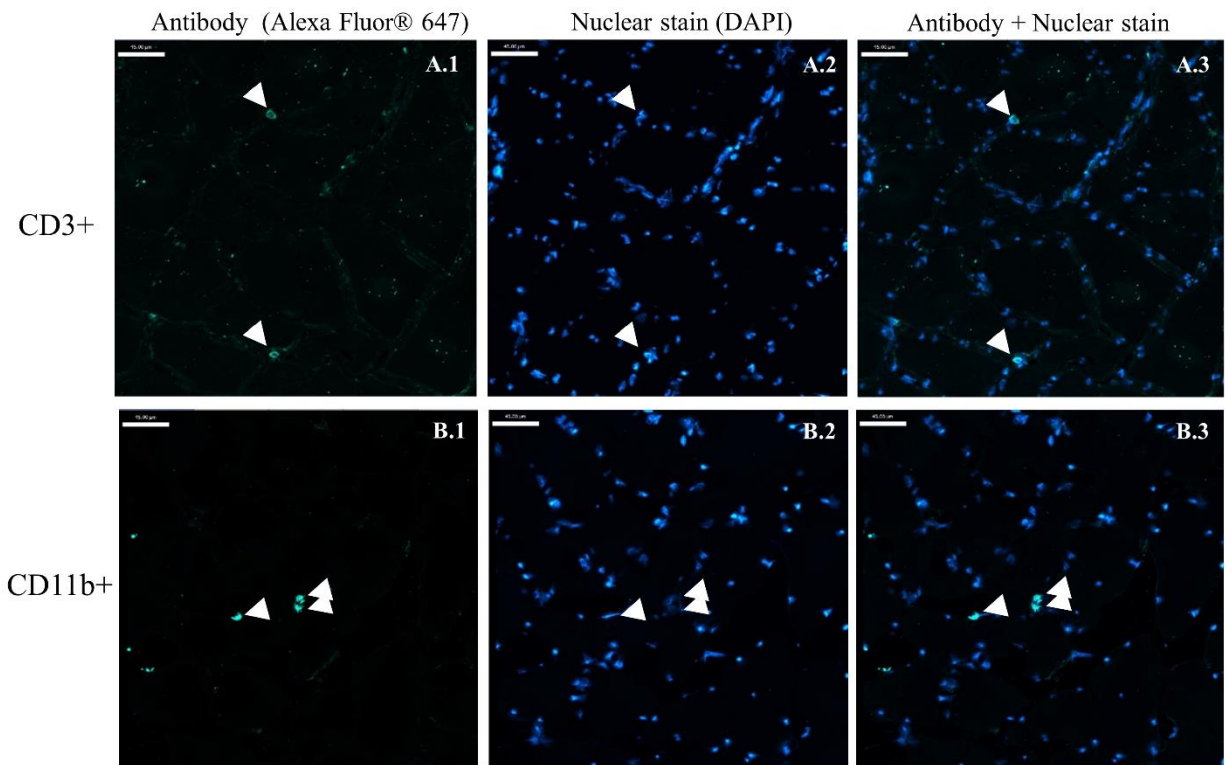


Fig. 4.3 Distribution of immune cells within muscle tissue

Representation of the distribution of more than one immune cell localized on a muscle cross-section. Immunostaining of CD3+ (A) and CD11b+ (B). A.1 and B.1 Antibody detected by Alexa Fluor® 647. A.2 and B.2 Nuclear stain (DAPI). A.3 and B.3 Antibody and nuclear stain. Scale bar 45 μ m

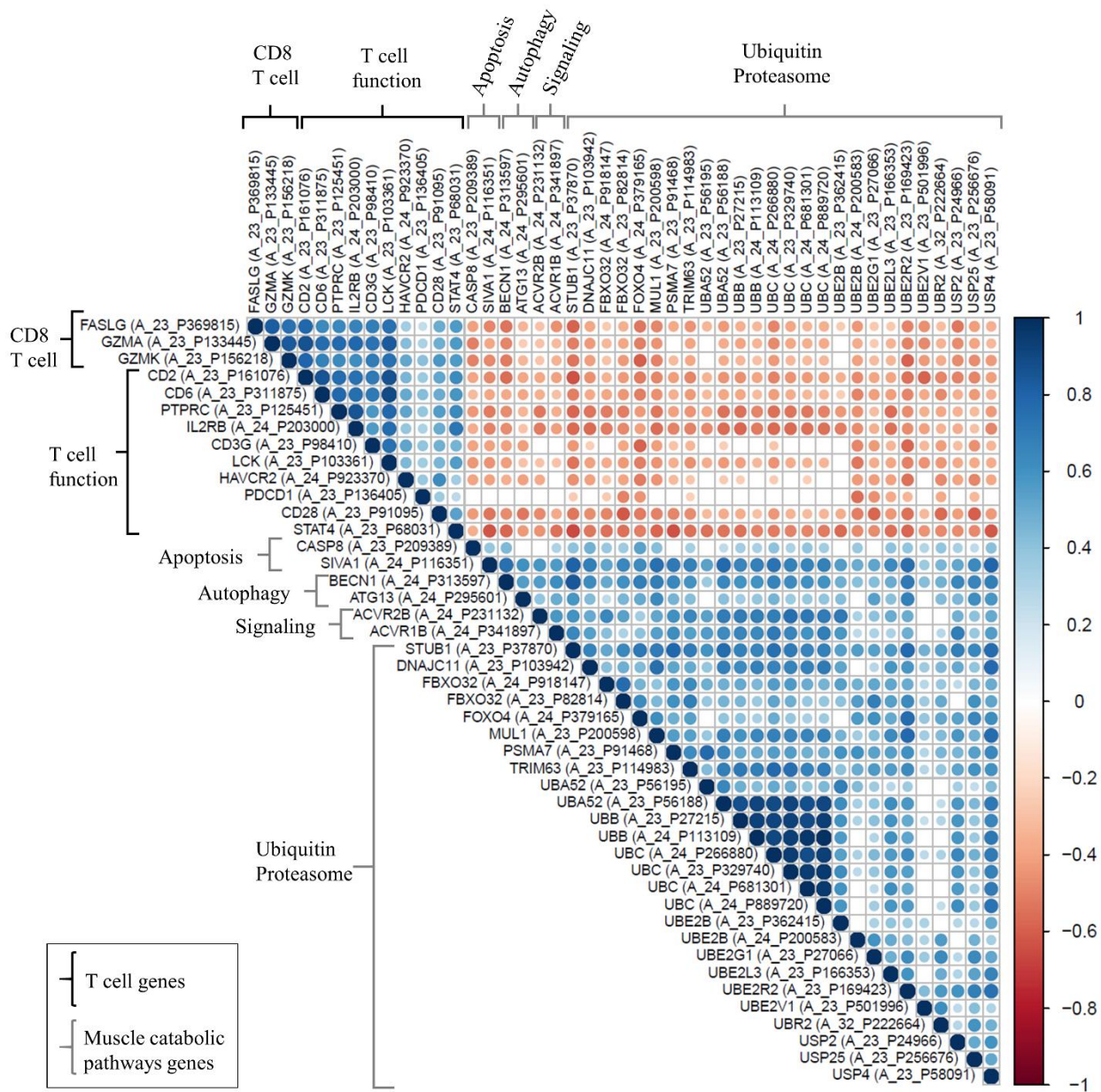


Fig.4.4 Correlation matrix of T cells genes and muscle catabolic pathway genes.

Strength of the correlation is represented by the size and color intensity of each spot, positive in blue and negative in red. Pearson correlation analysis. Gene arrays from rectus abdominis muscle from secondary male cohort (n=69)

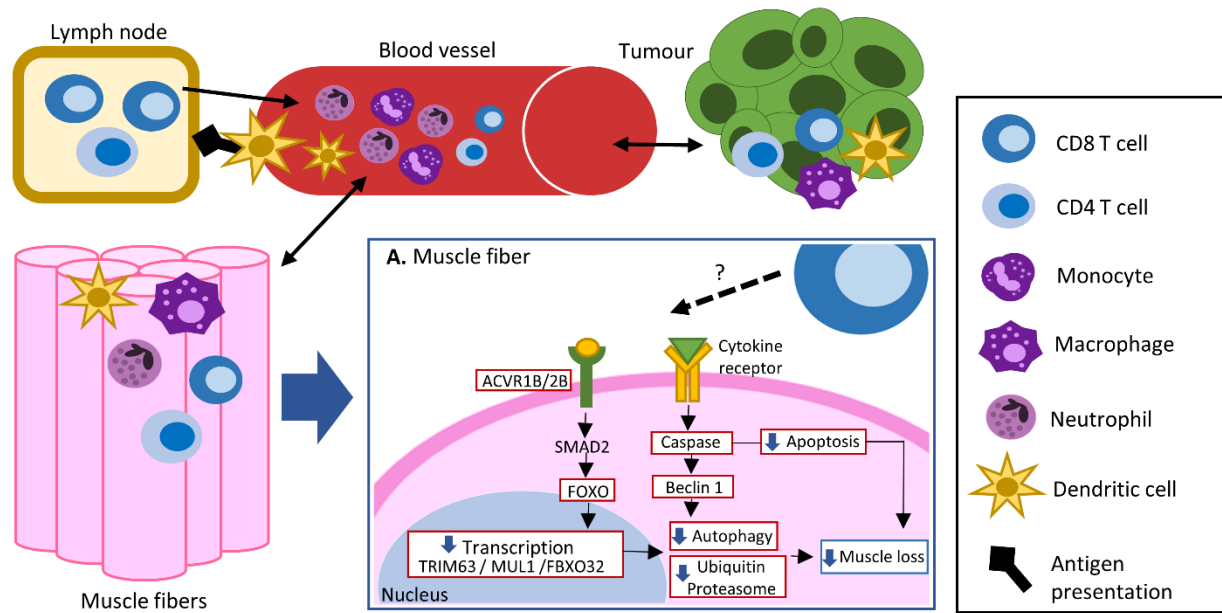


Fig. 4.5 Presence of immune cells in skeletal muscle tissue during cancer and potential role of CD8 T cells in muscle mass preservation

During cancer, changes in immune cell populations occur. Inflammatory mediators secreted by the tumor are capable of activating and mobilizing circulating and tissue resident immune cells. Presence of T cells (CD8 and CD4) within muscle tissue occurs in collaboration of antigen presenting cells (i.e. dendritic cells) that travel from the tissues into the bloodstream and lymph nodes. Once in the muscle, cytokine secretion by T cells, granulocytes (i.e. neutrophils) and phagocytes (i.e. macrophages and dendritic cells) promotes further recruitment and phenotype polarization (inflammatory or anti-inflammatory) of immune cells. A. Close-up of muscle fiber and nucleus. Gene correlation analysis suggest an inverse relationship of CD8 T cells with diverse components (in red boxes) of muscle catabolic pathways which might impact muscle mass.

Chapter 5: Immune cell migratory signaling in skeletal muscle in response to a tumor and irinotecan/5-fluorouracil chemotherapy in a ward colorectal cancer rodent model

5.1 Introduction

In cancer, immune cell migration into skeletal muscle is suspected to be a relevant event occurring in the host in response to a tumor and chemotherapy. For instance, cancer provokes an inflammatory response that leads to a complex recurrent immune response involving the activation and mobilization of immune cells from the innate and adaptive immune response, such as myeloid cells (e.g., neutrophils, eosinophils, macrophages and dendritic cells) and lymphocytes (e.g., T and B cells) respectively (Coffelt et al., 2016; Hanahan et al., 2011; Mumm et al., 2011; Zarour, 2016). While chemotherapy, as an additional source of inflammation, induces perturbations in host immunity, and has direct cytotoxic and pro-catabolic effects in muscle (Barreto et al., 2017; Damrauer et al., 2018a; Schiessel et al., 2018; Sjøblom et al., 2015; Xue et al., 2009). Neutrophils, macrophages and T cells have been identified within muscle of humans (see Chapter 4) and rodents with cancer (Berardi et al., 2008); however, immune cell migration into skeletal muscle during malignancy and chemotherapy has been less explored.

In skeletal muscle, immune cell migration is a dynamic time-dependent process that occurs in acute and chronic inflammatory events, such as muscle injury and muscle inflammatory disease (e.g. muscle dystrophy, polymyositis, dermatomyositis) (Kastenschmidt et al., 2019; Loell et al., 2011; Porter et al., 2003; Tidball, 2017; Yang et al., 2018). As a result of stress and cell death, damage-associated molecules, such as heat shock proteins, are released from skeletal muscle (Lightfoot et al., 2009). Damage-associated molecules, which have endocrine and paracrine effects, are detected by Toll-like receptors (TLRs) expressed in skeletal muscle, as well as resident and circulating immune cells, triggering the activation of inflammatory pathways (i.e. NFκB) and immune cell migration into the site of damage (Lightfoot et al., 2009; Mojumdar et al., 2016; Pillon et al., 2017; Vidya et al., 2018). A link between immune migration and muscle loss during cancer has been revealed by the exploration of tumor-bearing rodent models (Burfeind et al., 2018, 2019a; Calore et al., 2018; Cannon et al., 2007; Henriques et al., 2018; Ruud et al., 2013; Zhang, Liu, Ding, Miao, et al., 2017). TLR signaling in muscle has been associated to muscle loss through the interaction with danger-associated molecules produced by the tumor (Calore et al., 2018; Zhang, Liu, Ding, Zhou, et al., 2017). Also, other molecules involved in the immune cell migration

process, such as chemokine receptors (i.e. CCR2) and cellular adhesion molecules (i.e. P-selectin), have shown a relation to cancer-associated muscle loss (Burfeind et al., 2019b; B. H. L. Tan et al., 2012).

Our research group developed a system to study interactions of tumor-bearing and irinotecan (CPT-11)/5-fluorouracil (5-FU) chemotherapy exposure (Almasud et al., 2017; Ebadi et al., 2017) in an established ward-colorectal cancer rodent model (Cao et al., 2000). A global gene expression dataset was generated using skeletal muscle of healthy, tumor-bearing, and tumor-bearing chemotherapy exposed rats at day 14 of tumor implantation and 7 days following exposure to one cycle of CPT11/5-FU. We hypothesize that immune cell migration is an event occurring in skeletal muscle in response to the presence of a tumor that is further altered with chemotherapy exposure. Therefore, our first objective was to explore the differential expression of genes encoding known participant in immune cell migration such as TLRs, chemokines, and cellular adhesion molecules, in tumor-bearing and chemotherapy exposed rodents. As our second objective, we decided to evaluate the global gene expression profiles using Ingenuity Pathway Analysis® (IPA) for evidence of differentially expressed genes associated to the presence of lymphocytes and neutrophils in muscle under tumor-bearing and chemotherapy exposure conditions.

5.2 Methods

5.2.1 Animal model

Animal experiments were approved by the University of Alberta Institutional Animal Care Committee. Guidelines of the Canadian Council on Animal Care were followed to conduct all experimental procedures. Female Fischer 344 rats (n=23) from Charles River Laboratories, St. Constant, Quebec, Canada were received at 11 to 12 weeks of age with an average (\pm SD) weight of 127 ± 18 g. Rats were acclimated during seven days (two rats per cage). The animals were maintained at constant temperature (21-22 °C) and air pressure, and at twelve hour light:dark cycle per day. Female rats were selected for the current experiments to facilitate comparisons with our previous work (Almasud et al., 2017; Ebadi et al., 2017; Xue et al., 2009).

5.2.2 Experimental design

A visual representation of the study design is presented in Figure 5.1. Briefly, all rodents [healthy (n=8), tumor-bearing (n=7) and tumor-bearing chemotherapy (n=8)] were handled similarly. Ward colorectal carcinoma (0.05 g, provided by Dr. Y Rustum, Roswell Park Institute Buffalo, NY,

USA) (Rustum, 1989) was implanted subcutaneously in the left flank under light anaesthesia (n=15). Tumor was left to grow for 14 days and at the end of that period rats were euthanized (tumor-bearing n=7). The remaining tumor bearing rats received sequential chemotherapy [tumor-bearing chemotherapy exposed (n=8)] was administered by intraperitoneal injection starting with irinotecan (CPT-11, 50 mg/Kg/day) at day 14, and 5-fluorouracil (5-FU, 50 mg/Kg/day) at day 15. Tumor-bearing chemotherapy exposed rodents (n=8) were euthanized after 7 days. All rats were euthanized using carbon dioxide asphyxiation.

5.2.3 Tumor volume and tumor-free body weight

Subcutaneous tumour length, width and height were measured using calipers, and tumor volume was calculated as previously described (Almasud et al., 2017; Xue et al., 2007). Tumor volume was recorded before CPT-11/5-FU exposure, and the following days. Body weight was assessed every other day for all groups, and at the same time as tumour volume assessment (Almasud et al., 2017). Body weight was converted to tumour-free body weight for analysis and interpretation of results and statistical analysis. For rodents exposed to chemotherapy, relative body weight was compared to the body weight prior to the chemotherapy injections.

5.2.4 Diet and food intake

Rodent diet for all experiments carried out in this study has been previously described (Almasud et al., 2017; Ebadi et al., 2017). Briefly, rodents were feed a basal diet (Teklad TD.84172 basal mix with fat omitted, Harlan Laboratories) with the lipid source added from a mixture of commercial oils (i.e. canola stearine, sunflower and canola) (Table 5.1). Rodent diet had 40% of total energy from carbohydrates, 20% from protein and 40% from lipids. Rats were allowed feed and water *ad libitum*. Food intake was assessed every other day for all groups, and daily after chemotherapy exposure. For rodents exposed to chemotherapy, relative food intake during treatment was compared to the average food intake prior to the intervention.

5.3.5 Muscle mass: total weight and muscle fiber Cross Sectional Area (CSA)

Handling of muscle tissue and morphological laboratory techniques have been previously described (Almasud et al., 2017). Briefly, gastrocnemius muscle was collected and weighed. For morphological preservation the whole muscle was frozen in cooled isopentane and stored at -80°C. Transverse sections of 10 µm thickness were cut with a cryostat (Leica model CM300). Hematoxylin stain was performed to visually delineate muscle fibers for CSA assessment (n=4 per

group). Muscle sections were visualized with a ZEISS AXIO Compound Light Microscope (AX10 Scope A.1, Carl Zeiss Group, Toronto, ON, Canada) at 200× magnification. Images were collated with the Colour images were taken with an Optronics MacroFire Digital Camera (Optronics, Goleta, CA, USA) using a Leica TCS-SP2 spectral confocal and multiphoton system (Leica Camera, Solms, Germany). Muscle fiber CSA from 200 fibers were evaluated. Images were analysed using Image J software.

5.2.6 Statistical considerations for animal and tumor characteristics

Analyses were conducted in IBM® SPSS ® Statistics software, version 24. Data pertaining to tumor volume, food intake, body weight, muscle mass and muscle CSA were reported as mean ± standard error of the mean (SEM), as described elsewhere (give Ref) unless indicated otherwise. Students T-test and one -way ANOVA was used for normally distributed data. Data was tested for normality, and log transformed where applicable. For multiple group comparisons, one-way ANOVA with Bonferroni post-hoc tests was used. Statistical significance was considered at p values less than 0.05 (two-sided).

5.2.7 Total RNA extraction

Total RNA was extracted as previously described (Almasud et al., 2017). Briefly, total RNA was extracted from gastrocnemius muscle (10 mg / n=5 per group) using the MagMax-96 total RNA isolation Kit (Ambion, Austin, TX, USA) following the manufacturer's protocol. For assessing RNA quantity and quality, a NanoDrop spectrophotometer (Thermo Scientific, Wilmington, DE) and Agilent 2100 Bioanalyzer (Agilent Technologies, Santa Clara, CA, USA) were used, respectively.

5.2.8 RNA-sequencing, differential expression analysis and statistical considerations for genomics

Services from PlantBiosis Ltd were used from library preparation to the generation of (.bam) files. RNA-seq libraries were prepared using TruSeq Stranded Total RNA with Ribo-Zero™ Human/Mouse/Rat, TruSeq Stranded Total RNA according to manufacturer's instructions. Total RNA (1µg per sample) was used as an input material, depleted of rRNA and the remaining RNA was purified, fragmented and used for cDNA synthesis. The samples were sequenced on Illumina NextSeq 500 using high-throughput 2x150 nt runs with the density of 35 samples per flow cell to generate 10-13 million reads per sample. Base-calling and de-multiplexing was performed using

Illumina CASAVA 1.9 with default settings. Adapter trimming was done using Trim Galore v.0.4.1. Quality control of the sequenced reads was performed using FastQC v.0.11.4. Trimmed sequences were aligned to the rat reference genome using Tophat 2.0.10 with Bowtie2. Rat Genome (Rnor 6, Ensembl) was downloaded from the iGENOME website and served as a rat reference genome. Aligned sequences were saved as .sam files which were then converted to .bam files and were used for further data processing. Data analysis of the (.bam) files was performed using Partek Flow software. mRNAs were annotated using Ensembl Rattus norvegicus Rnor-6.0.92. Differential Expression analysis was performed using DEseq2 (Fold-change cut-off ≥ 1.5 and P-value < 0.05). Ingenuity Pathway Analysis [®] was used for the functional annotation of the identified DE mRNAs.

5.2.9 Global gene expression profiling: Candidate gene search and Ingenuity Pathway

Analysis [®] (IPA)

In-house data on global gene expression [V. Mazurak and S. Damaraju laboratories] in skeletal muscle was interrogated for immune cell migration and involvement of lymphocytes and neutrophils. To enable such an analysis, data sets from tumor bearing *versus* healthy rats, tumor-bearing chemotherapy exposed *versus* non-exposed, and tumor-bearing chemotherapy exposed *versus* healthy rats were accessed. Initially, a candidate gene search was done to investigate immune cell migration as an event occurring in rodent muscle. Candidate genes were selected based on molecules reported of published literature searched on Pubmed and Google Scholar. First, candidate molecules were identified in the literature [see Appendix M for detailed information on this method]. Second, a search for the gene encoding each candidate molecule was done and confirmed (www.genecards.org) to elaborate a candidate gene list (Table 5.2).

IPA was used to identify genes associated with the presence of lymphocytes and neutrophils in muscle of the present rodent model. First, IPA was used to predict biological processes under an analysis known as “*disease and biological functions*” to identify genes associated to neutrophil and lymphocyte presence. Key words for lymphocytes (*lymphoid cells, lymphocyte, natural killer, B cell, B lymphocyte, T cells and T lymphocyte*) and neutrophils (*myeloid cells, granulocyte, phagocyte and neutrophil*) were searched to identify related *biological functions*. Second, using the gene lists obtained from the IPA *biological function analysis*, an additional search in the literature was done to identify genes encoding surface markers with relevance to lymphocyte and myeloid cell function, to identify those exclusively or highly expressed by immune cells. This

search was done due to the assumption that the gene lists provided by IPA were assembled based on the mRNA expression of myocytes with potential concurrent mRNA expression of other resident and recruited cells (e.g., a variety of immune cells, muscle stem cells and mesenchymal-derived cells), as well as other tissues (e.g., blood vessels, epithelial tissue and intra- and inter-cellular fat) (Farup et al., 2015; Goodpaster et al., 2000; Madaro et al., 2014; Pillon et al., 2017).

Note: For the prediction of biological processes, IPA calculates a separate p-value (p-value of overlap using Fischer's exact test). This p-value is distinct from the global differential expression analysis. Overlap p-value describes the association between expressed genes (molecules) in the interrogated data set and literature annotated molecules within IPA. *Biological functions* are constructed by grouping molecules identified for a specific disease or function by an exhaustive review of the literature.

5.3 Results

5.3.1 Changes in food intake, body weight and tumor volume during cancer trajectory

Food intake was similar during the acclimation period and tumour-bearing phase. Body weight did not decrease in tumor-bearing rats; when rats were exposed to CPT-11/ 5-FU, relative food intake and body weight decreased in the following two days, but recovered by the third day after exposure. Tumor volume was $1.38 \pm 0.22 \text{ cm}^3$ (~1% of body weight) at day 14 of implantation and reached $1.87 \pm 0.54 \text{ cm}^3$ ($p=0.47$) seven days following chemotherapy.

5.3.2 Moderate muscle atrophy is present in tumor-bearing and chemotherapy exposed rodents

Muscle atrophy occurred in tumor-bearing rats, with a reduction of muscle fiber CSA in tumor-bearing rodents (Fig. 5.2), while gastrocnemius weight showed no statistically significant differences ($p=0.16$) between the groups. Tumor-bearing rats had smaller fibers when compared to healthy rodents ($p=0.016$); and a greater reduction of fiber CSA was observed in chemotherapy exposed rodents when compared to healthy rats ($p=0.0003$) and tumor-bearing rats ($p=0.054$).

5.3.3 Candidate search of immune cell migration genes in muscle of tumor-bearing rodents versus healthy

Gene expression of skeletal muscle of tumor-bearing rodents was generated at day 14 following tumor implantation and compared to healthy rodents. There was downregulation of several genes

encoding TLRs, TLR co-receptors and TLR associated molecules which collectively participate in the activation and regulation of innate immune cell mobilization, as well as the induction of secretion of chemokines involved in immune cell migration (Table 5.3, column A) (Andersen-Nissen et al., 2007; Boyd et al., 2006; Dobrovolskaia et al., 2002; Kawasaki et al., 2014; Vidya et al., 2018). Genes encoding surface molecules for TLR-5 and CD14 co-receptor are known to be expressed by myocytes and myeloid cells (Henneke et al., 2001; Pillon et al., 2017). SELE, a gene encoding cellular adhesion molecule E-Selectin which is expressed in endothelial cells at initial stages of the cellular extravasation process, was 12.5 fold higher in the tumor-bearing rodents when compared to healthy rodents. Genes encoding ITGAD and ITGB2A, which together act as the integrin complex CD11d/CD18 expressed at later steps of the extravasation process (Schittenhelm et al., 2017; S.-M. Tan, 2012; Torres-Palsa et al., 2015) , were downregulated in tumor-bearing rodents.

5.3.4 Candidate search of immune cell migration genes in muscle of tumor-bearing exposed to chemotherapy

In tumor-bearing rodents, upregulation of three genes involved in signaling of extracellular TLRs (Kumar et al., 2009), as well as CCL6 gene encoding chemokine ligand CCL6 involved in migration of macrophages (LaFleur et al., 2004), was present after chemotherapy exposure when compared to non-exposed tumor bearing rodents (Table 5.3, column B). It was observed that gene for TLR-adaptor MAL was upregulated when comparing chemotherapy exposed group with healthy rodents (Table 5.3, column C). Gene SELE was upregulated and gene CXCR4 was downregulated in chemotherapy exposed *versus* healthy rodents, a similar fold change to tumor-bearing rodents confirmed that these genes are not further altered by chemotherapy exposure.

5.3.5 Ingenuity Pathway Analysis® (IPA) *biological functions* to identify genes associated with the presence of lymphocytes and neutrophils in muscle of tumor-bearing and chemotherapy exposed rodents

Identification of differentially expressed genes associated with IPA *biological functions* are reported in Figure 5.3 and 5.4 for (a) tumor-bearing *versus* healthy and (b) tumor-bearing chemotherapy exposed *versus* non-exposed rodents, respectively. *Biological functions* of neutrophils and lymphocytes are reported in Table 5.5 and Table 5.6 for group (a) and group (b), respectively, with the individual genes being displayed in Table 5.6 for group (a) and Table 5.7

for group (b). For both tables (Table 5.6 and 5.7), an additional column comparing (c) tumor-bearing chemotherapy exposed *versus* healthy rodents was added as a point of reference to evaluate the effect of the tumor presence and chemotherapy exposure (see Appendix N for overall comparisons of differentially expressed genes between groups).

Sixteen genes were identified as being relevant to lymphocyte and myeloid cell function (Table 5.8). The genes ITGAD, ITGB2, and CD6 were identified as genes exclusively expressed by immune cells; while CD86 and CD80 encode two T-cell costimulatory ligands recognized to be highly expressed by antigen presenting cells (macrophages, dendritic cells and B cells) (Collins et al., 2005; Porciello et al., 2016). CD86, CD80, ITGAD, ITGB2 were identified as differentially expressed in response to the tumor presence (Table 5.6), while CD6 was upregulated following chemotherapy exposure as showed in Table 5.7.

5.4 Discussion

In the present study, evidence of immune cell migration in skeletal muscle was revealed by differential expression of several genes encoding molecules involved in the immune migration process, such as TLR-signaling (TLR5, TLR co-receptor CD14 and TLR-negative regulator CYD), chemokine family (CXCL14 and CXCR4), and cellular adhesion molecules (SELE, ITGAD and ITGB2A) in skeletal muscle of tumor-bearing rodents when compared to healthy rodents. Chemotherapy exposure promoted further alteration on the expression of gene for TLR-negative regulator CYD, and promoted the differential expression on additional genes encoding TLR-adaptor MAL/TIRAP and TLR-associated enzyme IRAK4, as well as chemokine ligand CCL6. Gene exploration with Ingenuity Pathway Analysis® resulted in the identification of three genes (ITGAD, ITGB2, CD6) encoding surface molecules exclusively expressed in lymphocytes and/or myeloid cells, providing initial evidence of their potential presence within skeletal muscle in tumor-bearing rodents, as well as chemotherapy exposed rodents. A hypothetical overview of the expression of differentially expressed genes involved in immune cell migration is presented in Figure 5.5.

Immune cell migration in skeletal muscle under acute and chronic inflammatory events is a dynamic process that follows a time course and includes several phases of immune cell recruitment (Kastenschmidt et al., 2019; Tidball, 2017; Yang et al., 2018); therefore, evidence produced from the present study is considered to be dependent on the time point of assessment. At day 14 of tumor

implantation, several genes involved in activation, support and facilitation of immune cell migration were downregulated, while one gene (SELE) involved in initial steps of cell extravasation was highly upregulated. A pancreatic carcinoma mice model examining immune cell recruitment in brain reported that 10 days post tumor implantation T cell numbers were significantly increased in comparison to 5 days before (Burfeind et al., 2019a). This study suggests that in our model, initial events of immune cell mobilization and migration into muscle in response to the presence of a tumor may have occurred in the days prior to assessment and as in the case of SELE. A study exploring gene expression of chemokines and inflammatory mediators at 48 and 96 hours after cardiotoxin-induced injury (Hirata et al., 2003), suggests that genes that are extremely upregulated at the start of an inflammatory trigger can remain highly upregulated days later. In addition, downregulation of genes might be reflective of a series of regulatory processes post-leucocyte migration, models with experimental gene deletion or endogenous inhibition of TLR5, CD14, CXCL14, CX3CL1, CXCR4, and ITGB2A, suggest that immune cell migration could be negatively impacted by downregulation of any of these genes (Andersen-Nissen et al., 2007; Brass et al., 2007; Forlow et al., 2000; Jeyaseelan et al., 2005; Kesteman et al., 2008; Nara et al., 2007; Shurin et al., 2005; Suzuki et al., 2005; Vasyutina et al., 2005). Collectively, differential expression of genes identified by candidate gene search provided insight on immune cell migration as an event occurring in skeletal muscle in response to the presence of a tumor in a ward colorectal cancer rodent model but the events preceding and proceeding our assessment are not able to be elucidated in this model.

Chemotherapy consisting of CPT-11 and 5-FU agents, are commonly used for colorectal and gastrointestinal cancers (Ciombor et al., 2018; Leal et al., 2017; Wagner et al., 2017; Wang-Gillam et al., 2016). CPT-11, also known as irinotecan, impedes DNA replication, and 5-FU interferes with DNA synthesis (Huehls et al., 2015; Pommier, 2006). Skeletal muscle was assessed seven days after chemotherapy exposure, with a dose designed to limit adverse events (e.g., diarrhea, immunosuppression and death) and align with the clinical experience of cancer patients. Seven days after CPT-11/5-FU exposure there was upregulation of genes MAL/TIRAP, IRAK4 and CCL6, which suggest migration of immune cells, in particular those from the innate response, into muscle of tumor-bearing rodents (Bernard et al., 2013; Dunne et al., 2010; Matsunaga et al., 2011; Pennini et al., 2013; Verstak et al., 2009). Gene CCL6 in particular is known to maintain its upregulation in skeletal muscle days following acute injury or induction to chronic muscle

inflammatory disease (Hirata et al., 2003; Porter et al., 2003). In addition, expression of CCL6 at the gene level is transcribed into protein that localizes to both muscle fibres and mononuclear cells within muscle, as confirmed by immunohistochemistry in a muscle dystrophy mouse model (Porter et al., 2003). Upregulation of genes encoding TLR adaptor molecule MAL/TIRAP and TLR associated enzyme IRAK4 suggests a trigger of TLR signaling in skeletal muscle by introduction of pathogen-associated molecules or damage-associated molecules following chemotherapy exposure. Pathogen-associated molecules could be introduced by gut bacteria translocation as a consequence of the toxic effect of CPT-11/5-FU in the intestinal epithelial barrier (Kucuk et al., 2005; Lin et al., 2014; Nakao et al., 2012). On the other hand, in muscle, chemotherapy activates proteolysis via NF- κ B pathway which promotes secretion of damage-associated proteins in response to myocyte damage (Damrauer et al., 2018b; Thakur et al., 2019, 2018). Importantly, upregulation of cell migratory gene SELE was observed in response of the tumor but no further change was observed after chemotherapy exposure. Collectively, the net effect of the upregulated genes (MAL/TIRAP, IRAK4 and CCL6), suggests that at 7 days of chemotherapy exposure there is upregulation of TLR-signaling with potential migration of innate immune cells into muscle skeletal in tumor-bearing rodents.

Presence of lymphocytes and myeloid cells within muscle in response to the ward colorectal tumor and chemotherapy exposure was suggested by the identification of several genes exclusively expressed by immune cells, such as ITGAD and ITGB2A as well as CD11d/CD18 (Schittenhelm et al., 2017; S.-M. Tan, 2012; Torres-Palsa et al., 2015). Gene expression of CD18 in human skeletal muscle after exercise has been associated to leucocyte tissue infiltration (Hamada 2004). Other genes, such as CD86 and CD80 encode T cell costimulatory ligands recognized to be mainly expressed by antigen presenting cells (Collins et al., 2005; Porciello et al., 2016). Muscle precursor cells (myoblast) express CD86 and CD80 during *in vitro* stimulation with IL-4 (Behrens et al., 1998), suggesting that a simultaneous expression from diverse cell types could be occurring in the muscles of tumor-bearing rodents. Gene CD6, expressed by lymphocytes, was the only transcript identified for tumor-bearing rodents exposed to chemotherapy *versus* non-exposed, minimal mRNA expression of CD6 in murine muscle has been attributed to the presence of lymphocytes (Robinson et al., 1995). These findings provide initial evidence of the potential presence of lymphocytes and myeloid cells within skeletal muscle in response to a tumor and chemotherapy

exposure. As presence of specific immune cell types is not able to be defined based on IPA *biological function* analyses, further experiments are required to expand on these findings.

In addition to the previous results that support our overall hypothesis, the present rodent model experienced mild muscle atrophy, a gradual decline of muscle mass, after the introduction of the ward colorectal tumor, and during tumor progression with chemotherapy exposure. Studies that explored immune cells within muscle in rodents experiencing cancer cachexia syndrome, which involves muscle loss, weight loss, anorexia and inflammation (Fearon et al., 2011), suggest that there is a link between immune cells, muscle mass and cancer (Berardi et al., 2008; Inaba et al., 2018). However, the dynamics of immune cell migration, as well as the role of immune cells in relation to muscle mass degradation or preservation in cancer are unknown. Our findings on immune cell migration and potential involvement of lymphocytes and myeloid cells in the present ward colorectal cancer model, experiencing mild muscle atrophy without anorexia or weight loss, confirm that this area requires further investigation.

The present study, evaluated a global gene expression data set generated from muscle of rodents implanted with a ward colorectal tumor which growth rate and tissue wasting effects reflect clinical experience compared to other experimental models of wasting (e.g., C26 model) known to induce severe tissue wasting and rapid death in a short period of time (Aulino et al., 2010). Exploration of gene expression, in addition to protein expression, at additional time points would be helpful to expand on the sequence of events that occur in the muscle environment after the introduction of a malignant tumor and its short and long-term alterations following chemotherapy exposure. In addition, as the present study was developed in female rat model, confirmation in a male model will contribute to the conclusions of the current findings. In conclusion, this is the first study providing evidence of immune cell migration as a relevant event occurring in skeletal muscle in response to the presence of cancer. Further changes in gene expression after chemotherapy exposure provided insight on the presence of an additional immune cell migratory event occurring in skeletal muscle in response to CPT-11/5-FU anti-neoplastic agents during tumor-bearing conditions. Presence of lymphocytes and myeloid cells was suggested by the identification of differential expression of genes encoding surface molecules exclusively expressed using IPA *biological function* analysis; however, further investigation is required to confirm these findings.

5.1 Composition of rodent diet	
Ingredients	g/100g of diet
Tekland Basal mix (80% of w/w diet):	
Casein	22.7
DL-Methionine	0.3
Dextrose, monohydrate	20.4
Corn Starch	25.5
Vitamins (AOAC, 40055)	1.2
Minerals (Bemhart-Tomarelli, 170750)	4.1
Inositol	0.6
Choline Bitartrate	0.2
Cellulose	5.0
Lipid source (20% of w/w diet):	
Canola stearine	11.7
Sunflower oil	5.2
Canola oil	3.1
AOAC, Association of Official Agricultural Chemists. Lipid source is a mixture of commercial oils.	

Table. 5.2 Candidate gene list: genes encoding molecules with a role in immune cell migration	
Gene classes	Gene list
A. Toll-like receptors	
TLRs	TLR2, TLR3, TLR4, TLR5, TLR6, TLR7, TLR9, TLR10
TLR co-receptors	Ly96 (MD2), RP105, CD36 and CD14
TLR-adaptor molecules	MyD88, TRIF, TRAM, TIRAP (MAL), TRAM
TLR-associated proteins	IRAK1, IRAK4, TRAF6, TRAF3, AP1, TAK1 (MAP3K7), TAB1, TAB2, TAB3, ERK1, ERK2, MAPK14 (P38), JNK, IRF3, IRF7, RIP1, DEAF1, NEU1, SRC, BTK, SYK, LYN, UBE1, UBE2, UBE3, UBC13, UEV1A, PELI1, PELI2, PELI3, TRIAD3A, SMURF1, SMURF2, TBK1, IKKB, IKKA, IKKI, NEMO, IKKBE, IFNB1, IFNG, AP1
Endogenous TLR-associated proteins	GP96 (HSP90B1), CNPY93 (PRAT4A), CNPY4 (UNC93B1), AP3
TLR signaling negative regulators	SOCS1, SOCS3, SIGIRR, CYLD, A20, CBLB, SARM, TAG, DUBA, USP4, TANK, TRIM38, SHP
B. Chemokine ligands and receptors	
C class	Ligand: XCL1 Receptor: XCR1
CC class	Ligand: CCL1, CCL2, CCL3, CCL4, CCL5, CCL6, CCL7, CCL8, CCL9, CCL11, CCL12, CCL13, CCL15, CCL16, CCL17, CCL18, CCL19, CCL20, CCL21, CCL22, CCL23, CCL24, CCL25, CCL26, CCL27 and CCL18 Receptor: CCR1, CCR2, CCR3, CCR4, CCR5, CCR6, CCR7, CCR8, CCR9, CCR10
CXC class	Ligand: CXCL1, CXCL2, CXCL3, CXCL4, CXCL5, CXCL6, CXCL7, CXCL8, CXCL9, CXCL10, CXCL11, CXCL12, CXCL13, CXCL14, CXCL15, CXCL16, CXCL17 Receptor: CXCR2, CXCR3, CXCR4, CXCR5, CXCR6, CXCR7, CXCR8
CX3C class	Ligand: CX3CL1 Receptor: CX3CR1
C. Cellular adhesion molecules	
Immune cells	Selectin: PSGL1 (SELPLG), SELL Integrin: ITGB2, ITGAM, ITGAL, ITGAD, ITGB1, ITGAE, ITGB7 and ITGA4 Cell surface ligands involved in diapedesis: DNAM1 (CD226)
Endothelial cell	Selectin: SELE, SELP Intercellular adhesion molecules: ICAM1, ICAM2 Vascular adhesion molecules: VCAM1 Cell surface receptors involved in diapedesis: PECAM1, CD99, CD99L2, PVR, JAMA, ESAM, CD47
TLR, Toll-like receptors. Alternative names of genes were also searched (www.genecards.org)	

Table. 5.3 Candidate gene search: Differentially expressed genes identified in rodent muscle involved in immune cell migration

Gene Class	Gene ID	Gene description	A. Tumor-bearing <i>versus</i> healthy		B. Tumor-bearing chemotherapy exposed <i>versus</i> non-exposed		C. Tumor-bearing chemotherapy exposed <i>versus</i> healthy	
			P value	Fold change	P value	Fold change	P value	Fold change
A. Toll-like receptors								
TLR-signaling negative regulator	SOCS3	Suppressor of cytokine signaling 3	1.42E-06	-3.4	2.51E-03	2.6	NS	
TLR-associated protein	PELI3	Pellino E3 ubiquitin protein ligase family member 3	1.11E-02	-1.9	NS		NS	
TLRs	TLR5	Toll-like receptor 5	4.07E-02	-1.6	NS		NS	
TLR co-receptor	CD14	CD14 molecule	4.54E-02	-1.6	NS		NS	
TLR-associated protein	DEAF1	DEAF1 transcription factor	4.69E-03	-1.5	NS		NS	
TLR-associated protein	EGFR	Epidermal growth factor receptor	2.66E-03	-1.5	NS		NS	
TLR-associated protein	IRF3	Interferon regulatory factor 3	2.00E-02	1.6	NS		NS	
TLR-signaling negative regulator	CYLD	CYLD lysine 63 deubiquitinase	2.10E-03	1.6	1.74E-02	-1.6	NS	
TLR-associated protein	IRAK4	Interleukin-1 receptor-associated kinase 4	NS		3.63E-02	2.1	NS	
TLR adaptor	MAL (TIRAP)	Mal, T-cell differentiation protein	NS		1.24E-02	2.6	9.85E-04	3.5
B. Chemokine ligands and receptors								
Chemokine ligand	CCL6	Chemokine (C-C motif) ligand 6	NS		2.26E-02	1.5	NS	
Chemokine ligand	CCL24	C-C motif chemokine ligand 24	NS		NS		4.01E-02	-1.8
Chemokine ligand	CX3CL1	C-X3-C motif chemokine ligand 1	1.46E-02	-1.8	NS			
Chemokine ligand	CXCL14	C-X-C motif chemokine ligand 14	8.13E-04	-1.6	NS		NS	
Chemokine receptor	CXCR4	C-X-C motif chemokine receptor 4	1.23E-02	-1.5	NS		1.87E-02	-1.7
B. Chemokine ligands and receptors								
Leukocyte integrin	ITGAD	Integrin subunit alpha D	1.11E-02	-1.8	NS		NS	
Leukocyte integrin	ITGB2	Integrin subunit beta 2	3.50E-02	-1.7	NS		NS	
Selectin family	SELE	Selectin E	6.33E-03	12.5	NS		2.21E-02	12.4
Green= downregulated / Red= upregulated. Genes were identified by a candidate gene search based on published research and review articles.								

Table. 5.4 Tumor-bearing <i>versus</i> healthy rats - IPA® biological function analysis for identification of lymphocyte and neutrophil-related genes			
Functional Annotation	Diseases or Functions	p-value of overlap	# Molecules
Lymphocyte-related function			
Cellular Compromise	Clonal deletion of T lymphocytes	2.89E-03	3
Hematological System Development and Function	Quantity of suppressor T lymphocytes	3.00E-03	2
Neutrophil-related function			
Hematological System Development and Function	Quantity of neutrophils	1.51E-03	30
	Quantity of granulocytes	2.10E-03	39
	Quantity of phagocytes	2.61E-03	50

Table. 5.5 Tumor-bearing chemotherapy-exposed <i>versus</i> non-exposed rats- IPA® biological function analysis for identification of lymphocyte and neutrophil-related genes			
Functional Annotation	Diseases or Functions	p-value of overlap	# Molecules
Lymphocyte-related function			
Cell-mediated Immune Response	T cell development	1.14E-03	26
Cellular Development, Cellular Growth and Proliferation	Proliferation of lymphocytes	1.36E-03	33
Cellular Function and Maintenance	Lymphocyte homeostasis	1.54E-03	27
Neutrophil-related function			
Cell-To-Cell Signaling and Interaction	Recruitment of phagocytes	9.14E-05	17
	Recruitment of myeloid cells	8.36E-04	16
Cellular Movement	Cellular infiltration by myeloid cells	2.78E-04	19
Hematological System Development and Function	Quantity of myeloid cells	6.50E-04	25
Cellular Movement	Cell movement of myeloid cells	6.94E-04	28

Table. 5.6 Tumor-bearing <i>versus</i> healthy rats– Lymphocyte and neutrophil-related differentially expressed genes in rodent muscle identified by IPA® biological function analysis					
		Tumor-bearing <i>versus</i> healthy		Tumor-bearing chemotherapy vs. healthy*	
Gene ID	Gene description	P-value	Fold change	P-value	Fold change
Lymphocyte-related function:					
CD86	CD86 molecule	5.21E-03	1.9	NS	
BCL2	BCL2, apoptosis regulator	1.54E-02	2.4	NS	
CD80	CD80 molecule	3.00E-02	6.0	NS	
Neutrophil-related function:					
A. Neutrophil function					
SOCS3	Suppressor of cytokine signaling 3	1.42E-06	-3.4	NS	
FCGR2A	Fc Fragment Of igg Receptor Iia	2.01E-03	-2.9	NS	
ARID4B	AT-Rich Interaction Domain 4B	3.14E-02	-2.4	NS	
RBP1	Retinol binding protein 1	3.14E-02	-2.4	NS	
NOS2	Similar to Nitric oxide synthase, inducible (NOS type II)	2.34E-02	-2.2	NS	
IL2RB	Interleukin 2 receptor subunit beta	3.19E-02	-2.0	NS	
TGFB1	Transforming growth factor, beta 1	7.65E-03	-2.0	NS	
ORAI1	ORAI calcium release-activated calcium modulator 1	1.77E-04	-1.8	4.24E-02	-1.5

CMKLR1	Chemerin chemokine-like receptor 1	1.55E-02	-1.8	NS	
ARNTL	Aryl hydrocarbon receptor nuclear translocator-like	1.64E-02	-1.8	5.95E-03	-2.4
ADORA2A	Adenosine A2a receptor	2.28E-02	-1.7	NS	
ITGB2	Integrin subunit beta 2	3.50E-02	-1.7	NS	
TLR5	Toll-like receptor 5	4.07E-02	-1.6	NS	
ADAMTS12	ADAM metalloproteinase with thrombospondin type 1 motif, 12	7.25E-03	-1.5	NS	
TF	Transferrin	2.21E-03	-1.5	NS	
TIA1	TIA1 cytotoxic granule-associated RNA binding protein	1.42E-02	1.5	NS	
SERPINB1	Serpine1 mRNA binding protein 1	1.27E-02	1.6	NS	
TET1	Tet methylcytosine dioxygenase 1	3.28E-02	1.6	NS	
KLF5	Kruppel-like factor 5	4.62E-03	1.6	4.84E-02	1.5
DDIT3	DNA-damage inducible transcript 3	1.26E-02	1.7	NS	
SDC1	Syndecan 1	4.76E-02	1.8	NS	
CD1D	CD1d1 molecule	3.16E-03	1.8	NS	
CHST3	Carbohydrate sulfotransferase 3 Enzyme, extracellular communication	1.61E-02	2.3	5.92E-04	4.0
EZH2	Enhancer of zeste 2 polycomb repressive complex 2 subunit	5.03E-03	2.3	1.22E-02	2.5
VTCN1	V-set domain containing T cell activation inhibitor 1	2.60E-06	2.4	NS	
ADIPOQ	Adiponectin, C1Q and collagen domain containing	3.56E-02	2.7	NS	
SNAI2	Snail family transcriptional repressor 2	4.54E-02	3.1	NS	
IRF6	Interferon regulatory factor 6	2.20E-02	7.7	NS	
SELE	Selectin E	6.33E-03	12.5	2.21E-02	12.4
LEP	Leptin	5.53E-03	13.8	NS	
B. Granulocyte function					
CISH	Cytokine inducible SH2-containing protein	2.30E-03	-4.1	NS	
ALOX5	Arachidonate 5-lipoxygenase	1.23E-02	-1.7	NS	
ADGRE5	Adhesion G protein-coupled receptor E5	1.38E-03	-1.6	NS	
CD34	CD34 molecule	1.19E-02	-1.5	1.33E-02	-1.7
LGALS1	Galectin 1	2.14E-03	-1.5	NS	
ZFP35	Zinc finger protein 35	1.47E-02	1.8	NS	
IL17RB	Interleukin 17 receptor B	3.65E-02	3.0	NS	
FCER1A	Fc fragment of ige receptor Ia	2.11E-02	9.5	NS	
C. Phagocyte function					
LTB	Lymphotoxin beta	4.51E-02	-8.0	NS	
ADAM12	ADAM metalloproteinase domain 12	8.94E-03	-2.2	9.41E-03	-2.9
CIITA	Class II, major histocompatibility complex, transactivator	1.26E-02	-2.1	NS	
SREBF1	Sterol regulatory element binding transcription factor 1	2.32E-02	-2.0	NS	
CX3CL1	C-X3-C motif chemokine ligand 1	1.46E-02	-1.8	NS	
ITGAD	Integrin alpha D	1.11E-02	-1.8	NS	
IL34	Interleukin 34	1.82E-02	-1.7	NS	
STAB1	Stabilin 1	1.65E-03	-1.6	NS	

CXCL14	C-X-C motif chemokine ligand 14	8.13E-04	-1.6	NS	
CACNA1A	Calcium voltage-gated channel subunit alpha1 A	3.06E-02	-1.6	1.95E-02	-1.9
TNFSF13	TNF superfamily member 13	3.52E-02	-1.6	NS	
TMUB1	Transmembrane and ubiquitin-like domain containing 1	2.78E-04	-1.5	NS	
NFKBIB	NFKB inhibitor beta	7.41E-04	-1.5	1.05E-02	-1.5
TAL1	TAL bhlh transcription factor 1, erythroid differentiation factor	4.96E-02	1.5	NS	
RPS6KA3	Ribosomal protein S6 kinase A3	2.43E-02	1.6	NS	
IL12RB2	Interleukin 12 receptor subunit beta 2	4.20E-02	1.9	NS	
CD86	CD86 molecule	5.21E-03	1.9	NS	
FGF7	Fibroblast growth factor 7	1.31E-02	2.0	NS	
BCL2	BCL2, apoptosis regulator	1.54E-02	2.4	NS	

Green= downregulated / Red= upregulated, IPA®, Ingenuity Pathway Analysis.
 *Genes identified by IPA were also compared with differentially expressed genes from tumor-bearing chemotherapy exposed rodents versus healthy rodents.

Table. 5.7 Tumor-bearing chemotherapy-exposed versus non-exposed rats – Lymphocyte and neutrophil-related differentially expressed genes in rodent muscle identified by IPA® biological function analysis					
Gene ID	Gene description	Tumor-burden rodents: Chemotherapy vs non-exposed		Tumor-burden chemotherapy vs. healthy*	
		P-value	Fold change	P-value	Fold change
Lymphocyte-related function					
CD6	Cd6 molecule	5.58E-03	-4.9	NS	
NOS2	Similar to Nitric oxide synthase, inducible (NOS type II) (Inducible NO synthase) (Inducible NOS) (inos)	4.71E-02	-3.5	NS	
FOS	Fos proto-oncogene, AP-1 transcription factor subunit	6.81E-04	-2.8	1.46E-02	-2.1
PDP2	Pyruvate dehydrogenase phosphatase catalytic subunit 2	3.28E-02	-2.0	NS	
KDR	Kinase insert domain receptor	1.26E-03	-1.8	1.16E-03	-1.8
MYH6	Myosin heavy chain 6	3.33E-02	-1.7	NS	
MYH11	Myosin heavy chain 11	7.51E-03	-1.7	NS	
NOS1	Nitric oxide synthase 1	3.42E-02	-1.7	7.04E-04	-2.3
MLLT11	MLLT11, transcription factor 7 cofactor	2.93E-02	-1.7	6.03E-03	-1.9
DUSP1	Dual specificity phosphatase 1	2.29E-02	-1.6	3.26E-04	-2.2
CYLD	CYLD lysine 63 deubiquitinase	1.74E-02	-1.6	NS	
DCAF1	DDB1 and CUL4 associated factor 1	4.33E-03	-1.6	NS	
SMAD3	SMAD family member 3	4.11E-04	-1.6	5.03E-06	-1.8
PLEKHA2	Pleckstrin homology domain containing A2	3.62E-02	-1.5	NS	
APOE	Apolipoprotein E	4.28E-02	1.6	5.33E-03	1.9
BCL2L1	Bcl2-like 1	4.91E-02	1.6	NS	
NR2F6	Nuclear receptor subfamily 2, group F, member 6	2.68E-02	1.7	NS	
DPP4	Dipeptidylpeptidase 4	1.87E-02	1.7	NS	
PLA2G2D	Phospholipase A2, group IID	1.85E-02	1.8	NS	
S1PR1	Sphingosine-1-phosphate receptor 1	3.70E-04	1.8	2.58E-04	1.8

ZBTB16	Zinc finger and BTB domain containing 16	8.35E-03	1.8	1.11E-02	1.8
GATA2	GATA binding protein 2	6.19E-03	1.8	1.83E-03	2
E2F2	E2F transcription factor 2	4.49E-02	1.9	NS	
MAFB	MAF bzip transcription factor B	2.32E-02	1.9	NS	
NFKBIA	NFKB inhibitor alpha	3.61E-04	2.0	2.14E-02	1.6
ACKR4	Atypical chemokine receptor 4	2.37E-02	2.0	NS	
CTGF	Connective tissue growth factor	6.56E-04	2.1	NS	
CEBPB	CCAAT/enhancer binding protein beta	2.69E-03	2.1	NS	
IRAK4	Interleukin-1 receptor-associated kinase 4	3.63E-02	2.1	NS	
CD300C	Complement C4B (Chido blood group)	4.76E-03	2.1	NS	
TWIST1	Twist family bhlh transcription factor 1	3.94E-02	2.5	5.87E-06	2.6
ID1	Inhibitor of DNA binding 1, HLH protein	1.40E-03	2.6	5.74E-04	2.8
SOCS3	Suppressor of cytokine signaling 3	2.51E-03	2.6	NS	
PGF	Placental growth factor	2.12E-02	2.6	NS	
FCGR2A	Fc Fragment Of igg Receptor iia	1.42E-03	4.0	NS	
GADD45G	Growth arrest and DNA-damage-inducible, gamma	1.06E-04	4.1	2.71E-04	3.8
CISH	Cytokine inducible SH2-containing protein	7.45E-03	5.2	NS	
KCNA3	Potassium voltage-gated channel subfamily A member 3	1.99E-02	8.3	NS	
LTB	Lymphotoxin beta	1.31E-02	22.6	NS	
Neutrophil-related function					
A. Phagocyte function					
KDR	Kinase insert domain receptor	1.26E-03	-1.8	1.16E-03	-1.80
B4GALT6	Beta-1,4-galactosyltransferase 6	3.37E-03	-1.7	7.21E-03	-1.64
SMAD3	Smad family member 3	4.11E-04	-1.6	5.03E-06	-1.81
CLU	Clusterin	2.75E-02	1.5	5.31E-03	1.7
LYZ	Lysozyme 2	4.13E-02	1.6	NS	
NOD1	Nucleotide-binding oligomerization domain containing 1	1.30E-02	1.6	NS	
RHOB	Ras homolog family member b	5.98E-03	1.6	NS	
APOE	Apolipoprotein e	4.28E-02	1.6	5.33E-03	1.9
S1PR1	Sphingosine-1-phosphate receptor 1	3.70E-04	1.8	2.58E-04	1.8
FERMT3	Fermitin family member 3	3.14E-02	1.9	NS	
NFKBIA	Nfkb inhibitor alpha	3.61E-04	2.0	2.14E-02	1.6
F13A1	Coagulation factor xiii a1 chain	9.94E-03	2.0	NS	
MCPT4	Chymase 1	1.18E-02	2.3	NS	
TWIST1	Twist family bhlh transcription factor 1	3.94E-02	2.5	NS	
PGF	Placental growth factor	2.12E-02	2.6	NS	
MPZ	Myelin protein zero	4.23E-02	2.9	2.45E-02	3.3
FCGR2A	Fc fragment of igg receptor iia	1.42E-03	4.0	NS	
B. Myeloid cell functions					
NOS2	Similar to nitric oxide synthase, inducible (nos type ii) (inducible no synthase) (inducible nos) (inos)	4.71E-02	-3.5	NS	
LIPG	Lipase g, endothelial type	3.01E-03	-3.0	NS	
VTCN1	V-set domain containing t cell activation inhibitor 1	2.96E-04	-2.5	NS	
CXADR	Cxadr, ig-like cell adhesion molecule	4.09E-02	-1.9	NS	
NOS1	Nitric oxide synthase 1	3.42E-02	-1.7	7.04E-04	-2.3

DUSP1	Dual specificity phosphatase 1	2.29E-02	-1.6	3.26E-04	-2.2
TIA1	Tial cytotoxic granule-associated rna binding protein	3.37E-02	-1.6	NS	
NFYA	Nuclear transcription factor y subunit alpha	4.56E-02	-1.6	NS	
NFATC2IP	Nuclear factor of activated t-cells 2 interacting protein	3.84E-02	1.5	NS	
BCL2L1	Bcl2-like 1	4.91E-02	1.6	NS	
ELN	Elastin	4.24E-02	1.6	NS	
NDRG1	N-myc downstream regulated 1	2.92E-02	1.7	1.73E-02	1.8
DPP4	Dipeptidylpeptidase 4	1.87E-02	1.7	NS	
PCOLCE2	Procollagen c-endopeptidase enhancer 2	6.99E-03	1.8	NS	
PLA2G2D	Phospholipase a2, group iid	1.85E-02	1.8	NS	
ZBTB16	Zinc finger and btb domain containing 16	8.35E-03	1.8	1.11E-02	1.8
GATA2	Gata binding protein 2	6.19E-03	1.8	1.83E-03	2
IGFBP3	Insulin-like growth factor binding protein 3	5.64E-03	1.8	2.15E-04	2.3
C1QA	Complement c1q a chain	3.06E-03	1.9	NS	
CTGF	Connective tissue growth factor	6.56E-04	2.1	5.87E-06	2.6
C4A/C4B	Complement c4b (chido blood group)	4.76E-03	2.1	NS	
CMA1	Chymase 1	1.18E-02	2.3	NS	
SFRP5	Secreted frizzled-related protein 5	7.08E-03	2.4	NS	
P2RY6	Pyrimidineric receptor p2y6	1.13E-02	2.5	NS	
ID1	Inhibitor of dna binding 1, hlh protein	1.40E-03	2.6	5.74E-04	2.8
SOCS3	Suppressor of cytokine signaling 3	2.51E-03	2.6	NS	
RBP1	Retinol binding protein 1	4.38E-02	2.7	NS	
PDK4	Pyruvate dehydrogenase kinase 4	2.42E-02	3.0	NS	
CISH	Cytokine inducible sh2-containing protein	7.45E-03	5.2	NS	
LTB	Lymphotoxin beta	1.31E-02	22.6	NS	

Green= downregulated / Red= upregulated. IPA®, Ingenuity Pathway Analysis.

*Genes identified by IPA were also compared with differentially expressed genes from tumor-bearing chemotherapy exposed rodents versus healthy rodents.

Table 5.8 Genes encoding cell surface molecules with relevance to lymphocyte and myeloid cell function identified by IPA biological functions

Gene	Molecule description	Cellular expression in relevance to immune cells and skeletal muscle
CD86**	T cell costimulatory ligand from B7 family	Antigen presenting cells (macrophages, dendritic cells and B cells), and myoblasts stimulated with IL-4 (Behrens et al., 1998; Collins et al., 2005; Porciello et al., 2016)
CD80**	T cell costimulatory ligand from B7 family	Antigen presenting cells (macrophages, dendritic cells and B cells), and myoblasts stimulated with IL-4 (Behrens et al., 1998; Collins et al., 2005; Porciello et al., 2016)
ITGAD*	Integrin CD11d	Variety of immune cells, and its expression in muscle is associated to myeloid cells (Schittenhelm et al., 2017; Torres-Palsa et al., 2015)
ITGB2*	Integrin CD18	Variety of immune cells, and its expression muscle is associated to the macrophages and neutrophils (Schittenhelm et al., 2017; S.-M. Tan, 2012).

FCGR2A	Immunoglobulin receptor that triggers neutrophil phagocytosis	Phagocytes and endothelial cells (Sanders et al., 1995; Shashidharamurthy et al., 2009; Tanigaki et al., 2016).
TLR5	Toll-like receptor 5, innate immune receptor responsive to flagellin	Phagocytes, isolated myotubes and muscle tissue (Boyd et al., 2006; Metcalfe et al., 2010; Shibata et al., 2012; Simonin-Le Jeune et al., 2013; Uematsu et al., 2008) .
CD1D	Lipid antigen-presenting molecule	Cells of hematopoietic lineage and a variety of tissues including muscle (Brutkiewicz et al., 2003; Canchis et al., 1993).
VTCN1	T cell costimulatory ligand from B7 family	Dendritic cells, a variety of tissues including skeletal muscle and malignant tumors. (Bregar et al., 2017; Kryczek et al., 2006; Sica et al., 2003; Sun et al., 2006)
ADGRE5	CD97, adhesion receptor for cell-cell interactions	Highly expressed in lymphocyte and myeloid cells, and less in skeletal muscle (Veninga et al., 2008).
IL17RB	IL17 receptor	T helper cells and vascular endothelial cells (Hunninghake et al., 2011; Wang et al., 2012; Weathington et al., 2017) .
FCER1A*	Immunoglobulin receptor for IgE	Mast cells. Expression in muscle associated to presence of mast cells (Cheng et al., 2007; Potaczek et al., 2009) .
LTB	Membrane bounded cytokine lymphotoxin-beta from tumor necrosis factor family	Expressed in a variety of immune cells and tissues including muscle (Alimzhanov et al., 1997; Creus et al., 2012; Wolf et al., 2010).
STAB1	Scavenger receptor Stabilin-1	Macrophages, and myocytes (Kzhyshkowska et al., 2006; Park et al., 2016).
IL12RB2	Subunit for IL-12 receptor	T helper cells, and a variety of tissues including muscle (Kitz et al., 2017; Koch et al., 2012; Nam et al., 2013).
CD6*	Lymphocyte surface glycoprotein associated to T-cell receptor	T cells and B cells (Enyindah-Asonye et al., 2017; Orta-Mascaró et al., 2016; Singer et al., 1996).
S1PR1	Receptor for sphingosine 1-phosphate (chemoattractant)	Macrophages, lymphocytes and myocytes (Ieronimakis et al., 2013; Skon et al., 2013; Weichand et al., 2013).
*Genes exclusively expressed by immune cells. **Genes recognized to be highly expressed by immune cells. IL:interkelukin		

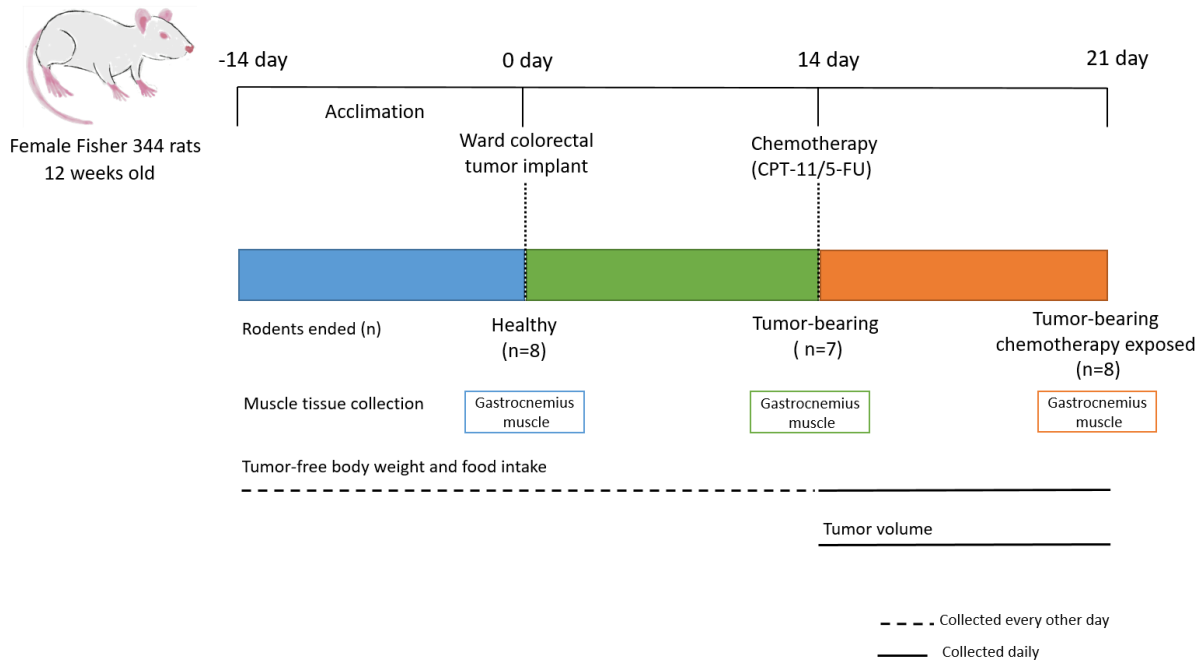


Figure 5.1 Experimental study design. Rats were acclimated for 14 days, prior to ward colorectal tumor implantation. Healthy rats (n=8) were euthanized after the acclimation period. Tumor was left to grow for 14 days in the remaining rats, at the end of that period tumour-bearing (n=7) rats were euthanized. The remaining rats (n=8) received a combination of chemotherapy (CPT-11 administered at day 14, and 5-FU administered at day 15), and were euthanized at day 7 of exposure. Gastrocnemius muscle was collected at all euthanization time points. Tumor-free body weight and food intake were collected every other day, until chemotherapy exposure wherein data was collected every day. Tumor volume was measured daily after chemotherapy exposure.

CPT-11, irinotecan; 5-FU, 5-fluorouracil.

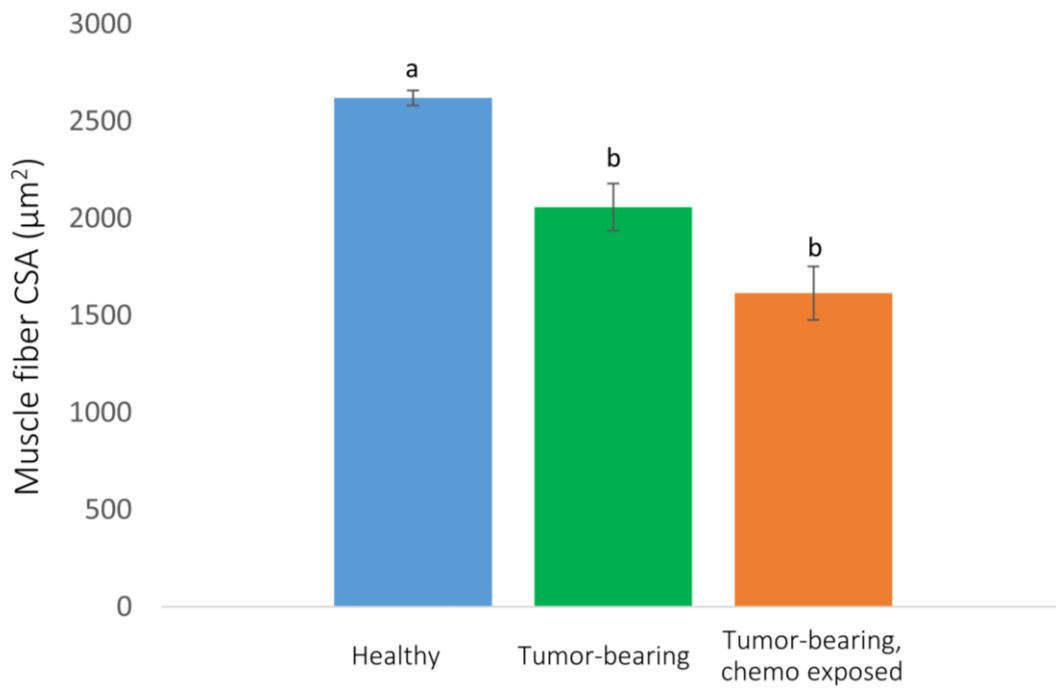


Figure 5.2 Muscle fiber cross sectional area (CSA) of gastrocnemius muscle in various treatment groups (n=4 per group). Tumor bearing and Tumor-bearing and chemo exposed groups were compared with healthy reference group in individual tests. Values are presented as mean±SEM. For multiple group comparisons one-way ANOVA with Bonferroni post-hoc test were selected. Small letter symbols were shown for each histogram. Overlap of these symbols indicate lack of statistically significant differences between the groups. Significance was reported at p value <0.05.

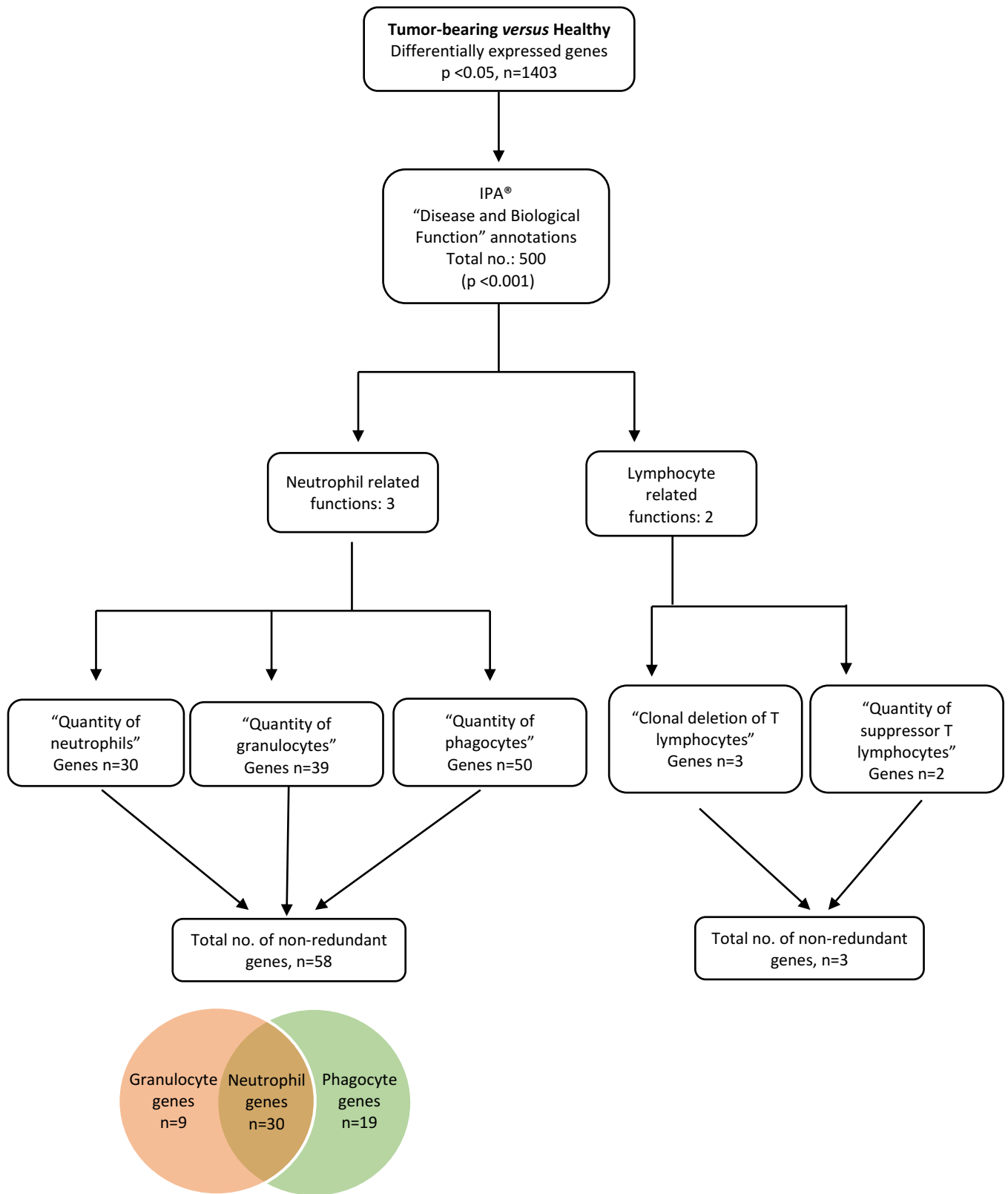


Fig.5.3 Tumor-bearing *versus* healthy (reference) - Flow chart of IPA® (Ingenuity pathway analysis) for biological functions and genes related to neutrophil and lymphocyte involvement.

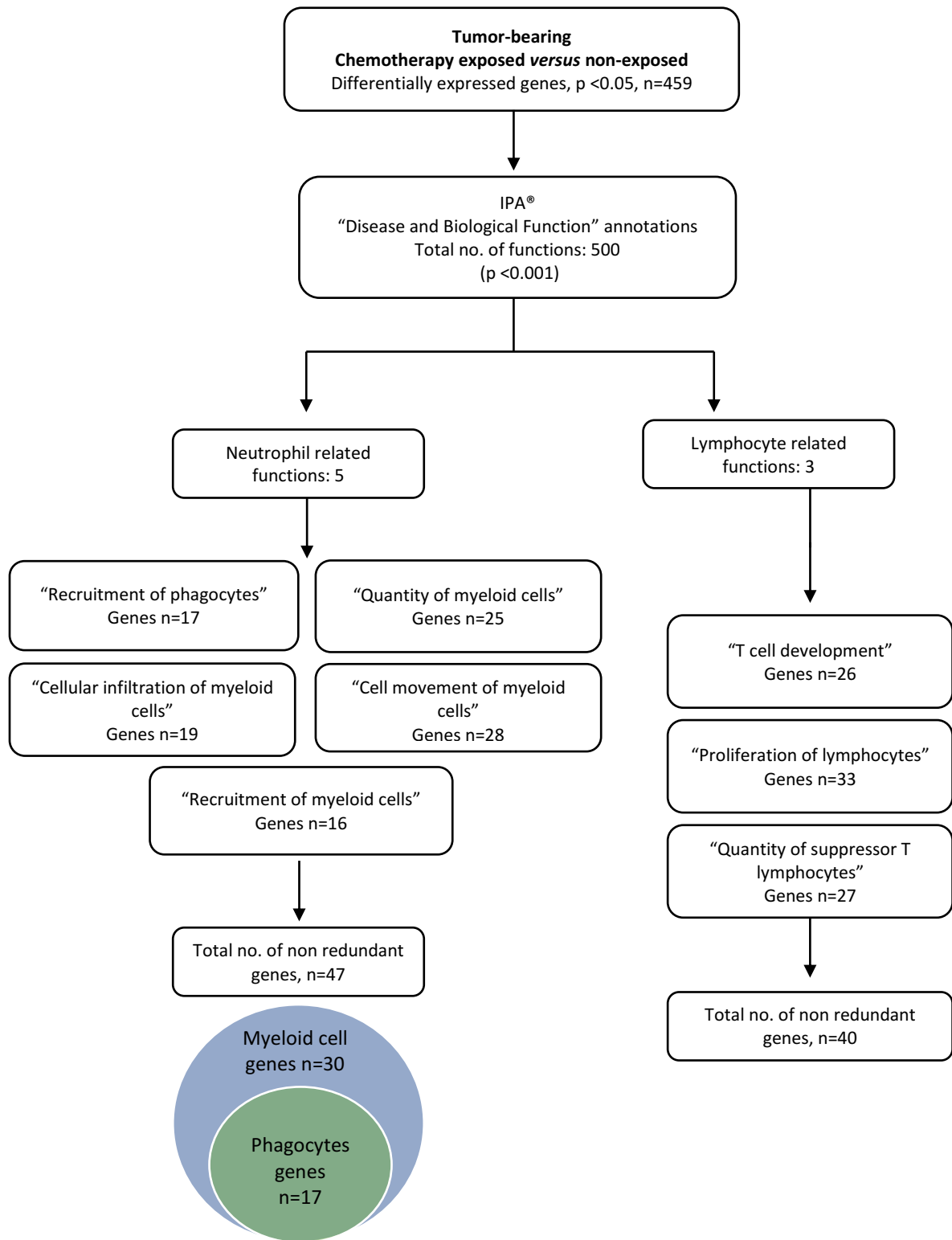


Fig. 5.4 Tumor-bearing chemotherapy exposed *versus* non-exposed - Flow chart of IPA® (Ingenuity pathway analysis) for biological functions and genes related to neutrophil and lymphocyte involvement.

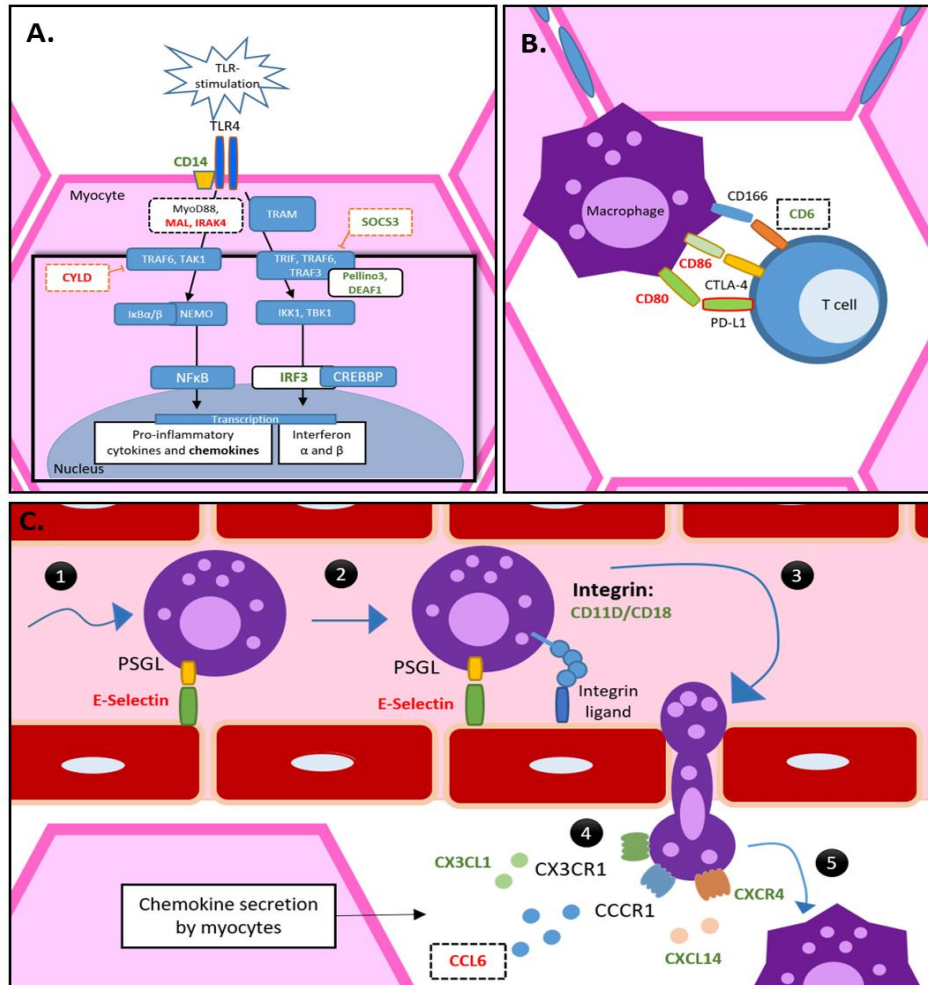


Figure 5.5 Hypothetical overview of molecules encoded by differentially expressed genes identified using candidate gene search and Ingenuity pathway analysis® biological functions for myeloid cells and lymphocytes in tumor-bearing rodents with and without chemotherapy exposure.

Green=downregulated | Red=upregulated | Non-bolded=relevant in the pathway but not identified.

Molecules without a box belong to differential expression of tumor-bearing rodents when compared to healthy. Dotted boxes are molecules of genes differentially expressed in tumor-bearing chemotherapy exposed rodents when compared to tumor-bearing.

A. Stimulation of TLRs occurs when in contact with danger-associated molecules secreted by damaged cells. For instance, stimulation of TLR4 leads to the activation of signaling cascade to translocate NF κ B or IRF3 for the transcription of chemokines and interferon α and β , respectively. Genes for SOCS3 and CYLD, negative regulators of TRAF3 and TRAF6 (Kawasaki et al., 2014), were differentially expressed in tumor and chemotherapy exposure conditions. SOCS3 was initially upregulated in the presence of the tumor and subsequently downregulated upon chemotherapy exposure. For CYLD, the pattern was opposite, being downregulated in the presence of tumor alone, and upregulated following chemotherapy exposure. **B.** The presence of myeloid cells is suggested by the upregulation of T cell costimulatory molecules from the B7 family (CD86 and CD80) in tumor-bearing rodents. After chemotherapy exposure, downregulation of lymphocyte receptor CD6 suggest the involvement of T and B lymphocytes. **C.** Collaboration between immune cell and vascular endothelium is necessarily to promote immune cell extravasation into muscle and genes involved in these processes appeared to be either up or down regulated at diverse steps of these processes for tumor-bearing rodents; while chemotherapy exposure promoted the upregulation of CCL6 gene only. Binding and interaction between of cellular adhesion molecules promotes the capture, slow rolling and total arrest of circulating immune cells. Transendothelial migration is supported by chemokine ligands. Migrating monocytes shift into macrophages once infiltrated into peripheral tissues (Fagerholm et al., 2019; Vestweber, 2015).

Chapter 6: Final discussion

6.1 General summary and review of objectives and hypotheses

Inflammation is recognized as a noted contributor to disease-associated muscle loss (Baracos et al., 2018; Fearon et al., 2011). During cancer, immune cells, as part of the inflammatory response, are suspected participants of cancer-associated muscle wasting. Anti-cancer therapy such as chemotherapy is an additional source of inflammation, which promotes alterations in host immunity and induces muscle wasting (Damrauer et al., 2018; Jung et al., 2015; Schiessel et al., 2018; Sjøblom et al., 2015; Xue et al., 2009). In the present work we were able to explore both human and animal models to expand the knowledge on the involvement of immune cells within muscle during cancer and their relation with cancer-associated muscle wasting. In our human cohort, we characterized and quantified the presence of T cells and granulocyte/phagocytes within muscle to evaluate their relationship with muscle mass. The animal model provided muscle for exploration of evidence for lymphocyte and neutrophil migration as an event occurring within muscle in response to cancer and chemotherapy exposure.

To provide a characterization of abdominal muscle biopsies (*rectus abdominis*) obtained from a well-powered sample size (n=190) to evaluate sources of variations in muscle biopsies such as risk of sampling bias and sexual dimorphisms.

This objective was addressed in Chapter 3, patients from across the whole muscle mass distribution for patients from the same geographical location with similar clinical characteristics were sampled. Sex dimorphisms were prominent for muscle fiber area, CT-derived muscle mass and radiodensity, as well as genes involved in growth, apoptosis and inflammation. Age did not appear to influence muscle fiber area or % of muscle fiber types. Chronic conditions such as diabetes, hypertension, cardiovascular disease and dyslipidemia were prevalent in cancer patients; medications used to control those conditions can independently interfere with muscle physiology. Importantly, this work provided reference ranges for several parameters of interest for *rectus abdominis* muscle for others to use and is contextualized based on a state-of-the-science review (n=59 studies) of the literature from human muscle biopsy material in the cancer setting. Sources of variations identified included sampling strategies, study design, population characteristics, poor data collection and analysis, and technical considerations. A variety of features such as age, sex, comorbidities,

medications, and antineoplastic treatment exposure were likely to be dismissed in the result analysis and interpretation of data. Technical considerations on muscle biopsy collection that must be reported are: time of collection during surgical procedures, transportation and experimental procedure waiting periods, removal of blood traces or unrelated tissue, biopsy handling and storage. Finally, recommendations for muscle biopsy processing and population characterization are provided in Table 3.8.

To investigate the relationship between immune cells from the innate (granulocytes/phagocytes: CD11b, CD15 and CD14) and adaptive (T cells: CD3, CD4 and CD8) immune response with muscle mass measures in cancer patients. It was hypothesized that cancer patients with lower muscle mass have more granulocytes/ phagocytes (CD11b, CD15 and CD14) and T cells (CD3, CD4 and CD8) within their muscle tissue.

This objective (addressed in Chapter 4) was the identification of CD11b⁺ phagocytes/granulocytes (subpopulations: CD11b⁺CD15⁺CD14⁺ cells and CD11b⁺CD15⁻CD14⁻ cells), and CD3⁺ T cells [subpopulations: CD4 (CD3⁺CD4⁺) and CD8 (CD3⁺CD4⁻)] within muscle of cancer patients. However, as opposed to our hypothesis, T cells and granulocyte/phagocytes were positively correlated to muscle mass measurements in our cancer cohort. Granulocytes/phagocytes (CD11b⁺CD15⁺CD14⁺), T cells (CD4 and CD8) and CD3⁻CD4⁺ cell were positively correlated with muscle fiber cross sectional area. In particular, CD8 T cells were the only cells positively correlated to both histological (i.e. muscle fiber cross sectional area) and radiological (i.e. SMI and SMI Z-score) assessments of muscle mass.

Given our rejection of the hypothesis in Chapter 4, further exploration was done in relation to CD8 T cells to further evaluate their potential role in the preservation of muscle mass in cancer. **The objective was to explore the relationship between CD8 T cell-related genes and genes involved in muscle catabolic pathways in cancer patients using transcriptomic analysis. It was hypothesized that an inverse correlation exists between CD8 T cell-related genes and genes involved in muscle catabolic pathways such as membrane signaling, autophagy, apoptosis and ubiquitin proteasome.** The hypothesis was confirmed, inverse correlations were observed between CD8 T cell-related genes and muscle catabolic genes involved in signaling

(ACVR2B), ubiquitin proteasome (FOXO4, TRIM63, FBXO32, MUL1, UBC, UBB, UBE2L3), and apoptosis/autophagy (CASP8, BECN1, ATG13, SIVA1).

To investigate if genes transcribing molecules involved in immune cell migration activation, signaling and extravasation, such as Toll-like receptors (TLR), chemokines and cell adhesion molecules, are differentially expressed in tumor-bearing rats when compared to healthy rodents, and if these genes are further altered by chemotherapy exposure. It is hypothesized that immune cell migration is an event occurring in skeletal muscle in response to the presence of a tumor that is further altered by chemotherapy exposure. This objective was evaluated in Chapter 5, where an analysis was conducted on a global gene expression of differentially expressed genes generated from muscle of (a) tumor-bearing *versus* healthy rodents, (b) tumor-bearing chemotherapy exposed *versus* non-exposed rodents and (c) tumor-bearing chemotherapy exposed *versus* healthy rodent. Evidence of immune cell migration in skeletal muscle was revealed by differential expression of several genes encoding molecules from TLR-signaling (TLR5, TLR co-receptor CD14 and TLR-negative regulator CYD), chemokine family (CXCL14 and CXCR4), and cellular adhesion molecules (SELE, ITGAD and ITGB2A) in skeletal muscle of tumor-bearing rodents when compared to healthy rodents. Chemotherapy exposure promoted further alteration on the expression of gene for TLR-negative regulator CYD, and promoted the differential expression on additional genes for TLR-adaptor MAL/TIRAP and TLR-associated enzyme IRAK4, as well as chemokine ligand CCL6.

As a secondary objective in Chapter 5 we evaluated the global gene expression profiles using Ingenuity Pathway Analysis® (IPA) for evidence of differentially expressed genes related to the presence of neutrophils and lymphocytes under conditions of tumor-bearing and chemotherapy exposure. The hypothesis was that there are differentially expressed genes that encode molecules exclusively or highly expressed in lymphocytes and neutrophils that suggest their presence within muscle in response to tumor burden and following chemotherapy exposure. Gene exploration resulted in the identification of three genes (ITGAD, ITGB2, CD6) encoding surface molecules exclusively expressed in lymphocytes and/or myeloid cells, providing initial evidence of their potential presence within skeletal muscle in tumor-bearing rodents, as well as chemotherapy exposed rodents. Further experiments are required to expand on these findings.

6.2 Considerations for future studies

In Chapter 3, it was identified that several studies using muscle biopsies in cancer patients have a small sample size and selection bias. In our cohort, we were able to characterize patients based on the muscle mass distribution of a larger cancer population from the same region and clinical characteristics (Martin et al., 2013). This characterization provided clarity on the muscle mass distribution of our patients, avoiding sample bias. The present approach is meant to enhance interpretation and comparability of future research done in clinical areas where CT body composition technique is emerging.

Importantly, our study cohort reflects the reality that oncology surgeons experience during their clinical practice in terms of the diagnosis diversity and clinical characteristics. The majority of patients had gastrointestinal malignancies, and underwent abdominal surgery as part of their cancer treatment from which a *rectus abdominis* muscle biopsy was obtained. Nutritional status was not included in our population characterization due to the absence of information in the clinical charts, because nutritional status assessments are not routinely collected in clinical practice. In particular, we noticed a complete absence of routine screening for malnutrition and weight assessment in our study population. For example, in the study cohort for Chapter 4 with a sample of 30 patients, only 6 patients were assessed for malnutrition, 3 patients had no record of their weight, and for 11 patients their weight was taken months before their surgical intervention. Implementation of malnutrition screening tools in the hospital setting is an ongoing effort worldwide (Álvaro Sanz et al., 2019; Arends et al., 2017; Hébuterne et al., 2014); evaluating nutritional status and including this information as part of the patient records provides a more comprehensive understanding of the biological characteristics of individuals experiencing muscle loss. Making CT-derived body composition assessment more accessible in clinical practice could enable improved prognostic characterization and ability to evaluate nutritional interventions that will result in beneficial outcomes for patients and a reduced financial burden to health care system.

In the present study, muscle biopsy evaluation was conducted at a single time point. Intraoperative muscle biopsies are optimal to keep patient discomfort to the essential minimum; however, longitudinal studies on surgical muscle biopsies is challenging as patients may not have repeated surgeries. Identification and validation of a biomarkers in blood and urine, not yet known, but of intense interest and alignment with the immune environment of skeletal muscle hold promise for longitudinal studies. For instance, unpublished data, generated the Mazurak/Baracos laboratories,

has shown an association between blood levels of C-reactive protein, a systemic inflammation biomarker, and genes involved in muscle tissue inflammation generated from *rectus abdominis muscle* of a cancer patient cohort. Involving translational preclinical animal model studies will expand on the knowledge generated by clinical models, and to help understand the dynamics between immune cells and muscle mass.

Flow cytometry was considered as a technique that would enable a robust exploration of the immune cell phenotypes and proportions in muscle. Despite several adjustments to the protocol and expertise of the Flow cytometry core team, numbers of mononuclear cell isolated and proportions of T cells and phagocytes/granulocytes were consistently low, which limited any further analyses with flow cytometry. Similar issues were reported in a study evaluating cancer cachexia in rodents, where few immune cells were isolated from limb muscles of rodents experiencing muscle loss (Inaba et al., 2018). Application and combination of state-of-the-art technologies that enable a large-scale study of genes (e.g. next generation sequencing) and proteins (e.g. proteomics) from limited tissue amount, will provide more robust understanding of the immune environment, their collective and individual role in muscle mass during cancer.

Evidence of potential immune cell migration was captured in Chapter 4 during the characterization of immune cells in muscle of patients with cancer (Appendix O). Later, in Chapter 5, transcriptomics generated from muscle of a preclinical rodent model confirmed that immune cell migration is a relevant event in muscle in response to cancer and chemotherapy. Gene and protein exploration at various time points will contribute to a more comprehensive understanding of the sequence of events around immune cell signaling (e.g. TLR signaling, damage-associated molecules and chemokine secretion) and their migratory response (e.g. expression of adhesion molecules) to cancer and chemotherapy exposure in muscle.

In the preclinical cancer model of Chapter 5, investigation on immune cell migration following chemotherapy provided information on chemotherapy as a factor that influences the immune cell mediated response of skeletal muscle which is already exhibiting cancer-induced muscle atrophy. In clinical practice, patients experience higher levels of chemotherapy toxicity when they have low muscle mass which leads to further exacerbation of muscle wasting (Daly et al., 2018; Kazemi-Bajestani et al., 2016; Pin et al., 2018); more exploration is required to understand the dynamics of several cycles of chemotherapy in the immune cell response in muscle and how does this impact

muscle mass. In addition, new antineoplastic therapies such as *immunotherapy*, which uses components of the immune system to treat tumors, are growing in clinical practice (Goel et al., 2014; Haanen et al., 2017; Kurra et al., 2016). A point of comparison with the use of chemotherapy is relevant to understand the implications and benefits of *immunotherapy* in relation to the inflammatory response and muscle mass in cancer.

Our findings on the immune environment of muscle (Chapter 4) and the involvement of immune cell migration in cancer (Chapter 5), integrate to a complex dynamic involving systemic and tissue-specific immune responses which individually and collectively seem to have an implication on muscle mass status during cancer. Individual and collective exploration in the number of immune cell phenotypes, as well as tumor and tissue interactions, are of value to understand their role in the preservation and loss of muscle mass during cancer (Figure 1.2). Also, dynamics between immune cells and their function in relation to other tissue cells is dependent on the host physical and nutritional status. For example, the presence of CD8 T cell represents danger to the integrity of muscle fibers during muscle inflammatory disease which has an autoimmune component (Hohlfeld et al., 1991; Loell et al., 2011; Pandya et al., 2016). While chronic appearance of CD8 T cells within a tissue is associated with transition into memory cells, which enter tissues for purposes of surveillance without necessarily inducing tissue damage in models without autoimmune disease (Gebhardt et al., 2009; Mueller et al., 2013; Wu et al., 2014); which could be potentially related to the phenotype of our findings. In addition, CD8 T cell presence is essential to promote an anti-inflammatory environment and support proper tissue repair following muscle injury under healthy conditions (Zhang et al., 2014).

In Chapter 4, characterization of the two classical subtypes of T cells (CD4 and CD8 T cells) was performed by exclusion using a CD4 antibody. There is the possibility that a small proportion of non-classical T cells (CD4- and/or CD8-) were combined with CD8 T cells as part of the CD3+CD4- phenotype. For example, gamma delta T cells could be present, however, they are known to represent a minor proportion of T cells (1 to 10%) in human blood (Garcillán et al., 2015).

In our main cancer cohort in Chapter 4, six patients had chemotherapy, one patient had chemo/radiotherapy and four patients experienced surgery (in relation to tumor biopsy), within nine months of surgical procedure where muscle biopsy was collected. It is suspected that the

exposure these treatments might have impacted the number CD8 T cells within the muscle tissue of these patients. Alterations in peripheral immune cell counts, as well as T cell subtypes proportions, are known to occur with exposure to a variety of cancer treatments in humans (Gustafson et al., 2017; He et al., 2017; van Meir et al., 2017). However, the effect of these treatments at a short, medium and long term in the immune cell environment of skeletal muscle is yet to be investigated.

Understanding features of the tumor immune microenvironment is relevant for studies evaluating immune system of the host and its role in muscle mass. An extensive immunogenomic analysis that characterized macrophage and lymphocyte genetic signatures from 33 cancer types identified six profiles of tumor immune-environment: wound healing, IFN-gamma dominant, TGF-beta dominant, lymphocyte depleted, and immunologically quiet (Thorsson et al., 2018). In addition, these diverse tumor immune-environments were associated with clinical outcomes such as survival and progression-free interval (Thorsson et al., 2018). The immune-environment of a tumor is likely to be influencing the characteristics of peripheral immune cells migrating or residing in muscle tissue, and their ability to perform in relation to muscle degradation, anabolism or repair. Inaba *et al.* explored the immune environment and regenerative process of skeletal muscle of rodents implanted with two different tumor types, a colon-26 (C26) which induced muscle wasting, and #KC which did not (Inaba et al., 2018). When muscle injury was induced, C26 implanted rodents exhibited a reduced accumulation of neutrophils and macrophages, as well as attenuated expression of chemokines CCL2 and CCL5, which lead to impaired muscle regeneration (Inaba et al., 2018). Immunogenomic explorations of muscle and tumor biopsies from individuals across the whole spectrum of muscle mass distribution, and patients exhibiting muscle wasting, could provide insight on the cross-talk between the immune microenvironment of tumor and skeletal muscle and their relevance to muscle mass during cancer.

During the development of this thesis from the point of a dietitian with expertise in skeletal muscle biology, cancer and immunology, it was obvious that “nutrition” is a topic often forgotten in the clinical and cancer setting that influences both muscle mass and the immune system. Nutritional interventions such as omega 3 fatty acids, are known to modulate inflammation through several mechanisms that include synthesis of anti-inflammatory mediators and immune cell signaling (Calder, 2007, 2015, 2017). In addition, omega 3 fatty acids have demonstrated significance in the

preservation of muscle mass and myosteatosis, a coexisting muscle abnormality with a biological process that is suggested to be cell-mediated immune response (Stretch et al., 2018), in the clinical setting and animal models (Ewaschuk et al., 2014). Omega 3 fatty acids have demonstrated beneficial effects during chemotherapy in the prevention of myosteatosis in the same animal model of Chapter 5 (Almasud et al., 2017) as well as in humans (Murphy et al., 2011). Currently, in our research laboratory, the exploration on the effect of Omega 3 fatty acids on immune response and muscle mass preservation in humans and animal models is being explored with confidence that it will bring stronger evidence to incorporate nutritional interventions, such as Omega 3 fatty acids, as part of a formal therapeutic approach for muscle wasting in cancer.

6.3 Conclusion

In conclusion, immune cells from the innate and adaptive immune response are present within skeletal muscle during cancer. Positive correlations between T cells and granulocyte/phagocyte numbers with histological and radiological assessments of muscle mass suggest that interactions between immune cells and muscle might play a role in muscle mass status during cancer. Exploration of transcriptomic events involving immune cell migration in a preclinical cancer model experiencing mild muscle atrophy enhanced our understanding on the participation of the local immune cell mediated response of skeletal muscle in response to cancer and its connection to cancer-induced muscle loss. Skeletal muscle as a tissue involved in pharmacokinetics is directly affected by chemotherapy. Chemotherapy exposure influences the immune environment of muscle by promoting the upregulation of immune cell migratory signals; however, further exploration is necessary to understand the long term effect of chemotherapy regimens on the immune environment of muscle. Our study highlights in the relevance of exploring the immune environment of muscle as a factor that influences muscle mass during cancer. Studies investigating biological characterizations of skeletal muscle from clinical cohorts with CT-derived muscle mass assessments can benefit from the critical review and recommendations provided as part of the literature review of Chapter 3. It is of great interest that this work provides a platform to better understand low muscle mass and muscle wasting in cancer, as well to identify and develop sustainable and accessible strategies for their prevention and treatment to enhance the quality of life and survival of people experiencing cancer. Overall the present work is an important contribution to the fields of skeletal muscle abnormalities in cancer, cancer cachexia and muscle disease.

Bibliography

Acharyya, S., Butchbach, M. E. R., Sahenk, Z., Wang, H., Saji, M., Carathers, M., ... Guttridge, D. C. (2005). Dystrophin glycoprotein complex dysfunction: A regulatory link between muscular dystrophy and cancer cachexia. *Cancer Cell*, 8(5), 421–432. <https://doi.org/10.1016/j.ccr.2005.10.004>

Agustsson, T., D'souza, M. A., Nowak, G., & Isaksson, B. (2011). Mechanisms for skeletal muscle insulin resistance in patients with pancreatic ductal adenocarcinoma. *Nutrition*, 27(7–8), 796–801. <https://doi.org/10.1016/j.nut.2010.08.022>

Alekseyev, Y. O., Fazeli, R., Yang, S., Basran, R., Maher, T., Miller, N. S., & Remick, D. (2018). A Next-Generation Sequencing Primer-How Does It Work and What Can It Do? *Academic Pathology*, 5, 2374289518766521. <https://doi.org/10.1177/2374289518766521>

Alimzhanov, M. B., Kuprash, D. V., Kosco-Vilbois, M. H., Luz, A., Turetskaya, R. L., Tarakhovsky, A., ... Pfeffer, K. (1997). Abnormal development of secondary lymphoid tissues in lymphotoxin beta-deficient mice. *Proceedings of the National Academy of Sciences of the United States of America*, 94(17), 9302–9307. <https://doi.org/10.1073/pnas.94.17.9302>

Almasud, A. A., Giles, K. H., Miklavcic, J. J., Martins, K. J. B., Baracos, V. E., Putman, C. T., ... Mazurak, V. C. (2017). Fish oil mitigates myosteatorsis and improves chemotherapy efficacy in a preclinical model of colon cancer. *PLOS ONE*, 12(8), e0183576. <https://doi.org/10.1371/journal.pone.0183576>

Álvaro Sanz, E., Garrido Siles, M., Rey Fernández, L., Villatoro Roldán, R., Rueda Domínguez, A., & Abilés, J. (2019). Nutritional risk and malnutrition rates at diagnosis of cancer in patients treated in outpatient settings: Early intervention protocol. *Nutrition*, 57, 148–153. <https://doi.org/10.1016/J.NUT.2018.05.021>

Andersen-Nissen, E., Hawn, T. R., Smith, K. D., Nachman, A., Lampano, A. E., Uematsu, S., ... Aderem, A. (2007). Cutting edge: Tlr5-/- mice are more susceptible to Escherichia coli urinary tract infection. *Journal of Immunology (Baltimore, Md. : 1950)*, 178(8), 4717–4720. <https://doi.org/10.4049/jimmunol.178.8.4717>

Anoveros-Barrera, A., Bhullar, A. S., Stretch, C., Esfandiari, N., Dunichand-hoedl, A. R., Karen, J. B., ... Mazurak, V. C. (2019). Clinical and biological characterization of skeletal muscle tissue biopsies of surgical cancer patients. *Journal of Cachexia, Sarcopenia and Muscle, (in press)*(December 2018). <https://doi.org/10.1002/jcsm.12466>

Anoveros-Barrera, A., Bhullar, A. S., Stretch, C., Dunichand-Hoedl, A. R., Martins, K. J. B., Rieger, A., ... Mazurak, V. C. (2019). Immunohistochemical phenotyping of T cells, granulocytes, and phagocytes in the muscle of cancer patients: association with radiologically defined muscle mass and gene expression. *Skeletal Muscle*, 9(1), 24. <https://doi.org/10.1186/s13395-019-0209-y>

Ansel, K. M., Harris, R. B. S., & Cyster, J. G. (2002). CXCL13 is required for B1 cell homing, natural antibody production, and body cavity immunity. *Immunity*, *16*(1), 67–76. [https://doi.org/10.1016/S1074-7613\(01\)00257-6](https://doi.org/10.1016/S1074-7613(01)00257-6)

Arden, N. K., & Spector, T. D. (1997). Genetic Influences on Muscle Strength, Lean Body Mass, and Bone Mineral Density: A Twin Study. *Journal of Bone and Mineral Research*, *12*(12), 2076–2081. <https://doi.org/10.1359/jbmr.1997.12.12.2076>

Arends, J., Bachmann, P., Baracos, V., Barthelemy, N., Bertz, H., Bozzetti, F., ... Preiser, J.-C. (2017). ESPEN guidelines on nutrition in cancer patients. *Clinical Nutrition*, *36*(1), 11–48. <https://doi.org/10.1016/J.CLNU.2016.07.015>

Argilés, J. M., Busquets, S., Stemmler, B., & López-Soriano, F. J. (2014). Cancer cachexia: understanding the molecular basis. *Nature Reviews Cancer*, *14*, 754–762. <https://doi.org/10.1038/nrc3829>

Arnold, L., Henry, A., Poron, F., Baba-Amer, Y., van Rooijen, N., Plonquet, A., ... Chazaud, B. (2007). Inflammatory monocytes recruited after skeletal muscle injury switch into antiinflammatory macrophages to support myogenesis. *The Journal of Experimental Medicine*, *204*(5), 1057–1069. <https://doi.org/10.1084/jem.20070075>

Aubrey, J., Esfandiari, N., Baracos, V. E., Buteau, F. A., Frenette, J., Putman, C. T., & Mazurak, V. C. (2014). Measurement of skeletal muscle radiation attenuation and basis of its biological variation. *Acta Physiologica*. <https://doi.org/10.1111/apha.12224>

Aulino, P., Berardi, E., Cardillo, V. M., Rizzuto, E., Perniconi, B., Ramina, C., ... Coletti, D. (2010). Molecular, cellular and physiological characterization of the cancer cachexia-inducing C26 colon carcinoma in mouse. *BMC Cancer*, *10*(1), 363. <https://doi.org/10.1186/1471-2407-10-363>

Aversa, Z., Bonetto, A., Penna, F., Costelli, P., Di Rienzo, G., Lacitignola, A., ... Muscaritoli, M. (2012). Changes in myostatin signaling in non-weight-losing cancer patients. *Annals of Surgical Oncology*, *19*(4), 1350–1356. <https://doi.org/10.1245/s10434-011-1720-5>

Aversa, Z., Pin, F., Lucia, S., Penna, F., Verzaro, R., Fazi, M., ... Muscaritoli, M. (2016). Autophagy is induced in the skeletal muscle of cachectic cancer patients. *Scientific Reports*, *6*, 1–11. <https://doi.org/10.1038/srep30340>

Banduseela, V., Ochala, J., Lamberg, K., Kalimo, H., & Larsson, L. (2007). Muscle paralysis and myosin loss in a patient with cancer cachexia. *Acta Myologica*, *26*(3), 136–144.

Baracos, V. E., Martin, L., Korc, M., Guttridge, D. C., & Fearon, K. C. H. (2018, January 18). Cancer-associated cachexia. *Nature Reviews Disease Primers*, Vol. 4, p. 17105. <https://doi.org/10.1038/nrdp.2017.105>

- Bardina, S. V., Michlmayr, D., Hoffman, K. W., Obara, C. J., Sum, J., Charo, I. F., ... Lim, J. K. (2015). Differential Roles of Chemokines CCL2 and CCL7 in Monocytosis and Leukocyte Migration during West Nile Virus Infection. *The Journal of Immunology*, *195*(9), 4306–4318. <https://doi.org/10.4049/jimmunol.1500352>
- Barret, M., Antoun, S., Dalban, C., Malka, D., Mansourbakht, T., Zaanan, A., ... Taieb, J. (2014). Sarcopenia Is Linked to Treatment Toxicity in Patients With Metastatic Colorectal Cancer. *Nutrition and Cancer*, *66*(4), 583–589. <https://doi.org/10.1080/01635581.2014.894103>
- Barreto, R., Kitase, Y., Matsumoto, T., Pin, F., Colston, K. C., Couch, K. E., ... Bonetto, A. (2017). ACVR2B/Fc counteracts chemotherapy-induced loss of muscle and bone mass. *Scientific Reports*, *7*(1), 14470. <https://doi.org/10.1038/s41598-017-15040-1>
- Barreto, R., Mandili, G., Witzmann, F. A., Novelli, F., Zimmers, T. A., & Bonetto, A. (2016). Cancer and Chemotherapy Contribute to Muscle Loss by Activating Common Signaling Pathways. *Frontiers in Physiology*, *7*, 472. <https://doi.org/10.3389/fphys.2016.00472>
- Barreto, R., Waning, D. L., Gao, H., Liu, Y., Zimmers, T. A., Bonetto, A., ... Bonetto, A. (2016). Chemotherapy-related cachexia is associated with mitochondrial depletion and the activation of ERK1/2 and p38 MAPKs. *Oncotarget*, *7*(28), 43442–43460. <https://doi.org/10.18632/oncotarget.9779>
- Basile, D., Parnofiello, A., Vitale, M. G., Cortiula, F., Gerratana, L., Fanotto, V., ... Cardellino, G. G. (2019). The IMPACT study: early loss of skeletal muscle mass in advanced pancreatic cancer patients. *Journal of Cachexia, Sarcopenia and Muscle*, *10*(2), 368–377. <https://doi.org/10.1002/jcsm.12368>
- Batchelor, T. T., Taylor, L. P., Thaler, H. T., Posner, J. B., & DeAngelis, L. M. (1997). Steroid myopathy in cancer patients. *Neurology*, *48*(5), 1234–1238.
- Baumann, K. (2010). Integrin's new partner. *Nature Reviews Molecular Cell Biology*, *11*(3), 164–164. <https://doi.org/10.1038/nrm2856>
- Baumgartner, R. N., Koehler, K. M., Gallagher, D., Romero, L., Heymsfield, S. B., Ross, R. R., ... Lindeman, R. D. (1998). Epidemiology of Sarcopenia among the Elderly in New Mexico. *American Journal of Epidemiology*, *147*(8), 755–763. <https://doi.org/10.1093/oxfordjournals.aje.a009520>
- Beaton, L. J., Allan, D. A., Tarnopolsky, M. A., Tiidus, P. M., & Phillips, S. M. (2002). Contraction-induced muscle damage is unaffected by vitamin E supplementation. *Medicine and science in sports and exercise*. <https://doi.org/10.1097/00005768-200205000-00012>
- Beudart, C., Reginster, J. Y., Petermans, J., Gillain, S., Quabron, A., Locquet, M., ... Bruyère, O. (2015). Quality of life and physical components linked to sarcopenia: The SarcoPhAge study. *Experimental Gerontology*, *69*, 103–110. <https://doi.org/10.1016/J.EXGER.2015.05.003>

- Behrens, L., Kerschensteiner, M., Misgeld, T., Goebels, N., Wekerle, H., & Hohlfeld, R. (1998). Human muscle cells express a functional costimulatory molecule distinct from B7.1 (CD80) and B7.2 (CD86) in vitro and in inflammatory lesions. *Journal of Immunology (Baltimore, Md. : 1950)*, *161*(11), 5943–5951.
- Bekiaris, V., Sedy, J. R., Rossetti, M., Spreafico, R., Sharma, S., Rhode-Kurnow, A., ... Ware, C. F. (2013). Human CD4+CD3- Innate-Like T Cells Provide a Source of TNF and Lymphotoxin- and Are Elevated in Rheumatoid Arthritis. *The Journal of Immunology*, *191*(9), 4611–4618. <https://doi.org/10.4049/jimmunol.1301672>
- Belizário, J. E., Lorite, M. J., & Tisdale, M. J. (2001). Cleavage of caspases-1, -3, -6, -8 and -9 substrates by proteases in skeletal muscles from mice undergoing cancer cachexia. *British Journal of Cancer*, *84*(8), 1135–1140. <https://doi.org/10.1054/bjoc.2001.1700>
- Berardi, E., Aulino, P., Murfunì, I., Toschi, A., Padula, F., Scicchitano, B. M., ... Adamo, S. (2008). Skeletal muscle is enriched in hematopoietic stem cells and not inflammatory cells in cachectic mice. *Neurological Research*, *30*(2), 160–169. <https://doi.org/10.1179/174313208X281046>
- Beretta, E., Dube, M. G., Kalra, P. S., & Kalra, S. P. (2002). Long-Term Suppression of Weight Gain, Adiposity, and Serum Insulin by Central Leptin Gene Therapy in Prepubertal Rats: Effects on Serum Ghrelin and Appetite-Regulating Genes. *Pediatric Research*, *52*(2), 189–198. <https://doi.org/10.1203/00006450-200208000-00010>
- Bernard, N. J., & O'Neill, L. A. (2013). Mal, more than a bridge to MyD88. *IUBMB Life*, *65*(9), 777–786. <https://doi.org/10.1002/iub.1201>
- Black, D., Mackay, C., Ramsay, G., Hamoodi, Z., Nanthakumaran, S., Park, K. G. M., ... Richards, C. H. (2017). Prognostic Value of Computed Tomography: Measured Parameters of Body Composition in Primary Operable Gastrointestinal Cancers. *Annals of Surgical Oncology*, *24*(8), 2241–2251. <https://doi.org/10.1245/s10434-017-5829-z>
- Blauth, K., Zhang, X., Chopra, M., Rogan, S., & Markovic-Plese, S. (2015). The role of fractalkine (CX3CL1) in regulation of CD4⁺ cell migration to the central nervous system in patients with relapsing-remitting multiple sclerosis. *Clinical Immunology*, *157*(2), 121–132. <https://doi.org/10.1016/j.clim.2015.01.001>
- Blauwhoff-Buskermolen, S., Versteeg, K. S., de van der Schueren, M. A. E., den Braver, N. R., Berkhof, J., Langius, J. A. E., & Verheul, H. M. W. (2016). Loss of Muscle Mass During Chemotherapy Is Predictive for Poor Survival of Patients With Metastatic Colorectal Cancer. *Journal of Clinical Oncology*, *34*(12), 1339–1344. <https://doi.org/10.1200/JCO.2015.63.6043>
- Bloise, F. F., Oliveira, T. S., Cordeiro, A., & Ortiga-Carvalho, T. M. (2018). Thyroid Hormones Play Role in Sarcopenia and Myopathies. *Frontiers in Physiology*, *9*, 560. <https://doi.org/10.3389/fphys.2018.00560>

Bodine, S. C., & Furlow, J. D. (2015). Glucocorticoids and skeletal muscle. *Advances in Experimental Medicine and Biology*, 872, 145–176. https://doi.org/10.1007/978-1-4939-2895-8_7

Bohlen, J., McLaughlin, S. L., Hazard-Jenkins, H., Infante, A. M., Montgomery, C., Davis, M., & Pistilli, E. E. (2018). Dysregulation of metabolic-associated pathways in muscle of breast cancer patients: preclinical evaluation of interleukin-15 targeting fatigue. *Journal of Cachexia, Sarcopenia and Muscle*, 9(4), 701–714. <https://doi.org/10.1002/jcsm.12294>

Bonetto, A., Penna, F., Aversa, Z., Mercantini, P., Baccino, F. M., Costelli, P., ... Muscaritoli, M. (2013). Early changes of muscle insulin-like growth factor-1 and myostatin gene expression in gastric cancer patients. *Muscle & Nerve*, 48(3), 387–392. <https://doi.org/10.1002/mus.23798>

Bossola, M., Muscaritoli, M., Costelli, P., Bellantone, R., Pacelli, F., Busquets, S., ... Doglietto, G. B. (2001). Increased muscle ubiquitin mRNA levels in gastric cancer patients. *American Journal of Physiology. Regulatory, Integrative and Comparative Physiology*, 280(5), R1518-23.

Bossola, Maurizio, Mirabella, M., Ricci, E., Costelli, P., Pacelli, F., Tortorelli, A. P., ... Doglietto, G. B. (2006). Skeletal muscle apoptosis is not increased in gastric cancer patients with mild-moderate weight loss. *International Journal of Biochemistry and Cell Biology*, 38(9), 1561–1570. <https://doi.org/10.1016/j.biocel.2006.03.015>

Bossola, Maurizio, Muscaritoli, M., Costelli, P., Grieco, G., Bonelli, G., Pacelli, F., ... Baccino, F. M. (2003). Increased Muscle Proteasome Activity Correlates with Disease Severity in Gastric Cancer Patients. *Annals of Surgery*, 237(3), 384–389. <https://doi.org/10.1097/01.SLA.0000055225.96357.71>

Bouchi, R., Fukuda, T., Takeuchi, T., Nakano, Y., Murakami, M., Minami, I., ... Ogawa, Y. (2017). Insulin Treatment Attenuates Decline of Muscle Mass in Japanese Patients with Type 2 Diabetes. *Calcified Tissue International*, 101(1), 1–8. <https://doi.org/10.1007/s00223-017-0251-x>

Boutbir, J., Singh, F., Charles, A.-L., Schlagowski, A.-I., Bonifacio, A., Echaniz-Laguna, A., ... Zoll, J. (2016). Statins Trigger Mitochondrial Reactive Oxygen Species-Induced Apoptosis in Glycolytic Skeletal Muscle. *Antioxidants & Redox Signaling*, 24(2), 84–98. <https://doi.org/10.1089/ars.2014.6190>

Boyd, J. H., Divangahi, M., Yahiaoui, L., Gvozdic, D., Qureshi, S., & Petrof, B. J. (2006). Toll-Like Receptors Differentially Regulate CC and CXC Chemokines in Skeletal Muscle via NF- κ B and Calcineurin. *Infection and Immunity*, 74(12), 6829–6838. <https://doi.org/10.1128/IAI.00286-06>

Bradfield, P. F., Amft, N., Vernon-Wilson, E., Exley, A. E., Parsonage, G., Rainger, G. E., ... Buckley, C. D. (2003). Rheumatoid fibroblast-like synoviocytes overexpress the chemokine stromal cell-derived factor 1 (CXCL12), which supports distinct patterns and rates of CD4+ and CD8+ T cell migration within synovial tissue. *Arthritis & Rheumatism*, 48(9), 2472–2482. <https://doi.org/10.1002/art.11219>

Brasier, A. R. (2010). The nuclear factor-kappaB-interleukin-6 signalling pathway mediating vascular inflammation. *Cardiovascular Research*, 86(2), 211–218. <https://doi.org/10.1093/cvr/cvq076>

Brass, D. M., Hollingsworth, J. W., McElvania-Tekippe, E., Garantziotis, S., Hossain, I., & Schwartz, D. A. (2007). CD14 is an essential mediator of LPS-induced airway disease. *American Journal of Physiology - Lung Cellular and Molecular Physiology*, 293(1). <https://doi.org/10.1152/ajplung.00282.2006>

Braun, T. P., Zhu, X., Szumowski, M., Scott, G. D., Grossberg, A. J., Levasseur, P. R., ... Marks, D. L. (2011). Central nervous system inflammation induces muscle atrophy via activation of the hypothalamic-pituitary-adrenal axis. *The Journal of Experimental Medicine*, 208(12), 2449–2463. <https://doi.org/10.1084/jem.20111020>

Bregar, A., Deshpande, A., Grange, C., Zi, T., Stall, J., Hirsch, H., ... Rueda, B. R. (2017). Characterization of immune regulatory molecules B7-H4 and PD-L1 in low and high grade endometrial tumors. *Gynecologic Oncology*, 145(3), 446–452. <https://doi.org/10.1016/j.ygyno.2017.03.006>

Brutkiewicz, R. R., Lin, Y., Cho, S., Hwang, Y. K., Sriram, V., & Roberts, T. J. (2003). CD1d-Mediated Antigen Presentation to Natural Killer T (NKT) Cells. *Critical Reviews in Immunology*, 23(5–6), 403–419. <https://doi.org/10.1615/CritRevImmunol.v23.i56.30>

Bruun, J. M., Helge, J. W., Richelsen, B., Stallknecht, B., & Bruun, J. M. (2006). Diet and exercise reduce low-grade inflammation and macrophage infiltration in adipose tissue but not in skeletal muscle in severely obese subjects. *Am J Physiol Endocrinol Metab*, 290, 961–967. <https://doi.org/10.1152/ajpendo.00506.2005.-Obesity>

Brzeszczynska, J., Johns, N., Schilb, A., Degen, S., Degen, M., Langen, R., ... Ross, J. A. (2016). Loss of oxidative defense and potential blockade of satellite cell maturation in the skeletal muscle of patients with cancer but not in the healthy elderly. *Aging*, 8(8), 1690–1702. <https://doi.org/10.18632/aging.101006>

Burd, N. A., Dickinson, J. M., Lemoine, J. K., Carroll, C. C., Sullivan, B. E., Haus, J. M., ... Trappe, T. A. (2010). Effect of a cyclooxygenase-2 inhibitor on postexercise muscle protein synthesis in humans. *American Journal of Physiology. Endocrinology and Metabolism*, 298(2), E354–61. <https://doi.org/10.1152/ajpendo.00423.2009>

Burfeind, K. G., Zhu, X., Levasseur, P. R., Michaelis, K. A., Norgard, M. A., & Marks, D. L. (2018). TRIF is a key inflammatory mediator of acute sickness behavior and cancer cachexia. *Brain, Behavior, and Immunity*, 73, 364–374. <https://doi.org/10.1016/j.bbi.2018.05.021>

Burfeind, K. G., Zhu, X., Norgard, M. A., Levasseur, P. R., Olson, B., Michaelis, K. A., ... Marks, D. L. (2019). “A distinct neutrophil population invades the central nervous system during pancreatic cancer.” *BioRxiv*, 659060. <https://doi.org/10.1101/659060>

Burks, T. N., Andres-Mateos, E., Marx, R., Mejias, R., Van Erp, C., Simmers, J. L., ... Cohn, R. D. (2011). Losartan Restores Skeletal Muscle Remodeling and Protects Against Disuse Atrophy in Sarcopenia. *Science Translational Medicine*, 3(82), 82ra37-82ra37. <https://doi.org/10.1126/scitranslmed.3002227>

Burzyn, D., Kuswanto, W., Kolodin, D., Shadrach, J. L., Jang, Y., Sefik, E., ... Wagers, A. J. (2013). A Special Population of Regulatory T cells Potentiates Muscle Repair, *155*(6), 1282–1295. <https://doi.org/10.1016/j.cell.2013.10.054.A>

Busquets, S., Deans, C., Figueras, M., Moore-Carrasco, R., López-Soriano, F. J., Fearon, K. C. H., & Argilés, J. M. (2007). Apoptosis is present in skeletal muscle of cachectic gastro-intestinal cancer patients. *Clinical Nutrition*, 26(5), 614–618. <https://doi.org/10.1016/j.clnu.2007.06.005>

Butterfield, T. A., Best, T. M., & Merrick, M. A. (2006). The Dual Roles of Neutrophils and Macrophages in Inflammation : A Damage and Repair. *Journal of Athletic Training*, 41(4), 457–465.

Butticè, G., Miller, J., Wang, L., & Smith, B. D. (2006). Interferon-gamma induces major histocompatibility class II transactivator (CIITA), which mediates collagen repression and major histocompatibility class II activation by human aortic smooth muscle cells. *Circulation Research*, 98(4), 472–479. <https://doi.org/10.1161/01.RES.0000204725.46332.97>

Caan, B. J., Meyerhardt, J. A., Kroenke, C. H., Alexeeff, S., Xiao, J., Weltzien, E., ... Prado, C. M. (2017). Explaining the Obesity Paradox: The Association between Body Composition and Colorectal Cancer Survival (C-SCANS Study). *Cancer Epidemiology Biomarkers & Prevention*, 26(7), 1008–1015. <https://doi.org/10.1158/1055-9965.EPI-17-0200>

Calder, P. C. (2007). Immunomodulation by omega-3 fatty acids. *Prostaglandins Leukotrienes and Essential Fatty Acids*, 77(5–6), 327–335. <https://doi.org/10.1016/j.plefa.2007.10.015>

Calder, P. C. (2015). Marine omega-3 fatty acids and inflammatory processes: Effects, mechanisms and clinical relevance. *Biochimica et Biophysica Acta - Molecular and Cell Biology of Lipids*, Vol. 1851, pp. 469–484. <https://doi.org/10.1016/j.bbalip.2014.08.010>

Calder, P. C. (2017). Omega-3 fatty acids and inflammatory processes: from molecules to man. *Biochemical Society Transactions*, 45, 1105–1115. <https://doi.org/10.1042/BST20160474>

Calore, F., Londhe, P., Fadda, P., Nigita, G., Casadei, L., Marceca, G. P., ... Croce, C. M. (2018). The TLR7/8/9 Antagonist IMO-8503 Inhibits Cancer-Induced Cachexia. *Cancer Research*, 78(23), 6680–6690. <https://doi.org/10.1158/0008-5472.CAN-17-3878>

Canchis, P. W., Bhan, A. K., Landau, S. B., Yang, L., Balkt, S. P., & Blumberg, R. S. (1993). Tissue distribution of the non-polymorphic major histocompatibility complex class I-like molecule, CD1d. *Immunology*, 80, 561-565.

Cannon, T. Y., Guttridge, D., Dahlman, J., George, J. R., Lai, V., Shores, C., ... Couch, M. E. (2007). The Effect of Altered Toll-like Receptor 4 Signaling on Cancer Cachexia. *Archives of Otolaryngology–Head & Neck Surgery*, *133*(12), 1263. <https://doi.org/10.1001/archotol.133.12.1263>

Cao, S., & Rustum, Y. M. (2000). Synergistic antitumor activity of irinotecan in combination with 5-fluorouracil in rats bearing advanced colorectal cancer: role of drug sequence and dose. *Cancer Research*, *60*(14), 3717–3721.

Castiglioni, A., Corna, G., Rigamonti, E., Basso, V., Vezzoli, M., Monno, A., ... Rovere-Querini, P. (2015). FOXP3+ T Cells Recruited to Sites of Sterile Skeletal Muscle Injury Regulate the Fate of Satellite Cells and Guide Effective Tissue Regeneration. *PLOS ONE*, *10*(6), e0128094. <https://doi.org/10.1371/journal.pone.0128094>

Cerutti, C., & Ridley, A. J. (2017, September 1). Endothelial cell-cell adhesion and signaling. *Experimental Cell Research*, Vol. 358, pp. 31–38. <https://doi.org/10.1016/j.yexcr.2017.06.003>

Cespedes Feliciano, E. M., Kroenke, C. H., Meyerhardt, J. A., Prado, C. M., Bradshaw, P. T., Kwan, M. L., ... Caan, B. J. (2017). Association of Systemic Inflammation and Sarcopenia With Survival in Nonmetastatic Colorectal Cancer. *JAMA Oncology*, *3*(12), e172319. <https://doi.org/10.1001/jamaoncol.2017.2319>

Cetrone, M., Mele, A., & Tricarico, D. (2014). Effects of the antidiabetic drugs on the age-related atrophy and sarcopenia associated with diabetes type II. *Current Diabetes Reviews*, *10*(4), 231–237. <https://doi.org/10.2174/1573399810666140918121022>

Chaparro, V., Leroux, L. P., Zimmermann, A., Jardim, A., Johnston, B., Descoteaux, A., & Jaramillo, M. (2019). Leishmania donovani lipophosphoglycan increases Macrophage-Dependent chemotaxis of CXCR6-Expressing cells via CXCL16 induction. *Infection and Immunity*, *87*(5). <https://doi.org/10.1128/IAI.00064-19>

Chatterjee, S. (2014). Artefacts in histopathology. *Journal of Oral and Maxillofacial Pathology*, *18*(Suppl 1), S111-6. <https://doi.org/10.4103/0973-029X.141346>

Chaudhry, S., Emond, J., & Griesemer, A. (2019). Immune Cell Trafficking to the Liver. *Transplantation*, *103*(7), 1323–1337. <https://doi.org/10.1097/TP.0000000000002690>

Chen, L., Liu, G. Q., Wu, H. Y., Jin, J., Yin, X., Li, D., & Lu, P. R. (2018). Monocyte chemoattractant protein 1 and fractalkine play opposite roles in angiogenesis via recruitment of different macrophage subtypes. *International Journal of Ophthalmology*, *11*(2), 216–222. <https://doi.org/10.18240/ijo.2018.02.06>

Cheng, C., Li, Y., Ohno, H., Sawanobori, K., Li, Y., Shimada, O., & Atsumi, S. (2007). Mast Cells Appearing in Long-Term Skeletal Muscle Cell Cultures of Rat. *1430*(September), 1424–1430. <https://doi.org/10.1002/ar.20595>

Cho, Y., Kim, J. W., Keum, K. C., Lee, C. G., Jeung, H. C., & Lee, I. J. (2018). Prognostic Significance of Sarcopenia With Inflammation in Patients With Head and Neck Cancer Who Underwent Definitive Chemoradiotherapy. *Frontiers in Oncology*, *8*, 457. <https://doi.org/10.3389/fonc.2018.00457>

Christensen, J. F., Jones, L. W., Tolver, A., Jørgensen, L. W., Andersen, J. L., Adamsen, L., ... Daugaard, G. (2014). Safety and efficacy of resistance training in germ cell cancer patients undergoing chemotherapy: A randomized controlled trial. *British Journal of Cancer*, *111*(1), 8–16. <https://doi.org/10.1038/bjc.2014.273>

Christensen, J. F., Schjerling, P., Andersen, J. L., Daugaard, G., Rasmussen, M., & Mackey, A. L. (2016). Muscle satellite cell content and mRNA signaling in germ cell cancer patients – effects of chemotherapy and resistance training. *Acta Oncologica*, *55*(9–10), 1246–1250. <https://doi.org/10.3109/0284186X.2016.1170200>

Chung, K.-J., Mitroulis, I., Wiessner, J. R., Zheng, Y. Y., Siegert, G., Sperandio, M., & Chavakis, T. (2014). A novel pathway of rapid TLR-triggered activation of integrin-dependent leukocyte adhesion that requires Rap1 GTPase. *Molecular Biology of the Cell*, *25*(19), 2948–2955. <https://doi.org/10.1091/mbc.e14-04-0867>

Ciombor, K. K., & Bekaii-Saab, T. (2018). A Comprehensive Review of Sequencing and Combination Strategies of Targeted Agents in Metastatic Colorectal Cancer. *The Oncologist*, *23*(1), 25–34. <https://doi.org/10.1634/theoncologist.2017-0203>

Coffelt, S. B., Wellenstein, M. D., & De Visser, K. E. (2016, July 10). Neutrophils in cancer: Neutral no more. *Nature Reviews Cancer*, Vol. 16, pp. 431–446. <https://doi.org/10.1038/nrc.2016.52>

Collins, M., Ling, V., & Carreno, B. M. (2005). The B7 family of immune-regulatory ligands. *Genome Biology*, *6*(6), 223. <https://doi.org/10.1186/gb-2005-6-6-223>

Constantin, G., Majeed, M., Giagulli, C., Piccio, L., Kim, J. Y., Butcher, E. C., & Laudanna, C. (2000). Chemokines trigger immediate beta2 integrin affinity and mobility changes: differential regulation and roles in lymphocyte arrest under flow. *Immunity*, *13*(6), 759–769.

Cooper, A. B., Slack, R., Fogelman, D., Holmes, H. M., Petzel, M., Parker, N., ... Katz, M. H. G. (2015). Characterization of Anthropometric Changes that Occur During Neoadjuvant Therapy for Potentially Resectable Pancreatic Cancer. *Annals of Surgical Oncology*, *22*(7), 2416–2423. <https://doi.org/10.1245/s10434-014-4285-2>

Costamagna, D., Costelli, P., Sampaolesi, M., & Penna, F. (2015). Role of Inflammation in Muscle Homeostasis and Myogenesis. *Mediators of Inflammation*, *2015*, 1–14. <https://doi.org/10.1155/2015/805172>

Costelli, P., Bossola, M., Muscaritoli, M., Grieco, G., Bonelli, G., Bellantone, R., ... Fanelli, F. R. (2002). Anticytokine treatment prevents the increase in the activity of ATP-ubiquitin- and Ca²⁺-

dependent proteolytic systems in the muscle of tumour-bearing rats. *Cytokine*, *19*(1), 1–5.
<https://doi.org/10.1006/cyto.2002.1036>

Cottle, D. L., McGrath, M. J., Wilding, B. R., Cowling, B. S., Kane, J. M., D'Arcy, C. E., ... Mitchell, C. A. (2009). SLIMMER (FHL1B/KyoT3) Interacts with the Proapoptotic Protein Siva-1 (CD27BP) and Delays Skeletal Myoblast Apoptosis. *Journal of Biological Chemistry*, *284*(39), 26964–26977. <https://doi.org/10.1074/jbc.M109.036293>

Crespo, J., Sun, H., Welling, T. H., Tian, Z., & Zou, W. (2013). T cell anergy, exhaustion, senescence, and stemness in the tumor microenvironment. *Current Opinion in Immunology*, *25*(2), 214–221. <https://doi.org/10.1016/j.coi.2012.12.003>

Creus, K. K., De Paepe, B., Weis, J., & De Bleeker, J. L. (2012). *The multifaceted character of lymphotoxin b in inflammatory myopathies and muscular dystrophies q*.
<https://doi.org/10.1016/j.nmd.2012.04.012>

Crouch, M. L., Knowels, G., Stuppard, R., Ericson, N. G., Bielas, J. H., Marcinek, D. J., & Syrjala, K. L. (2017). Cyclophosphamide leads to persistent deficits in physical performance and in vivo mitochondria function in a mouse model of chemotherapy late effects. *PLoS ONE*, *12*(7).
<https://doi.org/10.1371/journal.pone.0181086>

Cruz-Jentoft, A. J., Bahat, G., Bauer, J., Boirie, Y., Bruyère, O., Cederholm, T., ... Schols, J. (2019). Sarcopenia: revised European consensus on definition and diagnosis. *Age and Ageing*, *48*(1), 16–31. <https://doi.org/10.1093/ageing/afy169>

D'Orlando, C., Marzetti, E., François, S., Lorenzi, M., Conti, V., di Stasio, E., ... Bossola, M. (2014). Gastric cancer does not affect the expression of atrophy-related genes in human skeletal muscle. *Muscle & Nerve*, *49*(4), 528–533. <https://doi.org/10.1002/mus.23945>

D'Souza, D. M., Al-Sajee, D., & Hawke, T. J. (2013). Diabetic myopathy: impact of diabetes mellitus on skeletal muscle progenitor cells. *Frontiers in Physiology*, *4*, 379.
<https://doi.org/10.3389/fphys.2013.00379>

Dagdeviren, S., Jung, D. Y., Lee, E., Friedline, R. H., Noh, H. L., Kim, J. H., ... Kim, J. K. (2016). Altered Interleukin-10 Signaling in Skeletal Muscle Regulates Obesity-Mediated Inflammation and Insulin Resistance. *Molecular and Cellular Biology*, *36*(23), 2956–2966.
<https://doi.org/10.1128/MCB.00181-16>

Dai, C., Yao, X., Gordon, E. M., Barochia, A., Cuento, R. A., Kaler, M., ... Levine, S. J. (2016). A CCL24-dependent pathway augments eosinophilic airway inflammation in house dust mite-challenged Cd163 ^{-/-} mice. *Mucosal Immunology*, *9*(3), 702–717.
<https://doi.org/10.1038/mi.2015.94>

Dalakas, M. C. (2015). Inflammatory Muscle Diseases. *New England Journal of Medicine*, *372*(18), 1734–1747. <https://doi.org/10.1056/NEJMra1402225>

Daly, L. E., Ní Bhuachalla, É. B., Power, D. G., Cushen, S. J., James, K., & Ryan, A. M. (2018). Loss of skeletal muscle during systemic chemotherapy is prognostic of poor survival in patients with foregut cancer. *Journal of Cachexia, Sarcopenia and Muscle*, *9*(2), 315–325. <https://doi.org/10.1002/jcsm.12267>

Damrauer, J. S., Stadler, M. E., Acharyya, S., Baldwin, A. S., Couch, M. E., & Guttridge, D. C. (2018). Chemotherapy-induced muscle wasting: association with NF- κ B and cancer cachexia. *European Journal of Translational Myology*, *28*(2), 7590. <https://doi.org/10.4081/ejtm.2018.7590>

De Alvaro, C., Teruel, T., Hernandez, R., & Lorenzo, M. (2004). Tumor Necrosis Factor α Produces Insulin Resistance in Skeletal Muscle by Activation of Inhibitor κ B Kinase in a p38 MAPK-dependent Manner. *Journal of Biological Chemistry*, *279*(17), 17070–17078. <https://doi.org/10.1074/jbc.M312021200>

De Bleecker, J. L., De Paepe, B., Vanwalleghem, I. E., & Schröder, J. M. (2002). Differential expression of chemokines in inflammatory myopathies. *Neurology*, *58*(12), 1779–1785. <https://doi.org/10.1212/wnl.58.12.1779>

DeJong, C. H. C., Busquets, S., Moses, A. G. W., Schrauwen, P., Ross, J. A., Argiles, J. M., & Fearon, K. C. H. (2005). Systemic inflammation correlates with increased expression of skeletal muscle ubiquitin but not uncoupling proteins in cancer cachexia. *Oncology Reports*, *14*(1), 257–263.

Delafontaine, P., & Yoshida, T. (2016). The Renin-Angiotensin System And The Biology Of Skeletal Muscle: Mechanisms Of Muscle Wasting In Chronic Disease States. *Transactions of the American Clinical and Climatological Association*, *127*, 245–258. Retrieved from <http://www.ncbi.nlm.nih.gov/pubmed/28066057>

Deng, B. B., Wehling-Henricks, M., Villalta, S. A., Wang, Y., & Tidball, J. G. (2012). IL-10 triggers changes in macrophage phenotype that promote muscle growth and regeneration. *Journal of Immunology (Baltimore, Md. : 1950)*, *189*(7), 3669–3680. <https://doi.org/10.4049/jimmunol.1103180>

Dennis, K. L., Blatner, N. R., Gounari, F., & Khazaie, K. (2013). Current status of interleukin-10 and regulatory T-cells in cancer. *Current Opinion in Oncology*, *25*(6), 637–645. <https://doi.org/10.1097/CCO.0000000000000006>

Derbre, F., Ferrando, B., Gomez-Cabrera, M. C., Sanchis-Gomar, F., Martinez-Bello, V. E., Olaso-Gonzalez, G., ... Viña, J. (2012). Inhibition of Xanthine Oxidase by Allopurinol Prevents Skeletal Muscle Atrophy: Role of p38 MAPKinase and E3 Ubiquitin Ligases. *PLoS ONE*, *7*(10), e46668. <https://doi.org/10.1371/journal.pone.0046668>

Derstine, B. A., Holcombe, S. A., Ross, B. E., Wang, N. C., Su, G. L., & Wang, S. C. (2018). Skeletal muscle cutoff values for sarcopenia diagnosis using T10 to L5 measurements in a healthy US population. *Scientific Reports*, *8*(1), 11369. <https://doi.org/10.1038/s41598-018-29825-5>

Di Bari, M., Van De Poll-Franse, L. V., Onder, G., Kritchevsky, S. B., Newman, A., Harris, T. B., ... Health, Aging and Body Composition Study. (2004). Antihypertensive Medications and Differences in Muscle Mass in Older Persons: The Health, Aging and Body Composition Study. *Journal of the American Geriatrics Society*, 52(6), 961–966. <https://doi.org/10.1111/j.1532-5415.2004.52265.x>

Diaz, E. C., Herndon, D. N., Porter, C., Sidossis, L. S., Suman, O. E., & Børsheim, E. (2015). Effects of pharmacological interventions on muscle protein synthesis and breakdown in recovery from burns. *Burns : Journal of the International Society for Burn Injuries*, 41(4), 649–657. <https://doi.org/10.1016/j.burns.2014.10.010>

Disteldorf, E. M., Krebs, C. F., Paust, H. J., Turner, J. E., Nouailles, G., Tittel, A., ... Panzer, U. (2015). CXCL5 drives neutrophil recruitment in TH17-mediated GN. *Journal of the American Society of Nephrology*, 26(1), 55–66. <https://doi.org/10.1681/ASN.2013101061>

Dobrovolskaia, M. A., & Vogel, S. N. (2002). Toll receptors, CD14, and macrophage activation and deactivation by LPS. *Microbes and Infection*, Vol. 4, pp. 903–914. [https://doi.org/10.1016/S1286-4579\(02\)01613-1](https://doi.org/10.1016/S1286-4579(02)01613-1)

Dohlman, T. H., Chauhan, S. K., Kodati, S., Hua, J., Chen, Y., Omoto, M., ... Dana, R. (2013). The CCR6/CCL20 axis mediates Th17 cell migration to the ocular surface in dry eye disease. *Investigative Ophthalmology and Visual Science*, 54(6), 4081–4091. <https://doi.org/10.1167/iovs.12-11216>

Dolan, R. D., Almasaudi, A. S., Dieu, L. B., Horgan, P. G., McSorley, S. T., & McMillan, D. C. (2018, February 20). The relationship between computed tomography-derived body composition, systemic inflammatory response, and survival in patients undergoing surgery for colorectal cancer. *Journal of Cachexia, Sarcopenia and Muscle*, pp. 111–122. <https://doi.org/10.1002/jcsm.12357>

Dolan, R. D., McSorley, S. T., Horgan, P. G., Laird, B., & McMillan, D. C. (2017, August). The role of the systemic inflammatory response in predicting outcomes in patients with advanced inoperable cancer: Systematic review and meta-analysis. *Critical Reviews in Oncology/Hematology*. <https://doi.org/10.1016/j.critrevonc.2017.06.002>

Dorph, C., Englund, P., Nennesmo, I., & Lundberg, I. E. (2006). Signs of inflammation in both symptomatic and asymptomatic muscles from patients with polymyositis and dermatomyositis. *Annals of the Rheumatic Diseases*, 65(12), 1565–1571. <https://doi.org/10.1136/ard.2005.051086>

Dumont, N., Bouchard, P., & Frenette, J. (2008). Neutrophil-induced skeletal muscle damage: a calculated and controlled response following hindlimb unloading and reloading. *American Journal of Physiology-Regulatory, Integrative and Comparative Physiology*, 295(6), R1831–R1838. <https://doi.org/10.1152/ajpregu.90318.2008>

Dunne, A., Carpenter, S., Brikos, C., Gray, P., Strelow, A., Wesche, H., ... O'Neill, L. A. J. (2010). IRAK1 and IRAK4 Promote Phosphorylation, Ubiquitination, and Degradation of MyD88

Adaptor-like (Mal). *Journal of Biological Chemistry*, 285(24), 18276–18282.
<https://doi.org/10.1074/JBC.M109.098137>

Dustin, M. L. (2019, April 18). Integrins and Their Role in Immune Cell Adhesion. *Cell*, Vol. 177, pp. 499–501. <https://doi.org/10.1016/j.cell.2019.03.038>

Ebadi, M., Field, C. J., Lehner, R., & Mazurak, V. C. (2017). Chemotherapy diminishes lipid storage capacity of adipose tissue in a preclinical model of colon cancer. *Lipids in Health and Disease*, 16(1), 247. <https://doi.org/10.1186/s12944-017-0638-8>

Ebadi, M., Tandon, P., Moctezuma-Velazquez, C., Ghosh, S., Baracos, V. E., Mazurak, V. C., & Montano-Loza, A. J. (2018). Low subcutaneous adiposity associates with higher mortality in female patients with cirrhosis. *Journal of Hepatology*, 69(3), 608–616.
<https://doi.org/10.1016/j.jhep.2018.04.015>

Ebhardt, H. A., Degen, S., Tadini, V., Schilb, A., Johns, N., Greig, C. A., ... Jacobi, C. (2017). Comprehensive proteome analysis of human skeletal muscle in cachexia and sarcopenia: a pilot study. *Journal of Cachexia, Sarcopenia and Muscle*, 8(4), 567–582.
<https://doi.org/10.1002/jcsm.12188>

Edwards, B. K., Noone, A.-M., Mariotto, A. B., Simard, E. P., Boscoe, F. P., Henley, ; S Jane, ... Ward, E. M. (1975). Featuring Prevalence of Comorbidity and Impact on Survival Among Persons With Lung, Colorectal, Breast, or Prostate Cancer. *Cancer*, 120(9), 1290–1314.
<https://doi.org/10.1002/cncr.28509>

Egerman, M. A., & Glass, D. J. (2014). Signaling pathways controlling skeletal muscle mass. *Critical Reviews in Biochemistry and Molecular Biology*, 49(1), 59–68.
<https://doi.org/10.3109/10409238.2013.857291>

Eksteen, B., Miles, A., Curbishley, S. M., Tselepis, C., Grant, A. J., Walker, L. S. K., & Adams, D. H. (2006). Epithelial Inflammation Is Associated with CCL28 Production and the Recruitment of Regulatory T Cells Expressing CCR10. *The Journal of Immunology*, 177(1), 593–603.
<https://doi.org/10.4049/jimmunol.177.1.593>

Elazzazy, S., Eziada, S. S., & Zaidan, M. (2012). Rhabdomyolysis secondary to drug interaction between atorvastatin, omeprazole, and dexamethasone. *International Medical Case Reports Journal*, 5, 59–61. <https://doi.org/10.2147/IMCRJ.S34919>

Eley, H. L., Skipworth, R. J. E., Deans, D. A. C., Fearon, K. C. H., & Tisdale, M. J. (2008). Increased expression of phosphorylated forms of RNA-dependent protein kinase and eukaryotic initiation factor 2 α may signal skeletal muscle atrophy in weight-losing cancer patients. *British Journal of Cancer*, 98(2), 443–449. <https://doi.org/10.1038/sj.bjc.6604150>

Elsaid, O., Taylor, B., Zaleski, A., Panza, G., & Thompson, P. D. (2017). Rationale for investigating metformin as a protectant against statin-associated muscle symptoms. *Journal of Clinical Lipidology*, 11(5), 1145–1151. <https://doi.org/10.1016/j.jacl.2017.06.019>

Endharti, A. T., Rifá, M., Shi, Z., Fukuoka, Y., Nakahara, Y., Kawamoto, Y., ... Suzuki, H. (2005). Cutting Edge: CD8+CD122+ Regulatory T Cells Produce IL-10 to Suppress IFN- γ Production and Proliferation of CD8+ T Cells. *The Journal of Immunology*, 175(11), 7093–7097. <https://doi.org/10.4049/jimmunol.175.11.7093>

Englund, P., Nennesmo, I., Klareskog, L., & Lundberg, I. E. (2002). Interleukin-1 β expression in capillaries and major histocompatibility complex class I expression in type II muscle fibers from polymyositis and dermatomyositis patients: Important pathogenic features independent of inflammatory cell clusters in muscle tis. *Arthritis & Rheumatism*, 46(4), 1044–1055. <https://doi.org/10.1002/art.10140>

Enyindah-Asonye, G., Li, Y., Xin, W., Singer, N. G., Gupta, N., Fung, J., & Lin, F. (2017). CD6 Receptor Regulates Intestinal Ischemia/Reperfusion-induced Injury by Modulating Natural IgM-producing B1a Cell Self-renewal. *Journal of Biological Chemistry*, 292(2), 661–671. <https://doi.org/10.1074/JBC.M116.749804>

Eruslanov, E. B., Singhal, S., & Albelda, S. M. (2017). Mouse versus Human Neutrophils in Cancer: A Major Knowledge Gap. *Trends in Cancer*, Vol. 3, pp. 149–160. <https://doi.org/10.1016/j.trecan.2016.12.006>

Esashi, E., Ito, H., Ishihara, K., Hirano, T., Koyasu, S., & Miyajima, A. (2004). Development of CD4 + Macrophages from Intrathymic T Cell Progenitors Is Induced by Thymic Epithelial Cells. *The Journal of Immunology*, 173(7), 4360–4367. <https://doi.org/10.4049/jimmunol.173.7.4360>

Esfandiari, N., Ghosh, S., Prado, C. M. M., Martin, L., Mazurak, V., & Baracos, V. E. (2014). Age, Obesity, Sarcopenia, and Proximity to Death Explain Reduced Mean Muscle Attenuation in Patients with Advanced Cancer. *The Journal of Frailty & Aging*, 3(1), 3–8. <https://doi.org/10.14283/jfa.2014.1>

Essen, P., McNurlan, M. A., Wernerman, J., Vinnars, E., & Garlick, P. J. (1992). Uncomplicated surgery, but not general anesthesia, decreases muscle protein synthesis. *American Journal of Physiology-Endocrinology and Metabolism*, 262(3), E253–E260. <https://doi.org/10.1152/ajpendo.1992.262.3.E253>

Ewaschuk, J. B., Almasud, A., & Mazurak, V. C. (2014). Role of n-3 fatty acids in muscle loss and myosteatosis. *Applied Physiology, Nutrition, and Metabolism*. 662(January), 654–662. 4) <https://doi.org/10.1139/apnm-2013-0423>

Fagerholm, S. C., Guenther, C., Llorc Asens, M., Savinko, T., & Uotila, L. M. (2019). Beta2-Integrins and Interacting Proteins in Leukocyte Trafficking, Immune Suppression, and Immunodeficiency Disease. *Frontiers in Immunology*, 10, 254. <https://doi.org/10.3389/fimmu.2019.00254>

Faget, J., Biota, C., Bachelot, T., Gobert, M., Treilleux, I., Goutagny, N., ... Meñétrier-Caux, C. (2011). Early detection of tumor cells by innate immune cells leads to T reg recruitment through

CCL22 production by tumor cells. *Cancer Research*, 71(19), 6143–6152.
<https://doi.org/10.1158/0008-5472.CAN-11-0573>

Fan, J., Yang, X., Li, J., Shu, Z., Dai, J., Liu, X., ... Chen, N. (2017). Spermidine coupled with exercise rescues skeletal muscle atrophy from D-gal-induced aging rats through enhanced autophagy and reduced apoptosis via AMPK-FOXO3a signal pathway. *Oncotarget*, 8(11), 17475–17490. <https://doi.org/10.18632/oncotarget.15728>

Farup, J., Madaro, L., Puri, P. L., & Mikkelsen, U. R. (2015). Interactions between muscle stem cells, mesenchymal-derived cells and immune cells in muscle homeostasis, regeneration and disease. *Cell Death & Disease*, 6(7), e1830-13. <https://doi.org/10.1038/cddis.2015.198>

Fearon, K., Strasser, F., Anker, S. D., Bosaeus, I., Bruera, E., Fainsinger, R. L., ... Baracos, V. E. (2011). Definition and classification of cancer cachexia: an international consensus. *Lancet Oncology*, 12(5), 489–495. [https://doi.org/10.1016/S1470-2045\(10\)70218-7](https://doi.org/10.1016/S1470-2045(10)70218-7)

Feng, F., Zheng, G., Wang, Q., Liu, S., Liu, Z., Xu, G., ... Zhang, H. (2018). Low lymphocyte count and high monocyte count predicts poor prognosis of gastric cancer. *BMC Gastroenterology*, 18(1), 148. <https://doi.org/10.1186/s12876-018-0877-9>

Fernandes, C., Wanderley, C. W. S., Silva, C. M. S., Muniz, H. A., Teixeira, M. A., Souza, N. R. P., ... Lima-Júnior, R. C. P. (2018). Role of regulatory T cells in irinotecan-induced intestinal mucositis. *European Journal of Pharmaceutical Sciences*, 115, 158–166.
<https://doi.org/10.1016/J.EJPS.2018.01.006>

Fernández-Celemín, L., Pasko, N., Blomart, V., & Thissen, J.-P. (2002). Inhibition of muscle insulin-like growth factor I expression by tumor necrosis factor- α . *American Journal of Physiology-Endocrinology and Metabolism*, 283(6), E1279–E1290.
<https://doi.org/10.1152/ajpendo.00054.2002>.

Fernando, P., Kelly, J. F., Balazsi, K., Slack, R. S., & Megeney, L. A. (2002). Caspase 3 activity is required for skeletal muscle differentiation. *Proceedings of the National Academy of Sciences*, 99(17), 11025-11030. <https://doi.org/10.1073/pnas.162172899>

Figarella-branger, D., Civatte, M., Bartoli, C., & Ois Pellissier, J. (2003). Cytokines, Chemokines, and Cell Adhesion Molecules in Inflammatory Myopathies. *Muscle Nerve*, 28(December), 659–682. <https://doi.org/10.1002/mus.10462>

Fogelman, D. R., Holmes, H., Mohammed, K., Katz, M. H. G., Prado, C. M., Lieffers, J., ... Javle, M. Does IGF1R inhibition result in increased muscle mass loss in patients undergoing treatment for pancreatic cancer?. *Journal of Cachexia, Sarcopenia and Muscle*, 5 (4), 307-313.
<https://doi.org/10.1007/s13539-014-0145-y>

Forlow, S. B., White, E. J., Barlow, S. C., Feldman, S. H., Lu, H., Bagby, G. J., ... Ley, K. (2000). Severe inflammatory defect and reduced viability in CD18 and E-selectin double-mutant

mice. *The Journal of Clinical Investigation*, 106(12), 1457–1466.
<https://doi.org/10.1172/JCI10555>

Friedman, J. M., & Halaas, J. L. (1998). Leptin and the regulation of body weight in mammals. *Nature*, 395(6704), 763–770. <https://doi.org/10.1038/27376>

Frontera, W. R., & Ochala, J. (2015). Skeletal Muscle: A Brief Review of Structure and Function. *Calcified Tissue International*, 96(3), 183–195. <https://doi.org/10.1007/s00223-014-9915-y>

Fukushima, H., Takemura, K., Suzuki, H., & Koga, F. (2018). Impact of Sarcopenia as a Prognostic Biomarker of Bladder Cancer. *International Journal of Molecular Sciences*, 19(10), 2999. <https://doi.org/10.3390/ijms19102999>

Fukushima, H., Yokoyama, M., Nakanishi, Y., Tobisu, K., & Koga, F. (2015). Sarcopenia as a Prognostic Biomarker of Advanced Urothelial Carcinoma. *PLOS ONE*, 10(1), e0115895. <https://doi.org/10.1371/journal.pone.0115895>

Gallagher, I. J., Stephens, N. A., MacDonald, A. J., Skipworth, R. J. E., Husi, H., Greig, C. A., ... Fearon, K. C. H. (2012). Suppression of skeletal muscle turnover in cancer cachexia: Evidence from the transcriptome in sequential human muscle biopsies. *Clinical Cancer Research*, 18(10), 2817–2827. <https://doi.org/10.1158/1078-0432.CCR-11-2133>

Gallo, M., Gordon, T., Syrotuik, D., Shu, Y., Tyreman, N., MacLean, I., ... Putman, C. T. (2006). Effects of long-term creatine feeding and running on isometric functional measures and myosin heavy chain content of rat skeletal muscles. *Pflügers Archiv - European Journal of Physiology*, 452(6), 744–755. <https://doi.org/10.1007/s00424-006-0079-0>

Gani, F., Buettner, S., Margonis, G. A., Sasaki, K., Wagner, D., Kim, Y., ... Pawlik, T. M. (2016). Sarcopenia predicts costs among patients undergoing major abdominal operations. *Surgery*, 160(5), 1162–1171. <https://doi.org/10.1016/J.SURG.2016.05.002>

Gao, J. Q., Tsuda, Y., Han, M., Xu, D. H., Kanagawa, N., Hatanaka, Y., ... Nakagawa, S. (2009). NK cells are migrated and indispensable in the anti-tumor activity induced by CCL27 gene therapy. *Cancer Immunology, Immunotherapy*, 58(2), 291–299. <https://doi.org/10.1007/s00262-008-0554-x>

Gao, Y., Li, W., Chen, J., Wang, X., Lv, Y., Huang, Y., ... Xu, F. (2019). Pharmacometabolomic prediction of individual differences of gastrointestinal toxicity complicating myelosuppression in rats induced by irinotecan. *Acta Pharmaceutica Sinica B*, 9(1), 157–166. <https://doi.org/10.1016/J.APSB.2018.09.006>

Garcillán, B., Marin, A. V. M., Jiménez-Reinoso, A., Briones, A. C., Muñoz-Ruiz, M., García-León, M. J., ... Regueiro, J. R. (2015, January 29). $\gamma\delta$ T lymphocytes in the diagnosis of human T cell receptor immunodeficiencies. *Frontiers in Immunology*, Vol. 6. <https://doi.org/10.3389/fimmu.2015.00020>

Garg, B., Giri, B., Modi, S., Sethi, V., Castro, I., Umland, O., ... Dudeja, V. (2018). NFκB in Pancreatic Stellate Cells Reduces Infiltration of Tumors by Cytotoxic T Cells and Killing of Cancer Cells, via Up-regulation of CXCL12. *Gastroenterology*, 155(3), 880-891.e8. <https://doi.org/10.1053/j.gastro.2018.05.051>

Garman, K. S., Pieper, C. F., Seo, P., & Cohen, H. J. (2003). Function in elderly cancer survivors depends on comorbidities. *The Journals of Gerontology. Series A, Biological Sciences and Medical Sciences*, 58(12), M1119-24.

Gebhardt, T., Wakim, L. M., Eidsmo, L., Reading, P. C., Heath, W. R., & Carbone, F. R. (2009). Memory T cells in nonlymphoid tissue that provide enhanced local immunity during infection with herpes simplex virus. *Nature Immunology*, 10(5), 524–530. <https://doi.org/10.1038/ni.1718>

George-Gay, B., & Parker, K. (2003). Understanding the complete blood count with differential. *Journal of PeriAnesthesia Nursing*, 18(2), 96–117. <https://doi.org/10.1053/jpan.2003.50013>

Giglio, J., Kamimura, M. A., Lamarca, F., Rodrigues, J., Santin, F., & Avesani, C. M. (2018). Association of Sarcopenia With Nutritional Parameters, Quality of Life, Hospitalization, and Mortality Rates of Elderly Patients on Hemodialysis. *Journal of Renal Nutrition*, 28(3), 197–207. <https://doi.org/10.1053/J.JRN.2017.12.003>

Girbl, T., Lenn, T., Perez, L., Rolas, L., Barkaway, A., Thiriout, A., ... Nourshargh, S. (2018). Distinct Compartmentalization of the Chemokines CXCL1 and CXCL2 and the Atypical Receptor ACKR1 Determine Discrete Stages of Neutrophil Diapedesis. *Immunity*, 49(6), 1062-1076.e6. <https://doi.org/10.1016/j.immuni.2018.09.018>

Go, S., Park, M. J., Song, H., Kang, M. H., Park, H. J., Jeon, K. N., ... Lee, G. (2016). Sarcopenia and inflammation are independent predictors of survival in male patients newly diagnosed with small cell lung cancer. *Supportive Care in Cancer : Official Journal of the Multinational Association of Supportive Care in Cancer*, 24(5), 2075–2084. <https://doi.org/10.1007/s00520-015-2997-x>

Godfraind, T. (2017). Discovery and development of calcium channel blockers. *Frontiers in Pharmacology*, Vol. 8, p. 286. <https://doi.org/10.3389/fphar.2017.00286>

Goel, G., & Sun, W. (2014, September 1). Cancer immunotherapy in clinical practice—the past, Present, And future chinese journal of cancer. *Chinese Journal of Cancer*, Vol. 33, pp. 445–457. <https://doi.org/10.5732/cjc.014.10123>

Gonda, K., Shibata, M., Sato, Y., Washio, M., Takeshita, H., Shigeta, H., ... Sakuramoto, S. (2017). Elevated neutrophil-to-lymphocyte ratio is associated with nutritional impairment, immune suppression, resistance to S-1 plus cisplatin, and poor prognosis in patients with stage IV gastric cancer. *Molecular and Clinical Oncology*, 7(6), 1073–1078. <https://doi.org/10.3892/mco.2017.1438>

Goodpaster, B. H., Kelley, D. E., Thaete, F. L., He, J., Ross, R., Bret, H., ... Ross, R. (2000). Skeletal muscle attenuation determined by computed tomography is associated with skeletal muscle lipid content, *15261*, 104–110.

Goodpaster, B. H., Theriault, R., Watkins, S. C., & Kelley, D. E. (2000). Intramuscular lipid content is increased in obesity and decreased by weight loss. *Metabolism: Clinical and Experimental*, *49*(4), 467–472. [https://doi.org/DOI: 10.1016/S0026-0495\(00\)80010-4](https://doi.org/DOI: 10.1016/S0026-0495(00)80010-4)

Grant, M. J., & Booth, A. (2009). A typology of reviews: an analysis of 14 review types and associated methodologies. *Health Information & Libraries Journal*, *26*(2), 91–108. <https://doi.org/10.1111/j.1471-1842.2009.00848.x>

Gregor, C. E., Foeng, J., Comerford, I., & McColl, S. R. (2017). Chemokine-Driven CD4+ T Cell Homing: New Concepts and Recent Advances. In *Advances in Immunology* (Vol. 135, pp. 119–181). <https://doi.org/10.1016/bs.ai.2017.03.001>

Grivennikov, S. I., Greten, F. R., & Karin, M. (2010). Immunity, Inflammation, and Cancer. *Cell*, *140*(6), 883–899. <https://doi.org/10.1016/j.cell.2010.01.025>

Grossberg, A. J., Scarlett, J. M., Zhu, X., Bowe, D. D., Batra, A. K., Braun, T. P., & Marks, D. L. (2010). Arcuate Nucleus Proopiomelanocortin Neurons Mediate the Acute Anorectic Actions of Leukemia Inhibitory Factor via gp130. *Endocrinology*, *151*(2), 606–616. <https://doi.org/10.1210/en.2009-1135>

Grusby, M. J., Markowitz, J. S., Laufer, T. M., Lee, R., Auchincloss, H., & Glimcher, L. H. (1994). MHC Class II Mutant Mice. *Transgenesis and Targeted Mutagenesis in Immunology*, 297–307. <https://doi.org/10.1016/B978-0-12-105760-2.50022-4>

Grusby, M., Johnson, R., Papaioannou, V., & Glimcher, L. (1991). Depletion of CD4+ T cells in major histocompatibility complex class II-deficient mice. *Science*, *253*(5026), 1417–1420. <https://doi.org/10.1126/science.1910207>

Gu, L., Li, H., Chen, L., Ma, X., Li, X., Gao, Y., ... Zhang, X. (2016). Prognostic role of lymphocyte to monocyte ratio for patients with cancer: evidence from a systematic review and meta-analysis. *Oncotarget*, *7*(22), 31926–31942. <https://doi.org/10.18632/oncotarget.7876>

Günther, C., Bello-Fernandez, C., Kopp, T., Kund, J., Carballido-Perrig, N., Hinteregger, S., ... Carballido, J. M. (2005). CCL18 Is Expressed in Atopic Dermatitis and Mediates Skin Homing of Human Memory T Cells. *The Journal of Immunology*, *174*(3), 1723–1728. <https://doi.org/10.4049/jimmunol.174.3.1723>

Gustafson, M. P., Bornschlegl, S., Park, S. S., Gastineau, D. A., Roberts, L. R., Dietz, A. B., & Hallemeier, C. L. (2017). Comprehensive assessment of circulating immune cell populations in response to stereotactic body radiation therapy in patients with liver cancer. *Advances in Radiation Oncology*, *2*(4), 540–547. <https://doi.org/10.1016/j.adro.2017.08.003>

Haanen, J. B. A. G., Carbonnel, F., Robert, C., Kerr, K. M., Peters, S., Larkin, J., & Jordan, K. (2017). Management of toxicities from immunotherapy: ESMO Clinical Practice Guidelines for diagnosis, treatment and follow-up. *Annals of Oncology*, *28*, iv119–iv142. <https://doi.org/10.1093/annonc/mdx225>

Halvorsen, E. C., Hamilton, M. J., Young, A., Wadsworth, B. J., LePard, N. E., Lee, H. N., ... Bennewith, K. L. (2016). Maraviroc decreases CCL8-mediated migration of CCR5⁺ regulatory T cells and reduces metastatic tumor growth in the lungs. *OncoImmunology*, *5*(6), e1150398. <https://doi.org/10.1080/2162402X.2016.1150398>

Hanahan, D., & Weinberg, R. A. (2011). Hallmarks of Cancer: The Next Generation. *Cell*, *144*(5), 646–674. <https://doi.org/10.1016/j.cell.2011.02.013>

He, Q., Li, G., Ji, X., Ma, L., Wang, X., Li, Y., & Fan, C. (2017). Impact of the immune cell population in peripheral blood on response and survival in patients receiving neoadjuvant chemotherapy for advanced gastric cancer. *Tumor Biology*, *39*(5), 1010428317697571. <https://doi.org/10.1177/1010428317697571>

He, W. A., Calore, F., Londhe, P., Canella, A., Guttridge, D. C., & Croce, C. M. (2014). Microvesicles containing miRNAs promote muscle cell death in cancer cachexia via TLR7. *Proceedings of the National Academy of Sciences*, *111*(12), 4525–4529. <https://doi.org/10.1073/pnas.1402714111>

He, W. Z., Yang, Q. X., Xie, J. Y., Kong, P. F., Hu, W. M., Yang, L., ... Xia, L. P. (2018). Association of low skeletal muscle index with increased systematic inflammatory responses and interferon γ -induced protein 10 levels in patients with colon cancer. *Cancer Management and Research*, *10*, 2499–2507. <https://doi.org/10.2147/CMAR.S160901>

Hébuterne, X., Lemarié, E., Michallet, M., de Montreuil, C. B., Schneider, S. M., & Goldwasser, F. (2014). Prevalence of Malnutrition and Current Use of Nutrition Support in Patients With Cancer. *Journal of Parenteral and Enteral Nutrition*, *38*(2), 196–204. <https://doi.org/10.1177/01486071113502674>

Henneke, P., Takeuchi, O., van Strijp, J. A., Guttormsen, H.-K., Smith, J. A., Schromm, A. B., ... Golenbock, D. T. (2001). Novel Engagement of CD14 and Multiple Toll-Like Receptors by Group B Streptococci. *The Journal of Immunology*, *167*(12), 7069–7076. <https://doi.org/10.4049/jimmunol.167.12.7069>

Henriksen, T. I., Davidsen, P. K., Pedersen, M., Schultz, H. S., Hansen, N. S., Larsen, T. J., ... Scheele, C. (2017). Dysregulation of a novel miR-23b/27b-p53 axis impairs muscle stem cell differentiation of humans with type 2 diabetes. *Molecular Metabolism*, *6*(7), 770–779. <https://doi.org/10.1016/j.molmet.2017.04.006>

Henriques, F., Lopes, M. A., Franco, F. O., Knobl, P., Santos, K. B., Bueno, L. L., ... Batista, M. L. (2018). Toll-Like Receptor-4 Disruption Suppresses Adipose Tissue Remodeling and Increases

Survival in Cancer Cachexia Syndrome. *Scientific Reports*, 8(1), 18024.
<https://doi.org/10.1038/s41598-018-36626-3>

Hernandez, C., Huebener, P., & Schwabe, R. F. (2016). Damage-associated molecular patterns in cancer: a double-edged sword. *Oncogene*, 35(46), 5931–5941.
<https://doi.org/10.1038/onc.2016.104>

Hers, H. G., & van Hoof, F. (1966). Enzymes of glycogen degradation in biopsy material. *Methods in Enzymology*, 8, 525–532. [https://doi.org/10.1016/0076-6879\(66\)08094-7](https://doi.org/10.1016/0076-6879(66)08094-7)

Higuchi, I., Niiyama, T., Uchida, Y., Inose, M., Hu, J., Nakagawa, M., ... Osame, M. (2000). Microvascular endothelial abnormality in skeletal muscle from a patient with gastric cancer without dermatomyositis. *Acta Neuropathologica*, 100(6), 718–722.
<https://doi.org/10.1007/s004010000243>

Hindi, S. M., & Kumar, A. (n.d.). Toll-like receptor signalling in regenerative myogenesis: friend and foe. <https://doi.org/10.1002/path.4714>

Hirasawa, Y., Nakashima, J., Yunaiyama, D., Sugihara, T., Gondo, T., Nakagami, Y., ... Tachibana, M. (2016). Sarcopenia as a Novel Preoperative Prognostic Predictor for Survival in Patients with Bladder Cancer Undergoing Radical Cystectomy. *Annals of Surgical Oncology*, 23(S5), 1048–1054. <https://doi.org/10.1245/s10434-016-5606-4>

Hirata, A., Masuda, S., Tamura, T., Kai, K., Ojima, K., Fukase, A., ... Takeda, S. (2003). Expression profiling of cytokines and related genes in regenerating skeletal muscle after cardiotoxin injection: A role for osteopontin. *American Journal of Pathology*, 163(1), 203–215.
[https://doi.org/10.1016/S0002-9440\(10\)63644-9](https://doi.org/10.1016/S0002-9440(10)63644-9)

Hohlfeld, R., & Engel, A. G. (1990). Induction of HLA-DR expression on human myoblasts with interferon-gamma. *The American Journal of Pathology*, 136(3), 503–508.

Hohlfeld, R., & Engel, A. G. (1991). Coculture with autologous myotubes of cytotoxic T cells isolated from muscle in inflammatory myopathies. *Annals of Neurology*, 29(5), 498–507.
<https://doi.org/10.1002/ana.410290509>

Hohlfeld, Reinhard, & Engel, A. G. (1991). Coculture with autologous myotubes of cytotoxic T cells isolated from muscle in inflammatory myopathies. *Annals of Neurology*, 29(5), 498–507.
<https://doi.org/10.1002/ana.410290509>

Hounsfield, G. N. (1973). Computerized transverse axial scanning (tomography): Part 1. Description of system. *The British Journal of Radiology*, 46(552), 1016–1022.
<https://doi.org/10.1259/0007-1285-46-552-1016>

House, I. G., Savas, P., Lai, J., Chen, A. X. Y., Oliver, A. J., Teo, Z. L., ... Beavis, P. A. (2019). Macrophage derived CXCL9 and CXCL10 are required for anti-tumor immune responses

following immune checkpoint blockade. *Clinical Cancer Research : An Official Journal of the American Association for Cancer Research*. <https://doi.org/10.1158/1078-0432.CCR-19-1868>

Hsiao, Y.-W., Liao, K.-W., Chung, T.-F., Liu, C.-H., Hsu, C.-D., & Chu, R.-M. (2008). Interactions of host IL-6 and IFN- γ and cancer-derived TGF- β 1 on MHC molecule expression during tumor spontaneous regression. *Cancer Immunology, Immunotherapy*, *57*(7), 1091–1104. <https://doi.org/10.1007/s00262-007-0446-5>

Hu, J., Shi, D., Ding, M., Huang, T., Gu, R., Xiao, J., ... Liao, H. (2019). Calmodulin-dependent signalling pathways are activated and mediate the acute inflammatory response of injured skeletal muscle. *The Journal of Physiology*, *597*(21), 5161–5177. <https://doi.org/10.1113/JP278478>

Huang, D.-D., Ji, Y.-B., Zhou, D.-L., Li, B., Wang, S.-L., Chen, X.-L., ... Zhuang, C.-L. (2017). Effect of surgery-induced acute muscle wasting on postoperative outcomes and quality of life. *Journal of Surgical Research*, *218*, 58–66. <https://doi.org/10.1016/J.JSS.2017.05.045>

Huehls, A. M., Huntoon, C. J., Joshi, P. M., Baehr, C. A., Wagner, J. M., Wang, X., ... Karnitz, L. M. (2015). Genomically Incorporated 5-Fluorouracil that Escapes UNG-Initiated Base Excision Repair Blocks DNA Replication and Activates Homologous Recombination. *Molecular Pharmacology*, *89*(1), 53–62. <https://doi.org/10.1124/mol.115.100164>

Hunninghake, G. M., Chu, J., Sharma, S. S., Cho, M. H., Himes, B. E., Rogers, A. J., ... Raby, B. A. (2011). The CD4+ T-cell transcriptome and serum IgE in asthma: IL17RB and the role of sex. *BMC Pulmonary Medicine*, *11*(1), 17. <https://doi.org/10.1186/1471-2466-11-17>

Ieronimakis, N., Pantoja, M., Hays, A. L., Dosey, T. L., Qi, J., Fischer, K. A., ... Reyes, M. (2013). Increased sphingosine-1-phosphate improves muscle regeneration in acutely injured mdx mice. *Skeletal Muscle*, *3*(1), 20. <https://doi.org/10.1186/2044-5040-3-20>

Inaba, S., Hinohara, A., Tachibana, M., Tsujikawa, K., & Fukada, S. (2018). Muscle regeneration is disrupted by cancer cachexia without loss of muscle stem cell potential. *PLOS ONE*, *13*(10), e0205467. <https://doi.org/10.1371/journal.pone.0205467>

Jackson, W., Alexander, N., Schipper, M., Fig, L., Feng, F., & Jolly, S. (2014). Characterization of changes in total body composition for patients with head and neck cancer undergoing chemoradiotherapy using dual-energy x-ray absorptiometry. *Head and Neck*, *36*(9), 1356–1362. <https://doi.org/10.1002/hed.23461>

Jago, R. T., Redfern, C. P. F., Roberts, R. G., Gibson, G. J., & Goodship, T. H. J. (2002). Skeletal muscle mRNA levels for cathepsin B, but not components of the ubiquitin–proteasome pathway, are increased in patients with lung cancer referred for thoracotomy. *Clinical Science*, *102*(3), 353–361. <https://doi.org/10.1042/CS20010270>

Jameel, N. M., Thirunavukkarasu, C., Wu, T., Watkins, S. C., Friedman, S. L., & Gandhi, C. R. (2009). p38-MAPK- and caspase-3-mediated superoxide-induced apoptosis of rat hepatic stellate

cells: Reversal by retinoic acid. *Journal of Cellular Physiology*, 218(1), 157–166.
<https://doi.org/10.1002/jcp.21581>

Järvinen, T., Ilonen, I., Kauppi, J., Salo, J., & Räsänen, J. (2018). Loss of skeletal muscle mass during neoadjuvant treatments correlates with worse prognosis in esophageal cancer: a retrospective cohort study. *World Journal of Surgical Oncology*, 16(1), 27.
<https://doi.org/10.1186/s12957-018-1327-4>

Jeong, J., Kim, Y.-J., Yoon, S. Y., Kim, Y.-J., Kim, J. H., Sohn, K.-Y., ... Kim, J. W. (2016). PLAG (1-Palmitoyl-2-Linoleoyl-3-Acetyl-rac-Glycerol) Modulates Eosinophil Chemotaxis by Regulating CCL26 Expression from Epithelial Cells. *PLOS ONE*, 11(3), e0151758.
<https://doi.org/10.1371/journal.pone.0151758>

Jeyaseelan, S., Chu, H. W., Young, S. K., Freeman, M. W., & Worthen, G. S. (2005). Distinct roles of pattern recognition receptors CD14 and Toll-like receptor 4 in acute lung injury. *Infection and Immunity*, 73(3), 1754–1763. <https://doi.org/10.1128/IAI.73.3.1754-1763.2005>

Johns, N., Hatakeyama, S., Stephens, N. A., Degen, M., Degen, S., Friauff, W., ... Fearon, K. C. H. (2014). Clinical classification of cancer cachexia: Phenotypic correlates in human skeletal muscle. *PLoS ONE*, 9(1), 1–13. <https://doi.org/10.1371/journal.pone.0083618>

Johns, N., Stretch, C., Tan, B. H. L., Solheim, T. S., Sørhaug, S., Stephens, N. A., ... Fearon, K. C. H. (2017). New genetic signatures associated with cancer cachexia as defined by low skeletal muscle index and weight loss. *Journal of Cachexia, Sarcopenia and Muscle*, 8(1), 122–130.
<https://doi.org/10.1002/jcsm.12138>

Johnson, M. A., Polgar, J., Weightman, D., & Appleton, D. (1973). Data on the distribution of fibre types in thirty-six human muscles. An autopsy study. *Journal of the Neurological Sciences*, 18(1), 111–129. [https://doi.org/10.1016/0022-510X\(73\)90023-3](https://doi.org/10.1016/0022-510X(73)90023-3)

Joseph, P. R. B., Sawant, K. V., & Rajarathnam, K. (2017). Heparin-bound chemokine CXCL8 monomer and dimer are impaired for CXCR1 and CXCR2 activation: Implications for gradients and neutrophil trafficking. *Open Biology*, 7(11). <https://doi.org/10.1098/rsob.170168>

Joyce, N. C., Oskarsson, B., & Jin, L.-W. (2012). Muscle biopsy evaluation in neuromuscular disorders. *Physical Medicine and Rehabilitation Clinics of North America*, 23(3), 609–631.
<https://doi.org/10.1016/j.pmr.2012.06.006>

Jung, B., Staudacher, J. J., & Beauchamp, D. (2017). Transforming Growth Factor β Superfamily Signaling in Development of Colorectal Cancer. *Gastroenterology*, 152(1), 36–52.
<https://doi.org/10.1053/J.GASTRO.2016.10.015>

Jung, H.-W., Kim, J. W., Kim, J.-Y., Kim, S.-W., Yang, H. K., Lee, J. W., ... Kim, J. H. (2015). Effect of muscle mass on toxicity and survival in patients with colon cancer undergoing adjuvant chemotherapy. *Supportive Care in Cancer*, 23(3), 687–694. <https://doi.org/10.1007/s00520-014-2418-6>

- Juo, P., Kuo, C. J., Reynolds, S. E., Konz, R. F., Raingeaud, J., Davis, R. J., ... Blenis, J. (1997). Fas activation of the p38 mitogen-activated protein kinase signalling pathway requires ICE/CED-3 family proteases. *Molecular and Cellular Biology*, *17*(1), 24–35. <https://doi.org/10.1128/mcb.17.1.24>
- Kabashima, K., Shiraishi, N., Sugita, K., Mori, T., Onoue, A., Kobayashi, M., ... Tokura, Y. (2007). CXCL12-CXCR4 engagement is required for migration of cutaneous dendritic cells. *American Journal of Pathology*, *171*(4), 1249–1257. <https://doi.org/10.2353/ajpath.2007.070225>
- Kaech, S. M., Hemby, S., Kersh, E., & Ahmed, R. (2002). Molecular and Functional Profiling of Memory CD8 T Cell Differentiation. *Cell*, *111*(6), 837–851. [https://doi.org/10.1016/S0092-8674\(02\)01139-X](https://doi.org/10.1016/S0092-8674(02)01139-X)
- Kamimura, K., Matsumoto, Y., Zhou, Q., Moriyama, M., & Saijo, Y. (2016). Myelosuppression by chemotherapy in obese patients with gynecological cancers. *Cancer Chemotherapy and Pharmacology*, *78*(3), 633–641. <https://doi.org/10.1007/s00280-016-3119-2>
- Kandarian, S. C., Nosacka, R. L., Delitto, A. E., Judge, A. R., Judge, S. M., Ganey, J. D., ... Jackman, R. W. (2018). Tumour-derived leukaemia inhibitory factor is a major driver of cancer cachexia and morbidity in C26 tumour-bearing mice. *Journal of Cachexia, Sarcopenia and Muscle*, *9*(6), 1109–1120. <https://doi.org/10.1002/jcsm.12346>
- Kastenschmidt, J. M., Mannaa, A. H., Muñoz, K. J., & Villalta, S. A. (2019). Immune System Regulation of Muscle Injury and Disease. In *Muscle Gene Therapy* (pp. 121–139). https://doi.org/10.1007/978-3-030-03095-7_7
- Kawamura, T., Makuuchi, R., Tokunaga, M., Tanizawa, Y., Bando, E., Yasui, H., ... Terashima, M. (2018). Long-Term Outcomes of Gastric Cancer Patients with Preoperative Sarcopenia. *Annals of Surgical Oncology*, *25*(6), 1625–1632. <https://doi.org/10.1245/s10434-018-6452-3>
- Kawasaki, T., & Kawai, T. (2014). Toll-Like Receptor Signaling Pathways. *Frontiers in Immunology*, *5*, 461. <https://doi.org/10.3389/fimmu.2014.00461>
- Kazemi-Bajestani, S. M. R., Mazurak, V. C., & Baracos, V. (2016). Computed tomography-defined muscle and fat wasting are associated with cancer clinical outcomes. *Seminars in Cell and Developmental Biology*, *54*, 2–10. <https://doi.org/10.1016/j.semcdb.2015.09.001>
- Kesteman, N., Vansanten, G., Pajak, B., Goyert, S. M., & Moser, M. (2008). Injection of lipopolysaccharide induces the migration of splenic neutrophils to the T cell area of the white pulp: role of CD14 and CXC chemokines. *Journal of Leukocyte Biology*, *83*(3), 640–647. <https://doi.org/10.1189/jlb.0807578>
- Khal, J., Hine, A. V., Fearon, K. C. H., Dejong, C. H. C., & Tisdale, M. J. (2005). Increased expression of proteasome subunits in skeletal muscle of cancer patients with weight loss.

International Journal of Biochemistry and Cell Biology, 37(10 SPEC. ISS.), 2196–2206.
<https://doi.org/10.1016/j.biocel.2004.10.017>

Kim, E. Y., Kim, Y. S., Seo, J. Y., Park, I., Ahn, H. K., Jeong, Y. M., ... Kim, N. (2016). The relationship between sarcopenia and systemic inflammatory response for cancer cachexia in small cell lung cancer. *PLoS ONE*, 11(8). <https://doi.org/10.1371/journal.pone.0161125>

Kiss, N., Beraldo, J., & Everitt, S. (2018). Early Skeletal Muscle Loss in Non-Small Cell Lung Cancer Patients Receiving Chemoradiation and Relationship to Survival. *Supportive Care in Cancer*, 1–8. <https://doi.org/10.1007/s00520-018-4563-9>

Kitz, A., & Dominguez-Villar, M. (2017, November 1). Molecular mechanisms underlying Th1-like Treg generation and function. *Cellular and Molecular Life Sciences*, Vol. 74, pp. 4059–4075. <https://doi.org/10.1007/s00018-017-2569-y>

Klein, S. L., & Flanagan, K. L. (2016). Sex differences in immune responses. *Nature Reviews Immunology*, 16(10), 626–638. <https://doi.org/10.1038/nri.2016.90>

Kobayashi, Y., Konno, Y., Kanda, A., Yamada, Y., Yasuba, H., Sakata, Y., ... Ueki, S. (2019). Critical role of CCL4 in eosinophil recruitment into the airway. *Clinical and Experimental Allergy*, 49(6), 853–860. <https://doi.org/10.1111/cea.13382>

Koch, M. A., Thomas, K. R., Perdue, N. R., Smigielski, K. S., Srivastava, S., & Campbell, D. J. (2012). T-bet + Treg Cells Undergo Abortive Th1 Cell Differentiation due to Impaired Expression of IL-12 Receptor $\beta 2$. *Immunity*, 37(3), 501–510. <https://doi.org/10.1016/j.immuni.2012.05.031>

Kohno, S., Ueji, T., Abe, T., Nakao, R., Hirasaka, K., Oarada, M., ... Nikawa, T. (2011). Rantes secreted from macrophages disturbs skeletal muscle regeneration after cardiotoxin injection in Cbl-b-deficient mice. *Muscle & Nerve*, 43(2), 223–229. <https://doi.org/10.1002/mus.21829>

Kralova, J., Dvorak, M., Koc, M., & Kral, V. (2008). p38 MAPK plays an essential role in apoptosis induced by photoactivation of a novel ethylene glycol porphyrin derivative. *Oncogene*, 27(21), 3010–3020. <https://doi.org/10.1038/sj.onc.1210960>

Kryczek, I., Zou, L., Rodriguez, P., Zhu, G., Wei, S., Mottram, P., ... Zou, W. (2006). B7-H4 expression identifies a novel suppressive macrophage population in human ovarian carcinoma. *The Journal of Experimental Medicine*, 203(4), 871–881. <https://doi.org/10.1084/jem.20050930>

Kucuk, C., Ozkan, M., Akgun, H., Muhtaroglu, S., & Sozuer, E. (2005). The Effect of Granulocyte Macrophage-Colony Stimulating Factor on Bacterial Translocation after Administration of 5-Fluorouracil in Rats. *Journal of Surgical Research*, 128(1), 15–20. <https://doi.org/10.1016/J.JSS.2005.04.037>

Kumar, H., Kawai, T., & Akira, S. (2009). Toll-like receptors and innate immunity. *Biochemical and Biophysical Research Communications*, 388(4), 621–625. <https://doi.org/10.1016/j.bbrc.2009.08.062>

- Kuroki, L. M., Mangano, M., Allsworth, J. E., Menias, C. O., Massad, L. S., Powell, M. A., ... Thaker, P. H. (2015). Pre-operative Assessment of Muscle Mass to Predict Surgical Complications and Prognosis in Patients With Endometrial Cancer. *Annals of Surgical Oncology*, 22(3), 972–979. <https://doi.org/10.1245/s10434-014-4040-8>
- Kurra, V., Sullivan, R. J., Gainor, J. F., Hodi, F. S., Gandhi, L., Sadow, C. A., ... Lee, S. (2016). Pseudoprogession in cancer immunotherapy: Rates, time course and patient outcomes. *Journal of Clinical Oncology*, 34(15_suppl), 6580–6580. https://doi.org/10.1200/jco.2016.34.15_suppl.6580
- Kuwano, Y., Spelten, O., Zhang, H., Ley, K., & Zarbock, A. (2010). Rolling on E- or P-selectin induces the extended but not high-affinity conformation of LFA-1 in neutrophils. *Blood*, 116(4), 617–624. <https://doi.org/10.1182/blood-2010-01-266122>
- Kzhyshkowska, J., Workman, G., Cardó-Vila, M., Arap, W., Pasqualini, R., Gratchev, A., ... Sage, E. H. (2006). Novel Function of Alternatively Activated Macrophages: Stabilin-1-Mediated Clearance of SPARC. *The Journal of Immunology*, 176(10), 5825–5832. <https://doi.org/10.4049/jimmunol.176.10.5825>
- Lacomis, D. (2004). The utility of muscle biopsy. *Current Neurology and Neuroscience Reports*, 4(1), 81–86.
- Lacy, P. (2015). Editorial: secretion of cytokines and chemokines by innate immune cells. *Frontiers in Immunology*, 6, 190. <https://doi.org/10.3389/fimmu.2015.00190>
- LaFleur, A. M., Lukacs, N. W., Kunkel, S. L., & Matsukawa, A. (2004). Role of CC chemokine CCL6/C10 as a monocyte chemoattractant in a murine acute peritonitis. *Mediators of Inflammation*, 13(5–6), 349–355. <https://doi.org/10.1080/09629350400014172>
- Lamboley, C. R., Xu, H., Dutka, T. L., Hanson, E. D., Hayes, A., Violet, J. A., ... Lamb, G. D. (2017). Effect of androgen deprivation therapy on the contractile properties of type I and type II skeletal muscle fibres in men with non-metastatic prostate cancer. *Clinical and Experimental Pharmacology and Physiology*, (August 2017), 146–154. <https://doi.org/10.1111/1440-1681.12873>
- Langen, R. C. J., Gosker, H. R., Remels, A. H. V., & Schols, A. M. W. J. (2013). Triggers and mechanisms of skeletal muscle wasting in chronic obstructive pulmonary disease. *The International Journal of Biochemistry & Cell Biology*, 45(10), 2245–2256. <https://doi.org/10.1016/j.biocel.2013.06.015>
- Langstein, H. N., Doherty, G. M., Fraker, D. L., Buresh, C. M., & Norton, J. A. (1991). The roles of gamma-interferon and tumor necrosis factor alpha in an experimental rat model of cancer cachexia. *Cancer Research*, 51(9), 2302–2306.
- Larsen, B. A., Wassel, C. L., Kritchevsky, S. B., Strotmeyer, E. S., Criqui, M. H., Kanaya, A. M., ... Health ABC Study. (2016). Association of Muscle Mass, Area, and Strength With Incident

Diabetes in Older Adults: The Health ABC Study. *The Journal of Clinical Endocrinology & Metabolism*, 101(4), 1847–1855. <https://doi.org/10.1210/jc.2015-3643>

Lattermann, R., Carli, F., Wykes, L., & Schricker, T. (2002). Epidural blockade modifies perioperative glucose production without affecting protein catabolism. *Anesthesiology*, 97(2), 374–381.

Laviano, A., Gleason, J. R., Meguid, M. M., Yang, Z. J., Cangiano, C., & Rossi Fanelli, F. (2000). Effects of intra-VMN mianserin and IL-1ra on meal number in anorectic tumor-bearing rats. *Journal of Investigative Medicine : The Official Publication of the American Federation for Clinical Research*, 48(1), 40–48.

Lavine, K. J., & Sierra, O. L. (2017). Skeletal muscle inflammation and atrophy in heart failure. *Heart Failure Reviews*, 22(2), 179–189. <https://doi.org/10.1007/s10741-016-9593-0>

Leal, F., Ferreira, F. P., & Sasse, A. D. (2017). FOLFOXIRI Regimen for Metastatic Colorectal Cancer: A Systematic Review and Meta-Analysis. *Clinical Colorectal Cancer*, 16(4), 405–409.e2. <https://doi.org/10.1016/j.clcc.2017.03.012>

Leenders, M., Verdijk, L. B., van der Hoeven, L., Adam, J. J., van Kranenburg, J., Nilwik, R., & van Loon, L. J. C. (2013). Patients With Type 2 Diabetes Show a Greater Decline in Muscle Mass, Muscle Strength, and Functional Capacity With Aging. *Journal of the American Medical Directors Association*, 14(8), 585–592. <https://doi.org/10.1016/j.jamda.2013.02.006>

Lei, Y., Ripen, A. M., Ishimaru, N., Ohigashi, I., Nagasawa, T., Jeker, L. T., ... Takahama, Y. (2011). Aire-dependent production of XCL1 mediates medullary accumulation of thymic dendritic cells and contributes to regulatory T cell development. *Journal of Experimental Medicine*, 208(2), 383–394. <https://doi.org/10.1084/jem.20102327>

Leifer, C. A., & Medvedev, A. E. (2016). Molecular mechanisms of regulation of Toll-like receptor signaling. *Journal of Leukocyte Biology*, 100(5), 927–941. <https://doi.org/10.1189/jlb.2mr0316-117rr>

Lerner, L., Tao, J., Liu, Q., Nicoletti, R., Feng, B., Krieger, B., ... Gyuris, J. (2016). MAP3K11/GDF15 axis is a critical driver of cancer cachexia. *Journal of Cachexia, Sarcopenia and Muscle*, 7(4), 467–482. <https://doi.org/10.1002/jcsm.12077>

Li, L., Xu, L., Yan, J., Zhen, Z.-J., Ji, Y., Liu, C.-Q., ... Xu, J. (2015). CXCR2–CXCL1 axis is correlated with neutrophil infiltration and predicts a poor prognosis in hepatocellular carcinoma. *Journal of Experimental & Clinical Cancer Research*, 34(1), 129. <https://doi.org/10.1186/s13046-015-0247-1>

Liao, H., Franck, E., Fréret, M., Adriouch, S., Baba-Amer, Y., Authier, F.-J., ... Gherardi, R. K. (2012). Myoinjury transiently activates muscle antigen-specific CD8+ T cells in lymph nodes in a mouse model. *Arthritis & Rheumatism*, 64(10), 3441–3451. <https://doi.org/10.1002/art.34551>

- Liberati, A., Altman, D. G., Tetzlaff, J., Mulrow, C., Gotzsche, P. C., Ioannidis, J. P. A., ... Moher, D. (2009). The PRISMA statement for reporting systematic reviews and meta-analyses of studies that evaluate healthcare interventions: explanation and elaboration. *BMJ*, *339*(jul21 1), b2700–b2700. <https://doi.org/10.1136/bmj.b2700>
- Lieffers, J R, Bathe, O. F., Fassbender, K., Winget, M., & Baracos, V. E. (2012). Sarcopenia is associated with postoperative infection and delayed recovery from colorectal cancer resection surgery. *British Journal of Cancer*, *107*(6), 931–936. <https://doi.org/10.1038/bjc.2012.350>
- Lieffers, J. R., Mourtzakis, M., Hall, K. D., McCargar, L. J., Prado, C. M., & Baracos, V. E. (2009). A viscerally driven cachexia syndrome in patients with advanced colorectal cancer: contributions of organ and tumor mass to whole-body energy demands. *The American Journal of Clinical Nutrition*, *89*(4), 1173–1179. <https://doi.org/10.3945/ajcn.2008.27273>
- Lightfoot, A., McArdle, A., & Griffiths, R. D. (2009). Muscle in defense. *Critical Care Medicine*, *37*(SUPPL. 10). <https://doi.org/10.1097/CCM.0b013e3181b6f8a5>
- Lin, J., Zhang, W., Huang, Y., Chen, W., Wu, R., Chen, X., ... Wang, P. (2018). Sarcopenia is associated with the neutrophil/ lymphocyte and platelet/lymphocyte ratios in operable gastric cancer patients: A prospective study. *Cancer Management and Research*, *10*, 4935–4944. <https://doi.org/10.2147/CMAR.S175421>
- Lin, X. B., Farhangfar, A., Valcheva, R., Sawyer, M. B., Dieleman, L., Schieber, A., ... Baracos, V. (2014). The role of intestinal microbiota in development of irinotecan toxicity and in toxicity reduction through dietary fibres in rats. *PLoS ONE*, *9*(1). <https://doi.org/10.1371/journal.pone.0083644>
- Linge, H. M., Collin, M., Nordenfelt, P., Mörgelin, M., Malmsten, M., & Egesten, A. (2008). The human CXC chemokine granulocyte chemotactic protein 2 (GCP-2)/CXCL6 possesses membrane-disrupting properties and is antibacterial. *Antimicrobial Agents and Chemotherapy*, *52*(7), 2599–2607. <https://doi.org/10.1128/AAC.00028-08>
- Lissoni, P., Brivio, F., Ferrante, R., Vigore, L., Vaghi, M., Fumagalli, E., ... Fumagalli, L. (n.d.). Circulating immature and mature dendritic cells in relation to lymphocyte subsets in patients with gastrointestinal tract cancer. *The International Journal of Biological Markers*, *15*(1), 22–25.
- Liu, J., Chen, D., Nie, G. D., & Dai, Z. (2015). CD8(+)CD122(+) T-Cells: A Newly Emerging Regulator with Central Memory Cell Phenotypes. *Frontiers in Immunology*, *6*, 494. <https://doi.org/10.3389/fimmu.2015.00494>
- Liu, L.-Z., Zhang, Z., Zheng, B.-H., Shi, Y., Duan, M., Ma, L.-J., ... Gao, Q. (2019). CCL15 Recruits Suppressive Monocytes to Facilitate Immune Escape and Disease Progression in Hepatocellular Carcinoma. *Hepatology*, *69*(1), 143–159. <https://doi.org/10.1002/hep.30134>
- Liu, S. Z., Jemiolo, B., Lavin, K. M., Lester, B. E., Trappe, S. W., & Trappe, T. A. (2016). Prostaglandin E2/cyclooxygenase pathway in human skeletal muscle: influence of muscle fiber

type and age. *Journal of Applied Physiology (Bethesda, Md. : 1985)*, 120(5), 546–551. <https://doi.org/10.1152/jappphysiol.00396.2015>

Loell, I., & Lundberg, I. E. (2011). Can muscle regeneration fail in chronic inflammation: A weakness in inflammatory myopathies? *Journal of Internal Medicine*, 269(3), 243–257. <https://doi.org/10.1111/j.1365-2796.2010.02334.x>

Loell, I., Helmers, S. B., Dastmalchi, M., Alexanderson, H., Munters, L. a., Nennesmo, I., ... Esbjörnsson, M. (2011). Higher proportion of fast-twitch (type II) muscle fibres in idiopathic inflammatory myopathies - evident in chronic but not in untreated newly diagnosed patients. *Clinical Physiology and Functional Imaging*, 31(1), 18–25. <https://doi.org/10.1111/j.1475-097X.2010.00973.x>

Loomans, H. A., & Andl, C. D. (2014). Intertwining of Activin A and TGF β Signaling: Dual Roles in Cancer Progression and Cancer Cell Invasion. *Cancers*, 7(1), 70–91. <https://doi.org/10.3390/cancers7010070>

Lozano, D. D., Kahl, E. A., Wong, H. P., Stephenson, L. L., & Zamboni, W. A. (1999). L-Selectin and Leukocyte Function in Skeletal Muscle Reperfusion Injury. *Archives of Surgery*, 134(10), 1079. <https://doi.org/10.1001/archsurg.134.10.1079>

Lundholm, K., Bylund, A., Holm, J., & Schersten, T. (1976). Skeletal muscle metabolism in patients with malignant tumor. *European Journal of Cancer*, 12(6), 465–473.

Luo, J.-L., Hammarqvist, F., Andersson, K., & Wernerman, J. (1998). Surgical trauma decreases glutathione synthetic capacity in human skeletal muscle tissue. *American Journal of Physiology-Endocrinology and Metabolism*, 275(2), E359–E365. <https://doi.org/10.1152/ajpendo.1998.275.2.E359>

Lyons, Y. A., Wu, S. Y., Overwijk, W. W., Baggerly, K. A., & Sood, A. K. (2017). Immune cell profiling in cancer: molecular approaches to cell-specific identification. *Npj Precision Oncology*, 1(1), 26. <https://doi.org/10.1038/s41698-017-0031-0>

Ma, J. F., Sanchez, B. J., Hall, D. T., Tremblay, A. K., Di Marco, S., & Gallouzi, I. (2017). STAT 3 promotes IFN γ / TNF α -induced muscle wasting in an NF - κ B-dependent and IL -6-independent manner. *EMBO Molecular Medicine*, 9(5), 622–637. <https://doi.org/10.15252/emmm.201607052>

MacDonald, A. J., Johns, N., Stephens, N., Greig, C., Ross, J. A., Small, A. C., ... Preston, T. (2015). Habitual myofibrillar protein synthesis is normal in patients with upper GI cancer cachexia. *Clinical Cancer Research*, 21(7), 1734–1740. <https://doi.org/10.1158/1078-0432.CCR-14-2004>

Madaro, L., & Bouché, M. (2014). From innate to adaptive immune response in muscular dystrophies and skeletal muscle regeneration: The role of lymphocytes. *BioMed Research International*, 2014, 1–12. <https://doi.org/10.1155/2014/438675>

- Malietzis, G., Currie, A. C., Johns, N., Fearon, K. C., Darzi, A., Kennedy, R. H., ... Jenkins, J. T. (2016). Skeletal Muscle Changes After Elective Colorectal Cancer Resection: A Longitudinal Study. *Annals of Surgical Oncology*, 23(8), 2539–2547. <https://doi.org/10.1245/s10434-016-5188-1>
- Malietzis, G., Giacometti, M., Kennedy, R. H., Athanasiou, T., Aziz, O., & Jenkins, J. T. (2014). The Emerging Role of Neutrophil to Lymphocyte Ratio in Determining Colorectal Cancer Treatment Outcomes: A Systematic Review and Meta-Analysis. *Annals of Surgical Oncology*, 21(12), 3938–3946. <https://doi.org/10.1245/s10434-014-3815-2>
- Malietzis, G., Johns, N., Al-Hassi, H. O., Knight, S. C., Kennedy, R. H., Fearon, K. C. H., ... Jenkins, J. T. (2016). Low muscularity and myosteatosis is related to the host systemic inflammatory response in patients undergoing surgery for colorectal cancer. *Annals of Surgery*, 263(2), 320–325. <https://doi.org/10.1097/SLA.0000000000001113>
- Malietzis, G., Lee, G. H., Al-Hassi, H. O., Bernardo, D., Blakemore, A. I. F., Kennedy, R. H., ... Knight, S. C. (2016). Body composition of the host influences dendritic cell phenotype in patients treated for colorectal cancer. *Tumor Biology*, 37(8), 11359–11364. <https://doi.org/10.1007/s13277-016-5009-y>
- Malin, S. K., & Kashyap, S. R. (2014). Effects of metformin on weight loss. *Current Opinion in Endocrinology & Diabetes and Obesity*, 21(5), 323–329. <https://doi.org/10.1097/MED.0000000000000095>
- Malinin, N. L., Boldin, M. P., Kovalenko, A. V., & Wallach, D. (1997). MAP3K-related kinase involved in NF- κ B induction by TNF, CD95 and IL-1. *Nature*, 385(6616), 540–544. <https://doi.org/10.1038/385540a0>
- Malm, C., Nyberg, P., Engstrom, M., Sjodin, B., Lenkei, R., Ekblom, B., & Lundberg, I. (2000). Immunological changes in human skeletal muscle and blood after eccentric exercise and multiple biopsies. *The Journal of Physiology*, 529 Pt 1, 243–262. https://doi.org/PHY_0858
- Malm, Christer, Sjodin, B., Sjöberg, B., Lenkei, R., Renström, P., Lundberg, I. E., & Ekblom, B. (2004). Leukocytes, cytokines, growth factors and hormones in human skeletal muscle and blood after uphill or downhill running. *Journal of Physiology*, 556(3), 983–1000. <https://doi.org/10.1113/jphysiol.2003.056598>
- Mammucari, C., Milan, G., Romanello, V., Masiere, E., Rudolf, R., Del Piccolo, P., ... Sandri, M. (2007). FoxO3 Controls Autophagy in Skeletal Muscle In Vivo. *Cell Metabolism*, 6(6), 458–471. <https://doi.org/10.1016/j.cmet.2007.11.001>
- Marchildon, F., Fu, D., Lala-Tabbert, N., & Wiper-Bergeron, N. (2016). CCAAT/enhancer binding protein beta protects muscle satellite cells from apoptosis after injury and in cancer cachexia. *Cell Death & Disease*, 7(2), e2109–e2109. <https://doi.org/10.1038/cddis.2016.4>

Marino, M., Scuderi, F., Provenzano, C., & Bartoccioni, E. (2010). Skeletal muscle cells : from local inflammatory response to active immunity. *Gene Therapy*, *18*(2), 109–116. <https://doi.org/10.1038/gt.2010.124>

Marquis, K., Debigaré, R., Lacasse, Y., LeBlanc, P., Jobin, J., Carrier, G., & Maltais, F. (2002). Midthigh Muscle Cross-Sectional Area Is a Better Predictor of Mortality than Body Mass Index in Patients with Chronic Obstructive Pulmonary Disease. *American Journal of Respiratory and Critical Care Medicine*, *166*(6), 809–813. <https://doi.org/10.1164/rccm.2107031>

Martín, A. I., Gómez-SanMiguel, A. B., Priego, T., & López-Calderón, A. (2018). Formoterol treatment prevents the effects of endotoxin on muscle TNF/NF- κ B, Akt/mTOR, and proteolytic pathways in a rat model. Role of IGF-I and miRNA 29b. *American Journal of Physiology-Endocrinology and Metabolism*, *315*(4), E705–E714. <https://doi.org/10.1152/ajpendo.00043.2018>

Martin, L., Birdsell, L., MacDonald, N., Reiman, T., Clandinin, M. T., McCargar, L. J., ... Baracos, V. E. (2013). Cancer Cachexia in the Age of Obesity: Skeletal Muscle Depletion Is a Powerful Prognostic Factor, Independent of Body Mass Index. *Journal of Clinical Oncology*, *31*(12), 1539–1547. <https://doi.org/10.1200/JCO.2012.45.2722>

Martin, L., Gioulbasanis, I., Senesse, P., & Baracos, V. E. (2019). Cancer-Associated Malnutrition and CT-Defined Sarcopenia and Myosteatorsis Are Endemic in Overweight and Obese Patients. *Journal of Parenteral and Enteral Nutrition*. <https://doi.org/10.1002/jpen.1597>

Martin, L., Hopkins, J., Malietzis, G., Jenkins, J. T., Sawyer, M. B., Brisebois, R., ... Baracos, V. E. (2018). Assessment of Computed Tomography (CT)-Defined Muscle and Adipose Tissue Features in Relation to Short-Term Outcomes After Elective Surgery for Colorectal Cancer: A Multicenter Approach. *Annals of Surgical Oncology*, *25*(9), 2669–2680. <https://doi.org/10.1245/s10434-018-6652-x>

Martin, L., Senesse, P., Gioulbasanis, I., Antoun, S., Bozzetti, F., Deans, C., ... Baracos, V. E. (2015). Diagnostic Criteria for the Classification of Cancer-Associated Weight Loss. *Journal of Clinical Oncology*, *33*(1), 90–99. <https://doi.org/10.1200/JCO.2014.56.1894>

Martins, K. J. B., St-Louis, M., Murdoch, G. K., MacLean, I. M., McDonald, P., Dixon, W. T., ... Michel, R. N. (2012). Nitric oxide synthase inhibition prevents activity-induced calcineurin-NFATc1 signalling and fast-to-slow skeletal muscle fibre type conversions. *The Journal of Physiology*, *590*(6), 1427–1442. <https://doi.org/10.1113/jphysiol.2011.223370>

Marzani, B., Felzani, G., Bellomo, R. G., Vecchiet, J., & Marzatico, F. (2005). Human muscle aging: ROS-mediated alterations in rectus abdominis and vastus lateralis muscles. *Experimental Gerontology*, *40*(12), 959–965. <https://doi.org/10.1016/j.exger.2005.08.010>

Marzetti, E., Lorenzi, M., Landi, F., Picca, A., Rosa, F., Tanganelli, F., ... Bossola, M. (2017). Altered mitochondrial quality control signaling in muscle of old gastric cancer patients with cachexia. *Experimental Gerontology*, *87*, 92–99. <https://doi.org/10.1016/j.exger.2016.10.003>

Matsunaga, N., Tsuchimori, N., Matsumoto, T., & Ii, M. (2011). TAK-242 (resatorvid), a small-molecule inhibitor of Toll-like receptor (TLR) 4 signaling, binds selectively to TLR4 and interferes with interactions between TLR4 and its adaptor molecules. *Molecular Pharmacology*, 79(1), 34–41. <https://doi.org/10.1124/mol.110.068064>

Mayanagi, S., Tsubosa, Y., Omae, K., Niihara, M., Uchida, T., Tsushima, T., ... Yasui, H. (2017). Negative Impact of Skeletal Muscle Wasting After Neoadjuvant Chemotherapy Followed by Surgery on Survival for Patients with Thoracic Esophageal Cancer. *Annals of Surgical Oncology*, 24(12), 3741–3747. <https://doi.org/10.1245/s10434-017-6020-2>

Mayr, R., Fritsche, H.-M., Zeman, F., Reiffen, M., Siebertz, L., Niessen, C., ... Gierth, M. (2018). Sarcopenia predicts 90-day mortality and postoperative complications after radical cystectomy for bladder cancer. *World Journal of Urology*, 36(8), 1201–1207. <https://doi.org/10.1007/s00345-018-2259-x>

McGlory, C., Vliet, S., Stokes, T., Mittendorfer, B., & Phillips, S. M. (2019). The impact of exercise and nutrition on the regulation of skeletal muscle mass. *The Journal of Physiology*, 597(5), 1251–1258. <https://doi.org/10.1113/JP275443>

Mckay, B. R., Toth, K. G., Tarnopolsky, M. A., & Parise, G. (2010). Satellite cell number and cell cycle kinetics in response to acute myotrauma in humans : immunohistochemistry versus flow cytometry. *The Journal of Physiology*, 17(17), 3307–3320. <https://doi.org/10.1113/jphysiol.2010.190876>

McSorley, S. T., Black, D. H., Horgan, P. G., & McMillan, D. C. (2018). The relationship between tumour stage, systemic inflammation, body composition and survival in patients with colorectal cancer. *Clinical Nutrition*, 37(4), 1279–1285. <https://doi.org/10.1016/j.clnu.2017.05.017>

Medzhitov, R. (2008). Origin and physiological roles of inflammation. *Nature*, 454(7203), 428–435. <https://doi.org/10.1038/nature07201>

Merad, M., Sathe, P., Helft, J., Miller, J., & Mortha, A. (2013). The dendritic cell lineage: ontogeny and function of dendritic cells and their subsets in the steady state and the inflamed setting. *Annual Review of Immunology*, 31, 563–604. <https://doi.org/10.1146/annurev-immunol-020711-074950>

Metcalf, H. J., Best, A., Kanellos, T., La Ragione, R. M., & Werling, D. (2010). Flagellin expression enhances Salmonella accumulation in TLR5-positive macrophages. *Developmental and Comparative Immunology*, 34(8), 797–804. <https://doi.org/10.1016/j.dci.2010.02.008>

Meuter, S., Schaerli, P., Roos, R. S., Brandau, O., Bösl, M. R., von Andrian, U. H., & Moser, B. (2007). Murine CXCL14 is dispensable for dendritic cell function and localization within peripheral tissues. *Molecular and Cellular Biology*, 27(3), 983–992. <https://doi.org/10.1128/MCB.01648-06>

- Mikkelsen, U. R., Langberg, H., Helmark, I. C., Skovgaard, D., Andersen, L. L., Kjaer, M., & Mackey, A. L. (2009). Local NSAID infusion inhibits satellite cell proliferation in human skeletal muscle after eccentric exercise. *Journal of Applied Physiology (Bethesda, Md. : 1985)*. <https://doi.org/10.1152/jappphysiol.00707.2009>
- Milan, G., Romanello, V., Pescatore, F., Armani, A., Paik, J.-H., Frasson, L., ... Sandri, M. (2015). Regulation of autophagy and the ubiquitin–proteasome system by the FoxO transcriptional network during muscle atrophy. *Nature Communications*, *6*(1), 6670. <https://doi.org/10.1038/ncomms7670>
- Miller, A. E. J., MacDougall, J. D., Tarnopolsky, M. A., & Sale, D. G. (1993). Gender differences in strength and muscle fiber characteristics. *European Journal of Applied Physiology and Occupational Physiology*, *66*(3), 254–262. <https://doi.org/10.1007/BF00235103>
- Miller, K. D., Jones, E., Yanovski, J. A., Shankar, R., Feuerstein, I., & Falloon, J. (1998). Visceral abdominal-fat accumulation associated with use of indinavir. *The Lancet*, *351*(9106), 871–875. [https://doi.org/10.1016/S0140-6736\(97\)11518-5](https://doi.org/10.1016/S0140-6736(97)11518-5)
- Mitsiopoulos, N., Baumgartner, R. N., Heymsfield, S. B., Lyons, W., Gallagher, D., & Ross, R. (1998). Cadaver validation of skeletal muscle measurement by magnetic resonance imaging and computerized tomography. *Journal of Applied Physiology*, *85*(1), 115–122. <https://doi.org/10.1152/jappl.1998.85.1.115>
- Mittal, P., Romero, R., Kusanovic, J. P., Edwin, S. S., Gotsch, F., Mazaki-Tovi, S., ... Hassan, S. S. (2008). ORIGINAL ARTICLE: CXCL6 (Granulocyte Chemotactic Protein-2): A Novel Chemokine Involved in the Innate Immune Response of the Amniotic Cavity. *American Journal of Reproductive Immunology*, *60*(3), 246–257. <https://doi.org/10.1111/j.1600-0897.2008.00620.x>
- Miyamoto, Y., Hanna, D. L., Zhang, W., Baba, H., & Lenz, H.-J. (2016). Molecular Pathways: Cachexia Signaling—A Targeted Approach to Cancer Treatment. *Clinical Cancer Research*, *22*(16), 3999–4004. <https://doi.org/10.1158/1078-0432.CCR-16-0495>
- Mizukami, Y., Kono, K., Kawaguchi, Y., Akaike, H., Kamimura, K., Sugai, H., & Fujii, H. (2008). CCL17 and CCL22 chemokines within tumor microenvironment are related to accumulation of Foxp3+ regulatory T cells in gastric cancer. *International Journal of Cancer*, *122*(10), 2286–2293. <https://doi.org/10.1002/ijc.23392>
- Modesti, P. A., Reboldi, G., Cappuccio, F. P., Agyemang, C., Remuzzi, G., Rapi, S., ... Parati, G. (2016). Panethnic Differences in Blood Pressure in Europe: A Systematic Review and Meta-Analysis. *PloS One*, *11*(1), 1–21. <https://doi.org/10.1371/journal.pone.0147601>
- Mojumdar, K., Giordano, C., Lemaire, C., Liang, F., Divangahi, M., Qureshi, S. T., & Petrof, B. J. (2016). Divergent impact of Toll-like receptor 2 deficiency on repair mechanisms in healthy muscle versus Duchenne muscular dystrophy. *The Journal of Pathology*, *239*(1), 10–22. <https://doi.org/10.1002/path.4689>

Mori, K., Nishide, K., Okuno, S., Shoji, T., Emoto, M., Tsuda, A., ... Inaba, M. (2019). Impact of diabetes on sarcopenia and mortality in patients undergoing hemodialysis. *BMC Nephrology*, *20*(1), 105. <https://doi.org/10.1186/s12882-019-1271-8>

Mourtzakis, M., Prado, C. M. M., Lieffers, J. R., Reiman, T., McCargar, L. J., & Baracos, V. E. (2008). A practical and precise approach to quantification of body composition in cancer patients using computed tomography images acquired during routine care. *Applied Physiology, Nutrition, and Metabolism*, *33*(5), 997–1006. <https://doi.org/10.1139/H08-075>

Mueller, A., Meiser, A., McDonagh, E. M., Fox, J. M., Petit, S. J., Xanthou, G., ... Pease, J. E. (2008). CXCL4-induced migration of activated T lymphocytes is mediated by the chemokine receptor CXCR3. *Journal of Leukocyte Biology*, *83*(4), 875–882. <https://doi.org/10.1189/jlb.1006645>

Mueller, S. N., Gebhardt, T., Carbone, F. R., & Heath, W. R. (2013). Memory T Cell Subsets, Migration Patterns, and Tissue Residence. *Annual Review of Immunology*, *31*(1), 137–161. <https://doi.org/10.1146/annurev-immunol-032712-095954>

Mueller, T. C., Bachmann, J., Prokopchuk, O., Friess, H., & Martignoni, M. E. (2016). Molecular pathways leading to loss of skeletal muscle mass in cancer cachexia – can findings from animal models be translated to humans? *BMC Cancer*, *16*(1), 1–14. <https://doi.org/10.1186/s12885-016-2121-8>

Mumm, J. B., Emmerich, J., Zhang, X., Chan, I., Wu, L., Mauze, S., ... Oft, M. (2011). IL-10 Elicits IFN γ -Dependent Tumor Immune Surveillance. *Cancer Cell*, *20*(6), 781–796. <https://doi.org/10.1016/J.CCR.2011.11.003>

Murooka, T. T., Rahbar, R., Platanius, L. C., & Fish, E. N. (2008). CCL5-mediated T-cell chemotaxis involves the initiation of mRNA translation through mTOR/4E-BP1. *Blood*, *111*(10), 4892–4901. <https://doi.org/10.1182/blood-2007-11-125039>

Murphy, C. H., Shankaran, M., Churchward-Venne, T. A., Mitchell, C. J., Kolar, N. M., Burke, L. M., ... Phillips, S. M. (2018). Effect of resistance training and protein intake pattern on myofibrillar protein synthesis and proteome kinetics in older men in energy restriction. *The Journal of Physiology*, *596*(11), 2091–2120.

Murphy, R. A., Mourtzakis, M., Chu, Q. S. C., Baracos, V. E., Reiman, T., & Mazurak, V. C. (2011). Nutritional intervention with fish oil provides a benefit over standard of care for weight and skeletal muscle mass in patients with nonsmall cell lung cancer receiving chemotherapy. *Cancer*, *117*(8), 1775–1782. <https://doi.org/10.1002/cncr.25709>

Murphy, R. A., Mourtzakis, M., Chu, Q. S., Reiman, T., & Mazurak, V. C. (2010). Skeletal Muscle Depletion Is Associated with Reduced Plasma (n-3) Fatty Acids in Non-Small Cell Lung Cancer Patients. *The Journal of Nutrition*, *140*(9), 1602–1606. <https://doi.org/10.3945/jn.110.123521>

- Nakao, T., Kurita, N., Komatsu, M., Yoshikawa, K., Iwata, T., Utusnomiya, T., & Shimada, M. (2012). Irinotecan injures tight junction and causes bacterial translocation in rat. *Journal of Surgical Research*, *173*(2), 341–347. <https://doi.org/10.1016/j.jss.2010.10.003>
- Nalini, A., Narayanappa, G., & Nagappa, M. (2013). Major histocompatibility complex and inflammatory cell subtype expression in inflammatory myopathies and muscular dystrophies. *Neurology India*, *61*(6), 614. <https://doi.org/10.4103/0028-3886.125264>
- Nam, H., Ferguson, B. S., Stephens, J. M., & Morrison, R. F. (2013). Impact of obesity on IL-12 family gene expression in insulin responsive tissues. *Biochimica et Biophysica Acta - Molecular Basis of Disease*, *1832*(1), 11–19. <https://doi.org/10.1016/j.bbadis.2012.08.011>
- Nara, N., Nakayama, Y., Okamoto, S., Tamura, H., Kiyono, M., Muraoka, M., ... Hara, T. (2007). Disruption of CXC motif chemokine ligand-14 in mice ameliorates obesity-induced insulin resistance. *The Journal of Biological Chemistry*, *282*(42), 30794–30803. <https://doi.org/10.1074/jbc.M700412200>
- Narasimhan, A., Ghosh, S., Stretch, C., Greiner, R., Bathe, O. F., Baracos, V., & Damaraju, S. (2017). Small RNAome profiling from human skeletal muscle: novel miRNAs and their targets associated with cancer cachexia. *Journal of Cachexia, Sarcopenia and Muscle*, *8*(3), 405–416. <https://doi.org/10.1002/jcsm.12168>
- Narasimhan, A., Greiner, R., Bathe, O. F., Baracos, V., & Damaraju, S. (2018). Differentially expressed alternatively spliced genes in skeletal muscle from cancer patients with cachexia. *Journal of Cachexia, Sarcopenia and Muscle*, *9*(1), 60–70. <https://doi.org/10.1002/jcsm.12235>
- Narsale, A., Moya, R., Ma, J., Anderson, L. J., Wu, D., Garcia, J. M., & Davies, J. D. (2019). Cancer-driven changes link T cell frequency to muscle strength in people with cancer: a pilot study. *Journal of Cachexia, Sarcopenia and Muscle*, *jcsm.12424*. <https://doi.org/10.1002/jcsm.12424>
- Newman, N. B., Sidhu, M. K., Baby, R., Moss, R. A., Nissenblatt, M. J., Chen, T., ... Jabbour, S. K. (2016). Long-Term Bone Marrow Suppression During Postoperative Chemotherapy in Rectal Cancer Patients After Preoperative Chemoradiation Therapy. *International Journal of Radiation Oncology*Biophysics*Physics*, *94*(5), 1052–1060. <https://doi.org/10.1016/J.IJROBP.2015.12.374>
- Nilsen, T. S., Thorsen, L., Fosså, S. D., Wiig, M., Kirkegaard, C., Skovlund, E., ... Raastad, T. (2016). Effects of strength training on muscle cellular outcomes in prostate cancer patients on androgen deprivation therapy. *Scandinavian Journal of Medicine & Science in Sports*, *26*(9), 1026–1035. <https://doi.org/10.1111/sms.12543>
- Nilwik, R., Snijders, T., Leenders, M., Groen, B. B. L., van Kranenburg, J., Verdijk, L. B., ... Loon, L. J. C. Van. (2013). The decline in skeletal muscle mass with aging is mainly attributed to a reduction in type II muscle fiber size. *Experimental Gerontology*, *48*, 492–498. <https://doi.org/10.1016/j.exger.2013.02.012>

Nishikai-Yan Shen, T., Kanazawa, S., Kado, M., Okada, K., Luo, L., Hayashi, A., ... Tanaka, R. (2017). Interleukin-6 stimulates Akt and p38 MAPK phosphorylation and fibroblast migration in non-diabetic but not diabetic mice. *PLOS ONE*, *12*(5), e0178232. <https://doi.org/10.1371/journal.pone.0178232>

Noguchi, Y., Yoshikawa, T., Marat, D., Doi, C., Makino, T., Fukuzawa, K., ... Mitsuse, S. (1998). Insulin resistance in cancer patients is associated with enhanced tumor necrosis factor-alpha expression in skeletal muscle. *Biochem Biophys Res Commun*, *253*(3), 887–892. [https://doi.org/S0006-291X\(98\)99794-7](https://doi.org/S0006-291X(98)99794-7)

O'Brien, S., Twomey, M., Moloney, F., Kavanagh, R. G., Carey, B. W., Power, D., ... Ó'Súilleabháin, C. (2018). Sarcopenia and Post-Operative Morbidity and Mortality in Patients with Gastric Cancer. *Journal of Gastric Cancer*, *18*(3), 242. <https://doi.org/10.5230/jgc.2018.18.e25>

Ochiai, E., Sa, Q., Brogli, M., Kudo, T., Wang, X., Dubey, J. P., & Suzuki, Y. (2015). CXCL9 is important for recruiting immune T cells into the brain and inducing an accumulation of the T cells to the areas of tachyzoite proliferation to prevent reactivation of chronic cerebral infection with *Toxoplasma gondii*. *American Journal of Pathology*, *185*(2), 314–324. <https://doi.org/10.1016/j.ajpath.2014.10.003>

Odobasic, D., Kitching, A. R., & Holdsworth, S. R. (2016). Neutrophil-Mediated Regulation of Innate and Adaptive Immunity: The Role of Myeloperoxidase. *Journal of Immunology Research*, *2016*, 1–11. <https://doi.org/10.1155/2016/2349817>

Ogawa, K., Funaba, M., Chen, Y., & Tsujimoto, M. (2006). Activin A functions as a Th2 cytokine in the promotion of the alternative activation of macrophages. *Journal of Immunology (Baltimore, Md. : 1950)*, *177*(10), 6787–6794. <https://doi.org/10.4049/jimmunol.177.10.6787>

Oh, S. Y., Heo, J., Noh, O. K., Chun, M., Cho, O., & Oh, Y.-T. (2018). Absolute Lymphocyte Count in Preoperative Chemoradiotherapy for Rectal Cancer: Changes Over Time and Prognostic Significance. *Technology in Cancer Research & Treatment*, *17*, 153303381878006. <https://doi.org/10.1177/1533033818780065>

Oka, T., Sugaya, M., Takahashi, N., Takahashi, T., Shibata, S., Miyagaki, T., ... Sato, S. (2017). CXCL17 Attenuates Imiquimod-Induced Psoriasis-like Skin Inflammation by Recruiting Myeloid-Derived Suppressor Cells and Regulatory T Cells. *The Journal of Immunology*, *198*(10), 3897–3908. <https://doi.org/10.4049/jimmunol.1601607>

Onai, N. (2002). Pivotal role of CCL25 (TECK)-CCR9 in the formation of gut cryptopatches and consequent appearance of intestinal intraepithelial T lymphocytes. *International Immunology*, *14*(7), 687–694. <https://doi.org/10.1093/intimm/14.7.687>

Op den Kamp, C. M., Langen, R. C., Minnaard, R., Kelders, M. C., Snepvangers, F. J., Hesselink, M. K., ... Schols, A. M. (2012). Pre-cachexia in patients with stages I-III non-small cell lung cancer: Systemic inflammation and functional impairment without activation of skeletal muscle

ubiquitin proteasome system. *Lung Cancer*, 76(1), 112–117.
<https://doi.org/10.1016/j.lungcan.2011.09.012>

Op den Kamp, Celine M., Langen, R. C., Snepvangers, F. J., Theije, C. C. De, Schellekens, J. M., Laugs, F., ... Schols, A. M. (2013). Nuclear transcription factor k B activation and protein turnover adaptations in skeletal muscle of patients with progressive stages of lung cancer cachexia. *Am J Clin Nutr*, (1), 738–748. <https://doi.org/10.3945/ajcn.113.058388.1>

Op den Kamp, Celine M., Gosker, H. R., Lagarde, S., Tan, D. Y., Snepvangers, F. J., Dingemans, A. M. C., ... Schols, A. M. W. J. (2015). Preserved muscle oxidative metabolic phenotype in newly diagnosed non-small cell lung cancer cachexia. *Journal of Cachexia, Sarcopenia and Muscle*, (April), 164–173. <https://doi.org/10.1002/jcsm.12007>

Orta-Mascaró, M., Consuegra-Fernández, M., Carreras, E., Roncagalli, R., Carreras-Sureda, A., Alvarez, P., ... Lozano, F. (2016). CD6 modulates thymocyte selection and peripheral T cell homeostasis. *Journal of Experimental Medicine*, 213(8), 1387–1397.
<https://doi.org/10.1084/jem.20151785>

Otten, L., Stobäus, N., Franz, K., Genton, L., Müller-Werdan, U., Wirth, R., & Norman, K. (2019). Impact of sarcopenia on 1-year mortality in older patients with cancer. *Age and Ageing*, 48(3), 413–418. <https://doi.org/10.1093/ageing/afy212>

Paiva-Oliveira, E. L., Ferreira da Silva, R., Correa Leite, P. E., Cogo, J. C., Quirico-Santos, T., & Lagrota-Candido, J. (2012). TLR4 signaling protects from excessive muscular damage induced by Bothrops jararacussu snake venom. *Toxicon*, 60(8), 1396–1403.
<https://doi.org/10.1016/j.toxicon.2012.10.003>

Panduro, M., Benoist, C., & Mathis, D. (2018). Treg cells limit IFN- γ production to control macrophage accrual and phenotype during skeletal muscle regeneration. *Proceedings of the National Academy of Sciences of the United States of America*, 115(11), E2585–E2593.
<https://doi.org/10.1073/pnas.1800618115>

Pandya, J. M., Loell, I., Hossain, M. S., Zong, M., Alexanderson, H., Raghavan, S., ... Malmström, V. (2016). Effects of conventional immunosuppressive treatment on CD244+ (CD28null) and FOXP3+ T cells in the inflamed muscle of patients with polymyositis and dermatomyositis. *Arthritis Research and Therapy*, 18(1), 1–14. <https://doi.org/10.1186/S13075-016-0974-5>

Pandya, J. M., Venalis, P., Al-Khalili, L., Shahadat Hossain, M., Stache, V., Lundberg, I. E., ... Fasth, A. E. R. (2016). CD4+ and CD8+ CD28^{null} T Cells Are Cytotoxic to Autologous Muscle Cells in Patients With Polymyositis. *Arthritis & Rheumatology*, 68(8), 2016–2026.
<https://doi.org/10.1002/art.39650>

Paramanathan, A., Saxena, A., & Morris, D. L. (2014). A systematic review and meta-analysis on the impact of pre-operative neutrophil lymphocyte ratio on long term outcomes after curative

intent resection of solid tumours. *Surgical Oncology*, 23(1), 31–39.
<https://doi.org/10.1016/J.SURONC.2013.12.001>

Park, S. Y., Yun, Y., Lim, J. S., Kim, M. J., Kim, S. Y., Kim, J. E., & Kim, I. S. (2016). Stabilin-2 modulates the efficiency of myoblast fusion during myogenic differentiation and muscle regeneration. *Nature Communications*, 7. <https://doi.org/10.1038/ncomms10871>

Pascual-García, M., Bonfill-Teixidor, E., Planas-Rigol, E., Rubio-Perez, C., Iurlaro, R., Arias, A., ... Seoane, J. (2019). LIF regulates CXCL9 in tumor-associated macrophages and prevents CD8+ T cell tumor-infiltration impairing anti-PD1 therapy. *Nature Communications*, 10(1).
<https://doi.org/10.1038/s41467-019-10369-9>

Paulsen, G., Egner, I., Reinholt, F., Brorson, Á. S.-H., Koskinen, Á. S., Owe, S., & Lauritzen, Á. F. (2013). Inflammatory markers CD11b, CD16, CD66b, CD68, myeloperoxidase and neutrophil elastase in eccentric exercised human skeletal muscles. *Histochem Cell Biol*, 139, 691–715.
<https://doi.org/10.1007/s00418-012-1061-x>

Pedersen, J., Song, D. H., & Selber, J. C. (2014). Robotic, Intraperitoneal Harvest of the Rectus Abdominis Muscle. *Plastic and Reconstructive Surgery*, 134(5), 1057–1063.
<https://doi.org/10.1097/PRS.0000000000000586>

Penafuerte, C. A., Gagnon, B., Sirois, J., Murphy, J., MacDonald, N., & Tremblay, M. L. (2016). Identification of neutrophil-derived proteases and angiotensin II as biomarkers of cancer cachexia. *British Journal of Cancer*, 114(6), 680–687. <https://doi.org/10.1038/bjc.2016.3>

Peng, Q.-L., Zhang, Y.-L., Shu, X.-M., Yang, H.-B., Zhang, L., Chen, F., ... Wang, G.-C. (2015). Elevated Serum Levels of Soluble CD163 in Polymyositis and Dermatomyositis: Associated with Macrophage Infiltration in Muscle Tissue. *The Journal of Rheumatology*, 42(6), 979–987.
<https://doi.org/10.3899/jrheum.141307>

Pennini, M. E., Perkins, D. J., Salazar, A. M., Lipsky, M., & Vogel, S. N. (2013). Complete dependence on IRAK4 kinase activity in TLR2, but not TLR4, signaling pathways underlies decreased cytokine production and increased susceptibility to *Streptococcus pneumoniae* infection in IRAK4 kinase-inactive mice. *Journal of Immunology (Baltimore, Md. : 1950)*, 190(1), 307–316. <https://doi.org/10.4049/jimmunol.1201644>

Pessina, P., Conti, V., Pacelli, F., Rosa, F., Doglietto, G. B., Brunelli, S., & Bossola, M. (2010). Skeletal muscle of gastric cancer patients expresses genes involved in muscle regeneration. *Oncology Reports*, 24(3), 741–745.

Petrie Aronin, C. E., Zhao, Y. M., Yoon, J. S., Morgan, N. Y., Prüstel, T., Germain, R. N., & Meier-Schellersheim, M. (2017). Migrating Myeloid Cells Sense Temporal Dynamics of Chemoattractant Concentrations. *Immunity*, 47(5), 862-874.e3.
<https://doi.org/10.1016/j.immuni.2017.10.020>

Phillips, B. E., Smith, K., Liptrot, S., Atherton, P. J., Varadhan, K., Rennie, M. J., ... Williams, J. P. (2013). Effect of colon cancer and surgical resection on skeletal muscle mitochondrial enzyme activity in colon cancer patients: A pilot study. *Journal of Cachexia, Sarcopenia and Muscle*, 4(1), 71–77. <https://doi.org/10.1007/s13539-012-0073-7>

Pillon, N. J., & Krook, A. (2017). Innate immune receptors in skeletal muscle metabolism. *Experimental Cell Research*, 360(1), 47–54. <https://doi.org/10.1016/J.YEXCR.2017.02.035>

Pin, F., Barreto, R., Couch, M. E., Bonetto, A., & O'Connell, T. M. (2019). Cachexia induced by cancer and chemotherapy yield distinct perturbations to energy metabolism. *Journal of Cachexia, Sarcopenia and Muscle*, 10(1), 140–154. <https://doi.org/10.1002/jcsm.12360>

Pin, F., Couch, M. E., & Bonetto, A. (2018). Preservation of muscle mass as a strategy to reduce the toxic effects of cancer chemotherapy on body composition. *Current Opinion in Supportive and Palliative Care*, Vol. 12, pp. 420–426. <https://doi.org/10.1097/SPC.0000000000000382>

Plomgaard, P., Bouzakri, K., Krogh-Madsen, R., Mittendorfer, B., Zierath, J. R., & Pedersen, B. K. (2005). Tumor Necrosis Factor- Induces Skeletal Muscle Insulin Resistance in Healthy Human Subjects via Inhibition of Akt Substrate 160 Phosphorylation. *Diabetes*, 54(10), 2939–2945. <https://doi.org/10.2337/diabetes.54.10.2939>

Pommier, Y. (2006). Topoisomerase I inhibitors: camptothecins and beyond. *Nature Reviews Cancer*, 6(10), 789–802. <https://doi.org/10.1038/nrc1977>

Porciello, N., & Tuosto, L. (2016, April 1). CD28 costimulatory signals in T lymphocyte activation: Emerging functions beyond a qualitative and quantitative support to TCR signalling. *Cytokine and Growth Factor Reviews*, Vol. 28, pp. 11–19. <https://doi.org/10.1016/j.cytogfr.2016.02.004>

Porter, J. D., Guo, W., Merriam, A. P., Khanna, S., Cheng, G., Zhou, X., ... Kaminski, H. J. (2003). Persistent over-expression of specific CC class chemokines correlates with macrophage and T-cell recruitment in mdx skeletal muscle. *Neuromuscular Disorders*, 13(3), 223–235. [https://doi.org/10.1016/S0960-8966\(02\)00242-0](https://doi.org/10.1016/S0960-8966(02)00242-0)

Potaczek, D. P., Nishiyama, C., Sanak, M., Szczeklik, A., & Okumura, K. (2009, October). Genetic variability of the high-affinity IgE receptor α -subunit (Fc ϵ RI α). *Immunologic Research*, Vol. 45, pp. 75–84. <https://doi.org/10.1007/s12026-008-8042-0>

Pourhassan, M., Norman, K., Müller, M. J., Dziewas, R., & Wirth, R. (n.d.). Impact of Sarcopenia on One-Year Mortality Among Older Hospitalized Patients with Impaired Mobility. *The Journal of Frailty & Aging*, 7(1), 40–46. <https://doi.org/10.14283/jfa.2017.35>

Pourteymour, S., Eckardt, K., Holen, T., Langleite, T., Lee, S., Jensen, J., ... Hjorth, M. (2017). Global mRNA sequencing of human skeletal muscle: Search for novel exercise-regulated myokines. *Molecular Metabolism*, 6(4), 352–365. <https://doi.org/10.1016/J.MOLMET.2017.01.007>

Prado, C. M. M., Lieffers, J. R., McCargar, L. J., Reiman, T., Sawyer, M. B., Martin, L., & Baracos, V. E. (2008). Prevalence and clinical implications of sarcopenic obesity in patients with solid tumours of the respiratory and gastrointestinal tracts: a population-based study. *The Lancet Oncology*, *9*(7), 629–635. [https://doi.org/10.1016/S1470-2045\(08\)70153-0](https://doi.org/10.1016/S1470-2045(08)70153-0)

Prado, C. M., Sawyer, M. B., Ghosh, S., Lieffers, J. R., Esfandiari, N., Antoun, S., & Baracos, V. E. (2013). Central tenet of cancer cachexia therapy: Do patients with advanced cancer have exploitable anabolic potential? *American Journal of Clinical Nutrition*, *98*(4), 1012–1019. <https://doi.org/10.3945/ajcn.113.060228>

Prado, Carla M. M., & Heymsfield, S. B. (2014). Lean Tissue Imaging. *Journal of Parenteral and Enteral Nutrition*, *38*(8), 940–953. <https://doi.org/10.1177/0148607114550189>

Prado, Carla MM M, Lieffers, J. R., McCargar, L. J., Reiman, T., Sawyer, M. B., Martin, L., & Baracos, V. E. (2008a). Prevalence and clinical implications of sarcopenic obesity in patients with solid tumours of the respiratory and gastrointestinal tracts: a population-based study. *The Lancet Oncology*, *9*(7), 629–635. [https://doi.org/10.1016/S1470-2045\(08\)70153-0](https://doi.org/10.1016/S1470-2045(08)70153-0)

Pratt, V. C., Tredget, E. E., Clandinin, M. T., & Field, C. J. (2001). Fatty acid content of plasma lipids and erythrocyte phospholipids are altered following burn injury. *Lipids*, *36*(7), 675–682. <https://doi.org/10.1007/s11745-001-0772-y>

Prokopchuk, O., Steinacker, J. M., Nitsche, U., Otto, S., Bachmann, J., Schubert, E. C., ... Martignoni, M. E. (2017). IL-4 mRNA Is Downregulated in the Liver of Pancreatic Cancer Patients Suffering from Cachexia. *Nutrition and Cancer*, *69*(1), 84–91. <https://doi.org/10.1080/01635581.2017.1247885>

Puig-Vilanova, E., Rodriguez, D. A., Lloreta, J., Ausin, P., Pascual-Guardia, S., Broquetas, J., ... Barreiro, E. (2015). Oxidative stress, redox signaling pathways, and autophagy in cachectic muscles of male patients with advanced COPD and lung cancer. *Free Radical Biology and Medicine*, *79*, 91–108. <https://doi.org/10.1016/j.freeradbiomed.2014.11.006>

Purcell, S. A., Elliott, S. A., Baracos, V. E., Chu, Q. S. C., & Prado, C. M. (2016). Key determinants of energy expenditure in cancer and implications for clinical practice. *European Journal of Clinical Nutrition*, *70*(11), 1230–1238. <https://doi.org/10.1038/ejcn.2016.96>

Putman, C. T., Martins, K. J. B., Gallo, M. E., Lopaschuk, G. D., Pearcey, J. A., MacLean, I. M., ... Pette, D. (2007). α -Catalytic subunits of 5'AMP-activated protein kinase display fiber-specific expression and are upregulated by chronic low-frequency stimulation in rat muscle. *American Journal of Physiology-Regulatory, Integrative and Comparative Physiology*, *293*(3), R1325–R1334. <https://doi.org/10.1152/ajpregu.00609.2006>

Ramage, M. I., Johns, N., Deans, C. D. A., Ross, J. A., Preston, T., Skipworth, R. J. E., ... Fearon, K. C. H. (2018). The relationship between muscle protein content and CT-derived muscle radio-

density in patients with upper GI cancer. *Clinical Nutrition*, 37(2), 752–754. <https://doi.org/10.1016/j.clnu.2016.12.016>

Raman, D., & Sobolik-Delmaire, T. (2011). Chemokines in health and disease. *Experimental Cell Research*, 317(5), 575–589. <https://doi.org/10.1016/J.YEXCR.2011.01.005>

Ravoet, M., Sibille, C., Gu, C., Libin, M., Haibe-Kains, B., Sotiriou, C., ... Willard-Gallo, K. (2009). Molecular profiling of CD3-CD4⁺T cells from patients with the lymphocytic variant of hypereosinophilic syndrome reveals targeting of growth control pathways. *Blood*, 114(14), 2969–2983. <https://doi.org/10.1182/blood-2008-08-175091>

Rhoads, M. G., Kandarian, S. C., Pacelli, F., Doglietto, G. B., & Bossola, M. (2010). Expression of NF- κ B and I κ B proteins in skeletal muscle of gastric cancer patients. *European Journal of Cancer*, 46(1), 191–197. <https://doi.org/10.1016/j.ejca.2009.10.008>

Richards, C. H., Roxburgh, C. S. D., MacMillan, M. T., Isswiasi, S., Robertson, E. G., Guthrie, G. K., ... McMillan, D. C. (2012). The relationships between body composition and the systemic inflammatory response in patients with primary operable colorectal cancer. *PLoS ONE*, 7(8), e41883. <https://doi.org/10.1371/journal.pone.0041883>

Rier, H. N., Jager, A., Sleijfer, S., Maier, A. B., & Levin, M.-D. (2016). The Prevalence and Prognostic Value of Low Muscle Mass in Cancer Patients: A Review of the Literature. *The Oncologist*, 21(11), 1396–1409. <https://doi.org/10.1634/theoncologist.2016-0066>

Rigamonti, E., Touvier, T., Clementi, E., Manfredi, A. A., Brunelli, S., & Rovere-Querini, P. (2013). Requirement of inducible nitric oxide synthase for skeletal muscle regeneration after acute damage. *Journal of Immunology (Baltimore, Md. : 1950)*, 190(4), 1767–1777. <https://doi.org/10.4049/jimmunol.1202903>

Robinson, W. H., Prohaska, S. S., Santoro, J. C., Robinson, H. L., & Parnes, J. R. (1995). Identification of a mouse protein homologous to the human CD6 T cell surface protein and sequence of the corresponding cDNA. *Journal of Immunology (Baltimore, Md. : 1950)*, 155(10), 4739–4748.

Robson, N. C., Phillips, D. J., McAlpine, T., Shin, A., Svobodova, S., Toy, T., ... Maraskovsky, E. (2008). Activin-A: a novel dendritic cell-derived cytokine that potently attenuates CD40 ligand-specific cytokine and chemokine production. *Blood*, 111(5), 2733–2743. <https://doi.org/10.1182/blood-2007-03-080994>

Roeland, E. J., Ma, J. D., Nelson, S. H., Seibert, T., Heavey, S., Revta, C., ... Baracos, V. E. (2017). Weight loss versus muscle loss: re-evaluating inclusion criteria for future cancer cachexia interventional trials. *Supportive Care in Cancer*, 25(2), 365–369. <https://doi.org/10.1007/s00520-016-3402-0>

Rollins, K. E., Tewari, N., Ackner, A., Awwad, A., Madhusudan, S., Macdonald, I. A., ... Lobo, D. N. (2016). The impact of sarcopenia and myosteatorsis on outcomes of unresectable pancreatic

cancer or distal cholangiocarcinoma. *Clinical Nutrition*, 35(5), 1103–1109. <https://doi.org/10.1016/j.clnu.2015.08.005>

Ruel, M., Bianchi, C., Khan, T. A., Xu, S., Liddicoat, J. R., Voisine, P., ... Sellke, F. W. (2003). Gene expression profile after cardiopulmonary bypass and cardioplegic arrest. *The Journal of Thoracic and Cardiovascular Surgery*, 126(5), 1521–1530. <https://doi.org/10.1016/S0022>

Rustum, Y. M. (1989). Toxicity and antitumor activity of 5-fluorouracil in combination with leucovorin. Role of dose schedule and route of administration of leucovorin. *Cancer*, 63(6 Suppl), 1013–1017.

Ruud, J., Wilhelms, D. B., Nilsson, A., Eskilsson, A., Tang, Y.-J., Ströhle, P., ... Blomqvist, A. (2013). Inflammation- and tumor-induced anorexia and weight loss require MyD88 in hematopoietic/myeloid cells but not in brain endothelial or neural cells. *The FASEB Journal*, 27(5), 1973–1980. <https://doi.org/10.1096/fj.12-225433>

Sachdev, U., Cui, X., Xu, J., Xu, J., & Tzeng, E. (2014). MyD88 and TRIF mediate divergent inflammatory and regenerative responses to skeletal muscle ischemia. *Physiological Reports*, 2(5), e12006. <https://doi.org/10.14814/phy2.12006>

Salvatore, D., Simonides, W. S., Dentice, M., Zavacki, A. M., & Larsen, P. R. (2014). Thyroid hormones and skeletal muscle—new insights and potential implications. *Nature Reviews Endocrinology*, 10(4), 206–214. <https://doi.org/10.1038/nrendo.2013.238>

Salyer, A. C. D., & David, S. A. (2018). Transcriptomal signatures of vaccine adjuvants and accessory immunostimulation of sentinel cells by toll-like receptor 2/6 agonists. *Human Vaccines and Immunotherapeutics*, 14(7), 1686–1696. <https://doi.org/10.1080/21645515.2018.1480284>

Sánchez-Espiridión, B., Martín-Moreno, A. M., Montalbán, C., Jeffrey Medeiros, L., Vega, F., Younes, A., ... Garcia, J. F. (2012). Immunohistochemical markers for tumor associated macrophages and survival in advanced classical Hodgkin's lymphoma. *Haematologica*, 97(7), 1080–1084. <https://doi.org/10.3324/haematol.2011.055459>

Sanders, L. A., Feldman, R. G., Voorhorst-Ogink, M. M., de Haas, M., Rijkers, G. T., Capel, P. J., ... van de Winkel, J. G. (1995). Human immunoglobulin G (IgG) Fc receptor IIA (CD32) polymorphism and IgG2-mediated bacterial phagocytosis by neutrophils. *Infection and Immunity*, 63(1), 73–81.

Sandor, A., Lindsay, R. S., Gebbert, M., Bradley, B., Haskins, K., Jacobelli, J., & Friedman, R. S. (2018). CD11c+ cells are required for lymphocyte trafficking into previously infiltrated pancreatic islets during type 1 diabetes. *The Journal of Immunology*, 200(1 Supplement).

Sandri, M., Sandri, C., Gilbert, A., Skurk, C., Calabria, E., Picard, A., ... Goldberg, A. L. (2004). Foxo Transcription Factors Induce the Atrophy-Related Ubiquitin Ligase Atrogin-1 and Cause Skeletal Muscle Atrophy. *Cell*, 117(3), 399–412. [https://doi.org/10.1016/S0092-8674\(04\)00400-3](https://doi.org/10.1016/S0092-8674(04)00400-3)

- Sato, Y., Gonda, K., Harada, M., Tanisaka, Y., Arai, S., Mashimo, Y., ... Shibata, M. (2017). Increased neutrophil-to-lymphocyte ratio is a novel marker for nutrition, inflammation and chemotherapy outcome in patients with locally advanced and metastatic esophageal squamous cell carcinoma. *Biomedical Reports*, 7(1), 79–84. <https://doi.org/10.3892/br.2017.924>
- Sauty, A., Colvin, R. A., Wagner, L., Rochat, S., Spertini, F., & Luster, A. D. (2001). CXCR3 Internalization Following T Cell-Endothelial Cell Contact: Preferential Role of IFN-Inducible T Cell α Chemoattractant (CXCL11). *The Journal of Immunology*, 167(12), 7084–7093. <https://doi.org/10.4049/jimmunol.167.12.7084>
- Scandella, E., Men, Y., Legler, D. F., Gillessen, S., Prikler, L., Ludewig, B., & Groettrup, M. (2004). CCL19/CCL21-triggered signal transduction and migration of dendritic cells requires prostaglandin E2. *Blood*, 103(5), 1595–1601. <https://doi.org/10.1182/blood-2003-05-1643>
- Schiessel, D. L., & Baracos, V. E. (2018). Barriers to cancer nutrition therapy: excess catabolism of muscle and adipose tissues induced by tumour products and chemotherapy. *Proceedings of the Nutrition Society*, 1–9. <https://doi.org/10.1017/S0029665118000186>
- Schittenhelm, L., Hilken, C. M., & Morrison, V. L. (2017). β 2 Integrins As Regulators of Dendritic Cell, Monocyte, and Macrophage Function. *Frontiers in Immunology*, 8, 1866. <https://doi.org/10.3389/fimmu.2017.01866>
- Schmitt, T. L., Martignoni, M. E., Bachmann, J., Fechtner, K., Friess, H., Kinscherf, R., & Hildebrandt, W. (2007). Activity of the Akt-dependent anabolic and catabolic pathways in muscle and liver samples in cancer-related cachexia. *Journal of Molecular Medicine*, 85(6), 647–654. <https://doi.org/10.1007/s00109-007-0177-2>
- Schreiner, B., Voss, J., Wischhusen, J., Dombrowski, Y., Steinle, A., Lochmüller, H., ... Wiendl, H. (2006). Expression of toll-like receptors by human muscle cells in vitro and in vivo: TLR3 is highly expressed in inflammatory and HIV myopathies, mediates IL-8 release and up-regulation of NKG2D-ligands. *FASEB Journal*, 20(1), 118–120. <https://doi.org/10.1096/fj.05-4342fje>
- Schütze, S., Wiegmann, K., Machleidt, T., & Krönke, M. (1995). TNF-induced activation of NF-kappa B. *Immunobiology*, 193(2–4), 193–203. Retrieved from <http://www.ncbi.nlm.nih.gov/pubmed/8530143>
- Seo, P. H., Pieper, C. F., & Cohen, H. J. (2004). Effects of cancer history and comorbid conditions on mortality and healthcare use among older cancer survivors. *Cancer*, 101(10), 2276–2284. <https://doi.org/10.1002/cncr.20606>
- Shachar, S. S., Williams, G. R., Muss, H. B., & Nishijima, T. F. (2016, April 1). Prognostic value of sarcopenia in adults with solid tumours: A meta-analysis and systematic review. *European Journal of Cancer*. Pergamon. <https://doi.org/10.1016/j.ejca.2015.12.030>

Shanely, R. A., Zwetsloot, K. A., Triplett, N. T., Meaney, M. P., Farris, G. E., & Nieman, D. C. (2014). Human Skeletal Muscle Biopsy Procedures Using the Modified Bergström Technique. *Journal of Visualized Experiments*, (91), 51812. <https://doi.org/10.3791/51812>

Shashidharamurthy, R., Zhang, F., Amano, A., Kamat, A., Panchanathan, R., Ezekwudo, D., ... Selvaraj, P. (2009). Dynamics of the interaction of human IgG subtype immune complexes with cells expressing R and H allelic forms of a low-affinity Fc gamma receptor CD32A. *Journal of Immunology (Baltimore, Md. : 1950)*, 183(12), 8216–8224. <https://doi.org/10.4049/jimmunol.0902550>

Shaw, J. H., Humberstone, D. A., Douglas, R. G., & Koea, J. (1991). Leucine kinetics in patients with benign disease, non-weight-losing cancer, and cancer cachexia: studies at the whole-body and tissue level and the response to nutritional support. *Surgery*, 109(1), 37–50. Retrieved from <http://www.ncbi.nlm.nih.gov/pubmed/1984636>

Shen, W., Punyanitya, M., Wang, Z., Gallagher, D., St-Onge, M.-P., Albu, J., ... Heshka, S. (2004). Total body skeletal muscle and adipose tissue volumes: estimation from a single abdominal cross-sectional image. *Journal of Applied Physiology*, 97(6), 2333–2338. <https://doi.org/10.1152/jappphysiol.00744.2004>

Shibata, M., Takekawa, M., & Amano, S. (1998). Increased serum concentrations of soluble tumor necrosis factor receptor I in noncachectic and cachectic patients with advanced gastric and colorectal cancer. *Surgery Today*, 28(9), 884–888. <https://doi.org/10.1007/s005950050247>

Shibata, T., Takemura, N., Motoi, Y., Goto, Y., Karuppuchamy, T., Izawa, K., ... Miyake, K. (2012). PRAT4A-dependent expression of cell surface TLR5 on neutrophils, classical monocytes and dendritic cells. *International Immunology*, 24(10), 613–623. <https://doi.org/10.1093/intimm/dxs068>

Shurin, G. V, Ferris, R. L., Ferris, R., Tourkova, I. L., Perez, L., Lokshin, A., ... Shurin, M. R. (2005). Loss of new chemokine CXCL14 in tumor tissue is associated with low infiltration by dendritic cells (DC), while restoration of human CXCL14 expression in tumor cells causes attraction of DC both in vitro and in vivo. *Journal of Immunology (Baltimore, Md. : 1950)*, 174(9), 5490–5498. <https://doi.org/10.4049/jimmunol.174.9.5490>

Sica, G. L., Choi, I.-H., Zhu, G., Tamada, K., Wang, S.-D., Tamura, H., ... Chen, L. (2003). B7-H4, a Molecule of the B7 Family, Negatively Regulates T Cell Immunity. *Immunity*, 18(6), 849–861. [https://doi.org/10.1016/S1074-7613\(03\)00152-3](https://doi.org/10.1016/S1074-7613(03)00152-3)

Sierro, F., Dubois, B., Coste, A., Kaiserlian, D., Kraehenbuhl, J. P., & Sirard, J. C. (2001). Flagellin stimulation of intestinal epithelial cells triggers CCL20-mediated migration of dendritic cells. *Proceedings of the National Academy of Sciences of the United States of America*, 98(24), 13722–13727. <https://doi.org/10.1073/pnas.241308598>

Silva de Paula, N., de Aguiar Bruno, K., Azevedo Aredes, M., & Villaça Chaves, G. (2018). Sarcopenia and Skeletal Muscle Quality as Predictors of Postoperative Complication and Early

Mortality in Gynecologic Cancer. *International Journal of Gynecological Cancer : Official Journal of the International Gynecological Cancer Society*, 28(2), 412–420.
<https://doi.org/10.1097/IGC.0000000000001157>

Silva, K. A. S., Dong, J., Dong, Y., Dong, Y., Schor, N., Tweardy, D. J., ... Mitch, W. E. (2015). Inhibition of Stat3 activation suppresses caspase-3 and the ubiquitin-proteasome system, leading to preservation of muscle mass in cancer cachexia. *The Journal of Biological Chemistry*, 290(17), 11177–11187. <https://doi.org/10.1074/jbc.M115.641514>

Simonin-Le Jeune, K., Le Jeune, A., Jouneau, S., Belleguic, C., Roux, P.-F., Jaguin, M., ... Martin-Chouly, C. (2013). Impaired Functions of Macrophage from Cystic Fibrosis Patients: CD11b, TLR-5 Decrease and sCD14, Inflammatory Cytokines Increase. *PLoS ONE*, 8(9), e75667. <https://doi.org/10.1371/journal.pone.0075667>

Singer, N. G., Richardson, B. C., Powers, D., Hooper, F., Lialios, F., Endres, J., ... Fox, D. A. (1996). Role of the CD6 glycoprotein in antigen-specific and autoreactive responses of cloned human T lymphocytes. *Immunology*, 88(4), 537–543.

Sjøblom, B., Grønberg, B. H., Benth, J. Š., Baracos, V. E., Fløtten, Ø., Hjermstad, M. J., ... Jordhøy, M. (2015). Low muscle mass is associated with chemotherapy-induced haematological toxicity in advanced non-small cell lung cancer. *Lung Cancer*, 90(1), 85–91.
<https://doi.org/10.1016/J.LUNGCAN.2015.07.001>

Skon, C. N., Lee, J. Y., Anderson, K. G., Masopust, D., Hogquist, K. A., & Jameson, S. C. (2013). Transcriptional downregulation of S1pr1 is required for the establishment of resident memory CD8⁺ T cells. *Nature Immunology*, 14(12), 1285–1293. <https://doi.org/10.1038/ni.2745>

Skorokhod, A., Bachmann, J., Giese, N. A., Martignoni, M. E., & Krakowski-Roosen, H. (2012). Real-time imaging cDNA-AFLP transcript profiling of pancreatic cancer patients: Egr-1 as a potential key regulator of muscle cachexia. *BMC Cancer*, 12, 265. <https://doi.org/10.1186/1471-2407-12-265>

Smith, G. I., & Mittendorfer, B. (2016). Sexual dimorphism in skeletal muscle protein turnover. *Journal of Applied Physiology*, 120(6), 674–682. <https://doi.org/10.1152/jappphysiol.00625.2015>

Smith, I. J., Aversa, Z., Hasselgren, P.-O., Pacelli, F., Rosa, F., Doglietto, G. B., & Bossola, M. (2011). CALPAIN activity is increased in skeletal muscle from gastric cancer patients with no or minimal weight loss. *Muscle & Nerve*, 43(3), 410–414. <https://doi.org/10.1002/mus.21893>

Sokol, C. L., Camire, R. B., Jones, M. C., & Luster, A. D. (2018). The Chemokine Receptor CCR8 Promotes the Migration of Dendritic Cells into the Lymph Node Parenchyma to Initiate the Allergic Immune Response. *Immunity*, 49(3), 449-463.e6.
<https://doi.org/10.1016/j.immuni.2018.07.012>

- Srinivasan, M., Sedmak, D., & Jewell, S. (2002). Effect of Fixatives and Tissue Processing on the Content and Integrity of Nucleic Acids. *The American Journal of Pathology*, *161*(6), 1961–1971. [https://doi.org/10.1016/S0002-9440\(10\)64472-0](https://doi.org/10.1016/S0002-9440(10)64472-0)
- Standley, R. A., Liu, S. Z., Jemiolo, B., Trappe, S. W., & Trappe, T. A. (2013). Prostaglandin E2 induces transcription of skeletal muscle mass regulators interleukin-6 and muscle RING finger-1 in humans. *Prostaglandins, Leukotrienes, and Essential Fatty Acids*, *88*(5), 361–364. <https://doi.org/10.1016/j.plefa.2013.02.004>
- Starnes, T., Rasila, K. K., Robertson, M. J., Brahmi, Z., Dahl, R., Christopherson, K., & Hromas, R. (2006). The chemokine CXCL14 (BRAK) stimulates activated NK cell migration: Implications for the downregulation of CXCL14 in malignancy. *Experimental Hematology*, *34*(8), 1101–1105. <https://doi.org/10.1016/J.EXPHEM.2006.05.015>
- Steffen, S., Abraham, S., Herbig, M., Schmidt, F., Blau, K., Meisterfeld, S., ... Günther, C. (2018). Toll-Like Receptor-Mediated Upregulation of CXCL16 in Psoriasis Orchestrates Neutrophil Activation. *Journal of Investigative Dermatology*, *138*(2), 344–354. <https://doi.org/10.1016/j.jid.2017.08.041>
- Stephens, N. A., Gallagher, I. J., Rooyackers, O., Skipworth, R. J., Tan, B. H., Marstrand, T., ... Timmons, J. A. (2010). Using transcriptomics to identify and validate novel biomarkers of human skeletal muscle cancer cachexia. *Genome Medicine*, *2*(1), 1–12. <https://doi.org/10.1186/gm122>
- Stephens, N. A., Gray, C., MacDonald, A. J., Tan, B. H., Gallagher, I. J., Skipworth, R. J. E., ... Greig, C. A. (2012). Sexual dimorphism modulates the impact of cancer cachexia on lower limb muscle mass and function. *Clinical Nutrition*, *31*(4), 499–505. <https://doi.org/10.1016/j.clnu.2011.12.008>
- Stephens, N. A., Skipworth, R. J. E., Gallagher, I. J., Greig, C. A., Guttridge, D. C., Ross, J. A., & Fearon, K. C. H. (2015). Evaluating potential biomarkers of cachexia and survival in skeletal muscle of upper gastrointestinal cancer patients. *Journal of Cachexia, Sarcopenia and Muscle*, (March), 53–61. <https://doi.org/10.1002/jcsm.12005>
- Stephens, N. A., Skipworth, R. J. E., MacDonald, A. J., Greig, C. A., Ross, J. A., & Fearon, K. C. H. (2011). Intramyocellular lipid droplets increase with progression of cachexia in cancer patients. *Journal of Cachexia, Sarcopenia and Muscle*, *2*(2), 111–117. <https://doi.org/10.1007/s13539-011-0030-x>
- Stitt, T. N., Drujan, D., Clarke, B. A., Panaro, F., Timofeyeva, Y., Kline, W. O., ... Glass, D. J. (2004). The IGF-1/PI3K/Akt pathway prevents expression of muscle atrophy-induced ubiquitin ligases by inhibiting FOXO transcription factors. *Molecular Cell*, *14*(3), 395–403.
- Stoeckle, C., Gouttefangeas, C., Hammer, M., Weber, E., Melms, A., & Tolosa, E. (2009). Cathepsin W expressed exclusively in CD8+ T cells and NK cells, is secreted during target cell killing but is not essential for cytotoxicity in human CTLs. *Experimental Hematology*, *37*(2), 266–275. <https://doi.org/10.1016/j.exphem.2008.10.011>

- Stretch, C., Aubin, J. M., Mickiewicz, B., Leugner, D., Al-manasra, T., Tobola, E., ... Bathe, O. F. (2018). Sarcopenia and myosteatosis are accompanied by distinct biological profiles in patients with pancreatic and periampullary adenocarcinomas. *PLoS ONE*, *13*(5), e0196235: 1-17. <https://doi.org/10.1371/journal.pone.0196235>
- Stretch, C., Khan, S., Asgarian, N., Eisner, R., Vaisipour, S., Damaraju, S., ... Baracos, V. E. (2013). Effects of Sample Size on Differential Gene Expression, Rank Order and Prediction Accuracy of a Gene Signature. *PLoS ONE*, *8*(6), 1–6. <https://doi.org/10.1371/journal.pone.0065380>
- Strömberg, A., Olsson, K., Dijksterhuis, J. P., Rullman, E., Schulte, G., & Gustafsson, T. (2016). CX₃CL1—a macrophage chemoattractant induced by a single bout of exercise in human skeletal muscle. *American Journal of Physiology-Regulatory, Integrative and Comparative Physiology*, *310*(3), R297–R304. <https://doi.org/10.1152/ajpregu.00236.2015>
- Sun, Y. S., Ye, Z. Y., Qian, Z. Y., Xu, X. D., & Hu, J. F. (2012). Expression of TRAF6 and ubiquitin mRNA in skeletal muscle of gastric cancer patients. *Journal of Experimental and Clinical Cancer Research*, *31*(1), 81. <https://doi.org/10.1186/1756-9966-31-81>
- Sun, Y., Wang, Y., Zhao, J., Gu, M., Giscombe, R., Lefvert, A. K., & Wang, X. (2006). B7-H3 and B7-H4 expression in non-small-cell lung cancer. *Lung Cancer*, *53*(2), 143–151. <https://doi.org/10.1016/J.LUNGCAN.2006.05.012>
- Supinski, G. S., Ji, X., & Callahan, L. A. (2010). p38 Mitogen-Activated Protein Kinase Modulates Endotoxin-Induced Diaphragm Caspase Activation. *American Journal of Respiratory Cell and Molecular Biology*, *43*(1), 121–127. <https://doi.org/10.1165/rcmb.2008-0395OC>
- Suzuki, F., Nanki, T., Imai, T., Kikuchi, H., Hirohata, S., Kohsaka, H., & Miyasaka, N. (2005). Inhibition of CX3CL1 (fractalkine) improves experimental autoimmune myositis in SJL/J mice. *Journal of Immunology (Baltimore, Md. : 1950)*, *175*(10), 6987–6996. <https://doi.org/10.4049/jimmunol.175.10.6987>
- Svensson, M., Marsal, J., Ericsson, A., Carramolino, L., Brodén, T., Márquez, G., & Agace, W. W. (2002). CCL25 mediates the localization of recently activated CD8 $\alpha\beta$ ⁺ lymphocytes to the small-intestinal mucosa. *Journal of Clinical Investigation*, *110*(8), 1113–1121. <https://doi.org/10.1172/JCI15988>
- Talbert, E. E., Lewis, H. L., Farren, M. R., Ramsey, M. L., Chakedis, J. M., Rajasekera, P., ... Guttridge, D. C. (2018). Circulating monocyte chemoattractant protein-1 (MCP-1) is associated with cachexia in treatment-naïve pancreatic cancer patients. *Journal of Cachexia, Sarcopenia and Muscle*, *9*(2), 358–368. <https://doi.org/10.1002/jcsm.12251>
- Tan, B. H. L., Fladvad, T., Braun, T. P., Vigano, A., Strasser, F., Deans, D. A. C., ... Fearon, K. C. H. (2012). P-selectin genotype is associated with the development of cancer cachexia. *EMBO Molecular Medicine*, *4*(6), 462–471. <https://doi.org/10.1002/emmm.201200231>

Tan, B. H. L., Ross, J. A., Kaasa, S., Skorpen, F., Fearon, K. C. H., & European Palliative Care Research Collaborative. (2011). Identification of possible genetic polymorphisms involved in cancer cachexia: a systematic review. *Journal of Genetics*, *90*(1), 165–177.

Tan, B. H.L., Brammer, K., Randhawa, N., Welch, N. T., Parsons, S. L., James, E. J., & Catton, J. A. (2015). Sarcopenia is associated with toxicity in patients undergoing neo-adjuvant chemotherapy for oesophago-gastric cancer. *European Journal of Surgical Oncology*, *41*(3), 333–338. <https://doi.org/10.1016/j.ejso.2014.11.040>

Tan, S.-M. (2012). The leucocyte $\beta 2$ (CD18) integrins: the structure, functional regulation and signalling properties. *Bioscience Reports*, *32*(3), 241–269. <https://doi.org/10.1042/bsr20110101>

Tanigaki, K., Chambliss, K. L., Yuhanna, I. S., Sacharidou, A., Ahmed, M., Atochin, D. N., ... Mineo, C. (2016). Endothelial fcg receptor IIB activation blunts insulin delivery to skeletal muscle to cause insulin resistance in mice. *Diabetes*, *65*(7), 1996–2005. <https://doi.org/10.2337/db15-1605>

Tarnopolsky, M. A., Pearce, E., Smith, K., & Lach, B. (2011). Suction-modified Bergström muscle biopsy technique: Experience with 13,500 procedures. *Muscle & Nerve*, *43*(5), 716–725. <https://doi.org/10.1002/mus.21945>

Taskin, S., Stumpf, V. I., Bachmann, J., Weber, C., Martignoni, M. E., Friedrich, O., ... Friedrich, O. (2014). Motor protein function in skeletal abdominal muscle of cachectic cancer patients. *Journal of Cellular and Molecular Medicine*, *18*(1), 69–79. <https://doi.org/10.1111/jcmm.12165>

Ter-Pogossian, M. M. (1977). Computerized cranial tomography: Equipment and physics. *Seminars in Roentgenology*, *12*(1), 13–25. [https://doi.org/10.1016/0037-198X\(77\)90053-0](https://doi.org/10.1016/0037-198X(77)90053-0)

Thakur, S. S., James, J. L., Cranna, N. J., Chhen, V. L., Swiderski, K., Ryall, J. G., & Lynch, G. S. (2019). Expression and localization of heat-shock proteins during skeletal muscle cell proliferation and differentiation and the impact of heat stress. *Cell Stress and Chaperones*, *24*(4), 749–761. <https://doi.org/10.1007/s12192-019-01001-2>

Thakur, S. S., Swiderski, K., Ryall, J. G., & Lynch, G. S. (2018). Therapeutic potential of heat shock protein induction for muscular dystrophy and other muscle wasting conditions. *Philosophical Transactions of the Royal Society B: Biological Sciences*, Vol. 373. <https://doi.org/10.1098/rstb.2016.0528>

Thorley, A. J., Goldstraw, P., Young, A., & Tetley, T. D. (2005). Primary Human Alveolar Type II Epithelial Cell CCL20 (Macrophage Inflammatory Protein-3 α)–Induced Dendritic Cell Migration. *American Journal of Respiratory Cell and Molecular Biology*, *32*(4), 262–267. <https://doi.org/10.1165/rcmb.2004-0196OC>

Thorsson, V., Gibbs, D. L., Brown, S. D., Wolf, D., Bortone, D. S., Ou Yang, T.-H., ... Shmulevich, I. (2018). The Immune Landscape of Cancer. *Immunity*, 48(4), 812-830.e14. <https://doi.org/10.1016/J.IMMUNI.2018.03.023>

Tidball, J. G. (2017). Regulation of muscle growth and regeneration by the immune system. *Nature Reviews Immunology*, 17(3), 165–178. <https://doi.org/10.1038/nri.2016.150>

Torres-Palsa, M. J., Koziol, M. V., Goh, Q., Cicinelli, P. A., Peterson, J. M., & Pizza, F. X. (2015). Expression of intercellular adhesion molecule-1 by myofibers in *mdx* mice. *Muscle & Nerve*, 52(5), 795–802. <https://doi.org/10.1002/mus.24626>

Trappe, T. A., White, F., Lambert, C. P., Cesar, D., Hellerstein, M., & Evans, W. J. (2002). Effect of ibuprofen and acetaminophen on postexercise muscle protein synthesis. *American Journal of Physiology-Endocrinology and Metabolism*, 282(3), E551–E556. <https://doi.org/10.1152/ajpendo.00352.2001>

Trappe, Todd A, & Liu, S. Z. (2013). Effects of prostaglandins and COX-inhibiting drugs on skeletal muscle adaptations to exercise. *Journal of Applied Physiology (Bethesda, Md. : 1985)*, 115(6), 909–919. <https://doi.org/10.1152/jappphysiol.00061.2013>

Trendelenburg, A., Meyer, A., Jacobi, C., Feige, J. N., & Glass, D. J. (2012). TAK-1/p38/nNFκB signaling inhibits myoblast differentiation by increasing levels of Activin A. *Skeletal Muscle*, 2(1), 3. <https://doi.org/10.1186/2044-5040-2-3>

Truong, M., Liang, L., Kukreja, J., O'Brien, J., Jean-Gilles, J., & Messing, E. (2017). Cautery artifact understages urothelial cancer at initial transurethral resection of large bladder tumours. *Canadian Urological Association Journal = Journal de l'Association Des Urologues Du Canada*, 11(5), E203–E206. <https://doi.org/10.5489/cuaj.4172>

Tsukioka, T., Izumi, N., Mizuguchi, S., Kyukwang, C., Komatsu, H., Toda, M., ... Nishiyama, N. (2018). Positive correlation between sarcopenia and elevation of neutrophil/lymphocyte ration in pathological stage IIIA (N2-positive) non-small cell lung cancer patients. *General Thoracic and Cardiovascular Surgery*, 66(12), 716–722. <https://doi.org/10.1007/s11748-018-0985-z>

Turrin, N. P., Ilyin, S. E., Gayle, D. A., Plata-Salamán, C. R., Ramos, E. J. B., Laviano, A., ... Meguid, M. M. (2004). Interleukin-1beta system in anorectic catabolic tumor-bearing rats. *Current Opinion in Clinical Nutrition and Metabolic Care*, 7(4), 419–426. Retrieved from <http://www.ncbi.nlm.nih.gov/pubmed/15192445>

Uematsu, S., Fujimoto, K., Jang, M. H., Yang, B. G., Jung, Y. J., Nishiyama, M., ... Akira, S. (2008). Regulation of humoral and cellular gut immunity by lamina propria dendritic cells expressing Toll-like receptor 5. *Nature Immunology*, 9(7), 769–776. <https://doi.org/10.1038/ni.1622>

Uguccioni, M., Mackay, C. R., Ochensberger, B., Loetscher, P., Rhis, S., LaRosa, G. J., ... Dahinden, C. A. (1997). High expression of the chemokine receptor CCR3 in human blood

basophils. Role in activation by eotaxin, MCP-4, and other chemokines. *Journal of Clinical Investigation*, 100(5), 1137–1143. <https://doi.org/10.1172/JCI119624>

Van Der Werf, A., Langius, J. A. E., De Van Der Schueren, M. A. E., Nurmohamed, S. A., Van Der Pant, K. A. M. I., Blauwhoff-Buskermolen, S., & Wierdsma, N. J. (2018). Percentiles for skeletal muscle index, area and radiation attenuation based on computed tomography imaging in a healthy Caucasian population. *European Journal of Clinical Nutrition*, 72(2), 288–296. <https://doi.org/10.1038/s41430-017-0034-5>

Van Meir, H., Nout, R. A., Welters, M. J. P., Loof, N. M., de Kam, M. L., van Ham, J. J., ... van der Burg, S. H. (2017). Impact of (chemo) radiotherapy on immune cell composition and function in cervical cancer patients. *OncoImmunology*, 6(2), e1267095. <https://doi.org/10.1080/2162402X.2016.1267095>

Vanderlocht, J., Hellings, N., Hendriks, J. J. A., Vandenabeele, F., Moreels, M., Buntinx, M., ... Stinissen, P. (2006). Leukemia inhibitory factor is produced by myelin-reactive T cells from multiple sclerosis patients and protects against tumor necrosis factor- α -induced oligodendrocyte apoptosis. *Journal of Neuroscience Research*, 83(5), 763–774. <https://doi.org/10.1002/jnr.20781>

Vanderlocht, J., Hendriks, J. J. A., Venken, K., Stinissen, P., & Hellings, N. (2006). Effects of IFN- β , leptin and simvastatin on LIF secretion by T lymphocytes of MS patients and healthy controls. *Journal of Neuroimmunology*, 177(1–2), 189–200. <https://doi.org/10.1016/J.JNEUROIM.2006.04.012>

Varadhan, K. K., Constantin-Teodosiu, D., Constantin, D., Greenhaff, P. L., & Lobo, D. N. (2018). Inflammation-mediated muscle metabolic dysregulation local and remote to the site of major abdominal surgery. *Clinical Nutrition*, 37(6), 2178–2185. <https://doi.org/10.1016/j.clnu.2017.10.020>

Vasyutina, E., Stebler, J., Brand-Saberi, B., Schulz, S., Raz, E., & Birchmeier, C. (2005). CXCR4 and Gab1 cooperate to control the development of migrating muscle progenitor cells. *Genes & Development*, 19(18), 2187–2198. <https://doi.org/10.1101/gad.346205>

Veninga, H., Becker, S., Hoek, R. M., Wobus, M., Wandel, E., Kaa, J. van der, ... Hamann, J. (2008). Analysis of CD97 Expression and Manipulation: Antibody Treatment but Not Gene Targeting Curtails Granulocyte Migration. *The Journal of Immunology*, 181(9), 6574–6583. <https://doi.org/10.4049/JIMMUNOL.181.9.6574>

Verstak, B., Nagpal, K., Bottomley, S. P., Golenbock, D. T., Hertzog, P. J., & Mansell, A. (2009). MyD88 adapter-like (Mal)/TIRAP interaction with TRAF6 is critical for TLR2- and TLR4-mediated NF-kappaB proinflammatory responses. *The Journal of Biological Chemistry*, 284(36), 24192–24203. <https://doi.org/10.1074/jbc.M109.023044>

Vestweber, D. (2015). How leukocytes cross the vascular endothelium. *Nature Reviews Immunology*, 15(11), 692–704. <https://doi.org/10.1038/nri3908>

Vidya, M. K., Kumar, V. G., Sejian, V., Bagath, M., Krishnan, G., & Bhatta, R. (2018). Toll-like receptors: Significance, ligands, signaling pathways, and functions in mammals. *International Reviews of Immunology*, Vol. 37, pp. 20–36. <https://doi.org/10.1080/08830185.2017.1380200>

Vinet, L., & Zhedanov, A. (2011). A ‘missing’ family of classical orthogonal polynomials. *Journal of Physics A: Mathematical and Theoretical*, 44(8), 085201. <https://doi.org/10.1088/1751-8113/44/8/085201>

Voron, T., Tselikas, L., Pietrasz, D., Pigneur, F., Laurent, A., Compagnon, P., ... Azoulay, D. (2015). Sarcopenia Impacts on Short- and Long-term Results of Hepatectomy for Hepatocellular Carcinoma. *Annals of Surgery*, 261(6), 1173–1183. <https://doi.org/10.1097/SLA.0000000000000743>

Vuong, C., Van Uum, S. H. M., O’Dell, L. E., Lutfy, K., & Friedman, T. C. (2010). The Effects of Opioids and Opioid Analogs on Animal and Human Endocrine Systems. *Endocrine Reviews*, 31(1), 98–132. <https://doi.org/10.1210/er.2009-0009>

Vyas, D., Laput, G., & Vyas, A. K. (2014). Chemotherapy-enhanced inflammation may lead to the failure of therapy and metastasis. *OncoTargets and Therapy*. Dove Press. <https://doi.org/10.2147/OTT.S60114>

Wagner, A. D., Syn, N. L., Moehler, M., Grothe, W., Yong, W. P., Tai, B.-C., ... Unverzagt, S. (2017). Chemotherapy for advanced gastric cancer. *Cochrane Database of Systematic Reviews*, 8, CD004064. <https://doi.org/10.1002/14651858.CD004064.pub4>

Wang, J. (2018). Neutrophils in tissue injury and repair. *Cell and Tissue Research*, 371(3), 531. <https://doi.org/10.1007/S00441-017-2785-7>

Wang, T., Feng, X., Zhou, J., Gong, H., Xia, S., Wei, Q., ... Yu, L. (2016). Type 2 diabetes mellitus is associated with increased risks of sarcopenia and pre-sarcopenia in Chinese elderly. *Scientific Reports*, 6, 38937. <https://doi.org/10.1038/srep38937>

Wang, W., Fan, Y. Q., Lv, Z., Yao, X. J., Wang, W., Huang, K. W., ... Ying, S. (2012). Interleukin-25 promotes basic fibroblast growth factor expression by human endothelial cells through interaction with IL-17RB, but not IL-17RA. *Clinical & Experimental Allergy*, 42(11), 1604–1614. <https://doi.org/10.1111/j.1365-2222.2012.04062.x>

Wang, Y., Kuang, Z., Yu, X., Ruhn, K. A., Kubo, M., & Hooper, L. V. (2017). The intestinal microbiota regulates body composition through NFIL3 and the circadian clock. *Science (New York, N.Y.)*, 357(6354), 912–916. <https://doi.org/10.1126/science.aan0677>

Wang-Gillam, A., Li, C.-P., Bodoky, G., Dean, A., Shan, Y.-S., Jameson, G., ... Wong, M. (2016). Nanoliposomal irinotecan with fluorouracil and folinic acid in metastatic pancreatic cancer after previous gemcitabine-based therapy (NAPOLI-1): a global, randomised, open-label, phase 3 trial. *The Lancet*, 387(10018), 545–557. [https://doi.org/10.1016/S0140-6736\(15\)00986-1](https://doi.org/10.1016/S0140-6736(15)00986-1)

- Wardill, H. R., Gibson, R. J., Van Seville, Y. Z. A., Secombe, K. R., Coller, J. K., White, I. A., ... Bowen, J. M. (2016). Irinotecan-Induced Gastrointestinal Dysfunction and Pain Are Mediated by Common TLR4-Dependent Mechanisms. *Molecular Cancer Therapeutics*, 15(6), 1376–1386. <https://doi.org/10.1158/1535-7163.MCT-15-0990>
- Warren, G. L., Hulderman, T., Liston, A., & Simeonova, P. P. (2011). Toll-like and adenosine receptor expression in injured skeletal muscle. *Muscle & Nerve*, 44(1), 85–92. <https://doi.org/10.1002/mus.22001>
- Weathington, N. M., Kanth, S. M., Gong, Q., Londino, J., Hoji, A., Rojas, M., ... Mallampalli, R. K. (2017). IL-4 Induces IL17Rb Gene Transcription in Monocytic Cells with Coordinate Autocrine IL-25 Signaling. *American Journal of Respiratory Cell and Molecular Biology*, 57(3), 346–354. <https://doi.org/10.1165/rcmb.2016-0316OC>
- Weber, M. A., Kinscherf, R., Krakowski-Roosen, H., Aulmann, M., Renk, H., Künkele, A., ... Hildebrandt, W. (2007). Myoglobin plasma level related to muscle mass and fiber composition - A clinical marker of muscle wasting? *Journal of Molecular Medicine*, 85(8), 887–896. <https://doi.org/10.1007/s00109-007-0220-3>
- Weber, M. A., Krakowski-Roosen, H., Schröder, L., Kinscherf, R., Krix, M., Kopp-Schneider, A., ... Hildebrandt, W. (2009). Morphology, metabolism, microcirculation, and strength of skeletal muscles in cancer-related cachexia. *Acta Oncologica*, 48(1), 116–124. <https://doi.org/10.1080/02841860802130001>
- Weichand, B., Weis, N., Weigert, A., Grossmann, N., Levkau, B., & Brüne, B. (2013). Apoptotic cells enhance sphingosine-1-phosphate receptor 1 dependent macrophage migration. *European Journal of Immunology*, 43(12), 3306–3313. <https://doi.org/10.1002/eji.201343441>
- Weng, N., Araki, Y., & Subedi, K. (2012). The molecular basis of the memory T cell response: differential gene expression and its epigenetic regulation. *Nature Reviews. Immunology*, 12(4), 306–315. <https://doi.org/10.1038/nri3173>
- Wessels, B., Ciapaite, J., van den Broek, N. M. A., Nicolay, K., & Prompers, J. J. (2014). Metformin Impairs Mitochondrial Function in Skeletal Muscle of Both Lean and Diabetic Rats in a Dose-Dependent Manner. *PLoS ONE*, 9(6), e100525. <https://doi.org/10.1371/journal.pone.0100525>
- Weycker, D., Silvia, A., Richert-Boe, K., Bensink, M., Brady, J. O., Lamerato, L., ... Chandler, D. (2016). Use and Patterns of Supportive Care Among Patients Receiving Myelosuppressive Chemotherapy for Breast Cancer, Colorectal Cancer, Lung Cancer, or Non-Hodgkin's Lymphoma in US Clinical Practice. *Blood*, 128(22).
- White, J. P., Puppa, M. J., Gao, S., Sato, S., Welle, S. L., & Carson, J. A. (2013). Muscle mTORC1 suppression by IL-6 during cancer cachexia: a role for AMPK. *American Journal of Physiology-Endocrinology and Metabolism*, 304(10), E1042–E1052. <https://doi.org/10.1152/ajpendo.00410.2012>

- Williams, A., Sun, X., Fischer, J. E., & Hasselgren, P. O. (1999). The expression of genes in the ubiquitin-proteasome proteolytic pathway is increased in skeletal muscle from patients with cancer. *Surgery*, *126*(4), 744–750. [https://doi.org/10.1016/S0039-6060\(99\)70131-5](https://doi.org/10.1016/S0039-6060(99)70131-5)
- Williams, J. P., Phillips, B. E., Smith, K., Atherton, P. J., Rankin, D., Selby, A. L., ... Rennie, M. J. (2012). Effect of tumor burden and subsequent surgical resection on skeletal muscle mass and protein turnover in colorectal cancer patients. *AM J Clin Nutr*, *96*(5), 1064–1071. <https://doi.org/10.3945/ajcn.112.045708.1064>
- Wing, S. S. (2016). Deubiquitinating enzymes in skeletal muscle atrophy—An essential role for USP19. *The International Journal of Biochemistry & Cell Biology*, *79*, 462–468. <https://doi.org/10.1016/J.BIOCEL.2016.07.028>
- Wolf, M. J., Seleznik, G. M., Zeller, N., & Heikenwalder, M. (2010). The unexpected role of lymphotoxin β receptor signaling in carcinogenesis: from lymphoid tissue formation to liver and prostate cancer development. *Oncogene*, *29*(36), 5006–5018. <https://doi.org/10.1038/onc.2010.260>
- Wu, T., Hu, Y., Lee, Y.-T., Bouchard, K. R., Benechet, A., Khanna, K., & Cauley, L. S. (2014). Lung-resident memory CD8 T cells (T_{RM}) are indispensable for optimal cross-protection against pulmonary virus infection. *Journal of Leukocyte Biology*, *95*(2), 215–224. <https://doi.org/10.1189/jlb.0313180>
- Wüst, R. C. I., & Degens, H. (2007). Factors contributing to muscle wasting and dysfunction in COPD patients. *International Journal of Chronic Obstructive Pulmonary Disease*, *2*(3), 289–300. Retrieved from <http://www.ncbi.nlm.nih.gov/pubmed/18229567>
- Wynn, T. A., & Vannella, K. M. (2016). Macrophages in Tissue Repair, Regeneration, and Fibrosis. *Immunity*, *44*(3), 450–462. <https://doi.org/10.1016/j.immuni.2016.02.015>
- Xiao, J., Caan, B. J., Cespedes Feliciano, E. M., Meyerhardt, J. A., Kroenke, C. H., Baracos, V. E., ... Prado, C. M. (2019). The association of medical and demographic characteristics with sarcopenia and low muscle radiodensity in patients with nonmetastatic colorectal cancer. *The American Journal of Clinical Nutrition*, *109*(3), 615–625. <https://doi.org/10.1093/ajcn/nqy328>
- Xiao, J., Caan, B. J., Weltzien, E., Cespedes Feliciano, E. M., Kroenke, C. H., Meyerhardt, J. A., ... Prado, C. M. (2018). Associations of pre-existing co-morbidities with skeletal muscle mass and radiodensity in patients with non-metastatic colorectal cancer. *Journal of Cachexia, Sarcopenia and Muscle*, *9*(4), 654–663. <https://doi.org/10.1002/jcsm.12301>
- Xing, Y., Tian, Y., Kurosawa, T., Matsui, S., Touma, M., Yanai, T., ... Sugimoto, K. (2016). CCL11-induced eosinophils inhibit the formation of blood vessels and cause tumor necrosis. *Genes to Cells*, *21*(6), 624–638. <https://doi.org/10.1111/gtc.12371>

Xue, H., Field, C. J., Sawyer, M. B., Dieleman, L. A., & Baracos, V. E. (2009). Prophylactic ciprofloxacin treatment prevented high mortality, and modified systemic and intestinal immune function in tumour-bearing rats receiving dose-intensive CPT-11 chemotherapy. *British Journal of Cancer*, *100*(10), 1581–1588. <https://doi.org/10.1038/sj.bjc.6605051>

Xue, H., Le Roy, S., Sawyer, M. B., Field, C. J., Dieleman, L. A., & Baracos, V. E. (2009). Single and combined supplementation of glutamine and n -3 polyunsaturated fatty acids on host tolerance and tumour response to 7-ethyl-10-[4-(1-piperidino)-1-piperidino]carbonyloxy-camptothecin (CPT-11)/5-fluorouracil chemotherapy in rats bearing Ward col. *British Journal of Nutrition*, *102*(3), 434–442. <https://doi.org/10.1017/s0007114508199482>

Xue, H., Sawyer, M. B., Field, C. J., Dieleman, L. A., & Baracos, V. E. (2007). Nutritional modulation of antitumor efficacy and diarrhea toxicity related to irinotecan chemotherapy in rats bearing the ward colon tumor. *Clinical Cancer Research*, *13*(23), 7146–7154. <https://doi.org/10.1158/1078-0432.CCR-07-0823>

Xue, Hongyu, Le Roy, S., Sawyer, M. B., Field, C. J., Dieleman, L. A., & Baracos, V. E. (2009). Single and combined supplementation of glutamine and n -3 polyunsaturated fatty acids on host tolerance and tumour response to 7-ethyl-10-[4-(1-piperidino)-1-piperidino]carbonyloxy-camptothecin (CPT-11)/5-fluorouracil chemotherapy in rats bearing Ward col. *British Journal of Nutrition*, *102*(3), 434–442. <https://doi.org/10.1017/s0007114508199482>

Yadav, A., Chang, Y.-H., Carpenter, S., Silva, A. C., Rakela, J., Aqel, B. A., ... Carey, E. J. (2015). Relationship between sarcopenia, six-minute walk distance and health-related quality of life in liver transplant candidates. *Clinical Transplantation*, *29*(2), 134–141. <https://doi.org/10.1111/ctr.12493>

Yago, T., Shao, B., Miner, J. J., Yao, L., Klopocki, A. G., Maeda, K., ... McEver, R. P. (2010). E-selectin engages PSGL-1 and CD44 through a common signaling pathway to induce integrin α L β 2-mediated slow leukocyte rolling. *Blood*, *116*(3), 485–494. <https://doi.org/10.1182/blood-2009-12-259556>

Yago, T., Zhang, N., Zhao, L., Abrams, C. S., & McEver, R. P. (2018). Selectins and chemokines use shared and distinct signals to activate β 2 integrins in neutrophils. <https://doi.org/10.1182/bloodadvances.2017015602>

Yamamoto, T., Kawada, K., Itatani, Y., Inamoto, S., Okamura, R., Iwamoto, M., ... Sakai, Y. (2017). Loss of SMAD4 promotes lung metastasis of colorectal cancer by accumulation of CCR1 + tumor-associated neutrophils through CCL15-CCR1 axis. *Clinical Cancer Research*, *23*(3), 833–844. <https://doi.org/10.1158/1078-0432.CCR-16-0520>

Yamazaki, K., Beauchamp, G., Kupniewski, D., Bard, J., Thomas, L., & Boyse, E. (1988). Familial imprinting determines H-2 selective mating preferences. *Science*, *240*(4857), 1331–1332. <https://doi.org/10.1126/science.3375818>

Yang, L., Pang, Y., & Moses, H. L. (2010). TGF-beta and immune cells: an important regulatory axis in the tumor microenvironment and progression. *Trends in Immunology*, *31*(6), 220–227. <https://doi.org/10.1016/j.it.2010.04.002>

Yang, W., & Hu, P. (2018, April). Skeletal muscle regeneration is modulated by inflammation. *Journal of Orthopaedic Translation*, Vol. 13, pp. 25–32. <https://doi.org/10.1016/j.jot.2018.01.002>

Yao, L., Yago, T., Shao, B., Liu, Z., Silasi-Mansat, R., Setiadi, H., ... McEver, R. P. (2013). Elevated CXCL1 expression in gp130-deficient endothelial cells impairs neutrophil migration in mice. *Blood*, *122*(23), 3832–3842. <https://doi.org/10.1182/blood-2012-12-473835>

Yoshizumi, T., Nakamura, T., Yamane, M., Waliul Islam, A. H. M., Menju, M., Yamasaki, K., ... Matsuzawa, Y. (1999). Abdominal Fat: Standardized Technique for Measurement at CT. *Radiology*, *211*(1), 283–286. <https://doi.org/10.1148/radiology.211.1.r99ap15283>

Zalcberg, J., Kerr, D., Seymour, L., & Palmer, M. (1998). Haematological and non-haematological toxicity after 5-fluorouracil and leucovorin in patients with advanced colorectal cancer is significantly associated with gender, increasing age and cycle number. *European Journal of Cancer*, *34*(12), 1871–1875. [https://doi.org/10.1016/S0959-8049\(98\)00259-7](https://doi.org/10.1016/S0959-8049(98)00259-7)

Zampieri, S., Doria, A., Adami, N., Biral, D., Vecchiato, M., Savastano, S., ... Merigliano, S. (2010). Subclinical myopathy in patients affected with newly diagnosed colorectal cancer at clinical onset of disease: evidence from skeletal muscle biopsies. *Neurological Research*, *32*(1), 20–25. <https://doi.org/10.1179/016164110X12556180205997>

Zampieri, S., Valente, M., Adami, N., Biral, D., Ghirardello, A., Rampudda, M. E., ... Doria, A. (2010). Polymyositis, dermatomyositis and malignancy: A further intriguing link. *Autoimmunity Reviews*, *9*(6), 449–453. <https://doi.org/10.1016/j.autrev.2009.12.005>

Zampieri, S., Valente, M., Adami, N., Corbianco, S., Doria, A., Biral, D., ... Section, H. P. (2009). *Subclinical myopathy in patients affected with early stage colorectal cancer at disease onset : No evidence of inflammatory cells infiltration in the skeletal muscle biopsies harvested during diagnostic laparoscopy Immunohistochemical analysis*. *19*, 253–257.

Zarour, H. M. (2016). Reversing T-cell Dysfunction and Exhaustion in Cancer. *Clinical Cancer Research : An Official Journal of the American Association for Cancer Research*, *22*(8), 1856–1864. <https://doi.org/10.1158/1078-0432.CCR-15-1849>

Zeiderman, M. R., Gowland, G., Peel, B., & McMahon, M. J. (1991). the Influence of Short-Term Preoperative Intravenous Nutrition Upon Anthropometric Variables, Protein-Synthesis and Immunological Indexes in Patients With Gastrointestinal Cancer. *Clinical Nutrition*, *10*, 213–221. [https://doi.org/10.1016/0261-5614\(91\)90041-a](https://doi.org/10.1016/0261-5614(91)90041-a)

Zhang, C., Qiao, Y., Huang, L., Li, F., Zhang, Z., Ping, Y., ... Zhang, Y. (2018). Regulatory T cells were recruited by CCL3 to promote cryo-injured muscle repair. *Immunology Letters*, *204*, 29–37. <https://doi.org/10.1016/j.imlet.2018.10.004>

Zhang, G., Liu, Z., Ding, H., Miao, H., Garcia, J. M., & Li, Y. P. (2017). Toll-like receptor 4 mediates Lewis lung carcinoma-induced muscle wasting via coordinate activation of protein degradation pathways. *Scientific Reports*, 7(1), 1–8. <https://doi.org/10.1038/s41598-017-02347-2>

Zhang, G., Liu, Z., Ding, H., Zhou, Y., Doan, H. A., Sin, K. W. T., ... Li, Y.-P. (2017). Tumor induces muscle wasting in mice through releasing extracellular Hsp70 and Hsp90. *Nature Communications*, 8(1), 589. <https://doi.org/10.1038/s41467-017-00726-x>

Zhang, J., Xiao, Z., Qu, C., Cui, W., Wang, X., & Du, J. (2014). CD8 T cells are involved in skeletal muscle regeneration through facilitating MCP-1 secretion and Gr1(high) macrophage infiltration. *Journal of Immunology (Baltimore, Md. : 1950)*, 193(10), 5149–5160. <https://doi.org/10.4049/jimmunol.1303486>

Zhang, Y., Fu, S., Wang, J., Zhao, X., Zeng, Q., & Li, X. (2019). Association between Geriatric Nutrition Risk Index and low muscle mass in Chinese elderly people. *European Journal of Clinical Nutrition*, 73(6), 917–923. <https://doi.org/10.1038/s41430-018-0330-8>

Zhao, X., Sato, A., Dela Cruz, C. S., Linehan, M., Luegering, A., Kucharzik, T., ... Iwasaki, A. (2003). CCL9 Is Secreted by the Follicle-Associated Epithelium and Recruits Dome Region Peyer's Patch CD11b⁺ Dendritic Cells. *The Journal of Immunology*, 171(6), 2797–2803. <https://doi.org/10.4049/jimmunol.171.6.2797>

Zheng, Z. F., Lu, J., Xie, J. W., Wang, J. Bin, Lin, J. X., Chen, Q. Y., ... Li, P. (2018). Preoperative skeletal muscle index vs the controlling nutritional status score: Which is a better objective predictor of long-term survival for gastric cancer patients after radical gastrectomy? *Cancer Medicine*, 7(8), 3537–3547. <https://doi.org/10.1002/cam4.1548>

Zhou, F. H., Foster, B. K., Zhou, X.-F., Cowin, A. J., & Xian, C. J. (2006). TNF- α Mediates p38 MAP Kinase Activation and Negatively Regulates Bone Formation at the Injured Growth Plate in Rats. *Journal of Bone and Mineral Research*, 21(7), 1075–1088. <https://doi.org/10.1359/jbmr.060410>

Appendix

Appendix A (Chapter 3): Antibody information used for immunofluorescence experiments: muscle fiber types, laminin/dystrophin and nuclear stain.

Primary Antibody	Dilution factor-primary	Supplier	Secondary antibody	Dilution factor-secondary	Supplier (Code)	Isotype	Species
Laminin	1:200	SIGMA	AlexaFluor® 647	1:400	Fisher	IgG	Rabbit
Dystrophin	1:25	Abcam				IgG	Rabbit
MyHC I (BAD5)	1:400	American Type Culture Collection	AlexaFluor® 568	1:200	Fisher	IgG2b	Mouse
MyCH IID (6H1)	1:400	American Type Culture Collection	AlexaFluor® 488	1:400	Fisher	IgM	Mouse
MyCH IIA (SC71)	1:400	American Type Culture Collection	AlexaFluor® 405	1:200	Fisher	IgG1	Mouse
DAPI	300 nM	BD Biosciences					

Appendix B (Chapter 3): Complete extraction table of the reviewed articles in relevance of muscle biopsy collection in cancer patients

Section I: Quality assessment, study design, muscle group, surgical procedure, cancer type, cancer stage and population sample size

Section II: Age, weight loss, body composition, control group, control sample size and age

Section III: Anti-neoplastic treatment, % of weight loss, medical history, medications, exclusion criteria

Complete extraction table of the reviewed articles in relevance of muscle biopsy collection in cancer patients / Section I									
Author	Year	BIAS - Modified Newcastle-Ottawa scale - sample bias score (max. 3 points)	QUALITY - Quality Assessment score (NIH)	Study design	Muscle	Type of surgical procedure	Cancer type	Cancer stage	Population sample size, n (male%)
Acharyya	2005	1	3 out of 12	Cross-sectional	RA	NR	Gastric	NR	27(NR)
Agustsson	2011	1	3 out of 12	Cross-sectional	RA	Open surgery	Pancreatic and other (gastric, colon, ampulla of Vater, bile duct, small intestine and gallbladder)	NR	Pancreas=13 (30) / Other=8 (37)
Aversa	2016	1	6 out of 12	Cross-sectional	RA	Open surgery	Colorectal, pancreatic and gastric	Stage 1-4	29 (59), WS = 14 / WL =15
Aversa	2012	1	3 out of 12	Cross-sectional	RA and SA	Open surgery	NSCLC and gastric	Stage 1-4	39 (74)
Banduseela	2007	N/A	N/A	Case study	TA	N/A	NSCLC	NR	1 (100)
Bohlen	2018	0	4 out of 12	Cross-sectional	PM	Open surgery	Breast	Stage 1-4	14 (0)
Bonetto	2013	1	3 out of 12	Cross-sectional	RA	Open surgery	Gastric	Stage 1-4	16(NR)

Bossola	2006	1	5 out of 12	Cross-sectional	RA	Open surgery	Gastric	Stage 1-4	16 (50)
Bossola	2001	1	4 out of 12	Cross-sectional	RA	Open surgery	Gastric	NR	20 (55)
Bossola	2003	1	5 out of 12	Cross-sectional	RA	Open surgery	Gastric	NR	23 (61)
Brzezczynska	2016	0	2 out of 12	Cross-sectional	QF	Open surgery	Oesophageal, gastric and pancreatic	Stage 2-3	28 (75), NC = 18 (72) / CC = 10 (80)
Busquets	2007	0	3 out of 12	Cross-sectional	RA	Open surgery	Oesophageal, gastric and pancreatic	Stage 1-4	16(NR)
Christensen	2016	N/A	13 out of 14	Randomized controlled trial	VL	N/A	Testicular germ cell	NR	8 (100)
Christensen	2014	N/A	13 out of 14	Randomized controlled trial	VL	N/A	Testicular germ cell	NR	15 (100)
DeJong	2005	0	4 out of 12	Cross-sectional	RA	Open surgery	Pancreatic	Stage 1-4	16 (63)
D'Orlando	2014	1	6 out of 12	Cross-sectional	RA	Open surgery	Gastric	Stage 1-4	38 (66)
Ebhardt	2017	0	1 out of 12	Cross-sectional	QF	N/A	Oesophageal, gastric and pancreatic	NR	19 (79), NC = 14 (85) / CC = 5 (60)
Eley	2008	1	3 out of 12	Cross-sectional	RA	Open surgery	Oesophageal and gastric	Stage 1-4	15 (87)
Gallagher	2012	1	7 out of 14	Longitudinal	QF	N/A	Oesophageal, gastric and pancreatic	Stage1-3	12 (83)
Higuchi	2000	N/A	N/A	Case study	Gastroc	N/A	Gastric	NR	1 (100)
Jagoe	2002	0	1 out of 12	Cross-sectional	LD	Open surgery	Lung	Stage3-4	36 (75)

Johns	2017	2	9 out of 12	Cross-sectional	RA	Open surgery	Oesophageal, gastric and pancreatic, lung and other (not defined)	Stage 1-4	134 (51)
Johns	2014	0	5 out of 12	Cross-sectional	RA	Open surgery	Upper GI tract and pancreatic	NR	41 (73)
Khal	2005	0	1 out of 12	Cross-sectional	RA	Open surgery	Pancreatic and colorectal	NR	18 (67), WS = 5 (60) / WL = 13 (69)
Lamboley	2017	1	3 out of 12	Cross-sectional	VL	N/A	Prostate	Stage 2	8 (100)
Lundholm	1976	1	3 out of 12	Cross-sectional	RA	Open surgery	Oesophageal, gastric, pancreatic, choledochal, colorectal and liver, gall-bladder, renal and ovary	NR	43 (44)
MacDonald	2015	0	2 out of 12	Cross-sectional	RA and QF	Open surgery	Oesophageal and gastric	Stage 1-4	14 (57), WS = 6 (66) / WL = 8 (50)
Marzetti	2017	1	5 out of 12	Cross-sectional	RA	Open surgery	Gastric	Stage 1-4	18 (94), WS = 9 (100) / WL = 9 (89)
Narasimhan	2017	2	8 out of 12	Cross-sectional	RA	Open surgery	Pancreatic and colorectal	Stage 1-4	22 (41)
Narasimhan	2018	1	5 out of 12	Cross-sectional	RA	Open surgery	Pancreatic and colorectal	Stage 1-4	40 (43), WS = 19 (47) / WL = 21 (40)
Nilsen	2016	N/A	9 out of 14	Randomized controlled trial	VL	N/A	Prostate	NR	12 (100)

Noguchi	1998	0	3 out of 12	Cross-sectional	RA	Open surgery	Oesophageal, gastric and colorectal	Stage 1-4	10 (90)
Op den Kamp	2015	0	6 out of 12	Cross-sectional	VL	NR	NSCLC	Stage 3-4	26 (65), Pre-CC = 10 (80) / CC= 16 (56),
Op den Kamp	2012	0	3 out of 12	Cross-sectional	VL	NR	NSCLC	Stage 1-3	16 (93)
Op den Kamp	2013	0	5 out of 12	Cross-sectional	VL	NR	NSCLC	Stage 3-4	26 (65), Pre-CC = 10 (80) / CC= 16 (56),
Pessina	2010	1	6 out of 12	Cross-sectional	RA	Open surgery	Gastric	Stage 1-3	30 (57)
Phillips	2013	0	4 out of 14	Longitudinal	VL	Open surgery	Colorectal	Early stage	8 (50)
Prokopchuk	2016	0	4 out of 12	Cross-sectional	RA	Open surgery	Pancreas	Stage 1-4	25 (32), NC=13 (38) / CC=12 (25)
Puig-Vilanova	2014	1	3 out of 12	Cross-sectional	VL	NR	Lung	Stage 1-4	10 (100)
Ramage	2018	1	3 out of 12	Cross-sectional	RA	Open surgery	Oesophageal, gastric and pancreatic	Stage 1-4	32 (81)
Rhoads	2009	1	6 out of 12	Cross-sectional	RA	Open surgery	Gastric	Stage 1-4	14 (57), WS = 6 (66) / WL = 8 (50)

Schmitt	2007	0	2 out of 12	Cross-sectional	RA	Open surgery	Pancreatic	Stage 2 and 4	16 (63), NC= 8 (37) / CC = 8 (88)
Shaw	1991	0	6 out of 14	Non-randomized trial	RA and SCM	Open surgery	Colorectal and pancreatic, head and neck, thyroid, melanoma and sarcoma	NR	43 (42), WS = 25 (48) / WL = 18 (66)
Skorokhod	2012	0	1 out of 12	Cross-sectional	RA	Open surgery	Pancreatic	Stage 2-4	23 (61), WS = 13 (69) / WL = 10 (50)
Smith	2010	0	4 out of 12	Cross-sectional	RA	Open surgery	Gastric	Stage 1-4	15 (67)
Stephens	2011	0	2 out of 12	Cross-sectional	RA	Open surgery	Oesophageal, gastric, pancreatic, bile duct and rectal	Stage 2-4	19 (58)
Stephens	2010	1	3 out of 12	Cross-sectional	RA, VL and DIAPH	Open surgery	Oesophageal, gastric and pancreatic	NR	18 (66), WL
Stephens	2015	0	3 out of 12	Longitudinal	RA	Open surgery	Oesophageal, gastric, small-bowel, pancreatic and bile duct	Stage 1-4	92 (72), NC = 41 (82) / CC = 51(63),
Stretch	2013	0	4 out of 12	Cross-sectional	RA	Open surgery	Liver/Bile duct, GI tract, pancreatic, ovary/uterus, head & neck, skin and kidney	NR	134 (51)
Sun	2012	0	5 out of 12	Cross-sectional	RA	Open surgery	Gastric	Stage 1-4	102 (71)
Taskin	2014	0	1 out of 12	Cross-sectional	RA	Open surgery	Colorectal, pancreatic and gastric and lymphoma	NR	14 (50), NC= 8 (37) / CC = 6 (66)

Weber	2007	0	3 out of 12	Cross-sectional	VL	N/A	Gastric, pancreatic and leukemia	NR	17 (53)
Weber	2009	0	2 out of 12	Cross-sectional	VL	N/A	GI tract (malignancy types not defined)	NR	19 (52)
Williams	2012	0	5 out of 12	Longitudinal	VL	N/A	Colorectal	Early stage	13 (46)
Williams	1999	0	2 out of 12	Cross-sectional	RA	Open surgery	Colorectal	NR	6 (66)
Zampieri	2010	0	3 out of 12	Cross-sectional	RA (cancer group) / QF (control group)	Open surgery and Laparoscopy	Colorectal	NR	14 (36)
Zampieri	2009	0	1 out of 12	Cross-sectional	RA (cancer group) / QF or RA (control group)	Laparoscopy	Colorectal	Stage 2-3	10 (30)
Zampieri	2010	1	3 out of 12	Cross-sectional	RA (cancer group) / QF or RA (control group)	Laparoscopy	Colorectal	Stage 2-3	11 (36)
Zeiderman	1991	0	5 out of 12	Longitudinal	RA	Open surgery	Oesophageal, gastric, colorectal and pancreatic	NR	30 (70), Hospital diet = 10 (70) / 3 days intervention = 10 (70) / 7 days

									intervention= 10 (70)
<p>Values reported as mean ± standard deviation (SD) unless indicated otherwise, *median (range) and ** median (interquartile range). NIH: National, Heart, Lung and Blood Institute; RA: Rectus Abdominis; TA: Tibialis anterior; QF: Quadriceps Femoris; VA: Vastus Lateralis; PM: Pectoralis Major; SA: Serratus Anterior; LD: Latissimus Dorsi; Gastroc: Gastrocnemius; SCM:Sternocleidomastoid;DIAPH:Diaphragm; GI: Gastrointestinal; NSCLC: Non-small cell lung carcinoma; N/A: Not applicable; NR: Not reported.</p>									

Complete extraction table of the reviewed articles in relevance of muscle biopsy collection in cancer patients / Section II								
Author	Year	Age (years), mean±SD	Patient weight loss or cancer cachexia criteria	Body composition analysis	Body composition used for muscle mass assessment	Control group type	Control group sample size, n (male %)	Control group age (years), mean±SD
Acharyya	2005	NR	N/A	No	No	Healthy	14 (NR)	NR
Agustsson	2011	Pancreas:70±2 / Other: 68±3	NR	No	No	Benign disease (age and sex matched)	Benign=8 (37) / Chronic pancreatitis= 8 (63)	53±4 / Chronic pancreatitis:52±3
Aversa	2016	68±10.7	5% WL over 6 months	Anthropometric and BIA	Yes	Benign disease	11 (63)	63±13.2
Aversa	2012	Lung:66+9 /Gastric:65+10	NR	No	No	Benign disease, weight stable	10 (50)	Abdominal: 63+10 / Thoracic:65+12
Banduseela	2007	63	NR	No	No	Muscle disease (acute quadriplegic myopathy, hereditary motor and sensory neuropathy of demyelinating, amyotrophic lateral sclerosis) and healthy	6 (50)	Healthy ♂: 42 and 56 / Myopathy ♂: 75 / Myopathy ♀: 30, 74 and 61

Bohlen	2018	56.5 ± 17.2	N/A	No	No	Prophylactic mastectomy or breast reconstruction surgery	6 (0)	44.2 ± 7.4
Bonetto	2013	64±11	>5% WL	Anthropometric	No	Benign disease	6 (NR)	62±17.4
Bossola	2006	60.8±11.2	WL Mild: 0–5%. WL Moderate: 6–10%. WL Severe: >10%	Anthropometric	No	Benign disease	5 (60)	65.6±7.5
Bossola	2001	61±79.6	WL Mild: 0–5%. Moderate: 6–10%. Severe: >10%	No	No	Benign disease, weight stable	10 (60)	62±45.8
Bossola	2003	59.5±16.1	>10% WL	No	No	Benign disease, weight stable	14 (64)	61.2±12.3
Brzeczczynska	2016	NC: 67±10.5 / CC: 65±8.1	>5% WL of pre-illness	DXA	Yes	Healthy elderly and healthy middle age	Elderly = 21 (52), Middle age = 20 (60)	Middle-age: 61±7 / Elderly: 79±3.6
Busquets	2007	66±10	>5% WL over 1 month	No	No	Benign disease, weight stable	11 (NR)	66±10.2
Christensen	2016	33.4±7.5	N/A	No	No	Malignant and healthy	Control =9 (100), Ref=13 (100)	Control:37.8±7.6 / Reference group:32.1±6.3
Christensen	2014	Intervention: 34.4±7.6 / Control: 35.8±8.9	N/A	DXA	Yes	Healthy (age matched)	19 (100)	31.5±6.0
DeJong	2005	66±8	N/A	No	No	Benign disease, weight stable	11 (81)	67±13.2
D'Orlando	2014	68.1±11.6	>5% WL over 6 months	No	No	Benign disease	12 (58)	64.2±11.6

Ebhardt	2017	Non- CC: 66.3±10.2 / CC:64±4.1	>5% WL of pre- illness	DXA	Yes	Healthy elderly: sarcopenic and non-sarcopenic	Non-sarcopenic = 10 (60), Sarcopenic = 8 (50)	Non-sarcopenic: 77.4±2.3 / Sarcopenic: 80.3±3.9
Eley	2008	66 (49 – 83) *	NR	No	No	Hernia, weight stable	9 (10)	56 (41 – 86) *
Gallagher	2012	65	NR	No	No	Benign disease, weight stable	6 (66)	58
Higuchi	2000	54	N/A	No	No	N/A	N/A	N/A
Jagoe	2002	64.1±9	Any % WL over 6 months	No	No	Benign disease (Thoracotomy)	10 (40)	51.3±15.1
Johns	2017	65±13	WL >5%, >10%, >15% and SMI with any degree of WL (>2%)	CT	Yes	N/A	N/A	N/A
Johns	2014	65 ± 12.8	>5% WL over past 6 months (in absence of simple starvation) and low muscularity with 2% WL	CT	Yes	Malignant, Weight stable	N/A	N/A
Khal	2005	WS:79.8±2.2 / WL:70.6±8.2,	WL Moderate: 1- 11%. WL Severe: >11%	No	No	Hernia, liver cyst and gall stones, weight stable	10 (80)	69.6±7.3
Lamboley	2017	68± 5.6	N/A	No	No	Healthy (age and physical activity matched)	14 (100)	71±3.7

Lundholm	1976	Male:62± 13.1 /Female: 63± 9.7	N/A	No	No	Uncomplicated gall bladder disease or peptic ulcer	55 (51)	56± 14.8
MacDonald	2015	WS: 62.5 (57.0- 70.3)** / WL: 63.4 (61.5-66.3)**	>5% WL	CT	Yes	Healthy	7 (42)	52.1 (51.5-53.1)**
Marzetti	2017	WS:70.6±8.63 /WL:66.8±12.5	>5% WL over 6 months	No	No	Benign disease, weight stable (age- matched)	9 (88)	57.4±15.9
Narasimhan	2017	64.9 ±10	>5% pre-illness WL within 6 months or BMI of <20 with WL >2% and sarcopenia	CT	Yes	Malignant, Weight stable	20 (45)	63.6±7.9
Narasimhan	2018	WS:64±8 /WL: 66±11	WL >5%, >10%, >15% and sarcopenic (Skeletal Muscle Index) with any degree of WL (>2%)	CT	Yes	N/A	N/A	N/A
Nilsen	2016	67±7	N/A	No	No	Prostate cancer without physical training	11 (100)	64 ±6
Noguchi	1998	56 (50 to 63)*	N/A	No	No	N/A	N/A	N/A

Op den Kamp	2015	Pre-CC:62.4±10.4 / CC:59.8±8.2	>5% WL over 6 months	DXA	Yes	Healthy	22 (59)	61.4±7.0
Op den Kamp	2012	65.9±7.5	10% WL over 6 months	DXA	Yes	Healthy	10 (70)	63.7±5.6
Op den Kamp	2013	Pre-CC:62.4±10.4 / CC:59.8±8.2	5% WL over 6 months, 2% WL with BMI 20 or sarcopenic (Skeletal Muscle Index)	DXA	Yes	Healthy	22 (59)	61.4±7.02
Pessina	2010	63.8±2.8	N/A	No	No	Benign disease, weight stable (age-matched)	8 (62)	64.2±2.6
Phillips	2013	62.5±23.4	N/A	DXA	Yes	Healthy	8 (50)	70.7±4.5
Prokopchuk	2016	NC:67 (36-87) / CC:70 (52-83)*	>10% WL 6 months previous to surgery	CT	Yes	Diverticular disease, seous cystadenoma of pancreas, nodular hyperplasia of liver, gallstones, liver rupture and chronic pancreatitis.	Benign=15 (80) / Chronic pancreatitis=9 (45)	Benign:67 (32-73) / Chronic pancreatitis: 49.5 (40-75)*
Puig-Vilanova	2014	65±9	Fat Free Mass Index: <18.5kg/m2	Anthropometric	Yes	Healthy and COPD cachexia	Healthy = 10 (100) / COPD = 16 (100)	65±11 and 64±9

Ramage	2018	64.5 (43-83)	>5% WL of pre-illness	CT	Yes	N/A	N/A	N/A
Rhoads	2009	64.2±3.8	NR	Anthropometric	No	Benign disease	10 (60)	63.9±2.8
Schmitt	2007	NC: 62±8.5 / CC:53±11.3	>10% WL in the last 6 months	No	No	N/A	N/A	N/A
Shaw	1991	WS:61±20 / WL: 64±12.7	>15% WL of pre-illness	No	No	Benign disease, weight stable	18 (33)	57±16.9
Skorokhod	2012	WS: 66 (51-69) / WL: 65 (57-74)	>10% WL of pre-illness	No	No	N/A	N/A	N/A
Smith	2010	66±11.6	>5% WL	No	No	Cholelithiasis, weight stable	15 (80)	57±19.3
Stephens	2011	67±10	>10% WL in 6 months	No	No	Benign disease, weight stable	6 (33)	53±8
Stephens	2010	67±8.4	>5% WL	Anthropometric	No	Benign disease	3 (66)	45±3.4
Stephens	2015	All: 65±10 / NC:68±9/ CC:63±9	>5% WL	No	No	Hernia and cholecystectomy	15 (53)	56±17

Stretch	2013	♂:59±13 / ♀:63±13	N/A	CT	Yes	N/A	N/A	N/A
Sun	2012	62.13±6.54	>10% WL	No	No	Benign disease, (age and sex matched)	29 (72)	61.8±6.4
Taskin	2014	NC: 68±5 / CC: 70±15	>10% WL in 6 months, weight stable <5%	No	No	Benign disease	5 (40)	77±5
Weber	2007	52.5±6.5	>10% WL in 6 months	BIA	Yes	Healthy	27 (52)	57.9±12.4
Weber	2009	58±9	>10% WL in 6 months	BIA	Yes	Healthy, weight stable (age, sex and height matched)	19 (53)	56±7
Williams	2012	66±10.8	N/A	DXA	Yes	Healthy (age and sex matched)	8 (50)	71±5.6
Williams	1999	67 (53-76) *	N/A	No	No	Benign disease	6 (83)	54(22-92) *
Zampieri	2010	65.1 ±10.3	N/A	No	No	Muscle disease (Polymyositis and dermatomyositis) and healthy	Muscle disease= 13 (38) / Healthy = 19	Healthy: 30.1±13.3 / Myopathy: 64.3±6.3

Zampieri	2009	65.1 ± 10.3	N/A	No	No	Healthy	10 (NR)	22.7±2.6
Zampieri	2010	65.1 ± 10.3	N/A	No	No	Benign disease, weight stable	7 (0)	44.5±18.3
Zeiderman	1991	Hospital diet: 67±9.5 /3 days intervention:72±3. 2 / 7 days intervention: 67±6.3	> 5 kg WL over 3 months	Anthropometric	Yes	N/A	N/A	N/A

WL: Weight loss. NC: non-cachexia. CC: Cancer cachexia. BMI: BMI. SMI: Skeletal Muscle Index. . BIA: Bio-electrical impedance analysis. DXA: dual-energy x-ray absorptiometry. CT: Computed Tomography. N/A: Not applicable; NR: Not reported

Complete extraction table of the reviewed articles in relevance of muscle biopsy collection in cancer patients / Section III								
Author	Year	Anti-neoplastic treatment exposure previous to biopsy	Cancer Patients, weight loss % (mean±SD)	Controls, weight loss % (mean±SD)	Comorbidity history	Medication history	Medication used as an exclusion criteria	Comorbidities used as an exclusion criteria
Acharyya	2005	NR	NR	NR	NR	NR	NR	NR
Agustsson	2011	NR	Pancreas:6±3 / Other:3±3	2±2 / Chronic pancreatitis:6±3	NR	NR	NR	Diabetes
Aversa	2016	NR	13.2±7.7,0.6±1.1	0	NR	NR	NR	Liver failure, diabetes, metabolic acidosis, acute and chronic renal failure, sepsis, AIDS, inflammatory bowel diseases, acute and chronic hepatitis, autoimmune disorders and chronic obstructive pulmonary disease.

Aversa	2012	NR	Lung:3.7±4.6, Gastric: 5.6±5.9	0	NR	NR	NR	Acute and chronic renal failure, liver failure, diabetes, metabolic acidosis, sepsis, AIDS, inflammatory bowel disease, autoimmune disorders, acute and chronic hepatitis, and chronic obstructive pulmonary disease.
Banduseela	2007	NR	N/A	N/A	Type 2 diabetes	Corticosteroids	NR	NR
Bohlen	2018	Naïve, except six patients undergoing chemotherapy	N/A	N/A	NR	NR	NR	NR
Bonetto	2013	NR	5.3±4.8	0.5±0.09	NR	NR	NR	Liver failure, diabetes, acute or chronic renal failure, metabolic acidosis, AIDS, inflammatory bowel disease, autoimmune disorders, sepsis, chronic obstructive pulmonary disease, chronic heart failure, hepatitis, hyperthyroidism.
Bossola	2006	NR	6±2	0.5±0.1	NR	NR	NR	Acute or chronic renal failure, liver failure, diabetes, metabolic acidosis, sepsis, AIDS, inflammatory bowel disease, autoimmune disorders, chronic heart failure, acute and chronic hepatitis, hyperthyroidism, and chronic obstructive pulmonary disease.
Bossola	2001	NR	5.6±21.9	0.8±1.2	NR	NR	NR	Acute or chronic renal failure, liver failure, diabetes, metabolic acidosis, sepsis, AIDS, inflammatory bowel disease, autoimmune disorders, chronic heart failure, and hyperthyroidism.
Bossola	2003	NR	5.2±4.7	0.7±0.3	NR	NR	NR	Acute or chronic renal failure, liver failure, diabetes, metabolic acidosis, sepsis, AIDS, inflammatory bowel disease, autoimmune disorders, chronic heart failure, acute and chronic hepatitis, hyperthyroidism, and chronic obstructive pulmonary disease.
Brzeszczynska	2016	NR	NC:6.5±9.3, CC:9.3±7.8	NR	NR	NR	NR	NR
Busquets	2007	Naïve	5.1±4.4	1.4±2.6	NR	NR	Corticosteroid or β-blocking	Endocrine disease

							medication. Prior exposure to chemotherapy or radiotherapy.	
Christensen	2016	Chemotherapy	N/A	N/A	NR	NR	NR	Cardiomyopathy, coronary heart disease, diabetes mellitus and chronic obstructive pulmonary disease.
Christensen	2014	Chemotherapy	N/A	N/A	NR	NR	NR	Cardiomyopathy, coronary heart disease, diabetes mellitus and chronic obstructive pulmonary disease.
DeJong	2005	NR	18.4±14.8	2.2±6.3	NR	No corticosteroids or beta blockers	Corticosteroids, beta blockers	Endocrine disease
D'Orlando	2014	NR	4.2±4.1	1.4±0.6	NR	No	Chronic corticosteroid treatment	Renal failure, diabetes mellitus, sepsis, HIV infection, inflammatory bowel disease, congestive heart failure, acute or chronic hepatitis, thyroid disorders, chronic obstructive pulmonary disease
Ebhardt	2017	Naïve	Non-sarcopenic: 2.3±3.2, Sarcopenic: 15.9±6.8	NR	NR	NR	NR	NR
Eley	2008	Naïve	7.8 (0-27.5) *	0	NR	No	NR	NR
Gallagher	2012	Naïve, except five patients with previous chemotherapy exposure, but no treatment within 4 weeks before surgery.	Baseline: 7.3±2.7, follow up: 13.8±2.7	0	NR	No under anabolic or catabolic agents	Anabolic/catabolic agents	Uncontrolled diabetes or thyroid disorders.
Higuchi	2000	Naïve	N/A	N/A	NR	NR	NR	NR
Jagoe	2002	NR	2.9±6.6	2.7±9.8 (gain)	NR	NR	NR	NR
Johns	2017	NR	6±9	6±9		NR	Corticosteroids.	Cognitive impairment and infection
Johns	2014	NR	> 5% WL: 12±4, > 10% 15±7, low muscularity: 6±5, Low muscularity +2% WL: 11±4	> 5% WL: 0±1, > 10% WL: 2±1, low muscularity: 5±3, Low	NR	NR	NR	NR

				muscularity +2% WL:2±1				
Khal	2005	NR	14±9, 0	0	NR	NR	NR	NR
Lamboley	2017	Naïve	N/A	N/A	NR	NR	NR	Cardiovascular disease and type 1 diabetes.
Lundholm	1976	NR	N/A	N/A	NR	NR	NR	NR
MacDonald	2015	No chemotherapy exposure within 4 weeks before surgery	10 (7.6-12.1) **	0	NR	NR	NR	NR
Marzetti	2017	NR	WS: 1.8±0.8, WL:7±0.8,	0.1±0.1	NR	NR	Corticosteroids.	Acute or chronic renal failure, liver failure, heart failure, chronic obstructive pulmonary disease, diabetes mellitus, thyroid disorders, metabolic acidosis, sepsis, HIV infection, inflammatory bowel disease, acute or chronic hepatitis, autoimmune disorders
Narasimhan	2017	Naïve, except one patient under chemotherapy	11.4±6.6	NR	NR	NR	NR	NR
Narasimhan	2018	Naïve	11.4±6.5	N/A	NR	NR	NR	NR
Nilsen	2016	Radiotherapy and Androgen deprivation therapy	N/A	N/A	NR	NR	Osteoporosis medication	NR
Noguchi	1998	NR	N/A	N/A	NR	NR	NR	NR
Op den Kamp	2015	NR	Pre-CC: 1.7±1.4, CC:12±5.5	0	NR	NR	Corticosteroids or hormonal therapy	Chronic obstructive pulmonary disease, cardiac failure, severe endocrine, hepatic or renal disorders, other malignancies in the last 3 years, and chronic inflammatory diseases, or acute infection.

Op den Kamp	2012	NR	3.1±4.4	0.6 ±2 (gain)	NR	NR	NR	NR
Op den Kamp	2013	NR	Pre-CC: 1.7±1.4, CC:12±5.5	0	NR	NR	Hormones or continual oral corticosteroids, antitumor therapy	Chronic obstructive pulmonary disease, Congestive Heart Failure and active infectious disease, other malignant disease.
Pessina	2010	NR	10±3.1	0	NR	NR	NR	Acute or chronic renal failure, liver failure, diabetes, metabolic acidosis, sepsis, AIDS, inflammatory bowel disease, auto-immune disorders, chronic heart failure, acute and chronic hepatitis, hyperthyroidism, and chronic obstructive pulmonary disease.
Phillips	2013	Naïve	N/A	N/A	NR	NR	NR	Metastasis, metabolic, respiratory or cardiovascular disorders.
Prokopchuk	2016	NR	NC:4.9 (0-9.1), CC:14.3 (8.6-26.7)	0 (0-6) / Chronic pancreatitis:3.7 (0-29.5)	NR	NR	NR	NR
Puig-Vilanova	2014	NR	1-8 kg	N/A	NR	NR	NR	NR
Ramage	2018	NR	3.7 (-25 to +10.9)*	N/A	NR	No under anabolic or catabolic agents	NR	NR
Rhoads	2009	NR	11±4	0	NR	NR	NR	Acute or chronic renal failure, liver failure, diabetes, metabolic acidosis, sepsis, AIDS, inflammatory bowel disease, autoimmune disorders, chronic heart failure, acute and chronic hepatitis, hyperthyroidism, and chronic obstructive pulmonary disease.
Schmitt	2007	NR	NC:5.2±3.9, CC:12.4±2.8	N/A	NR	Diabetes treatment (unclear) for 3 patients	NR	NR
Shaw	1991	NR	WS:1.6±3, WL:18±4.2	2±2.1	NR	NR	Intotropic and antiarrhythmic agents	Hemodynamic treatments
Skorokhod	2012	NR	WS:2 (0-5.5) *, WL:13.9 (10-19.2)	N/A	NR	NR	NR	NR
Smith	2010	NR	1.2±1.9	0.5±0.73	NR	Corticosteroids excluded	NR	Renal failure, diabetes, sepsis, acquired immunodeficiency syndrome (AIDS), inflammatory bowel disease, chronic heart failure, acute and chronic

								hepatitis, hyperthyroidism, chronic pulmonary disease, and corticosteroid treatment.
Stephens	2011	Naive, except 3 patients that finished chemotherapy cycles before the surgery	6±7.1	0.3±1.4 (gain)	NR	NR	Anabolic/catabolic agents	Metastatic disease, undergoing palliative surgery, uncontrolled diabetes or known thyroid disorders.
Stephens	2010	NR	8.9±6.7	0	NR	NR	NR	NR
Stephens	2015	No chemotherapy exposure within 4 weeks before surgery	NC:0.8±3.0, CC:13.9±8.6	0	No subjects had uncontrolled diabetes or thyroid disorders.	No subjects were knowingly taking anabolic/catabolic agents	NR	NR
Stretch	2013	NR	N/A	N/A	NR	NR	NR	NR
Sun	2012	NR	N/A	N/A	NR	NR	NR	Acute or chronic renal failure, liver failure, diabetes, metabolic acidosis, sepsis, AIDS, inflammatory bowel disease, autoimmune disorders, chronic heart failure, and hyperthyroidism.
Taskin	2014	NR	12.15 (10.6-14)*	NR	NR	NR	NR	NR
Weber	2007	Chemotherapy and Radiotherapy	22.3±115.4	NR	NR	NR	NR	NR
Weber	2009	NR	>10	NR	NR	NR	NR	Severe heart failure, severe pulmonary disease, pregnancy, or myocardial infarction within the preceding two weeks. cardiovascular, metabolic, respiratory, renal, hepatic, neurological, psychiatric or inflammatory disease, cancer (type of cancer other than the aforementioned type admitted to the group of cachectic patients).
Williams	2012	Naïve	N/A	N/A	NR	NR	NR	Metabolic, respiratory, or cardiovascular disorders or other contraindications to a healthy status.

Williams	1999	NR	N/A	N/A	NR	NR	NR	NR
Zampieri	2010	Naïve	N/A	N/A	NR	NR	NR	Patients under chemotherapy treatment or taking drugs known to induce myopathy as main side effect.
Zampieri	2009	Naïve	N/A	N/A	NR	NR	NR	Patients under chemotherapy treatment or taking drugs known to induce myopathy as main side effect.
Zampieri	2010	Naïve	N/A	N/A	NR	NR	NR	Patients reporting fatigue, weakness or asymptomatic for muscle pain.
Zeiderman	1991	NR	Hospital diet = 16.4±8.8 Intervention 1 = 19.7±13.5, Intervention 2 = 19.2±10.1	N/A	NR	NR	NR	NR

N/A: Not applicable; NR: Not reported

Appendix C (Chapter 3): Skeletal muscle gene expression for genes associated with cancer cachexia in cancer patients

Biological function	Gene symbol	Gene name	Agilent transcript ID [Refseq RNA ID]	Female (n=64)	Male (n=69)	p-value
Atrophy	FBXO32	F-box protein 32	A_23_P82814 [NM_058229]	1.08 ± 0.59	1.06 ± 0.6	0.9
			A_24_P218259 [NM_058229]	1.18 ± 0.54	1.10 ± 0.57	0.4
			A_24_P918147 [NM_058229]	0.99 ± 0.48	1.07 ± 0.53	0.3
	FOXO1	forkhead box O1	A_23_P151426 [NM_002015]	1.43 ± 1.11	1.17 ± 0.66	0.6
			A_24_P22079	1.53 ± 1.04	1.11 ± 0.68	0.005
	FOXO3	forkhead box O3	A_23_P345575 [NM_001455]	1.10 ± 0.53	1.03 ± 0.51	0.4
			A_32_P102062 [NM_001455]	1.16 ± 0.59	1.05 ± 0.54	0.3
	TRIM63	tripartite motif containing 63	A_23_P114983 [NM_032588]	1.03 ± 0.36	1.10 ± 0.41	0.4
UCP1	uncoupling protein 1	A_23_P30091 [NM_021833]	1.21 ± 0.85	1.28 ± 1.35	1	
Autophagy	BECN1	beclin 1	A_23_P433071 [NM_003766]	0.91 ± 0.27	1.03 ± 0.3	0.05
			A_23_P89410 [NM_003766]	1.00 ± 0.27	1.11 ± 0.33	0.05
			A_24_P313597 [NM_003766]	0.98 ± 0.18	1.07 ± 0.27	0.1
	CTSB	cathepsin B	A_23_P215944 [NM_147780]	1.04 ± 0.5	1.19 ± 0.5	0.1
			A_24_P303770 [NM_147780]	1.08 ± 0.4	1.1 ± 0.38	0.7
			A_24_P397928 [NM_147780]	1.08 ± 0.46	1.09 ± 0.55	0.9
	CTSC	cathepsin C	A_23_P1552 [NM_001814]	1.10 ± 0.51	1.00 ± 0.43	0.4
			A_24_P115762 [NM_148170]	1.12 ± 0.48	1.06 ± 0.54	0.3
	CTSH	cathepsin H	A_23_P14774 [NM_004390]	1.05 ± 0.33	1.02 ± 0.34	0.5
	CTSL1	cathepsin L1	A_23_P94533 [NM_001912]	1.05 ± 0.29	1.04 ± 0.36	0.8
	CTSL2	cathepsin L2	A_23_P146456 [NM_001333]	1.31 ± 0.57	0.99 ± 0.44	<0.0001
	CTSS	cathepsin S	A_23_P46141 [NM_004079]	1.58 ± 2.69	1.27 ± 1.48	0.2
			A_24_P242646 [NM_004079]	1.10 ± 0.44	1.14 ± 0.48	0.6
	HIF1A	hypoxia inducible factor 1, alpha subunit	A_24_P56388 [NM_181054]	1.06 ± 0.53	1.08 ± 0.55	0.9
	Apoptosis	APAF1	apoptotic peptidase activating factor 1	A_23_P36611 [NM_181861]	1.04 ± 0.37	1.08 ± 0.42

	BAX	BCL2-associated X protein	A_23_P208706 [NM_138764]	1.04 ± 0.31	1.06 ± 0.36	0.7
			A_23_P346311 [NM_138764]	1.11 ± 0.43	1.01 ± 0.3	0.2
			A_23_P346309 [NM_138763]	2.81 ± 4.72	2.65 ± 4.53	0.7
	BCL2	B-cell CLL/lymphoma 2	A_23_P352266 [NM_000633]	1.09 ± 0.48	1.22 ± 0.61	0.3
	CASP3	caspase 3	A_23_P92410 [NM_004346]	1.07 ± 0.29	1.11 ± 0.51	0.9
	CASP8	caspase 8	A_23_P209389 [NM_033355]	0.97 ± 0.32	1.09 ± 0.38	0.08
			A_24_P157087 [NM_033355]	1.07 ± 0.41	1.1 ± 0.65	0.8
			A_24_P148499 [NM_033358]	1.68 ± 2.08	1.25 ± 0.79	0.1
	CASP9	caspase 9	A_23_P97309 [NM_001229]	0.95 ± 0.19	1.06 ± 0.25	0.008
			A_24_P111342 [NM_001229]	0.97 ± 0.22	1.08 ± 0.31	0.03
	FASLG	Fas ligand	A_23_P369815 [NM_000639]	1.31 ± 0.83	1.25 ± 0.94	0.4
			A_24_P54220 [NM_000639]	1.45 ± 1.45	1.25 ± 1.13	0.4
Muscle growth	AKT1	v-akt murine thymoma viral oncogene homolog 1	A_23_P2960 [NM_005163]	1.23 ± 0.52	1.04 ± 0.35	0.03
	DMD	dystrophin	A_23_P321860 [NM_004019]	1.04 ± 0.44	1.25 ± 1.11	0.1
			A_24_P342388 [NM_004019]	1.34 ± 0.67	0.94 ± 0.29	<0.000 1
			A_24_P185854 [NM_004010]	1.11 ± 0.27	0.94 ± 0.23	<0.000 1
			A_24_P34186 [NM_004010]	1.19 ± 0.55	0.97 ± 0.39	0.01
			A_32_P199796 [NM_004023]	1.27 ± 0.66	0.98 ± 0.42	0.005
	IGF1	insulin-like growth factor 1	A_23_P13907 [NM_000618]	1.15 ± 0.95	1.34 ± 1.35	0.1
			A_24_P304419 [NM_000618]	1.14 ± 0.9	1.32 ± 1.36	0.2
			A_24_P304423 [NM_000618]	1.19 ± 1.08	1.42 ± 1.76	0.2
			A_24_P398572 [NM_000618]	1.86 ± 2.57	2.23 ± 2.66	0.2
	IGF1R	insulin-like growth factor 1 receptor	A_23_P205986 [NM_000875]	1.06 ± 0.41	1.04 ± 0.37	0.9
			A_23_P417282 [NM_000875]	1.07 ± 0.3	1.00 ± 0.27	0.2
	MAPK14	mitogen-activated protein kinase 14	A_23_P426292 [NM_001315]	1.03 ± 0.19	1.03 ± 0.19	1
			A_24_P283288 [NM_139013]	1.03 ± 0.31	1.08 ± 0.37	0.5
			A_24_P397566 [NM_139013]	1.1 ± 0.37	1.01 ± 0.28	0.2

	MSTN	myostatin	A_23_P165727 [NM_005259]	1.71 ± 2.43	2.74 ± 3.74	0.02
	MTOR	mechanistic target of rapamycin	A_23_P34606 [NM_004958]	1.04 ± 0.25	1.04 ± 0.26	0.9
	MYOD1	myogenic differentiation 1	A_24_P30257 [NM_002478]	1.12 ± 0.70	1.24 ± 0.79	0.4
	MYOG	myogenin	A_23_P160438 [NM_002479]	1.73 ± 2.56	1.38 ± 1.33	0.7
			A_24_P311036 [NM_002479]	1.74 ± 2.53	1.43 ± 1.57	0.7
	PAX7	paired box 7	A_23_P126225 [NM_013945]	0.99 ± 0.49	1.08 ± 0.39	0.05
			A_23_P500985 [NM_013945]	0.96 ± 0.45	1.03 ± 0.33	0.09
	PDGFRA	platelet-derived growth factor receptor, alpha polypeptide	A_23_P300033 [NM_006206]	1.01 ± 0.32	0.98 ± 0.31	0.6
	PPARGC1 A	peroxisome proliferator-activated receptor gamma, coactivator 1 alpha	A_23_P18447 [NM_013261]	1.11 ± 0.58	1.05 ± 0.46	0.6
			A_24_P303052 [NM_013261]	1.22 ± 0.77	1.00 ± 0.51	0.07
	SMAD2	SMAD family member 2	A_23_P15937 [NM_001003652]	1.01 ± 0.19	1.05 ± 0.15	0.1
			A_24_P202527 [NM_001003652]	1.01 ± 0.23	1.00 ± 0.18	0.9
			A_32_P109002 [NM_001003652]	0.98 ± 0.44	1.05 ± 0.42	0.2
			A_32_P12580 [NM_001003652]	1.06 ± 0.29	1.06 ± 0.27	1
	SMAD3	SMAD family member 3	A_23_P48936 [NM_005902]	1.14 ± 0.42	1.00 ± 0.28	0.07
	TGFB1	transforming growth factor, beta 1	A_24_P79054 [NM_000660]	1.42 ± 1.47	1.06 ± 0.54	0.01
Inflammation	IFNG	interferon, gamma	A_23_P151294 [NM_000619]	1.04 ± 0.32	1.09 ± 0.34	0.3
	IL1A	interleukin 1, alpha	A_23_P72096 [NM_000575]	1.02 ± 0.3	1.07 ± 0.34	0.4
	IL1B	interleukin 1, beta	A_23_P79518 [NM_000576]	5.74 ± 16.9	5.60 ± 23.8	0.6
	IL6	interleukin 6	A_23_P71037 [NM_000600]	19.9 ± 63.8	26.6 ± 100	0.6
	IL6R	interleukin 6 receptor	A_24_P379413 [NM_000565]	1.35 ± 1.20	1.33 ± 1.13	0.9
	JAK1	Janus kinase 1	A_23_P97005 [NM_002227]	1.09 ± 0.37	1.05 ± 0.32	0.7
			A_24_P410678 [NM_002227]	0.92 ± 0.37	1.15 ± 0.43	0.001
	JAK2	Janus kinase 2	A_23_P123608 [NM_004972]	1.21 ± 0.48	1.06 ± 0.45	0.03
	JAK3	Janus kinase 3	A_23_P329112 [NM_000215]	1.03 ± 0.46	1.19 ± 0.57	0.09
			A_24_P308096 [NM_000215]	1.12 ± 0.56	1.11 ± 0.52	1
A_24_P59667 [NM_000215]			1.28 ± 0.74	1.33 ± 1.32	0.4	

NFKB1	Nuclear factor kappa B subunit 1	A_23_P30024 [NM_003998]	1.07 ± 0.22	1.03 ± 0.24	0.2
STAT3	signal transducer and activator of transcription 3	A_23_P100795 [NM_213662]	1.11 ± 1.05	0.44 ± 0.44	0.4
		A_23_P107206 [NM_213662]	1.21 ± 1.02	0.53 ± 0.35	0.02
		A_24_P116805 [NM_213662]	1.17 ± 1.00	0.50 ± 0.31	0.0
STAT5A	signal transducer and activator of transcription 5A	A_23_P207367 [NM_003152]	1.12 ± 1.01	0.32 ± 0.34	0.03
		A_24_P173088 [NM_003152]	1.19 ± 1.00	0.47 ± 0.45	0.005
STAT5B	signal transducer and activator of transcription 5B	A_23_P100788 [NM_012448]	1.05 ± 1.00	0.36 ± 0.36	0.3
TNF	tumor necrosis factor	A_23_P376488 [NM_000594]	1.27 ± 0.93	1.44 ± 1.21	0.4
		A_24_P50759 [NM_000594]	0.99 ± 0.35	1.15 ± 0.44	0.03
TNFSF12	tumor necrosis factor (ligand) superfamily, member 12	A_24_P245298 [NM_003809]	1.01 ± 0.24	1.05 ± 0.32	0.6
Values (unitless) reported as mean ± standard deviation					

Appendix D (Chapter 4): Primary antibody panel for immunohistochemistry

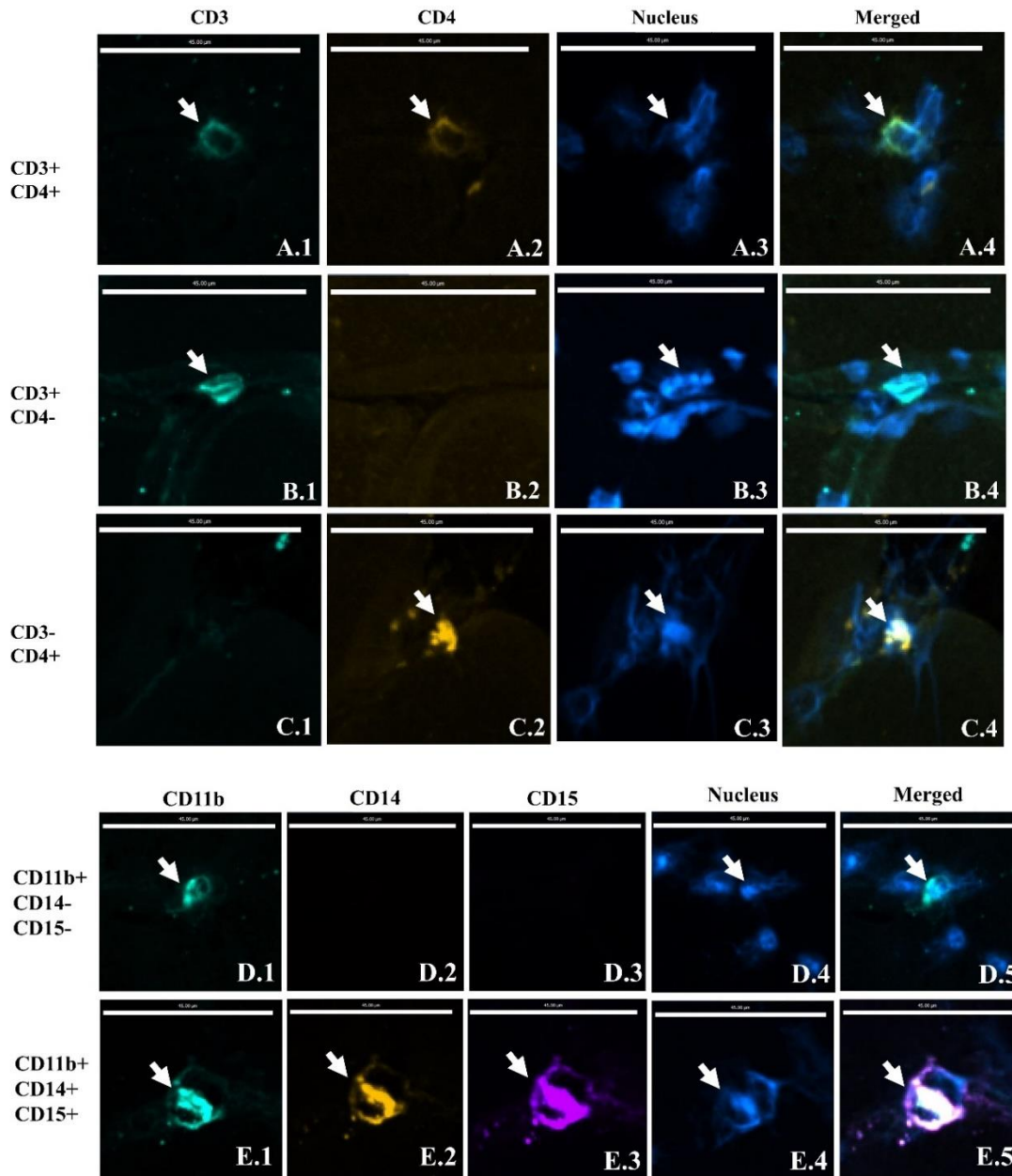
Primary Antibody	Clone	Species	Clonality	Dilution	Supplier		Function
CD3	SP7	Rabbit	Monoclonal	1:100	Abcam	ab16669	T cell receptor complex
CD4	IF6	Mouse	Monoclonal	1:100	Abcam	ab846	Accessory molecule for interaction with MHC class II
CD11b	EP1345y	Rabbit	Monoclonal	1:200	Abcam	ab52478	Classical myeloid lineage marker. Integrin, leukocyte adhesion and migration
CD14	5A3	Mouse	Monoclonal	1:200	ThermoFisher (Invitrogen)	MA5-14773	Lipopolysaccharide pattern recognition co-receptor (toll like receptor)
CD15	MY1	Mouse	Monoclonal	1:50	ThermoFisher (Invitrogen)	MA1-26235	Adhesion, chemotaxis and phagocytosis
Laminin	-	Rabbit	Polyclonal	1:200	SIGMA	L9393	Major constituents of muscle cell membranes.
Dystrophin	-	Rabbit	Polyclonal	1:25	Abcam	ab15277	

Appendix E (Chapter 4): Secondary antibody panel for immunohistochemistry with corresponding primary antibodies

Primary Antibody (Clone)	Secondary antibody	Dilution	Supplier		Isotype	Species	Clonality
CD3 (SK7)	AlexaFluor® 647	1:400	Fisher	A-21245	IgG	Rabbit	Polyclonal
CD4 (IF6)	AlexaFluor® 568	1:400	Fisher	A-21144	IgG1	Mouse	Polyclonal
CD11b (EP1345y)	AlexaFluor® 647	1:400	Fisher	A-21245	IgG	Rabbit	Polyclonal
CD14 (5A3)	AlexaFluor® 568	1:400	Fisher	A-21144	IgG1	Mouse	Polyclonal
CD15 (MY1)	AlexaFluor® 488	1:400	Fisher	A-11008	IgM	Mouse	Polyclonal
Laminin	AlexaFluor® 647	1:400	Fisher	A-21245	IgG	Rabbit	Polyclonal
Dystrophin					IgG		

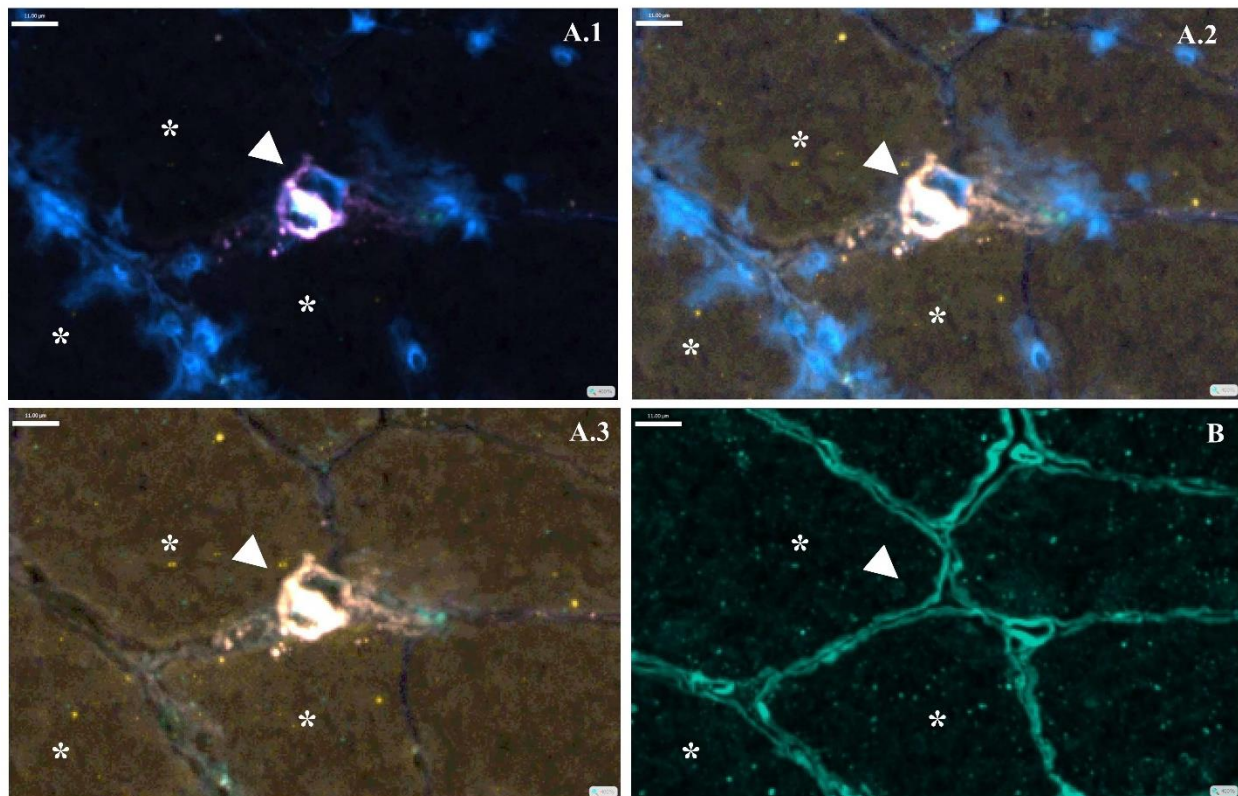
Appendix F (Chapter 4): Immune cell characterization by immunofluorescence

Immunostaining of CD3+CD4+ (A), CD3+CD4- (B), CD3-CD4+ (C), CD11b+CD14-CD15- (D) and CD11b+CD14+CD15+ (E) cells. Immune cells pointed by the white arrow. A.1, B.1, C.1, D.1 and E.1 antibody detected by Alexa Flour® 647. A.2, B.2, C.2, D.2 and E.2 antibody detected by Alexa Flour® 568. D.3 and E.3 antibody detected by Alexa Flour® 488. A.3, B.3, C.3, D.4 and E.4 nuclear stain detected by DAPI. A.4, B.4, C.4, D.5 and E.5 Merged images. Scale bar 45 μ m.



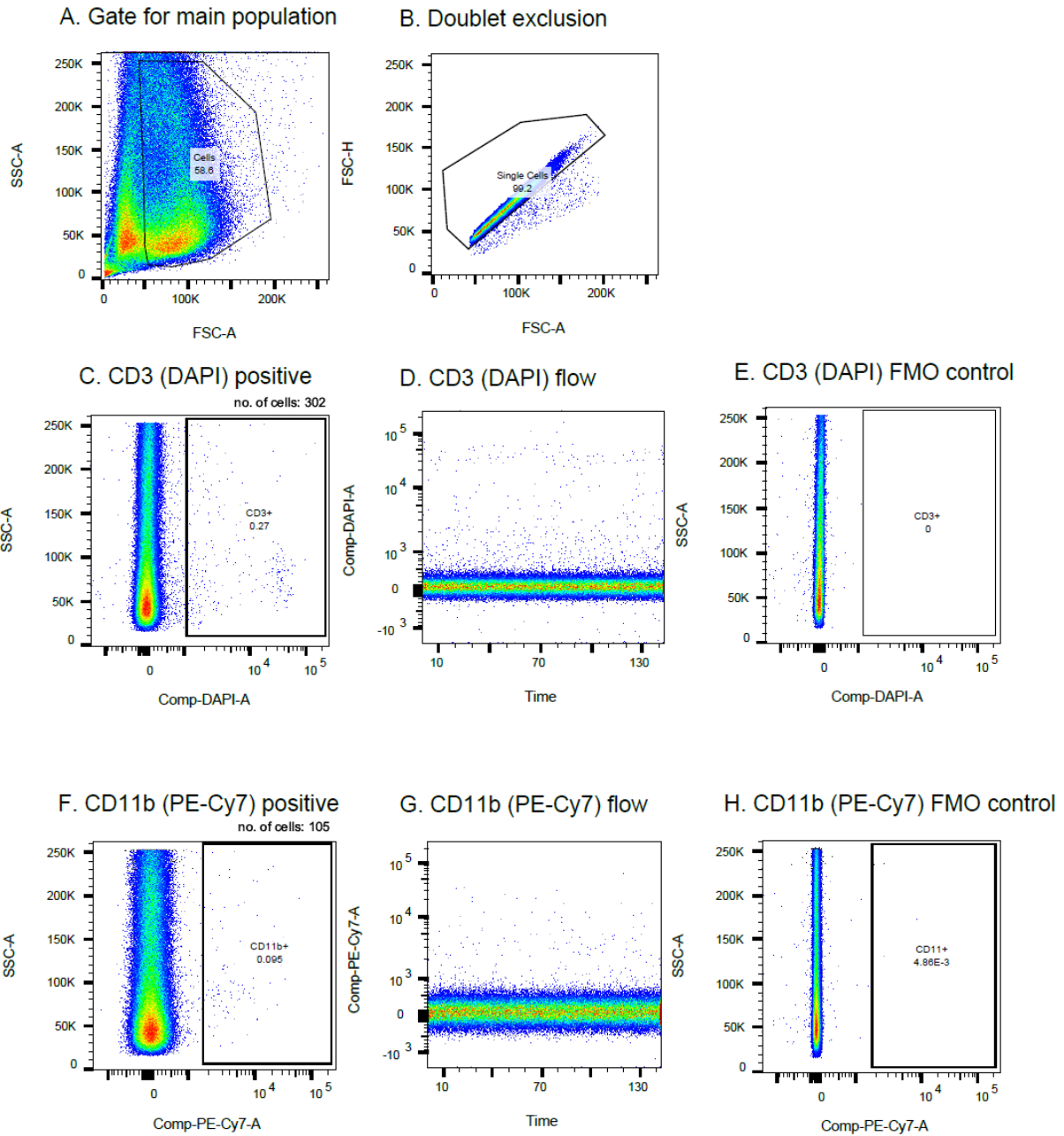
Appendix G (Chapter 4): Immunostaining of serial cross-sections of muscle tissue

CD11b+CD14+CD15+ cells (A) and laminin-dystrophin (B). Stained nuclei in blue. A.1 Original image with no brightness manipulation. A.2 and A.3 Brightness was increased to visually appreciate the location of the CD11b+CD14+CD15+ cell (arrow) on the endomysial area. B. Serial cross-section used to confirm the location of immune cells on the periphery of muscle fibers (endomysium). Asterisks mark muscle fibers used as a reference point, and immune cell location is pointed by the white arrow. Scale bar 11 μ m.



Appendix H (Chapter 4): Flow cytometry analysis for CD3+ and CD11b+ cells

Flow cytometry analyses done using FlowJo© software [FlowJo, LLC]. A. Gating strategy for the main cell population. B. Exclusion of doublets. C and F. Gating strategy for CD3 and CD11b positive populations. D and G. Stable flow stream for CD3 and CD11b. E and H. FMO controls for CD3 and CD11b. FMO: Fluorescence minus one control



Appendix I (Chapter 4): Patient characteristics, secondary cohort with microarray analysis in rectus abdominis muscle

	Males (n=69)	Females (n=64)
Age, mean years \pm SD (Min-Max)	59 \pm 13 (19-87)	63 \pm 14 (21-88)
Tumor type, % (n):		
Colorectal	39 (27)	14 (9)
Pancreas	14 (10)	23(15)
Liver or intrahepatic bile ducts	7 (5)	5 (3)
Biliary tract	4 (3)	8 (5)
Others gastrointestinal*	9 (6)	3 (2)
Others*	8 (4)	22 (14)
Non-malignant disease	20 (14)	25 (16)
Presence of metastasis, n	35	16
Chemotherapy exposure within 3 months previous to surgery, n	20	11
BMI (kg/m²), mean \pm SD	27 \pm 4	28 \pm 7
BMI classification**, n:		
Underweight	0	1
Normal	23	16
Overweight	28	14
Obesity I	9	6
Obesity II	3	8
Obesity III	0	2
Comorbidities, n:		
Diabetes type II	6 (4)	9 (6)
Hypertension	9 (6)	16 (10)
CVD	9 (6)	5 (3)
Dyslipidemia	1 (1)	0 (0)
Computed tomography body composition analysis**, mean \pm SD:		
L3 Muscle CSA (cm ²)	161.8 \pm 28.3	135.8 \pm 37.3
SMI (cm ² /m ²)	52.9 \pm 7.8	46.8 \pm 9.5
SMI z-score (SD)	0.0 \pm 0.9	0.0 \pm 1.0
L3 Muscle radiodensity (HU)	36.4 \pm 9.3	34.7 \pm 9.4
L3 VAT CSA (cm ²)	175.9 \pm 111.3	138.1 \pm 100.5
*Others gastrointestinal: appendix, stomach and small intestine. *Others: gallbladder, skin, uterus, ovary, soft tissue, kidney, head and neck. **BMI: Males n=63 / Females n=47 **Computed tomography analysis: Males n=50 / Females=42. BMI, Body Mass Index; CVD, Cardiovascular disease; L3, Lumbar 3; CSA, Cross-sectional area; SMI, Skeletal muscle index; HU, Hounsfield Unit; VAT, Visceral adipose tissue; SAT, Subcutaneous adipose tissue; TAT, Total adipose tissue; SD, Standard deviation. Population has been previously described by Stretch et.al. <i>PLOS One</i> 2013 [DOI: 10.1371/journal.pone.0065380].		

Appendix J (Chapter 4): Negative univariate associations ($r \leq -0.50$) between T cell related genes and genes involved in muscle catabolic pathways of rectus abdominis muscle of male cohort (n=69)

T cell category	Gene name	Muscle catabolic pathway	Gene name	r	p
T cell function	CD3G	Ubiquitin proteasome	FOXO4	-0.59	1.20E-07
		Ubiquitin proteasome	UBE2R2	-0.58	2.16E-07
	LCK	Ubiquitin proteasome	STUB1	-0.53	2.24E-06
		Ubiquitin proteasome	UBE2B	-0.53	3.14E-06
		Ubiquitin proteasome	FOXO4	-0.51	8.55E-06
	HAVCR2	Ubiquitin proteasome	UBE2R2	-0.55	1.23E-06
		Ubiquitin proteasome	FOXO4	-0.52	5.21E-06
	PDCD1	Ubiquitin proteasome	UBE2B	-0.56	5.93E-07
	CD28	Ubiquitin proteasome	FBXO32	-0.61	2.33E-08
		Ubiquitin proteasome	USP25	-0.59	9.54E-08
		Ubiquitin proteasome	UBE2G1	-0.57	2.47E-07
		Ubiquitin proteasome	UBR2	-0.57	3.58E-07
		Ubiquitin proteasome	UBE2R2	-0.54	1.31E-06
		Ubiquitin proteasome	STUB1	-0.52	4.40E-06
		Ubiquitin proteasome	FOXO4	-0.52	5.36E-06
		Ubiquitin proteasome	UBE2B	-0.51	9.54E-06
		Signaling	ACVR2B	-0.55	1.26E-06
		Autophagy	ATG13	-0.52	3.99E-06
		Apoptosis	SIVA1	-0.53	2.18E-06
	STAT4	Ubiquitin proteasome	STUB1	-0.66	8.60E-10
		Ubiquitin proteasome	PSMA7	-0.63	5.49E-09
		Ubiquitin proteasome	USP4	-0.62	1.84E-08
		Ubiquitin proteasome	MUL1	-0.58	1.80E-07
		Ubiquitin proteasome	UBE2R2	-0.57	2.64E-07
		Ubiquitin proteasome	UBE2B	-0.56	5.32E-07
		Ubiquitin proteasome	UBE2L3	-0.55	1.03E-06
		Ubiquitin proteasome	UBB	-0.55	1.13E-06
		Ubiquitin proteasome	UBA52	-0.55	1.16E-06
		Ubiquitin proteasome	FBXO32	-0.55	1.23E-06
		Ubiquitin proteasome	FBXO32	-0.55	1.23E-06
		Ubiquitin proteasome	TRIM63	-0.54	1.37E-06
		Ubiquitin proteasome	UBA52	-0.54	1.82E-06
		Ubiquitin proteasome	FOXO4	-0.53	2.53E-06
Ubiquitin proteasome		DNAJC11	-0.52	3.72E-06	
Ubiquitin proteasome		UBC	-0.52	4.84E-06	
Ubiquitin proteasome		UBC	-0.52	5.67E-06	
Ubiquitin proteasome		FOXO4	-0.50	1.02E-05	
Signaling		ACVR1B	-0.55	1.21E-06	
Signaling	ACVR2B	-0.53	2.72E-06		

		Apoptosis/Autophagy	BECN1	-0.61	2.28E-08	
		Apoptosis/Autophagy	BECN1	-0.58	2.21E-07	
		Apoptosis	SIVA1	-0.62	1.29E-08	
	CD2		Ubiquitin proteasome	FOXO4	-0.52	4.96E-06
			Ubiquitin proteasome	STUB1	-0.63	4.94E-09
			Ubiquitin proteasome	UBE2V1	-0.59	1.00E-07
			Ubiquitin proteasome	UBE2R2	-0.55	1.19E-06
			Apoptosis/Autophagy	BECN1	-0.55	7.62E-07
	CD6		Ubiquitin proteasome	FOXO4	-0.50	1.15E-05
			Ubiquitin proteasome	STUB1	-0.50	1.18E-05
	PTPRC (CD45)		Ubiquitin proteasome	STUB1	-0.58	1.98E-07
			Ubiquitin proteasome	UBC	-0.55	1.19E-06
			Ubiquitin proteasome	UBA52	-0.54	1.30E-06
			Ubiquitin proteasome	UBB	-0.54	1.65E-06
			Ubiquitin proteasome	DNAJC11	-0.54	1.97E-06
			Ubiquitin proteasome	UBC	-0.53	2.56E-06
			Ubiquitin proteasome	UBC	-0.53	2.95E-06
			Ubiquitin proteasome	MUL1	-0.52	4.09E-06
			Ubiquitin proteasome	FBXO32	-0.52	5.02E-06
			Ubiquitin proteasome	FBXO32	-0.51	9.04E-06
			Signaling	ACVR2B	-0.53	3.52E-06
			Signaling	ACVR2B	-0.50	1.18E-05
			Apoptosis	SIVA1	-0.52	5.09E-06
	IL2RB		Ubiquitin proteasome	UBB	-0.58	2.04E-07
			Ubiquitin proteasome	UBC	-0.57	4.00E-07
			Ubiquitin proteasome	UBC	-0.56	4.63E-07
			Ubiquitin proteasome	STUB1	-0.56	4.87E-07
			Ubiquitin proteasome	DNAJC11	-0.56	4.93E-07
			Ubiquitin proteasome	UBA52	-0.55	7.95E-07
			Ubiquitin proteasome	MUL1	-0.55	8.43E-07
			Ubiquitin proteasome	UBC	-0.54	1.35E-06
			Ubiquitin proteasome	UBC	-0.54	1.49E-06
			Ubiquitin proteasome	UBE2L3	-0.54	1.61E-06
Ubiquitin proteasome			UBB	-0.52	5.27E-06	
Ubiquitin proteasome			FBXO32	-0.51	6.77E-06	
Ubiquitin proteasome			UBE2B	-0.51	8.55E-06	
Signaling			ACVR2B	-0.52	5.83E-06	
Signaling			ACVR2B	-0.51	6.22E-06	
Apoptosis/Autophagy			BECN1	-0.51	8.78E-06	
CD8 T cell specific function			FASLG	Ubiquitin proteasome	STUB1	-0.58
	Ubiquitin proteasome	USP2		-0.53	3.62E-06	
	Ubiquitin proteasome	FOXO4		-0.52	4.58E-06	
	Apoptosis/Autophagy	BECN1		-0.54	1.79E-06	

	GZMA	Ubiquitin proteasome	FOXO4	-0.50	1.07E-05
		Ubiquitin proteasome	STUB1	-0.50	1.18E-05
		Apoptosis	CASP8	-0.51	7.66E-06
	GZMK	Ubiquitin proteasome	FOXO4	-0.59	8.30E-08
		Ubiquitin proteasome	UBE2R2	-0.58	1.54E-07
		Ubiquitin proteasome	STUB1	-0.53	2.35E-06
		Apoptosis/Autophagy	BECN1	-0.52	5.35E-06

r= Pearson's correlation coefficient. p = <0.05: statistical significance.

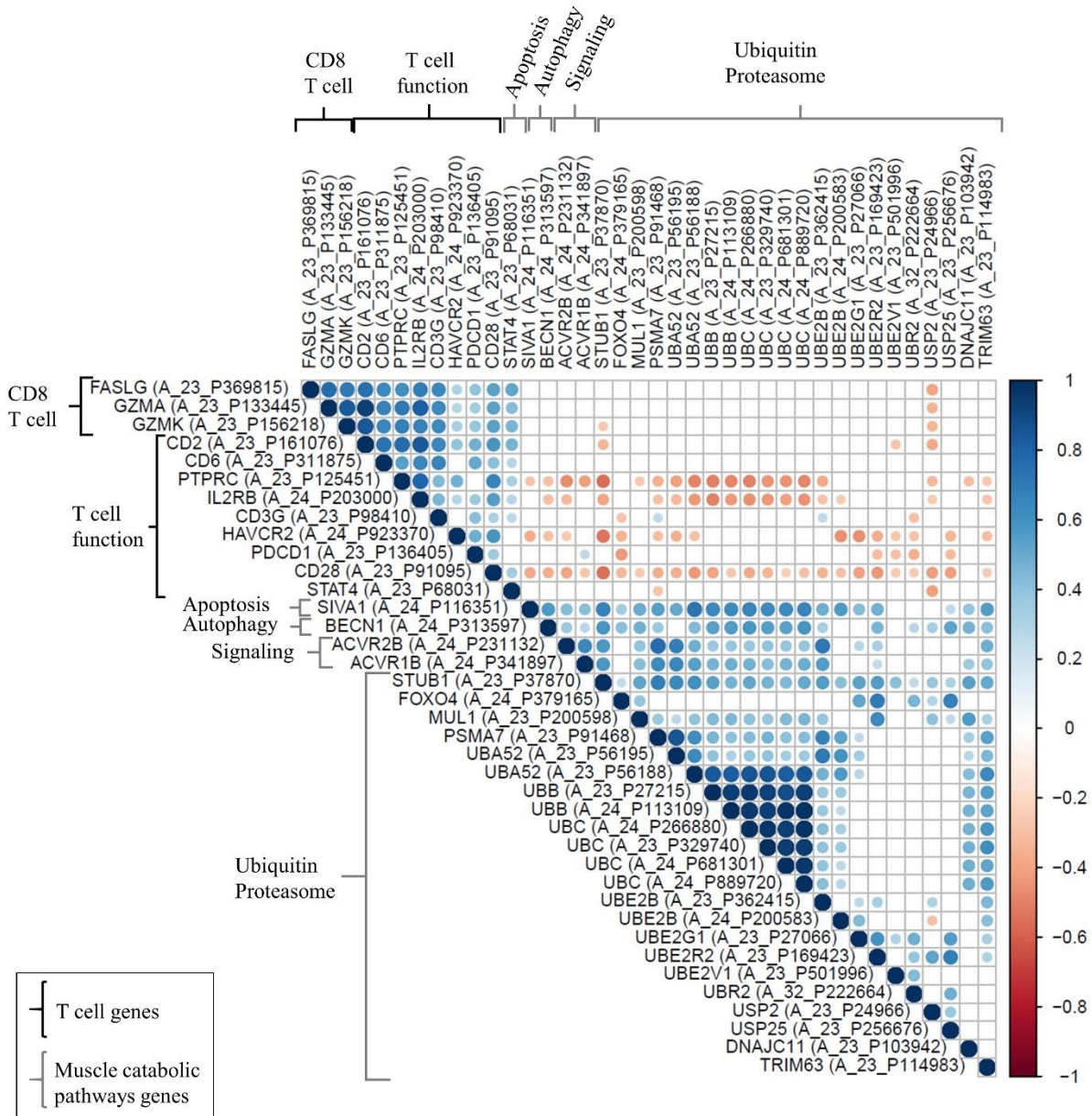
Appendix K (Chapter 4): Negative univariate associations between T cell related genes and genes involved in muscle catabolic pathways of rectus abdominis muscle of secondary female cohort (n=64)

T cell category	Gene name	Muscle catabolic pathway	Gene name	r	p
T cell function	CD3G	Ubiquitin proteasome	UBR2	-0.30	1.76E-02
		Ubiquitin proteasome	FOXO4	-0.28	2.47E-02
	HAVCR2	Apoptosis	BECN1	-0.30	1.80E-02
		Ubiquitin proteasome	UBE2L3	-0.32	1.02E-02
		Ubiquitin proteasome	TRIM63	-0.30	1.55E-02
		Ubiquitin proteasome	UBR2	-0.28	2.40E-02
	PDCD1	Ubiquitin proteasome	UBAP2	-0.61	1.04E-07
		Ubiquitin proteasome	UBR3	-0.50	2.31E-05
		Ubiquitin proteasome	FOXO4	-0.42	4.93E-04
		Ubiquitin proteasome	UBR2	-0.35	4.02E-03
		Ubiquitin proteasome	FOXO4	-0.32	1.05E-02
		Ubiquitin proteasome	USP25	-0.31	1.21E-02
		Ubiquitin proteasome	UBE2R2	-0.31	1.38E-02
		Ubiquitin proteasome	UBE2V1	-0.30	1.68E-02
		Ubiquitin proteasome	UBE2V1	-0.25	4.93E-02
	CD28	Apoptosis	SIVA1	-0.37	2.32E-03
		Apoptosis	BECN1	-0.36	3.91E-03
		Signaling	ACVR2B	-0.39	1.42E-03
		Signaling	ACVR1B	-0.27	2.79E-02
		Ubiquitin proteasome	UBC	-0.37	2.59E-03
		Ubiquitin proteasome	PSMA7	-0.36	3.67E-03
		Ubiquitin proteasome	UBE2V1	-0.35	4.15E-03
		Ubiquitin proteasome	FOXO4	-0.33	8.25E-03
		Ubiquitin proteasome	UBC	-0.29	1.80E-02
		Ubiquitin proteasome	UBE2B	-0.29	1.88E-02
		Ubiquitin proteasome	UBA52	-0.29	2.07E-02
		Ubiquitin proteasome	UBB	-0.27	2.82E-02
		Ubiquitin proteasome	TRIM63	-0.26	4.03E-02
		Ubiquitin proteasome	UBR2	-0.25	4.28E-02
		Ubiquitin proteasome	UBC	-0.25	4.75E-02
	STAT4	Ubiquitin proteasome	PSMA7	-0.28	2.56E-02
	CD2	Ubiquitin proteasome	USP2	-0.37	2.38E-03
		Ubiquitin proteasome	STUB1	-0.33	7.25E-03
		Ubiquitin proteasome	UBE2V1	-0.32	1.09E-02
		Ubiquitin proteasome	UBE2V1	-0.28	2.55E-02
		Ubiquitin proteasome	FOXO4	-0.28	2.78E-02
	CD6	Ubiquitin proteasome	FOXO4	-0.29	1.88E-02
	PTPRC (CD45)	Apoptosis	BECN1	-0.30	1.65E-02
		Apoptosis	SIVA1	-0.27	3.07E-02
		Signaling	ACVR2B	-0.47	9.17E-05
		Signaling	ACVR1B	-0.41	7.61E-04
		Ubiquitin proteasome	STUB1	-0.55	2.10E-06
		Ubiquitin proteasome	UBB	-0.51	2.00E-05
		Ubiquitin proteasome	UBA52	-0.50	3.16E-05
		Ubiquitin proteasome	UBC	-0.49	3.62E-05
		Ubiquitin proteasome	UBC	-0.48	5.33E-05
Ubiquitin proteasome		UBB	-0.48	5.70E-05	
Ubiquitin proteasome	UBC	-0.45	2.25E-04		

		Ubiquitin proteasome	UBC	-0.44	2.34E-04
		Ubiquitin proteasome	UBA52	-0.41	8.11E-04
		Ubiquitin proteasome	UBE2R2	-0.37	2.48E-03
		Ubiquitin proteasome	UBA52	-0.36	3.60E-03
		Ubiquitin proteasome	PSMA7	-0.35	4.17E-03
		Ubiquitin proteasome	USP2	-0.32	9.14E-03
		Ubiquitin proteasome	DNAJC11	-0.30	1.49E-02
		Ubiquitin proteasome	TRIM63	-0.26	3.67E-02
		Ubiquitin proteasome	MUL1	-0.27	3.29E-02
		Ubiquitin proteasome	FOXO4	-0.26	3.68E-02
		Ubiquitin proteasome	UBE2V1	-0.26	4.09E-02
	IL2RB	Apoptosis	BECN1	-0.31	1.39E-02
	IL2RB	Signaling	ACVR2B	-0.33	8.24E-03
	IL2RB	Ubiquitin proteasome	UBC	-0.46	1.36E-04
	IL2RB	Ubiquitin proteasome	UBC	-0.44	2.58E-04
	IL2RB	Ubiquitin proteasome	UBC	-0.40	9.27E-04
	IL2RB	Ubiquitin proteasome	FOXO4	-0.32	9.18E-03
CD8 T cell specific function	FASLG	Ubiquitin proteasome	USP2	-0.40	1.09E-03
	FASLG	Ubiquitin proteasome	FOXO4	-0.30	1.50E-02
	GZMA	Ubiquitin proteasome	USP2	-0.35	4.75E-03
	GZMK	Ubiquitin proteasome	USP2	-0.33	6.89E-03
	GZMK	Ubiquitin proteasome	STUB1	-0.27	3.32E-02
<p>r = Pearson's correlation coefficient. $p = <0.05$: statistical significance. Genes analyzed in the preset table are based on the univariate negative gene correlations from the secondary male cohort (a 46 gene list). No significant or negative correlations were observed for LCK, CASP8, ATG13, FBXO32, UBE2L3 and USP4.</p>					

Appendix L (Chapter 4): Gene arrays from rectus abdominis muscle from secondary female cohort (n=64)

Correlation matrix of T cells genes and muscle catabolic pathway genes. Strength of the correlation is represented by the size and color intensity of each spot, positive in blue and negative in red. Pearson correlation analysis.



Appendix M (Chapter 5): Candidate molecules for elaboration of candidate gene list

A search of the literature was conducted to determine candidate gene molecules associated with the pathways of interest. Toll-like receptors investigated in skeletal muscle associated with immune cell migration (Appendix M.1), search terms: Toll-like receptor # [TLR #] AND immune cell [OR synonyms for immune cell phenotypes] AND skeletal muscle. Toll-like receptors investigated in skeletal muscle associated with secretion of chemokines involved in immune cell migration (Appendix M.2), search terms: Toll-like receptor # [OR TLR #] AND chemokine AND skeletal muscle. For TLRs adaptor molecules and associated proteins (Appendix M.3), a search of current literature summarizing TLRs signaling mechanisms was done with terms: Toll-like receptor signaling [review]. For chemokines with relevance to immune cell migration (Appendix M.4), a recent review paper had identified chemokines and literature in relevance of these process (David et al., 2019); literature in relevance to chemokine activity on immune cell migration was search as: a) chemokine name AND chemoattractant AND immune cells / b) chemokine name AND immune cells AND migration [OR trafficking]. Search for cellular adhesion molecules was limited to selectin family, leukocyte-related selectin ligands, leukocyte-related integrins, intercellular adhesion molecules (ICAM), vascular adhesion molecules (VCAM), and cell surface receptors participating in diapedesis. Molecules were identified from a search on current literature summarizing the immune migration process search as: name of cellular adhesion molecule family AND leucocyte extravasation process (Appendix M.5).

M.1 TLRs investigated in skeletal muscle associated with immune cell recruitment				
Author	TLR	Model and exposure	Muscle group	Results
Mojumdar 2016	TLR2	TLR2 -/- mice. Cardiotoxin injury and muscle dystrophy.	TA	Reduced macrophage (F4/80+CD11b+) numbers in cardiotoxin exposed and muscle dystrophy mice when compared to WT. Neutrophil recruitment was not influenced.
Hu 2019	TLR3	C57BL/6 male and female mice. Cardiotoxin injury with Calmodulin (CAM) inhibitor or agonist	TA	CAM agonist promoted monocyte/macrophages recruitment with was associated to the upregulation of TLR3.
Paiva-Oliveira 2012	TLR4	C3H/HeJ mice with non-functional TLR4. <i>Bothrops jararacussu</i> snake venom injury.	GA	Reduced macrophage (F4/F80+) numbers when compared to TLR4-functional mice
Warren 2011	TLR9	C57BL/6 mice. Freeze-induced muscle injury.	TA	High expression of TLR9 at day 3 day post-injury, colocalized expression with tissue recruitment of macrophages (F4/F80+ and CD11b+)

TLR: Toll-like receptor. WT: wild type. TA: Tibialis anterior. GA: gastrocnemius.

M.2 Toll-like receptors investigated in skeletal muscle associated with secretion of chemokines involved in immune cell migration.

Author	TLR	Model and exposure	Results
Boyd 2006	TLR2/TLR4	C2CL2 myoblasts and myofiber isolation from C57BL/6 mice. LPS stimulation.	Enhanced gene expression of CCL2 (MCP-1) and CXCL1 (KC) *Protein expression in diaphragm and TA confirmed.
	TLR5	C2CL2 myoblasts and myofiber isolation from C57BL/6 mice. Flagellin + IFN-gamma stimulation.	Enhanced gene expression of CCL2 and CXCL1. *Protein expression in diaphragm and TA confirmed.
	TLR3 and TLR7	C2CL2 myoblasts and C57BL/6 mice	Absence of protein expression in C2CL2 myoblast. Absence of protein expression in diaphragm and TA.
	TLR9	C2CL2 myoblasts and C57BL/6 mice. IFN-gamma stimulation.	Protein expression in C2CL2 myoblasts. Protein expression in diaphragm and TA. No changes in gene expression of CCL2 and CXCL1.
Salyer 2018	TLR2/TLR6	Human myoblasts isolated from non-myopathic patients and cultured. TLR2/TLR6 agonist	TLR2/TLR6 agonist induce secretion of CCL20 and CXCL6
Schreiner 2006	TLR3	Human myoblasts isolated from non-myopathic patients and cultured. IFN-gamma and poly (I:C).	Strong upregulation with IFN-gamma and poly (I:C). TLR3 stimulation induced the NF-KB activation and secretion of CCL8.
	TLR1-7 and TLR9	Human myoblasts isolated from non-myopathic patients and cultured.	mRNA expression detected at low levels. No stimulation assay done for this TLRs.
	TLR8	Human myoblasts isolated from non-myopathic patients and cultured.	mRNA expression not detected
TLR: toll-like receptor. IFN: interferon. Poly (I:C): polycytidylic acid.			

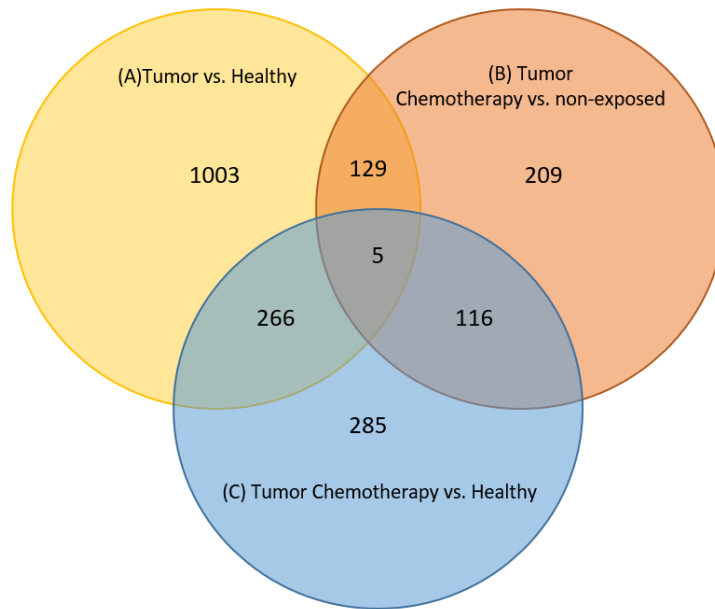
M.3 TLRs adaptor molecules and associated proteins involved in TLR signaling	
Review (Author, year)	TLR-adaptor molecules and associated proteins
Vidya 2018	TLR adaptors: MyD88, MAL, TRIF, TIRAP, TRAM Associated proteins: LRR, IRAK1, IRAK4, E3 Ub TRAF6, TRAF3 AP1, TAK1, TAB1, TAB2, MAPK, IKb, NFkB, IRF3, RIP1, IKKi, TBK1, Pellino1, DEAF1, IFNbeta Negative regulators: SOCS1, SIGIRR, T1/ST2
Leifer 2016	TLR adaptor molecules: MAL, MYD88, TRAM, TRIF, TIR domain Co-receptors: Ly96 (MD2), RP105/MD1 complex and CD14 Associated proteins for endogenous TLRs: gp96 (GRP94+Hsp90b1), CNPY93 (PRAT4A), CNPY4 (UNC93B1), LRR59, AP3, LRR14, LRR15 Negative regulator: SIGIRR, CYLD, A20 Kinases: Neu1, Src, Btk, Syk, Lyn, IRAK kinases (IRAK1, IRAK4), TBK1 and IKK- ε. Ubiquitins: E1 Ub, E2 Ub, E3 Ub, Pellino-1, Pellino-2, Pellino 3, TRAF6 Other associated proteins: TRIAD3A, SOCS1, Smurf1/2, Cbl-b, RIPI, TAK1, IKK, IRF3
Kawasaki 2014	Co-receptors: CD14, MD2, CD36 TLR adaptor molecules: MyD88, TRIF, TIRAP (MAL), TRAM Associated proteins for endogenous TLR: UNC93B1, gp96, IRF7, CNPY93 (PRAT4A), TRAF6 and TRAF3. Associated proteins: IRF3, MAPK family (ERK1, ERK2, p38 and JNK), AP1, type 1 IFN, IRAK1, TRAF6, UBC13, UEV1A, TAK1 complex (TAB1, TAB2 and TAB3), IKK complex (IKKalpha, IKKbeta, IKKgamma), NFkB, RIP1, Pellino-1, IRF3, DEAF1, IFNbeta promoter, TBK1 Negative regulators for: -MyD88: SOCS1, and Cbl-b -TRIF: SARM and TAG -TRAF3: SOCS3 and DUBA -TRAF6: USP4, CYLD, TANK, TRIM38, and SHP -TAK1: TRIM30α and A20
Kumar 2009	TLR1/2: TIRAP, MYD88 TLR2: TIRAP, MYD88 (Co-receptor: CD36, RP105) TLR3: TRIF TLR4: TIRAP, MYD88 (Co-receptor: CD14, LBP, RP105) TLR5: MYD88 TLR6/2: TIRAP, MYD88 TLR8, TLR9, TLR11: MYD88 Associated proteins: IRF3,7, IRAK4,1,2, TRAF6,3, RIP1, TAK1, TBK1/IKKI, IKK-alpha, IKK-beta, IKKgamma, IRF3, IRF7, MAP kinases (p38, JNKs and ERK1/2), NFkB, IKK complex
GRP: glucose-regulated protein, Hsp: heat shock protein	

M.4 Chemokine ligands with relevance on immune cell migration*		
Chemokine ligand	Chemokine receptor related	Immune cell migration relevance
XCL1	XCR1	Dendritic cell thymic accumulation (Lei et al., 2011).
CXCL1, CXCL2, CXCL3, CXCL5, CXCL6, CXCL7, CXCL8	CXCR2	Neutrophil trafficking from circulation into tissues (Disteldorf et al., 2015; Girbl et al., 2018; Joseph et al., 2017; Li et al., 2015; Linge et al., 2008; Mittal et al., 2008; Yao et al., 2013).
CXCL4 (Released by platelets)	CXCR3	T cell migration (Mueller et al., 2008).
CXCL9 and CXCL10	CXCR3	CD8+ T cell tissue migration (House et al., 2019; Ochiai et al., 2015; Pascual-García et al., 2019).
CXCL11	CXCR3	T cell recruitment (endothelium) (Sauty et al., 2001).
CXCL12	CXCR4	Dendritic cells and neutrophils (Petrie Aronin et al., 2017). CXCL12 inhibition promotes CD8+ T cell migration (Garg et al., 2018).
CXCL13	CXCR5	B cell recruitment/homing (Ansel et al., 2002).
CXCL14	CXCR4	Natural killer trafficking (Starnes et al., 2006). Macrophages and dendritic cell recruitment from circulation (Meuter et al., 2007).
CXCL15	Unknown	Neutrophil trafficking (Eruslanov et al., 2017).
CXCL16	CXCR6	T cell, macrophage and neutrophil trafficking and mobilization (Chaparro et al., 2019; Sandor et al., 2018; Steffen et al., 2018).
CXCL17	CXCR8	Myeloid cells and T regulatory cells recruitment (Oka et al., 2017).
CX3CL1	CX3CR1	Macrophage and CD4+ T cells recruitment (Blauth et al., 2015; Chen et al., 2018; Strömberg et al., 2016).
CCL1	CCR8	T regulatory cell recruitment (Blauth et al., 2015; Chen et al., 2018; Strömberg et al., 2016)
CCL2	CCR2	Macrophage recruitment (J. Zhang et al., 2014).
CCL3	CCR1, CCR5	T regulatory cell recruitment (C. Zhang et al., 2018).
CCL4	CCR5	Eosinophil recruitment (Kobayashi et al., 2019).
CCL5	CCR1, CCR3, CCR5	T cell migration (Murooka et al., 2008).
CCL6	CCR1	Myeloid cell migration (LaFleur et al., 2004).
CCL7	CCR1, CCR2, CCR3, CCR5	Neutrophils and T cell migration (Bardina et al., 2015).
CCL8	CCR8	Dendritic cell and T regulatory cell migration (Halvorsen et al., 2016; Sokol et al., 2018).
CCL9	CCR1	Dendritic cells (Zhao et al., 2003).
CCL11	CCR3	Eosinophil recruitment (Xing et al., 2016).
CCL12	CCR2	Dendritic cell, CD4+ and CD8+ T cell migration (Bradfield et al., 2003; Kabashima et al., 2007).

CCL13	CCR1, CCR2, CCR3	Granulocyte migration (Ugucioni et al., 1997).
CCL15	CCR1, CCR3	Myeloid cells (Liu et al., 2019; Yamamoto et al., 2017).
CCL16	CCR1, CCR2, CCR5	CD4 T cell mobilization (Gregor et al., 2017).
CCL17	CCR4	T regulatory cells recruitment (Mizukami et al., 2008).
CCL18	CCR8	CD8+ T memory cell recruitment/homing (Günther et al., 2005).
CCL19/CCL21	CCR7	Dendritic cell migration (Scandella et al., 2004).
CCL20	CCR6	T cell and dendritic cell migration (Dohlman et al., 2013; Sierro et al., 2001; Thorley et al., 2005).
CCL22	CCR4	T regulatory cell recruitment (Faget et al., 2011; Mizukami et al., 2008).
CCL23	CCR1	T cell recruitment (Chaudhry et al., 2019).
CCL24, CCL26	CCR3	Eosinophils (Dai et al., 2016; Jeong et al., 2016).
CCL25	CCR9	T cells (Onai, 2002; Svensson et al., 2002).
CCL27	CCR10	T cells (Gao et al., 2009).
CCL28	CCR10	T cells (Eksteen et al., 2006).
*Chemokine identification based on David et al. <i>Immunological reviews</i> (2019). 289 (1):9-30.		

M5. Summary of cell surface receptors and ligands involved in the leukocyte extravasation process		
Cellular expression	Molecules	Reviewed by:
Immune cells	Selectin ligands: PSGL-1, L-Selectin Integrin family: ITGAL (LFA-1), ITGAM (CD11b), ITAGD (CD11d), ITGB2 (CD18/Mac-1), ITGB1(CD29), ITGAE (CD103), ITGB7, ITGA4 (VLA-4) Cell surface ligands involved in diapedesis: DNAM1 (CD226)	Vestweber et al. 2015, Fagerholm et al. 2019, and Schittenhelm et al. 2017
Endothelial cell	Selectin family: E-Selectin, P-Selectin Intercellular adhesion molecules: ICAM1, ICAM2 Vascular adhesion molecules:VCAM1 Cell surface receptors involved in diapedesis: PECAM1, CD99, CD99L2, PVR, JAMA, ESAM, CD47	Cerutti et al. 2017, Vestweber et al. 2015, and Dustin et.al 2019

Appendix N (Chapter 5): Overlapping of differentially expressed genes between (A) tumor-bearing versus healthy rodents, (B) tumor-bearing chemotherapy exposed versus non-exposed rodents, and (C) tumor-bearing chemotherapy exposed versus healthy rodents.



Appendix O (Chapter 6): Granulocytes located in blood vessel and infiltrated in muscle tissue

Muscle cross section from a 38 year old individual with cancer. Image with increased brightness to visually appreciate location of a large blood vessel (area below to the left) and muscle fibers (area on top to the right, example of muscle fiber identified with an asterisk). Granulocytes CD11b+ cells are located on periphery of muscle fibers (arrows) and inside the vascular epithelium (Circle). Scale bar 45 μ m.

